Control architecture for adaptive and cooperative car-following

Carlos Flores

THÈSE DE DOCTORAT

de l'Université de recherche Paris Sciences et Lettres
PSL Research University

Préparée à MINES ParisTech

Architecture de contrôle pour le car-following adaptatif et coopératif
Control architecture for adaptive and cooperative car-following

École doctorale n°432

SCIENCES DES MÉTIERS DE L'INGÉNIEUR (SMI)

Spécialité MATHÉMATIQUES, INFORMATIQUE TEMPS-RÉEL, ROBOTIQUE

COMPOSITION DU JURY :

Mme. Concepción MONJE
Universidad Carlos III, Rapporteur

M. Olivier SENAME
GIPSA-lab Grenoble, Rapporteur

M. Steven SHLADOVER
PATH Berkeley, Examinateur

M. Philippe MARTINET
INRIA Sophia Antipolis, Président du jury

M. Fawzi NASHASHIBI
INRIA Paris, Examinateur

M. Vicente MILANÉS
Renault, Examinateur

Soutenue par
Carlos Eduardo FLORES PINO
le 14 Décembre 2018

Dirigée par **Fawzi Nashashibi**
Co-encadrée par **Vicente Milanés**

MINES ParisTech

PSL RESEARCH UNIVERSITY PARIS

To Luis and Marilú,

With whom I will never be grateful enough,

This accomplishment is also yours.

Acknowledgements

This thesis work is an outcome of three years of challenging, but rewarding times which I would not have made it through by my own. In my opinion, achievements are worth having, only if gratitude is at the very base of them. This is why acknowledging those that made it possible is more than fair:

I would like express gratitude in the first place to God, for being the compass that guides my life and for continuously blessing it.

I wish to thank my parents for their loving patience and aid, which have been fundamental in the accomplishment of this. Heartfelt gratitude also to Ariana for being a big part of this, whose support and company have been essential along this years.

My sincerest gratitude to Fawzi and Vicente for opening the doors of this unique opportunity on this challenging journey. This work would not have been possible without their invaluable guidance, patience and friendship.

To all of my friends, colleagues and people that somehow were part of this, great thanks to you all. Special thanks to Raoul, Luis, Fernando, Rafael, Chantal, Van, Julio and Jean-Marc for your help, as well as for those valuable experiences and discussions.

Special thanks to Gerardo, because he has always made me feel like one of his "academic sons" and for being such an amazing human being. To Joshue, great thanks for its unconditional support and being a great person with which I can luckily count on. Without their support and uninterested care, this work would not be a reality.

Contents

List of Figures

List of Tables

Chapitre 1

Introduction

Below is a French summary of the following chapter "Introduction".

Ce chapitre introduit le cadre, la motivation, les objectifs et les contributions de ce travaux de thèse. La croissance des problèmes liés au transport routière, notamment les embouteillages, les accidents ou bien les émissions CO_2, ont encouragé la recherche des solutions basés sur l'amélioration de la performance des véhicules. Les techniques car-following ont émergées de l'étude de la gestion de l'espacement entre véhicules par des conducteurs humains. Cela, ajouté à l'introduction des capteurs qui mesurent les inter-distances et l'automatisation longitudinale, a permis la conception des systèmes d'automatisation qui gèrent l'écart en distance avec le véhicule précédant. Les réseaux de communication "Vehicle-to-vehicle" (V2V) ont aussi permis d'étendre les avantages de ces systèmes en augmentant la perception des véhicules et en permettant de la coopération.

Néanmoins, la recherche pour des systèmes car-following plus performants est toujours en cours, surtout ciblant des inter-distances plus courts, une régulation de l'écart plus stable et la possibilité d'avoir véhicules des différents dynamiques dans la même formation. La notion de stabilité de la chaîne, ou stabilité du convoi stricte, est aussi l'une des métriques fondamentales de ce travaux, vu qu'elle définit la façon dont les perturbation se propagent dans la formation.

Les objectifs et les contributions de ce travaux sont ensuite mentionnés:

- Une architecture modulaire de contrôle pour le développement et validation des différents algorithmes de car-following coopératif et automatisé. D'ailleurs, une manipulation de l'écart temporel pour la gestion de l'espacement plus optimale est envisagé pour l'ACC et CACC, non seulement pour des environnements d'autoroute mais aussi urbains.
- Utilisation des méthodes de calcul (comme le calcul d'ordre fractionnaire) qui permettent la conception des systèmes de contrôle en feedback plus performants, en prenant en compte principalement la stabilité du convoi.
- La conception et validation de algorithmes basés sur des stratégies de coopération feedforward qui permettent d'assurer la performance, robustesse et stabilité désirées malgré la différence de dynamiques parmi les véhicules du convoi.

Finalement, le reste du manuscrit est décrit avec une résumée de chaque chapitre et la liste des publications est fournie.

Chapter 1

Introduction

The increasing population density that most of cities are experiencing has significantly increased the demand on road mobility infrastructure. This has brought as consequence that road congestion, traffic jams and accidents have become of the major issues in the road transport sector. For instance, commuters from cities like Los Angeles or New York spent in average more than 90 hours stuck in traffic jams in 2017[1]. Although road fatalities and injuries have decreased since 2006, the total of fatalities remains above 25 thousands per year in the European Union[2] and over 1.25 million in the entire world[3]. Another consequences of the increasing traffic jams are the elevated CO_2 emissions, air pollution and noise [Künzli et al., 2000]. When increasing road infrastructure size or augmenting the average speed is no longer feasible, the best solution is to optimize the way vehicles manage their inter-distances. For decades, mathematical analysis has been done over the way human surveys the distance towards the preceding vehicle, observing that it is being done in a non-optimal fashion. These studies have not only permitted to better understand road transportation problems, but also to seek alternatives as designing reference car-following models.

1.1 Background and motivation

The need for solving the aforementioned society problems and the advances on vehicular technology, have encouraged to explore solutions with automation capabilities of passenger and heavy duty vehicles. Given that the vehicle longitudinal motion determines the interaction with vehicles in the same lane and vulnerable road users (VRU), research and industrial agents are putting efforts on the integration of perception sensors with longitudinal automation systems. As an outcome, not only faster reactions to hazardous situations are feasible, but also the possibility to define the reference or ideal car-following behavior becomes achievable.

In addition, organizations as the European Commission are actively promoting the inclusion of wireless vehicle-to-vehicle (V2V) communication links[4] through research projects deployment to increase safety and extend vehicles' control capabilities. This would make possible to form cooperative vehicular networks, by means of applications as Cooperative Adaptive Cruise Control (CACC) and platooning. Their potential to significantly enhance not only the spacing gap regulation task in terms of stability and safety, but also the traffic throughput and string stability

[1] https://www.statista.com/chart/12830/the-cities-with-the-biggest-traffic-jams/

[2] https://ec.europa.eu/transport/road_safety/sites/roadsafety/files/pdf/statistics/dacota/asr2017.pdf

[3] https://www.cdc.gov/features/globalroadsafety/index.html

[4] https://ec.europa.eu/research/participants/data/ref/h2020/wp/2018-2020/main/h2020-wp1820-transport_en.pdf

has been demonstrated in recent years [Shladover et al., 2012]. If the inter-distances are short enough, platooning strategies have demonstrated to bring fuel economy capabilities up to a 15% of savings [Tsugawa, 2013]. Nevertheless, research towards even more performing car-following systems is still ongoing, targeting shorter inter-vehicular distances with safety and stable tracking over the entire speed range. For instance, string stability is a key notion that has been gaining interest mainly for its capacity to describe how the traffic oscillations are propagated, giving a performance metric of the string behavior [Swaroop and Hedrick, 1996]. The string stability is highly dependant on the gap-regulation control system, but most importantly on the adopted reference car-following model or spacing policy. For this reason the desired time gap not only describes the string geometry, but also defines the overall system performance–i.e. the shorter the time gap, the more exigent becomes the gap-regulation task [Naus et al., 2009]. Most of current car-following works are under the vehicles homogeneity assumption, which is unlikely to happen and also restricts the widespread employment of these techniques. Relaxing this assumption and considering vehicles dynamics heterogeneity is mandatory for the viability of automated car-following systems, despite the additional complexity that this signifies.

Although remarkable advances has been obtained so far over automated car-following systems, the benefits of current cooperative driving and platooning are still field of discussion [Van Arem et al., 2006]. For this reason, this work is motivated by the necessity of a more functional safety-aware car-following control structure, focusing on the trade-off between performance with time gap reduction (traffic capacity increase with fuel economy) and individual/string stability both in urban and highway scenarios. Since the consideration of strings of non-identical vehicles is still an open research subject, this work is also focused on developing control structures and algorithms that ensure the desired system performance regardless the string heterogeneity. This thesis has been carried out in the framework of the french National Research Agency (ANR) project VALET ANR-15-CE22-0013[5], which proposes the employment of platooning to redistribute fleets of shared electrical cars.

1.2 Objectives and contributions

Based on the presented motivation statements, this thesis has as main purpose the design and development of automated car-following control algorithms to further extend their benefits over traffic capacity and string stability. Sensor-based, but mostly communication-based car-following systems, are aimed through a modular hierarchical control architecture, where each of its blocks are designed with complementary objectives that enhance the overall performance both at individual and cooperative level. This thesis faces the next challenges:

- The proposal of a modular hierarchical control architecture for the development and validation of different cooperative automated car-following algorithms. With the purpose of extending the ACC and CACC benefits, focus on time gap-based strategies that ensure safety and stability over urban and highway scenarios.
- Exploration of novel calculus techniques and architectures for the development of more performing gap-regulation control systems, with special emphasis on the system string stability without losing individual stability and robustness.
- Design and validation of cooperative strategies that ensure the desired performance despite the heterogeneity of the string of vehicles and the temporal communication delays

[5]http://www.agence-nationale-recherche.fr/Project-ANR-15-CE22-0013

The aforementioned challenges have led to the next main contributions:

- A modular control structure employable with ACC or CACC, based on a two-layer control strategy where each of its blocks have different complementary objectives. A low level control layer is designed based on the vehicle longitudinal dynamics and its actuators, yielding a closed loop form of a reference speed tracking block. This is employed in cascade by the high level layer or gap-regulation control structure. An outer feedback loop defines the reference car-following model, for which a full range spacing policy that seeks safety, string stability and traffic throughput increase is proposed. To provide loop robustness and gap-regulation stability, a high level feedback controller is employed. The reference tracking performance and string stability is enhanced using an inverse model-based feedforward approach.

- An architecture for cooperative driving over urban environments is proposed and validated with real platforms experimentations. Based on a state machine, the architecture handles cooperative automated car-following and emergency braking in case a possible pedestrian collision is detected. It performs a gap-closing maneuver based on time gap manipulation once the collision has been avoided, thus rejoining the string and resuming the car-following state at the desired time gap.

- The proposal and validation of different design algorithms for feedback control based on optimization, targeting different car-following performance objectives. Three strategies are proposed that seek the optimal closed loop frequency response in terms of different exigencies, using fractional-order feedback controllers. The first consists on enhancing the string stability and reducing the time gap, without losing individual stability and response bandwidth. Robustness against plant gain variations is sought with the second design algorithm, finding an optimal control configuration for flat phase around the gain-cross frequency. Finally, the third algorithm proposes to employ template functions that shape the desired loop response, analyzing the load disturbance sensitivity, complementary sensitivity and control effort.

- An analysis of the effects of vehicles' dynamics heterogeneity in a string of cooperative car-following is provided. Two solutions are proposed to ensure the desired robust performance for strings of non-identical vehicles. The first solution aims preceding-only topologies, based on online feedforward structure adaptation in function of the ego-preceding vehicles' dynamics relation. It employs sequential Monte-Carlo or particle filtering to model the preceding vehicle behavior, which permits to attain the ideal feedforward model inversion and enhance the closed loop performance. The second solution proposes to extend the feedforward capabilities including the leader reference speed, which reduces the control effort of vehicles with slower dynamics and improves the system string stability, specially for short time gaps and considerable V2V communication delays.

1.3 Manuscript organization

This PhD thesis has been organized in seven chapters. Detailed description concerning the state of the art of cooperative car-following control, as well as the proposed control strategy for time gap regulation in homogeneous and heterogeneous strings is provided. A brief overview of each of the remaining chapters is given below:

Chapter 2, State of the art: Introduces the motivation and firsts advanced driver assistance systems that have been developed, based on longitudinal automation. Cruise control is reviewed,

as well as its evolution the Adaptive Cruise Control, leading to study the car-following notion. A review of human driving car-following and its models is provided firstly, introducing the automated car-following. Definitions and a literature overview are provided related to spacing policy and string stability notions, which are fundamental for cooperative driving. CACC is defined together with platooning, whose objectives and benefits are also described. An extensive literature review related to research projects and industrial developments is provided, focusing on cooperative automated driving and platooning. A final discussion is presented about the conclusions of the literature review, as well as some open challenges that have been identified.

Chapter 3, Car-following control structure: Provides an insight of the employed control structures and communication topologies that have been used in the literature. Afterwards, the proposed hierarchical control structure is described, based on a low level reference speed tracking control and a high level time gap-regulation system. The vehicular longitudinal dynamics are detailed, introducing the low level speed control strategy. For the high level system, an inverse model-based feedforward strategy is employed to improve the reference tracking, while an outer feedback loop is employed to set the desired time gap, defining not only the string geometry but also its stability. A state machine-based architecture for cooperative driving in urban scenarios is detailed, which accounts with cooperative car-following, pedestrian interaction and gap-closing capabilities. Finally, the motivation for a novel full range time gap spacing policy is described, as well as its operation, benefits and design procedure.

Chapter 4, Homogeneous strings control: Presents an introduction of the control of homogeneous strings or strings of similar vehicles, where a motivation for the employment of fractional-order calculus to design more performing feedback control systems is provided. An overview of the theory and applications of fractional-order calculus is presented, with control examples and methods to study stability of non-integer order systems. A list of approximation-based implementation tools is provided both for continuous and discrete time systems. Subsequently, three design methods for feedback fractional-order controllers for improving gap-regulation capabilities are detailed, under the assumption of identical vehicles within the same string. Each method targets different performance objectives: strings stability with reduced time gap, robustness against plant gain variations and loop-shaped robust performance.

Chapter 5, Heterogeneous strings control: Focuses on the control of strings of vehicles with non-identical dynamics. A literature survey is provided with state-of-the-art strategies, which conclusions motivate the proposal of an identification algorithm over the preceding vehicle dynamics, yielding the ideal inverse model-based feedforward performance. Another approach is presented, which proposes the employment of the leader vehicle reference speed on feedforward to improve string performance and reduce the risk of actuator saturation. An algorithm for the management of both feedforward links is proposed based on the ego-preceding vehicles dynamics relation.

Chapter 6, Validation results: Presents the validation experiments, both over numerical simulations and real platforms. For simulations, MATLAB Simulink and RTMaps models are employed, while the INRIA RITS team platforms are used for real experiment validations. The low level control layer design is validated over the Cycab and Citröen C1 platforms. Benefits of the proposed full range spacing policy are demonstrated in this chapter, over ACC and CACC strings. The architecture for urban cooperative driving operation is demonstrated over a real scenario with vehicles and pedestrians. Design methods for feedback control are applied for the vehicle dynamics and further validated with stability studies in simulations and real experiments, under the assumption of homogeneity on the string. Both approaches for heterogeneous strings are validated with extensive numerical experiments. Moreover, the model identification algorithm is

tested, which results are further employed over the heterogeneous CACC string control evaluations both over preceding-only and leader-predecessor topologies.

Chapter 7, Conclusions: Includes the concluding remarks of this thesis work related to the proposed approaches, having as a starting point the described state-of-the-art. Research perspective and some open subjects that could be derived from this work are provided at the end of this chapter.

1.4 Publications

The scientific contributions derived as a result of the developed research work are listed below:

Title: Using Fractional Calculus for Cooperative Car-Following Control
Authors: C. Flores, V. Milanés, and F. Nashashibi
Conference: 19$^{\text{th}}$ International IEEE Conference on Intelligent Transportation Systems (ITSC)
Place: Rio de Janeiro, Brazil **Date:** November, 2016

Title: A Time Gap-Based Spacing Policy for Full-Range Car-Following
Authors: C. Flores, V. Milanés, and F. Nashashibi
Conference: 20$^{\text{th}}$ International IEEE Conference on Intelligent Transportation Systems (ITSC)
Place: Yokohama, Japan **Date:** October, 2017

Title: Online Feedforward/Feedback Structure Adaptation for Heterogeneous CACC Strings
Authors: C. Flores, V. Milanés, and F. Nashashibi
Conference: American Control Conference (ACC)
Place: Milwaukee, USA **Date:** June, 2018

Title: A Cooperative Car-Following/Emergency Braking System With Prediction-based Pedestrian Avoidance Capabilities
Authors: C. Flores, P. Merdrignac, R. de Charette, F. Navas, V. Milanés, and F. Nashashibi
Journal: IEEE Transactions on Intelligent Transportations Systems
Status: Accepted **Date:** June, 2018

Title: Fractional-Order-Based ACC/CACC Algorithm for Improving String Stability
Authors: C. Flores, V. Milanés
Journal: Transportation Research Part C: Emerging Technologies
Status: Accepted **Date:** July, 2018

Title: On Feedforward Strategies for Cooperative Heterogeneous Strings
Authors: C. Flores, V. Milanés, F. Nashashibi
Journal: IEEE Transactions on Intelligent Transportations Systems
Status: In progress

Title: Multi Model Adaptive Control for CACC applications
Authors: F. Navas, V. Milanés, C. Flores, F. Nashashibi
Journal: Control Engineering Practice. A Journal of IFAC, the International Federation of Automatic Control
Status: In review

Title: Youla-Kucera based Fractional Controller for Stable Cut-in/Cut-out Transitions in Cooperative Adaptive Cruise Control Systems
Authors: F. Navas, R. de Charette, C. Flores, V. Milanés, F. Nashashibi
Journal: IEEE Transactions on Intelligent Transportation Systems
Status: In review

Chapitre 2

Etat-de-l'art

Below is a French summary of the following chapter "State-of-the-art".

Ce chapitre décrit les concepts fondamentales et l'état-de-l'art du car-following automatisé. D'abord, les origines et l'évolution des quelques systèmes d'automatisation longitudinale du véhicule sont décrits, notamment le contrôle croisière et le contrôle croisière adaptatif. Une brève littérature est fourni des modèles mathématiques qui représentent la façon dont les humains gèrent l'écart avec le véhicule précédent. Le deux notions les plus importants lors des études de car-following sont définies et leur état-de-l'art revues: les politiques d'espacements et la stabilité du convoi. Cette dernière est présentée avec ses différents définitions que l'on peut trouver dans la littérature, ainsi que ses applications.

Ensuite, la coopération dans la conduite automatisé, spécialement sur le car-following, est introduite et revue. Le contrôle croisière adaptatif coopératif (CACC) est défini et ses objectifs sont mentionnés, ainsi que la structure de contrôle requis pour sa mise en œuvre. Puis, le concept du platooning est introduit, en remarquant ses différences par rapport au CACC. Une vaste révision est présenté de la plupart des différents projets déroulés sur la ligne de recherche du car-following automatisé et coopératif, depuis 1997 jusqu'à présent. Dernièrement, une discussion sur l'état-de-l'art est fournie avec la tendance ses ce derniers années selon l'auteur, ainsi que des défis ouvertes dans la littérature que seront ciblés dans ce travaux de thèse.

Chapter 2

State of the art

2.1 Introduction

Human drivers account with limited perception and considerable reaction lags towards changes in their environment, which may lead to non-optimal spacing management, unsafe maneuvers and shockwaves. In recent years, significant efforts have been deployed towards the conception of vehicle automation systems to solve road transportation problems as safety, traffic jams and CO_2 emissions. Given that the car-following behavior defines the traffic flow evolution, safety and stability of the driving task; studying the motion and vehicles' interaction over the longitudinal axis is of utmost importance. For this reason, first embedded automation systems were designed to act over such axis. Commercially available systems as the Adaptive Cruise Control (ACC) or emergency braking systems rely on embedded sensors, actuators and a processing unit to significantly improve driver's reaction capabilities.

Connectivity between vehicles is being introduced more and more into the road transportation sector, opening possibilities to improve vehicle control systems and extend the car-following capabilities. It permits that each vehicle can rely in other information sources than its own sensors, as well as reaching cooperation between vehicles that drive in the same environment. Cooperation over car-following is a concept that has been gaining interest in recent years over industrial and research agents, to explore its capabilities to improve urban mobility.

This chapter introduces the evolution of the automation systems that act on the vehicle longitudinal axis is described. The fundamentals of car-following is defined in detail, from the first car-following models that represent the way how human driving manage inter-distances, to the reference car-following models that surge with longitudinal automation and ranging sensors. The condition of avoiding shockwaves or attenuating the speed changes of forward vehicles, or string stability, is introduced with its importance on the design of gap-regulation control systems. Cooperative driving is detailed after, focusing on the CACC and platooning techniques evolution and their potential benefits. Finally, a review is provided of most of research projects on cooperative driving benefits over passenger vehicles and heavy-duty trucks. Some concluding remarks are provided as well as the context of this thesis work with respect to the described state-of-the-art of car-following systems.

2.2 Longitudinal Automation: Historical Review

2.2.1 Cruise control

One of the first active automation systems that was implemented over real vehicles is the cruise control. Nowadays, most of commercial vehicles account with cruise control systems that maintain a set speed selected by the driver, being the initial point for current car-following applications.

Since most of highways are composed by long, flat, low curvature parts; it results convenient to assist the driver or even delegate completely the speed regulation task to an embedded system. This would not only reduce driver fatigue and increase comfort, but also optimize the energy consumption via the management of vehicle propulsion. Studies have showed that cruise control systems can improve the way energy is employed, providing up to fuel savings from 1.1 to 10.7% [Shaout and Jarrah, 1997]. One can summarize cruise control objectives in three points: 1) increase driver comfort by delegating throttle pressing to the system and reducing fatigue overall in long distance trips, 2) avoid exceeding speed limit since the system handles the vehicle longitudinal speed and maximize fuel economy and, 3) introducing an efficient control loop dedicated to the speed regulation task.

With the evolution of cruise control over the years, the aforementioned objectives have been satisfied in a more efficient fashion and at a lower cost with more robustness.

2.2.1.1 Origins

First cruise control systems were developed in the 50's based on mechanical components, having a limited functionality. Besides, strategies as maintaining a fixed throttle position or proportional feedback were proposed at the beginning. They yielded a speed tracking that led often to saturations when the real speed was around 16 km/h below the desired value, with a lack of robustness to different road conditions. Later versions came up around 1980's incorporating microprocessors. This increased the system's reliability and capability to implement a more performing cruise control.

From 1990's to present, cruise control systems have been standardized and composed by four main elements [Winkelman and Liubakka, 1993]:

- Vehicle speed sensor: such as in-wheel encoders to measure the vehicle longitudinal speed.
- User interface: Through which the driver is able to handle the reference speed and decouple the system if necessary, composed by switches.
- Electronic control module: Composes the control/automation layer, which receives the measured and target speeds to generate the throttle command.
- Throttle actuator: Receives the command from the electronic control module and acts over the vehicle propulsion in form of a PWM or airflow inlet control.

From the automation/control point of view, most of cruise control systems are based on a simple feedback as the one presented in Fig. 2.1. A set-point or desired speed is compared with the wheels odometers measured speed, so the controller can act over the pedal actuator and regulate the longitudinal speed with the applied torque over the vehicle chassis. The external disturbances that modify the vehicle dynamics behavior will be detailed in chapter 3.

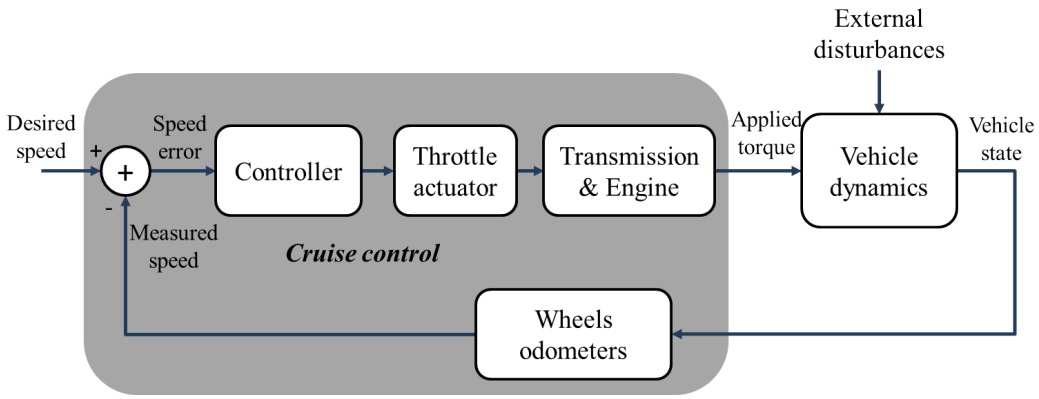

Figure 2.1: General control structure scheme for a conventional cruise control system

2.2.1.2 Evolution

Nowadays, almost all commercially available vehicles are equipped with cruise control systems, being of the most popular and accepted vehicular technologies. Medium and high range vehicles have this type of systems aiming mainly to increase driver comfort when driving over highways. Later cruise control technologies incorporated fuzzy-based solutions, with the purpose Although cruise control systems have provided satisfactory results and have been widely implemented in several commercial vehicles, they lose their benefits and become less advantageous when driving in dense traffic scenarios (either in highways or urban roads). This is caused by the frequent requirement of speed change due to traffic interaction, traffic lights, urban congestion, intersections and others. To mitigate this issue and increase the efficacy of longitudinal automated systems, ranging sensors and brake actuator automation have been proposed to extend cruise control capabilities. The resulting system has been named Adaptive Cruise Control (ACC).

2.2.2 Adaptive cruise control

In recent years, ACC systems have been entering the market after years of industrial, academic and governmental research over their technologies and benefits. Being one of the firsts ADAS that proposed to employ exteroceptive sensors in the loop, it has surged as a powerful tool to target some of the most relevant problems in transportation. ACC overcomes classical cruise control by incorporating a brake pedal actuator that allows higher deceleration than down-shifting, in case of overpassing the desired reference velocity. It also incorporates a ranging sensor (usually a radar, but can also be camera or LiDAR) to measure the inter-distance and relative velocity with respect to the preceding vehicle. Its main purpose is to regulate ego-vehicle's speed to keep a desired safe spacing gap towards the preceding car, mainly conceived for highways scenarios. Generally, market-available ACC operates from 40 to 160 km/h and under a maximum braking deceleration of 0.4g [Rajamani, 2011]. The ACC can be understood as an extension of the conventional cruise control where the reference velocity fed to the CC is generated to keep a safe headway. Its main objective is to assist the driver in the distance regulation task, acting primarily as a comfort-aimed feature for highway scenarios where speed changes are frequent due to headway traffic interaction. ACC systems have surged as an evolution of the cruise control, profiting from the advances on embedded vehicular technology in recent years to provide an enhanced driving performance.

2.2.2.1 Origins

ACC developments were derived from the conventional cruise control advances between the 1950s and 1980s. First developments were carried out by industrial agents as General Motors and Radio Corporation of America. Later on in middle 1960's, academic entities as The Ohio State University and University of Michigan through the Automatically Controlled Highway Systems (ACHS) program started research on automatic vehicle-following [Xiao and Gao, 2010]. Diamond and Lawrence designed a system to regulate vehicle speed and spacing, using mechanical actuators control [Diamond and Lawrence, 1966]. First scientific developments were published in a technical paper by Fenton's group at Ohio State University [Fenton and Mayhan, 1991] seeking an automatic vehicle following system, which was continued by the US Bureau of Public Roads over simulations and test tracks.

The increase of vehicles density, pollution and reduced infrastructure led to increase worldwide (almost all Europe, US and Japan) efforts towards ACC deployment. From 1986, the European community's PROMETHEUS program took the initiative by gathering several industrial agents to focus efforts on vehicle-dedicated technologies, demonstrating in 1991 for the first time what was called Autonomous Intelligent Cruise Control (AICC) [Brackstone and McDonald, 2000]. At the same time, California Department of Transportation (Caltrans), Ford Motor Company and California Partners for Advanced Transportation Technology (PATH) carried out research to design and test ACC controllers to study their traffic impact [Shladover, 1995]. Private European automakers and their suppliers invested later on in the integration of AICC systems on their vehicles in the frame of PROMETHEUS in mid-1994 [Brackstone and McDonald, 2000]. This constituted the first time that an ACC technology is embedded over real system architectures [Bishop, 2005], in parallel with Mitsubishi in Japan and several agents along US in 1995. From 1997, the technology has been available on commercial vehicles and the general focus changed towards the study of its impact and performance assessment over urban environments and large-scale ACC field operations. With time, developments served as a basis to switch research interests from Automated Highway Systems (AHS) to Intelligent Vehicles.

2.2.2.2 Evolution

Over the 2000's, technical problems were almost fixed, but marketing issues were still a major challenge. From that moment until now, numerous companies along the world have been incorporating ACC capabilities to their top-of-the-line cars and even some mid-range vehicles, mainly as a comfort enhancer feature. In fact, results have demonstrated that ACC systems makes the driving task less stressful and reduces the workload compared to manual driving [Piccinini et al., 2014]. A common structure of an ACC system that is implemented in nowadays vehicles is depicted in Fig. 2.2. The main difference with respect to CC structure in Fig. 2.1 appears in the outer feedback loop for gap-regulation with the ranging sensor. Another augmentation in terms of longitudinal automation with respect to the cruise control, is observed with the brake line control.

Extensive work has been continued in recent years, investigating drivers' feedback when using ACC systems ([De Winter et al., 2017], and references therein). Results show that passengers rate the system with 8.0 on a scale from 1.0 (extraordinarily negative) to 10.0 (extraordinarily positive). It has been concluded that the degree of pleasure when using ACC is directly correlated to the technological capabilities–e.g. ACC with stop-&-go capabilities were better rated than simpler versions– and the drivers' age and driving style. Nevertheless, since commercial ACC systems have operational limits as cut-in situations or emergency scenarios handling, drivers stated to feel displeased when this sort of situations arrived. The real benefits at large scale over traffic flow and

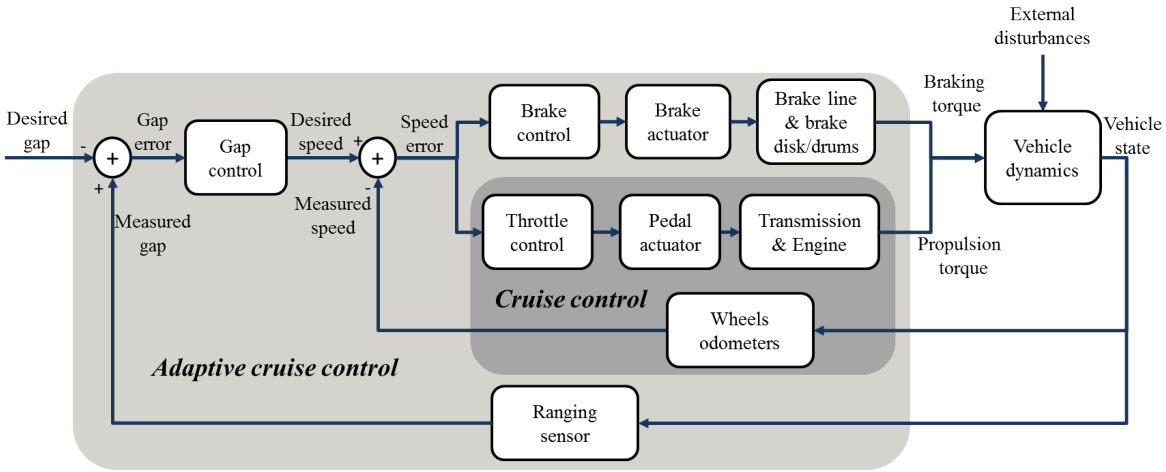

Figure 2.2: General control structure scheme for a conventional cruise control system

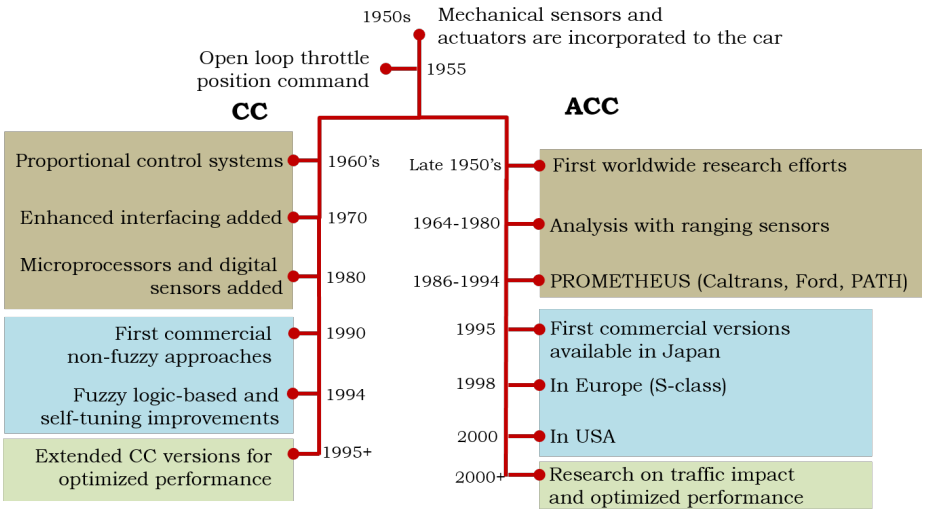

Figure 2.3: Timeline of advances in longitudinal automation prior to car-following

safety have been subject of debate [Marsden et al., 2001] [Li et al., 2017b].

A summary of the origin evolution of longitudinal automation (specifically CC and ACC) is provided in Fig. 2.3. With increasing market penetration, widespread usage and research, ACC systems have also opened the doors to several technologies as collision warning, collision avoidance or automated car-following applications, as promising solutions to road transportation mobility problems.

2.3 Car-following

In this section, the notion of car-following is described in detail. It can be understood as the action of commanding the vehicle behavior in its longitudinal axis, given a observed/measured relative motion with respect to the preceding vehicle in its same driving lane. The notion of car-following is revised in this section from mathematical models that intend to study and approximate how

drivers perform car-following, to closed loop automated car-following with ranging sensors and longitudinal automation to produce a desired performance.

2.3.1 Human driving car-following models

After extensive analysis of traffic flow theory at both individual and macroscopic level, the car-following concept gained attention in the scientific field. It refers to the way drivers maintain the spacing gap towards the preceding vehicle, predicting the traffic flow behavior from a higher scale point of view. In other words, car-following models predict the motion of a vehicle driven by a human in the position (i) of a vehicular stream, by studying the trajectory over time of the (i-1) and consequently the spacing between both vehicles.

Conceptualized for the first time by Pipes [Pipes, 1953] and Reuschel [Chandler et al., 1958], different car-following models have been proposed in the literature to simulate driving behavior at a microscopic level. They have been further employed in transportation science and engineering for safety and traffic capacity studies. An extensive literature review of car-following models can be found in [Toledo, 2007] or in [Brackstone and McDonald, 1999] where five groups can be distinguished:

- **Gazis-Herman-Rothery (GHR) or GM model:** proposed by General Motors in 1958, based on the fact that drivers react to stimuli in the environment, which define the vehicle acceleration. Such model was extended by Herman and Rothery when they realized the asymmetry between braking and throttling, proposing to use two set of parameters for the model.
- **Collision-avoidance (CA) model:** presented in [Kometani, 1959], considering that drivers aim a safe target distance that allows to avoid rear-end collisions, being in function of the driver reaction time, ego and predecessor vehicles' speeds.
- **Linear model:** Derivated from the GHR model and proposed in [Helly, 1959], employs ego speed and acceleration, with the relative distance and velocity with respect to predecessor vehicle. This approach yields a simpler expression, which permits to fit model parameters more accurately.
- **Psychophysical or action-point model:** Based on the assumption that drivers only react to stimuli (relative speed, spacing) that overcome a determined stimulus threshold [Michaels, 1963].
- **Fuzzy logic-based models:** Employing fuzzy sets and inference with logical operators, this model produces a fuzzy output that emulates car-following behavior. One example has been proposed in [Kikuchi and Chakroborty, 1992], showing the difficulty of defining the membership functions.

Along years, the aforementioned models served as a basis to elaborate more complex yet accurate models. The Gipps' car-following model [Gipps, 1981], which is a CA-based model, has become one of the most widely employed approaches both in research and practice due to its accuracy. Another model that has gained a lot of attention and is currently used in the literature belongs to Treiber et al. [Treiber et al., 2000], called Intelligent Driver Model (IDM). In [Treiber and Helbing, 2003], the model has been extended considering driver's adaptation effect using memory functions. This model has served as a basis for the development of ACC systems, since it accounts with controllable stability properties at the same time that implements an intelligent braking strategy with smooth transitions between acceleration and deceleration. More recently, a modified version of the IDM (IDM+) has been proposed for traffic flow study [Schakel et al., 2010].

Although these car-following models has been studied and employed widely in the literature, they are not designed to be optimal in terms of traffic flow, safety or stability; but to predict and imitate as closely as possible the human behavior. The study of these models has permitted to analyze the cause of road transportation issues, which has encouraged to propose solutions based on these results. When longitudinal automation is included with ranging sensors, an ideal reference car-following model can be implemented to define a vehicle behavior that improves traffic performance. These reference models that suggest the ideal separation between vehicles in the same lane are also defined as spacing policies.

2.3.2 Spacing policies for automated car-following

Having observed the great variety of human driver car-following models, one can conclude that they all try to predict in major scale the humans' behavior while driving, which results a major challenge. In fact, most of time gap-based spacing policies are based on human driving car-following models with some modifications for better results. Vehicle longitudinal automation has proven the capability to define an "ideal" spacing between vehicles in the same lane, following a desired behavior. Generally, spacing policies employ variables of ego and predecessor vehicles, with the exception of few approaches that employ other external variables. By knowing the spacing policy that the string members are tracking, one can model the complete behavior of the vehicle formation. A review of the different spacing strategies that have been proposed in the literature is presented below.

2.3.2.1 State-of-the-art spacing policies

Spacing policies are designed in function of the desired performance that is targeted. In other words, the string of vehicles that adopts such spacing policy will behave and perform as determined by the policy design objectives. Some of the most intended performance objectives in the literature are: traffic throughput increase, safety, comfort and string stability. Keeping these objectives in mind, a survey over the different strategies that have been proposed in the state-of-the-art is necessary. One can classify the spacing policies that can be found in the literature as presented in Fig. 2.4.

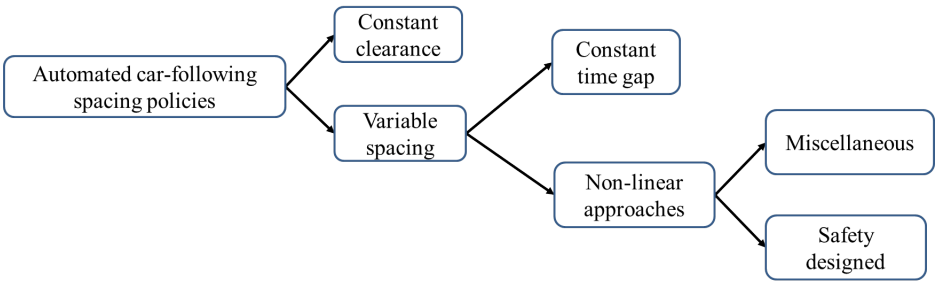

Figure 2.4: Spacing policies classification in function of the inter-distance evolution

Constant clearance constitutes the first spacing strategy that has been conceived for platooning applications [Swaroop et al., 1994]. In 1997, the PATH program used this strategy in a highway dedicated lane, over an 8-vehicle fleet to demonstrate platooning applications' benefits. This approach consists on maintaining a fixed inter-distance regardless the speed of the vehicles, which results ideal for tightly-coupled strings, increasing significantly the highway capacity. Drafting

is another benefit of such technique, which consists on the aerodynamic drag reduction when vehicles are close enough. When this strategy is adopted, dedicated lanes are required due to the short separations and difficulties to interact with other road users than the string members–i.e. merging, splitting–. Another obstacle that hinders the wide employment of constant clearance is that control stability is only achieved if all members account with a low latency Dedicated Short Range Communication (DSRC) towards the leader vehicle [Swaroop et al., 1994].

On the other hand, variable spacing policies permit a more flexible management of inter-vehicular distances, thus providing to the control designer a tool to target different performance metrics. One of the firsts variable spacing strategies, and the most employed one, is the Constant Time Gap (CTG) [Swaroop and Hedrick, 1999]. The time gap is interpreted as the time in seconds since the rear bumper of predecessor vehicle passes a fixed location on the road until the front bumper does the same [Shladover et al., 2015]. CTG is the strategy that fits the best the behavior humans driver have when car-following, for this reason it is the most adopted spacing policy by commercially available ACC systems. From the control point of view, CTG yields a spacing proportional to the ego-vehicle speed added to a fixed standstill distance. In fact, constant clearance can be interpreted as a special case of CTG where the time gap is set to zero.

Other than the two aforementioned strategies, are the non-linear approaches. They have gained a lot of attention for maintaining spacings defined by non-linear functions of the ego-velocity or even some variables of other neighboring vehicles. Two main groups can be distinguished, the ones based on human behavior aiming to increase safety in car-following and the rest of strategies that target miscellaneous objectives as string stability, traffic throughput, traffic flow stability and fuel consumption economy.

Several approaches have been proposed to target safety through automated car-following. One of the most cited is the Constant Safety Factor (CSF) [Michael et al., 1998]. It proposes to use a second order polynomial of the ego-velocity to define the reference spacing, suggesting high inter-distances. This approach aims cases where vehicles account with different braking capabilities, specially when the follower has less deceleration capacities than the predecessor vehicle. One of the targeted scenarios is the case when an constant clearance homogeneous platoon performs hard braking and a following platoon with less braking capabilities encounters the former in their way. Considerable separation and knowledge of deceleration capacities are required to avoid inter-platoon collision, which is approached using a quadratic function of the next platoon leader velocity. Under the same framework, [Zhao et al., 2009] took also the traffic flow stability into consideration. An extension of this technique can be found in [Ioannou and Chien, 1993]. In the mentioned strategy the required safe distance is yielded analyzing Newtonian motion in a worst case scenario–i.e. the predecessor is braking at its maximal capacity while ego-vehicle is at maximum acceleration. The technique results in an expression that penalizes the difference between adjacent vehicles square speed. Another safety-dedicated approach with special focus on stop-&-go scenarios is [Martinez and Canudas-de Wit, 2007]. A more human-like behavior is sought for low speed, while for high speeds more conservative yet comfortable distances are suggested.

Finally, a wide group of strategies has been proposed in the state-of-the-art to target one or more transportation issues through the spacing manipulation for either urban or highway environments. [Yanakiev and Kanellakopoulos, 1995] proposed a variable time gap approach for heavy-duty vehicles, where the time gap is set to vary in function of the relative speed between ego and predecessor vehicles. In [Mammar et al., 2012], a control strategy is proposed where different spacing reference models are adopted and switched in function of different safety car-following zones. A flatbed tow truck model is employed in [Ali et al., 2015] with the purpose of reaching constant spacing in steady state and a velocity-dependent policy at transitory states. Strategies for improv-

Table 2.1: Review of state-of-the-art spacing policies

Strategy	*Advantages*	*Disadvantages*
Constant clearance [Swaroop et al., 1994]	Traffic capacity increase	Requires dedicated lanes and low latency V2V links with leader
Constant time gap (CTG) [Swaroop and Hedrick, 1999]	String stability and safety in uniform driving	Traffic flow stability not ensured
Safety distance spacing [Ioannou and Chien, 1993]	Safety in worst case braking	Reduced traffic capacity
Constant safety factor (CSF) [Michael et al., 1998]	Safety in case of braking and string stability	Reduced traffic capacity
Non-linear spacing for heavy duty vehicles [Yanakiev and Kanellakopoulos, 1995]	Safety towards scenarios with high relative velocities	Sensitive to noise in relative speed measurement
"Ideal" spacing policy [Santhanakrishnan and Rajamani, 2003]	Traffic flow stability and string stability	Safety is not ensured in low/medium speeds and high spacing is suggested at high speeds
Flatbed truck model [Ali et al., 2015]	Traffic capacity increase, string stability	Safety not ensured in high speeds braking
Safe spacing for ACC Stop-&-Go [Martinez and Canudas-de Wit, 2007]	Safety in case of hard braking	String stability is not targeted
Range policy for ACC [Zhao et al., 2009]	Traffic flow stability	Traffic capacity is not considerably improved

ing traffic flow stability or traffic flow density is proposed in [D. and R., 1999], through a spacing policy. A comparison between spacing strategies defined by linear, quadratic and power functions of ego-speed is presented in [Zhou and Peng, 2005].

It is clear that the most targeted performance objectives are traffic throughput increase, safety guarantee and string stability, as visible in Tab. 2.1. The first refers directly to how many vehicles per time unit can circulate over a single lane, while the second refers to how risky the spacing policy is in terms of collision probability considering actuation lags or possible delays. The last objective, string stability has gained a lot of attention, becoming the main performance metric of most recent and advanced automated car-following systems. It is important to state that the chosen spacing policy together with the car-following control, defines the string stability of the system.

2.3.3 String stability

In the theory of interconnected systems, the states of an individual element and their propagation are correlated with the states of one or several other elements of the same group. The notion of string stability has been employed for more than 50 years. The term was introduced for the first time by [Peppard, 1974] and further employed in the context of car-following systems in [Chu, 1974], seeking conditions for decentralized optimal control solutions. A more formal definition was firstly stated by [Sheikholeslam and Desoer, 1992a] and later developed in [Swaroop and Hedrick, 1996], implying that all states of the interconnected system should remain uniformly bounded if initial states are as well.

In contrast with the notion of individual stability concept, which studies the time evolution of states under perturbations of initial conditions, the string stability focuses more on the evolution of such states along a cascade of systems in the sense of their indexes. Formal stability-like definitions have been proposed, suggesting to study string stability from the scope of Lyapunov asymptotic stability, specially studying the initial condition perturbations over interconnected systems. In such work, authors set sufficient "weak coupling"–i.e. relaxation of formation rigidity– conditions to guarantee string stability and asymptotic stability under disturbances. Another interpretation of the string stability notion has been employed to analyze infinite length strings of interconnected systems, both employing centralized [Mazzola and Schaaf, 2014] and decentralized control solutions [Stanger and del Re, 2013]. In [Swaroop and Hedrick, 1996], extensive analysis is carried out on the properties of interconnected systems. It formulates firstly a state space representation and subsequently a Z-transform over the index axis instead of the discrete time. For the first time, a model that describes the behavior of a car-following string as a whole is proposed. String stability can be evaluated through the state space model eigenvalues. Nevertheless, this infinite-length approximation may differ of the one of a finite-order, given that small variations or heterogeneity in the vehicle-controller configuration will make the performances diverge [Curtain et al., 2009].

A more practical interpretation of the string stability notion is the performance-oriented approach. It interprets a certain platoon as "string stable" when any perturbation of leader vehicles states is effectively attenuated in upstream direction. The fulfillment of such condition guarantees not only driver comfort and no head-to-tail collisions, but also would permit to extend the string length boundlessly. The studied variable can be either spacing error, control input, position, velocity and acceleration. Such method is adopted in this work and has been widely used in the literature of control design of automated car-following, given thats it provides sufficient conditions to develop string stable interconnected control systems. In [Sheikholeslam and Desoer, 1992a] this approach is used to control formations with and without leader vehicle information. Limitations of the performance over Linear Time Invariant (LTI) with limited communication range is studied in [Middleton and Braslavsky, 2010] and a control framework is proposed in [González-Villaseñor et al., 2007] as a solution to solve this issue. The mathematical interpretation that is taken into account in this work, shares the performance-oriented scope, which is:

$$sup_{\omega}|T_i(j\omega)| \equiv sup_{\omega}\left|\frac{Z_i(j\omega)}{Z_{i-1}(j\omega)}\right| \leq 1\,;\;\; 2 \leq i \leq m \tag{2.1}$$

where $|T_i(j\omega)|$ represents the relation between the frequency-domain variables $Z_i(j\omega)$ of interest of vehicles of index (i) and $(i-1)$ in a string of length m. The term $T_i(j\omega)$ is employed because for Single Input Single Output (SISO), it matches the complementary sensitivity. Note that the Eq. 2.1 results equivalent to the maximum value over all frequency components $\omega > 0$, which matches the ∞-norm of the scoped variable. This encourages the study of such norm at the moment of

designing string stable car-following control systems. Nevertheless, this method remains valid only for LTI systems. More recently, [Ploeg et al., 2014b] proposed an extension of the performance-oriented string stability notion, including initial state conditions in the definition. It consists on the $\mathcal{L}_2$ string stability notion proposed for interconnected non-linear or linear systems, where the expression $\mathcal{L}_p$ refers to the p-norm of a vector or system. A remarkable difference between the proposed definition and Lyapunov-based approaches, is that the former focuses on the system output rather than the states. It is stated that at any time, the difference between the output of the system of index (i) and the output at equilibrium point should not be higher in magnitude than that of the $(i\text{-}1)$ system.

2.3.3.1 Types of string stability

After reviewing the starting evolution of string stability notion, and adding some more recent work contributions [Ploeg et al., 2014a], one can highlight some practical string stability interpretations that have been frequently adopted in the literature.

- String stability margin (SSM). Introduced in [Liang and Peng, 2000], it scopes mixed strings where manually driven and ACC vehicles are randomly positioned in the same string. It proposes to examine the entire stability of the string as a whole, stating that the SSM of vehicle of index (i) corresponds to the inverse of the product of all preceding vehicles' complementary sensitivity $T_i(j\omega)$.

- Semi-strict $\mathcal{L}_2$ string stability or weak string stability. Such definition has been employed mostly in automated car-following control systems where the ego-vehicle considers other vehicles than its predecessor on its control strategy. It proposes that any vehicle that belongs to the controlled string, should not amplify the leader vehicle's output to be semi-strictly string stable. In other words, $|Z_i(j\omega)|_{\mathcal{L}_2} \leq |Z_1(j\omega)|_{\mathcal{L}_2}$ for every $\omega > 0$ and $2 \leq i \leq m$.

- Strict $\mathcal{L}_2$ string stability. In contrast with the aforementioned definition, the strict string stability requires each of the vehicles to not amplify their immediately preceding vehicle's output. Hence it demands a more strict performance requirement–i.e. $|Z_i(j\omega)|_{\mathcal{L}_2} \leq |Z_{i-1}(j\omega)|_{\mathcal{L}_2}$ for every $\omega > 0$ and $2 \leq i \leq m$.

- Bounded string stability. This notion is a relaxed interpretation of the semi-strict string stability that seeks to provide a definition to string stability that is valid for heterogeneous strings. It states the spacing error of any vehicle inside the string formation must not exceed a certain limit value γ_e ($|e_i(t)|_\infty < \gamma_e$; $\forall\, i \geq 2$), regardless the relation between adjacent vehicle dynamics. Such notion was employed in [Shaw and Hedrick, 2007a] and [Shaw and Hedrick, 2007b].

Fig. 2.5 presents an illustration of the different possible behaviors in function of the adopted string stability type. The left one corresponds to a weak string stable formation. It is visible the overall attenuation of leader vehicle oscillations, but from the fifth follower one can see that the peak magnitude are increasing as they propagate. The middle figure shows a string unstable behavior, since every follower is amplifying their immediate predecessor perturbation. Finally, a strict $\mathcal{L}_2$ string stable performance is observed on the right plot, where the initial perturbation introduced by the leader vehicle is absolutely attenuated by each of the vehicles in upstream direction.

Regarding the scoped variable over which examine the system string stability, different interpretations can be found in the literature. Firsts developments stated that for a system to be string

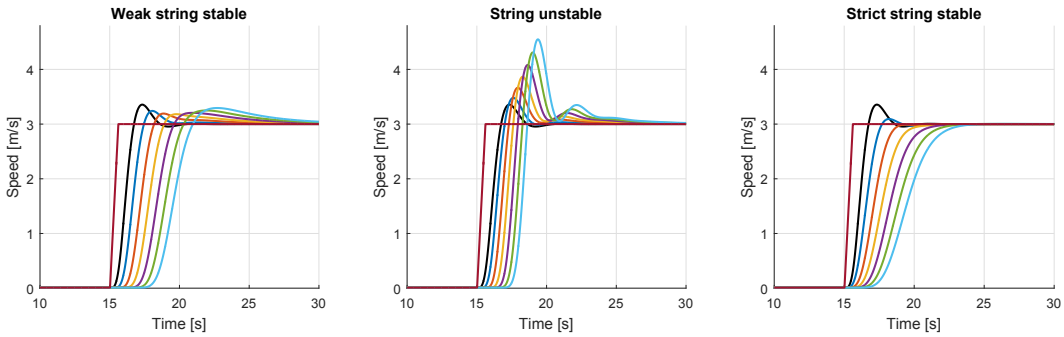

Figure 2.5: Illustration of the most commonly observed string behaviors

stable, "*it is required to ensure that the distance errors do not amplify upstream from vehicle to vehicle in a platoon*" [Swaroop et al., 1994], [Swaroop and Hedrick, 1999]. In the work of [Eyre et al., 1998], authors added to the $\mathcal{L}_\infty$ string stability definition that all vehicles' spacing errors should not only decrease in magnitude as they propagate, but also remain of the same sign than the input error during the disturbance propagation. The spacing error has been taken into consideration as the evaluation variable to study string stability in the early developments of car-following and platooning [Shladover, 1991]. The control effort or input, has been also employed in the string stability analysis in [Ploeg et al., 2014a] over one and two-vehicle look-ahead cooperative strategies.

Even if in the literature distance errors, control effort, position, velocity and acceleration have been employed to study the string stability, the first two are actually limited to analysis over homogeneous strings. When vehicles have either different dynamics or control configuration; the distance errors and control efforts evolve differently than the vehicle position, velocity or acceleration [Wang and Nijmeijer, 2015a]. This is due to the fact that spacing errors and control action variables are strongly related to each individual control structure and vehicle dynamics. Hence, in more recent works and in most of literature of heterogeneous strings, the vehicle position, velocity and acceleration are employed as the string stability criteria [Naus et al., 2010], [Liang and Peng, 2000], [Bose and Ioannou, 2003]. In this work, the strict $\mathcal{L}_2$ string stability criterion is adopted with $Z_i(j\omega)$ as the position of vehicle of index (i) in the frequency domain. This also agrees with the conclusions on [Naus et al., 2009] for string stability analysis over ACC and CACC applications.

When V2V communication links are added to the control structure of each vehicle, not only shorter inter-distances are possible but also faster reaction towards state perturbations in the leader vehicle, allowing an improved string stability. For this reason platooning, and more recently cooperative driving, have attired extensive research demonstrating promising results to solve road mobility issues.

2.4 Cooperative driving

The incorporation of communication links over vehicular systems has opened the doors for the introduction of different ITS, assisting and optimizing the infrastructure-vehicle and vehicle-vehicle interaction. The term cooperative driving comes from the idea of having connected road agents, making automated vehicles able to collaborate with their environment (either infrastructure or other vehicles) to drive and interact more effectively and efficiently. Some of the possible benefits of cooperative driving are: cooperative collision avoidance, warning of hazardous situations, automated traffic negotiation for cooperative maneuvers, CACC formations for enhanced traffic flow

and also platooning maneuvers for aerodynamic drafting and lane capacity increase [Shladover, 2017]. The cooperation may not only be for a single-lane string of vehicles, but can also include more complex environments such as intersection management, lane change assistance [Swaroop and Yoon, 1999], highway on-ramp handling [Rios-Torres and Malikopoulos, 2017], overtaking assessment, among other possible road scenarios. In fact, a framework has been proposed for the first time in [Burger et al., 2017] that assess and rate how cooperative is a driving behavior. This demonstrates the growing interest on increasing communication and cooperative systems penetration rate over urban and highway mobility. Cooperation has also gained attention through the incorporation of Infrastructure-to-Vehicle communication links, where the infrastructure communicates variable speed limits to improve bottleneck traffic efficiency and arterial coordinated start. Fig. 2.6 pictures an example of a cooperative driving system.

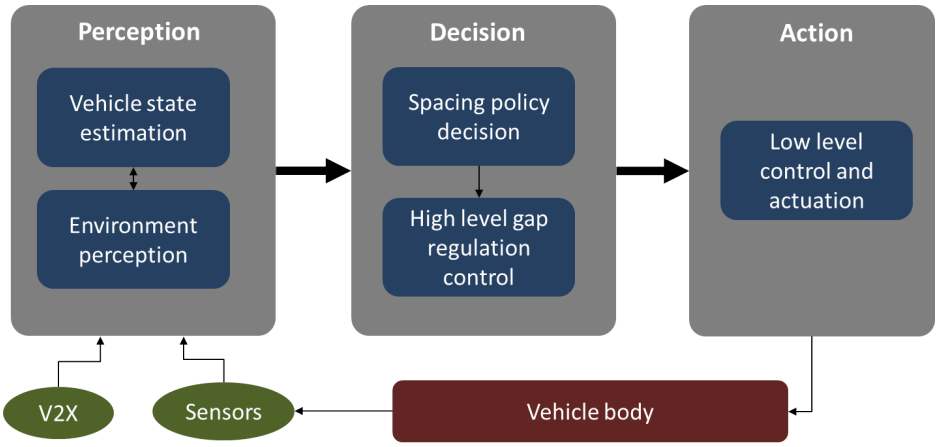

Figure 2.6: General architecture of a cooperative automated vehicle

The architecture is composed by three main blocks. Within perception, both the ego-vehicle and the surrounding vehicles states are estimated. For the latter, Vehicle-to-Anything (V2X) communication links are employed to extend the vehicle perception for variables that are not measurable with exteroceptive sensors. The decision block is composed by the choice of the desired spacing policy in function of the detected situation–e.g. merging, splitting, car-following–and the gap-regulation structure that generates the reference speed. This stage profits from the V2X extended perception to yield enhanced car-following performance through cooperation. Finally, the action block is in charge of commanding the actuators in function of the current ego-vehicle state and the received reference longitudinal speed.

The fundamental applications based on cooperative driving are the CACC and platooning. CACC systems have gained a lot of attention in recent years for its potential to increase traffic throughput and yield a more efficient and safe driving. Platooning adopts the same principles of CACC, but intends to minimize fuel reduction by aerodynamic drafting, which requires keeping constant clearance policies with dedicated lanes and restricted interaction with other vehicles [Shladover et al., 2015]. One can see then platooning as a special application of CACC techniques, mainly aimed for heavy duty trucks.

2.4.1 CACC

The widespread employment of ACC has motivated the deployment of automated car-following techniques. Research advances led to the idea that wireless links between ACC-equipped vehicles could significantly increase the benefits of car-following systems, yielding the CACC technique. It proposes to take advantage of V2V-received data to anticipate changes in forward vehicles motion before they are perceived by the on-board sensors. This permits to have significantly faster reactions towards oscillations arriving from downstream. This feature has encouraged CACC systems incorporation over traffic environments, which motivation can be better understood through their objectives [Shladover et al., 2014]:

- Increase the traffic throughput allowing shorter inter-distances among vehicles in the same lane, without losing car-following stability
- Reduce the risk of rear-end collisions, by increasing the reaction speed to forward vehicles' changes and capacity to communicate with forward vehicles
- Improve driver comfort not only serving as an ADAS, but also damping the propagated string disturbances
- Reduce the fuel consumption by improving traffic flow and aerodynamic drafting if distances are close enough

An illustration of a common control structure employed in CACC systems is provided in Fig. 2.7, where it is visible the main differences and advances from cruise control to ACC, and finally to CACC.

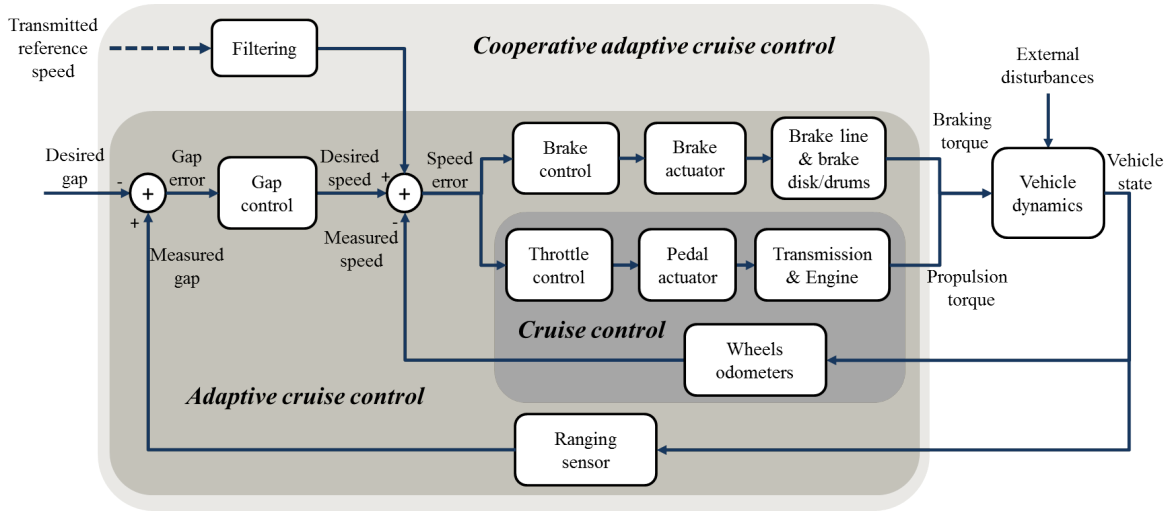

Figure 2.7: Control structure of a CACC-equipped vehicle

Even if for ACC systems, consequences over traffic flow are still unclear (they highly depend on road density and drivers' preferences), it has been widely demonstrated that adding communications in the gap-regulation control lead to enhanced performance in terms of safety and string stability [Zwaneveld and Van Arem, 1997]. Benefits of CACC systems over simulation and

on-field experiments have been investigated in the literature. In [Ryus et al., 2011], traffic capacity increase was demonstrated outperforming manual driving from 2000 to 4200 veh/hour/lane when having 100% CACC market penetration rate. Microsimulations with car-following models of CACC [Van Arem et al., 2006] in highway merging scenarios demonstrate improvements over traffic flow stability, average speed and slight enhancement of traffic throughput. Subsequent studies [Schakel et al., 2010] demonstrated CACC capabilities to outperform human drivers on mitigating the effects of shockwaves over large scale traffic, however near 50% of penetration market rate is required to observe the promised improvements, which agrees with similar conclusions obtained on [Shladover et al., 2012] claiming that high CACC penetration rate can increase traffic capacity. More recent studies over CACC models on a macroscopic level of on-ramp scenarios show that even with a fraction of 30 % of CACC-equipped vehicles, traffic congestion can be reduced and capacity increased [Delis et al., 2016]. In [Melson et al., 2018], a more dynamic and realistic study of CACC effects on medium and large scale traffic is presented. It concludes that high penetration rate of CACC systems can significantly reduce traffic congestion, but low deployment rates would cause an increase on the travel time.

Not only the traffic throughput has been demonstrated to be increased with CACC, but also the risk of rear-end collisions as can be expected since CACC increases the reaction speed towards hazardous situations. In [Li et al., 2017c], IDM models are adapted to CACC behaviors and analysis is done to evaluate the rear-end collision risk (employing the time-to-collision parameter), showing significant improvement at high market penetration rate.

When increasing the speed, the air resistance force becomes more and more significant producing higher losses, which is quadratic function of the vehicle speed. Nevertheless, when short inter-distances are kept, aerodynamic drafting is possible thus reducing losses not only for the follower vehicle but also for the predecessor. This has a great impact due to its potential on reducing not only the travel cost for fuel consumption but also the CO_2 emissions, which is of the main causes of nowadays contamination and global warming. To extend the energy saving capabilities, the platooning concept has been introduced in the 1990's to explore its potential benefits on private vehicles, but mostly on heavy duty trucks.

2.4.1.1 Platooning

Dedicated lanes and tightly coupled string formations are required to effectively carry out platooning. It consists on the formation of groups of reduced number (normally between two and five) of vehicles named platoons. The vehicles that compose the platoon travel on the same lane and direction with almost no interaction with other lane vehicles–i.e. no split or merge handling. The platoon members account with CACC capabilities and require low latency DSRC to be able to maintain stability at high speeds with constant clearance–i.e. fixed spacing between vehicles. The aerodynamic drag losses are faced by vehicles that drive at high speeds, due to the pressure differential between its front and rear surfaces, where high and low air pressure fields are experienced respectively. Small gaps between following vehicles can not only reduce the high pressure in the follower, but also increase the pressure in the rear part of leader vehicle, mitigating the drag created by the vacuum (see Fig. 2.8). For platoons with more than two members, the middle vehicles are the ones that earn the most benefit from aerodynamic drafting, since the drag is reduced both in its front and rear surface. Generally, it has been demonstrated that the shorter the gaps, the highest the fuel savings result for all platooning vehicles.

Even if this strategy is employable in any type of road mobility vehicles, platooning for heavy duty trucks has attracted the most attention for its economical benefits for fleet management and mostly aimed for highway environments with low interaction. On-field experimental results over

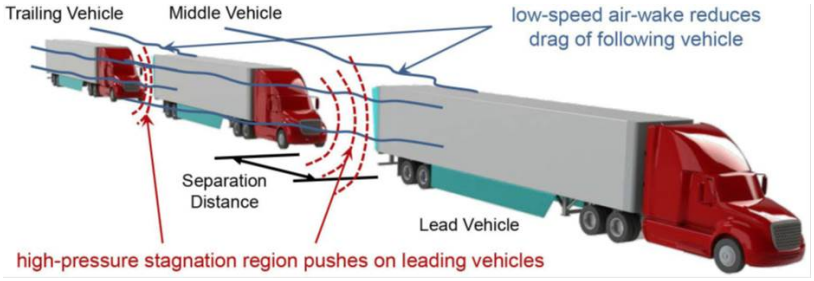

Figure 2.8: Schematic of a three truck platoon, demonstrating pressure variation areas. Source [McAuliffe et al., 2018]

two tandem trucks [Browand et al., 2004] show that savings between 8 and 11% can be achieved. Other extensive evaluation was done in [McAuliffe et al., 2018] on energy savings influence of truck platooning, showing a combined fuel saving of 14.2% with the middle vehicle showing the most savings among the three vehicles during the maneuver, thus providing design guidelines and encouraging future investment on these technologies.

Along the years, significant effort has been deployed towards investigating the possible applications and benefits of CACC and platooning techniques. A review of the different research and industrial projects is presented below for better understanding of the cooperative driving evolution.

2.4.2 Literature survey

Being of the most promising ITS, CACC and platooning strategies have been focus of research and developments worldwide. Truck platooning research has been increasing in the last 25 years, due to its demonstrated capabilities to improve fuel economy using constant clearance strategies and low latency DSRC. On the other hand, CACC efforts are more recent and have been more focused on passenger vehicles and considering more flexible interactions and maneuvers. A timeline of research projects is presented in Fig. 2.9.

2.4.2.1 PATH

The Partners for Advanced Transit and Highways (PATH) program is one of the first institutional collaborations between public and private institutions, seeking to apply advanced technologies to improve significantly highway capacity, reducing traffic congestion and energy consumption. Prior tests of PATH research consisted on studying kinematic behavior of platoon driving to increase highway capacity, which was subsequently validated with a four-car platoon holding 4 meters gaps in 1994. PATH also collaborated with the National Automated Highway Systems Consortium (NAHSC), General Motors, Delphi Automotive an Hughes Aircraft to perform the Demo '97 [Rajamani and Shladover, 2001] in 1997. It consisted in a 8-vehicle platoon scenario over dedicated lanes in the highways of San Diego, being one of the biggest AHS demonstrations ever done. They successfully demonstrated the benefits of tightly coupled platooning systems in terms of traffic throughput, travel time and energy consumption. Vehicles were equipped with complete automation, low latency DSRC links with the leader vehicle, vision-based lane detection and magnetic marker sensing for lateral guidance. A radar was used for measuring inter-vehicular distances. Platoon formation and decoupling were also considered at the beginning and ending points respectively.

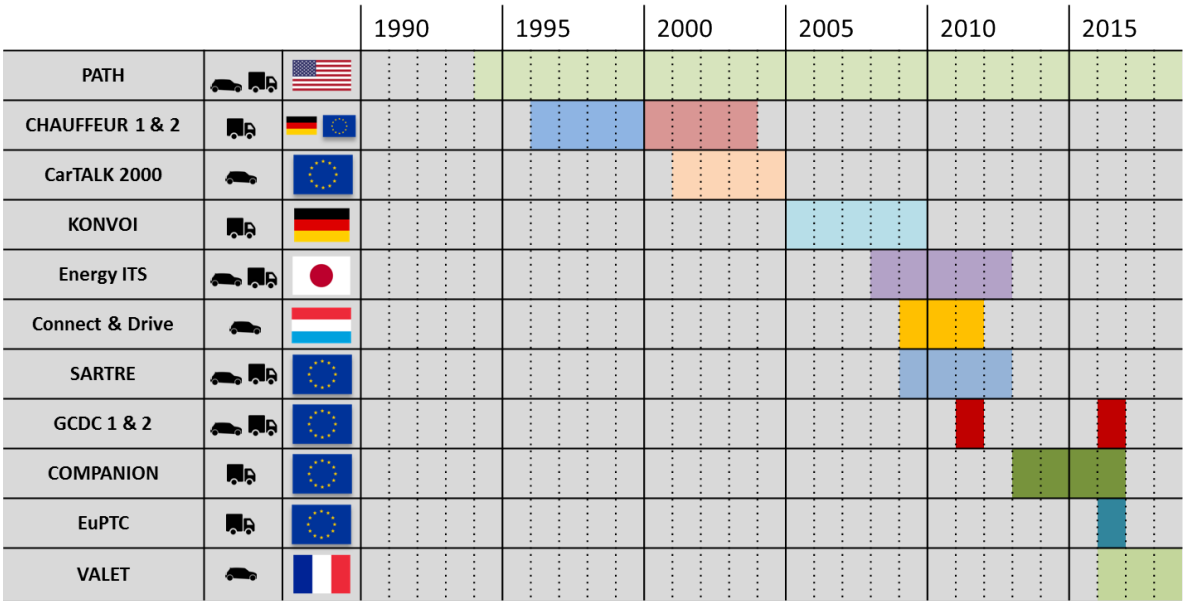

Figure 2.9: Timeline of worldwide projects focused on cooperative driving, CACC and platooning; with their name, vehicle types, countries that participated on it and duration

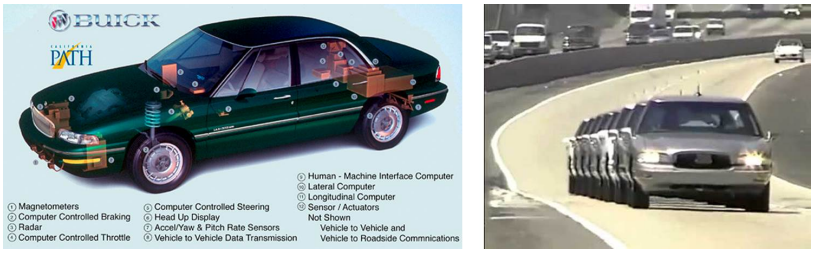

Figure 2.10: Platoon demonstration in PATH Demo '97. Source [Shladover, 2009]

Platooning maneuvers were resumed in 2003 with two-truck tests at 3 m gaps and three-truck tests at 4m spacing in 2011 and 2017 as well, showing platooning technical feasibility and an energy consumption reduction of 5% for the leader vehicle and from 10 to 15% for the followers [Browand et al., 2004]. PATH research lines have also evolved to the consideration of more complex scenarios as cut-in cut-out maneuvers [Milanés and Shladover, 2016], *ad hoc* platoon clustering, string stability and CACC behavior modeling [Milanés and Shladover, 2014]. Several works have been done to evaluate the impact of CACC systems in terms of human factors through extensive on-field tests, having different drivers and requesting their feedback on time gap preferences and system trust [Nowakowski et al., 2010a] on conventional vehicles and trucks [Yang et al., 2018]. More recent work focuses on high level platoon coordination and technology feasibility over trucks for energy consumption reduction.

2.4.2.2 CHAUFFEUR I & II

The CHAUFFEUR program was carried out by the European Commission in two phases, CHAUFFEUR 1 and 2 [Fritz et al., 2004]. In these projects, the concept of "electronic tow-bar" was in-

vestigated for closely coupled trucks over highways, providing good results and technical advances for truck platooning applications. Developments include an integrated system compatible with all partners' platforms, having as features: vision-based lane recognition, radar-based obstacle detection and ACC longitudinal layered control for distance keeping with a lateral lane keeping system. The overall architecture suggested to have automation levels of 2 and 4 [SAE, 2016] for the leader and follower trucks respectively, being the driver on the leader vehicle responsible for operational surveillance. At the end of the first phase, the project lacked on the management of platoon coupling from a logistic point of view. Such problem was targeted in the second phase, relying more on cooperation with the infrastructure and enabling platoon coupling and decoupling via V2V links, while increasing the platoon size from two to three trucks. Differentiation between constant clearance for fully automated trucks and constant time gap for semi-autonomous vehicles was also added.

2.4.2.3 KONVOI

The KONVOI project [Kunze et al., 2010] was founded by German's Federal Ministry of Economics and Technology in collaboration with RWTH Aachen University, industry and public institutions. Its main objective was to explore potential benefits of electronically coupled truck convoys over traffic capacity and fuel economy. One of its scenarios, called driver organized truck platoons, targets the systematic grouping of compatible trucks suggesting that drivers should schedule the meeting place, destination and vehicle features employing a Driver Information System (DIS). High interaction with the driver through HMIs is present over all platforms, so the platoon negotiation, joining and splitting could be triggered by the driver through the DIS. From the implementation point of view, the leading vehicle is driven manually while the followers account with a lateral control system that considers lane relative position and leading vehicle lateral offset. For the longitudinal axis, each follower has an embedded ACC system commanded with a reference acceleration given by the gap regulation control, which also employs V2V communication and radar, camera and LiDAR in the loop. The KONVOI system was tested in motorways at speeds between 37 and 50 mph, achieving fuel savings up to 21% with 10 meter gaps between trucks inside platoons of maximum five members.

2.4.2.4 Energy ITS

Started in 2008, the Energy ITS project investigated the benefits of truck platooning for energy saving and global warming prevention through ITS technologies. The development was carried out over one automated leader vehicle (level 2), as well as three fully autonomous heavy duty trucks and one fully automated light truck. The proposed system accounted with features as vision-based lane mark detection, LiDAR and 76 GHz radar for obstacle detection and spacing gap measurement. Platforms were also linked through 5.8 GHz DSRC and infrared to exchange data as reference velocity, acceleration, braking signal, among others. Even if the main objective was fuel saving demonstration, interaction with other road users, normal/harsh braking and driver interventions were also targeted later on in the project. Experiments included tests at 80 km/h with interdistances as short as 4 meters, observing a reduction in the drag coefficient up to 50% for the middle and 20% for leader vehicle. In [Tsugawa, 2013], it is stated that the project outperforms previous developments in reliability for future possible market introduction, while little detail was given on how platoons and drivers responsibilities were organized. A method to evaluate CO_2 emissions in platooning was also a contribution of this project (see Fig. 2.11). Simulations were carried out, whose results show that when penetration rate reaches 40%, reductions of 2.1 and

4.8% are seen with gaps of 10 and 4 meters respectively.

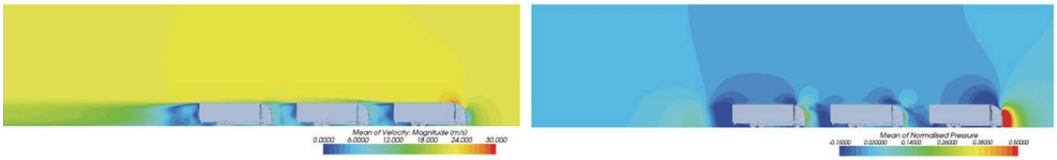

Figure 2.11: Computational fluid dynamic simulation of a three-truck platoon at 80 km/h with a 4 meters gap. Source [Tsugawa, 2013]

2.4.2.5 Connect & Drive

In the frame of the Dutch founded project Connect & Drive [El Ghouti et al., 2009], industrial, public and private academic entities gathered efforts to accomplish more performing CACC systems. Solutions for shockwave effects mitigation (due to possible cut-in or exit) and traffic congestion damping are sought, using ACC, CACC and a human-in-the-loop cooperative cruising control. The consortium is more focused on individual mobility rather than high scale public mobility deployment. One of the targets is to deal with platoon creation, modification and driving under real traffic disturbances. With respect to the shockwave effect, CACC solutions were developed with more performing engine/brake control systems showing promising results in terms of string stability. Several simulations, hardware-in-the-loop tests and real platforms experiments were carried out to validate the proposed technologies. The project demonstrated the advantages of using CACC together with the infrastructure, showing as well significant improvements over manual or ACC conventional traffic. Technologies were tested on seven Toyota Prius in Helmond, Netherlands; demonstrating the string stability enhancement during traffic disturbances.

2.4.2.6 SARTRE

Safe Road Trains for the Environment (SARTRE) [Chan et al., 2012] is an European Union project that included organizations from Spain, Germany and Sweden; aiming to develop strategies and technologies for public highway platooning. Its objective was to demonstrate the feasibility of mixed platooning and its benefits in terms of safety and fuel consumption using already commercial technologies. A less technical but fundamental objective, was the conception of a coordination/operation system that manages the platoon formation and its correct deployment over the highways, taking into consideration limited leader drivers available to perform platooning.

In such framework, a cooperative system was proposed where the leader vehicle is driven manually by a trained professional driver and the followers account with V2V links and sensors, as well as an embedded ACC and lateral automation for gap regulation and leader lateral positioning following respectively. The proposed longitudinal control is able not only to perform speed changes, but also to change the target gap while handling harsh braking and platoon joining. Results were obtained at spacing gaps between 3 and 15 meters, showing energy savings from 7 to 15%. In this project, mixed type of vehicles were scheduled in the same formation for the first time, showing promising results that encourage industrials and academic agents to put efforts on platooning development and deployment.

2.4.2.7 Grand Cooperative Driving Challenge I & II

The first edition of the Grand Cooperative Driving Challenge (GCDC) [Ploeg et al., 2012] was organized by TNO and it was inspired on the U.S. Defense Advanced Research Projects Agency (DARPA) Challenge, gathering nine teams from Europe, both from academy and industry. For the first time, the notion of cooperation was being taken into account as a judgment criteria in the system evaluation besides the technical performance. The main purpose of the first GCDC was to encourage the deployment of cooperative systems, specially real-time CACC over mixed strings of vehicles. The demonstration of traffic throughput enhancement and the system feasibility were of the main purposes of this initiative. Fault tolerancy or fail-safety capabilities, wireless communication for inter-vehicular interaction and the real time structure of each competitor was examined. Urban and highway scenarios were part of the evaluated use cases, analyzing mainly the vehicles' longitudinal behavior. An illustration of GCDC 2011 is showed in Fig. 2.12. Some issues were detected concerning data losses handling and fault tolerance, as well as the lack of more complex and realistic scenarios.

Figure 2.12: Illustration of the highway use case of the mixed platooning of GCDC 2011. Source [Ploeg et al., 2012].

For this reason, in the second edition of the GCDC [Ploeg et al., 2018], three new use cases were proposed for the teams to manage: platoon merging, intersection with assigned vehicles priority and emergency vehicle scenarios. As in the first edition, the focus remained on encouraging not only V2V but also V2I cooperation for an enhanced and optimal traffic management, but considering more realistic traffic situations. Conclusions of such challenge are: 1) reliable communication links are of fundamental relevance to implement cooperative maneuvers, 2) more studies are required to make systems more robust and reactive to communication dis-functioning.

2.4.2.8 COMPANION

Cooperative Mobility solutions for supervised platooning, or COMPANION EU project [Eilers et al., 2015], focused on platooning capabilities for fuel economy, safety and traffic capacity increase on heavy-duty trucks. It proposed a platoon management system composed by an off-board platform for platoons coordination, together with an on-board operational system for platooning maneuvers and interfaces between them. Other objectives as legislation and standardization of platooning systems are aimed, as well as demonstrations over European roads. For carrying this out, a three-layer approach is proposed that consists on strategic, tactical and operational layers; from high to low hierarchy. Human factors, platoon coordination and information interfacing, are scoped in the frame of this project, rather than proposing technical solutions for more performing platoon strategies. It has been concluded that vehicle-infrastructure coordination with a distributed net-

work is essential to guarantee the correct convergence and coordination of heavy-duty trucks on a platoon formation. Results were dependent not only on the market penetration rate, but also on the assumed platoon speed; showing up to 9% fuel savings at the best.

2.4.2.9 European Truck Platooning Challenge

The European Truck Platooning Challenge initiative [Eckhardt et al., 2015] took place as a showcase in 2016 from different European locations heading to the Rotterdam port. Its main objective was to gather several authorities and manufacturing entities from different countries (Germany, Netherlands, Belgium, Sweden and Denmark), to highlight the importance of cross border smart mobility, in this case through a major truck platooning demonstration.

Figure 2.13: Photo of Volvo Trucks platooning during the showcase.

Another purpose of such initiative was to encourage the creation of cross border corridors where truck platooning is allowed. Special attention was put to the legal, logistic and human factors issues of this technique, due to the high interaction between National Road Authorities, OEMs and European entities. A benchmark for exemptions was another result of such showcase, given that each of the OEMs had to apply for exemptions at each country they were going to cross. From the technical point of view, Society of Automotive Engineers (SAE) automation level 1 [SAE, 2016] was applied with only longitudinal actuation through CACC capabilities, steering was responsibility of each truck driver. All vehicles received V2V commands from the platoon leader vehicle, aiming a 0.5 seconds time gap under a leader-following topology. Tests were carried out at daytime with conventional driving conditions.

2.4.2.10 VALET

The VALET project[1], founded by the french National Research Agency (ANR), focuses on cooperative driving solutions to solve car-sharing distribution problems. It proposes to optimize the redistribution process by equipping vehicles with perception, automation and V2X capabilities, making platooning maneuvers feasible with a manually driven leader that is responsible of taking them to a parking place or to another service station for charging and posterior distribution. A fleet operator is in charge of managing optimally the drivers' operation in function of the stations requirements and locations. Finally, automated parking is also suggested once the platoon decouples at destination and each vehicle goes to its parking slot assigned by the parking operator. The project aims also to propose a system to encourage the electrical vehicles employment and a smarter usage of road transport inside densely populated cities. Another cooperative driving issues that are covered are pedestrian interaction, infrastructure cooperation, among others; relying on communication links with other road agents.

[1]http://www.agence-nationale-recherche.fr/Project-ANR-15-CE22-0013

2.4.2.11 Industrial deployments

In recent years, increasing interest on platooning has encouraged industrial entities to start investing in cooperative and automated car-following solutions. Most of efforts have been deployed to develop improved systems for truck platooning. Energy saving capabilities over tightly coupled homogeneous truck formations are the main target of industrial proposals. This motivation is shared for example by Scania, focusing more on minimizing fuel consumption, being the largest cost for fleet owners. This company made collaborations with The Royal Institute of Technology (KTH) and the Swedish government, to deploy two main projects called: Distributed Control of a Heavy Duty Vehicle Platoon and iQFleet. Both projects showed good results with road tests using on-board sensors and V2V communications in the platooning system. Another initiative was founded in 2011 named Peloton Technology[2]. They proposed to implement their so-called Peloton system, which permits a conventional heavy duty truck to perform platooning with other compatible vehicles. The company currently states that truck platooning will be the first semi-autonomous system implemented in public roads within a decade from 2017, through a recent collaboration with Omnitracs. Peloton Technology is constantly performing demonstration over highways, focusing on driver-vehicle interaction and V2V DSRC between vehicles. A picture of two trucks equipped with the Peloton system is presented in Fig. 2.14[3] performing platooning on US highways.

Figure 2.14: Image of two platooning trucks performing on-road tests

Another start-up named OTTO surged in recent years (acquired in 2016 by Uber), proposing a solution for safer and more fuel-efficient commercial platooning trucks in the US. It is important to highlight the amount of industrial agents that participated in the aforementioned European Truck Platooning Challenge 2016. Companies as Volvo Trucks, Scania, DAF Trucks, Daimler, MAN Trucks and IVECO showcased at this demonstration, proving the interest and benefits of platooning over mixed strings of automated and connected trucks. Although trucks have been the main employed vehicle for platooning initiatives like Toyota Fuel-Efficient CACC, or TNO research[4] in the Netherlands, have demonstrated good results in terms of fuel efficiency, CO_2 emissions reduction and traffic throughput increase.

[2]https://peloton-tech.com
[3]http://www.ttnews.com/articles/peloton-demonstrates-platoon-system-michigan
[4]https://www.tno.nl

2.5 Discussion

Recent advances on embedded vehicular technology and the increase of urban mobility issues, have encouraged the research and development on systems based on longitudinal automation, specially automated car-following. Analysis of traffic issues started with the modeling of the human driving way to survey inter-distances, resulting on several different car-following models that contributed to understand the causes. Longitudinal automation and ranging sensors later permitted the conception of reference car-following models, dictating the ideal behavior to overcome the different traffic issues. Although the introduction of ACC systems started the deployment of car-following systems on commercial vehicles, studies have demonstrated that ACC does not provide significant benefits in terms of traffic capacity and stability with respect to human driving. Instead, they are rather employed only as comfort systems in medium- and high-end vehicles. For this reason, most recent research and developments on the state-of-the-art focus on the cooperation via V2V communication links, together with longitudinal automation and ranging sensors, as stated in [Shladover et al., 2015]. This agrees with the efforts deployed by institutions as the European Commission[5] towards introducing V2X in public roads.

Along this chapter, a literature review of car-following evolution and its concepts is provided, starting from the models that describe the human driving in terms of inter-distance keeping. A review of the state-of-the-art reference car-following models, or spacing policies, has been presented with a comparison of the most relevant strategies, their advantages and drawbacks. Afterwards, the notion of string stability has been described in detail, highlighting its correlation with the spacing policy and importance when designing a car-following system. The types of string stability have been also defined, with their context over which they have been employed. The most consistent definition for string stability (the one adopted for this work) results the strict $\mathcal{L}_2$ string stability introduced in [Ploeg et al., 2014b], since it refers to the immediate state variable propagation from the preceding to the ego-vehicle, being the vehicle position, speed or acceleration the variables of interest [Wang and Nijmeijer, 2015b].

The notion of cooperation on car-following structures is discussed through the definition of CACC and platooning techniques. Numerous institutions and research projects that have put efforts on the development of cooperative systems for solving mobility issues have been revised. Worldwide leading institutions as the California PATH, TNO, EU-funded research projects, among others; have demonstrated the potential of CACC and platooning to solve road mobility problems. Recent studies have been presented that analyze the impact of CACC and platooning over traffic capacity [Van Arem et al., 2006], stability [Schakel et al., 2010], fuel consumption [Shladover et al., 2012] and human acceptance [Nowakowski et al., 2010b, Nowakowski et al., 2010a]. These works have agreed that cooperative automated car-following is a promising solution for traffic jams, shockwaves, rear-end collisions and CO_2 emissions.

Although the notion of string stability for car-following is more than 20 years old, a consensus on the type of string stability that should be adopted is starting to be set on the literature. Hence, current and future developments must take into consideration this notion within the design objectives, given that it defines the traffic flow behavior and its evolution. The traffic heterogeneity is a subject that has been recently scoped (in GCDC 1,2 and SARTRE), which means that there is still a long path to achieve the same results that have been obtained for homogeneous strings. To target this issue, communication capabilities appear to be the promising feature that is required to design systems that are robust to string heterogeneity. Some open challenges can be outlined

[5] https://ec.europa.eu/research/participants/data/ref/h2020/wp/2018-2020/main/h2020-wp1820-transport_en.pdf

from the state-of-the-art review.

- Almost all approaches that have been proposed for CACC and platooning have been designed and validated over highway scenarios. The design of a cooperative car-following architecture that is able to bring the same benefits to urban environments is needed. This represents a major challenge, given that when driving on urban scenarios, the risk of collision with VRU and a platoon division increases.
- Most of spacing policies that have been proposed target specific scenarios or performance metrics, which encourages the design of a general purpose safety-aware framework that focuses on the time gap manipulation. Further investigation is required on the trade-off that exists between shortening the inter-distances/time gap and improving the string stability.
- The major part of current developments assume same dynamics in all vehicles in the string. This assumption restricts the formation of CACC strings of vehicles of different brand, type or dynamics. In other words, it is necessary to design cooperative automated systems that permit the widespread usage of these solutions without losing string stability, degrading traffic performance or leading to unsafe operation.

As a conclusion of the presented review of the evolution of automated car-following, one can state that the interest on investing in these type of solutions has grown and spread significantly. In fact, first significant deployments of automated vehicles are expected to be of platooning trucks, given their proven fuel efficiency and traffic flow increase. The incrementing incorporation of ADAS in heavy duty trucks, added to the imminent introduction of communication networks in vehicular environments, encourages to think that cooperation-based techniques as platooning are the closest to be adopted worldwide. Further approaches which fundamentals rely on cooperation are expected to focus on urban scenarios problems as intersection handling, lane merging, among others.

Focusing on cooperation for car-following, the robustness in the gap-regulation task performance is of major importance given the amount of factors that influence the system behavior–e.g. vehicle dynamics change, non-linearities, sensor/communication failures. Another major issue that is starting to be approached and gaining attention is the feasibility of multi-brand or heterogeneous string driving, which would significantly increment the interest among industrial and governmental entities to invest in cooperative driving solutions. In addition, strict $\mathcal{L}_2$ string stability has been becoming the main objective of every car-following system, given that it permits to represent the entire string performance in terms of safety, stability and actuation effort. Its fulfilment also permits to extend boundlessly the number of vehicles in a platoon without meaning any risk for high-index vehicles. Finally, reliability of the communication links and ranging sensors are important to guarantee the desired cooperation benefits, for which work has to be done by technology providers and vehicle manufacturers.

Chapitre 3

Structure de contrôle pour le car-following

Below is a French summary of the following chapter "Car-following control structure".

Le chapitre comprend la définition du cadre de cette thèse, le structure de contrôle car-following dans laquelle les différents algorithmes conçus seront développés. Des exemples d'architectures de contrôle qui ont été proposées dans la littérature sont décrits, ainsi que les différents topologies de communication utilisés lors de l'emploi de la coopération avec du contrôle car-following.

La structure proposée, basée sur une approche en cascade, est décrite en détail. Ensuite, la conception du système feedforward pour le CACC et de la couche de contrôle bas niveau est mentionnée, particulièrement la manière dont les actionneurs sont gérés pour atteindre le suivi de la vitesse de référence optimale. La structure est améliorée en proposant un algorithme basé sur une machine d'état capable de gérer l'interaction avec des usager vulnérables de la route et retourner à l'état d'équilibre. Finalement, une nouvelle politique d'espacement adaptable pour l'ACC et le CACC est proposée et expliquée en détail. Celle-ci a pour objectif la référence aux distances que permettent l'augmentation du taux de trafique, tout en garantissant la stabilité du convoi et la sécurité. Une discussion sur les différents contributions de ce chapitre est fournie.

Chapter 3

Car-Following Control Structure

3.1 Introduction

As discussed in the chapter 2, drivers maintain inter-vehicular distances in different ways and the extensive literature over car-following modeling demonstrates its complexity. Including automation over the vehicle actuators and on-board sensors permits to define the desired behavior for the spacing gap regulation task. This allows to target solutions that improve traffic throughput, safety, comfort and fuel efficiency; thus highlighting the impact that the correct definition of the adopted spacing policy has over traffic issues. To effectively implement automated car-following over a string of vehicles, not only an inter-distance management law is required, but also a system that is able to track the preceding vehicle and regulate in real time the spacing gap commanding the vehicle actuators. A control structure is employed for this task, which is designed in function of the performance requirements. Extensive literature over control structures for automated car-following can be found that propose different control techniques.

This chapter presents the adopted control structure for car-following, which set the framework for the development of control algorithms that satisfy different design objectives. The rest of the chapter is as follows: firstly, a review of the automated car-following structures and topologies is provided with examples and descriptions. This motivates the proposal of the employed control structure, which is detailed afterwards with the longitudinal dynamic model of the vehicle. The design of the inverse feedforward system and the low level control layer are described. Actuators management and control design objectives for the reference speed tracking task are discussed later on, which constitute the low level control system. The enhanced car-following structure for driving on urban environments is presented, whose state machine and all composing algorithms are detailed. A novel safe full range spacing policy for improving traffic flow and string stability is presented with its design procedure. Finally, a discussion is provided about the contributions of this chapter.

3.2 Review of automated car-following structures

From the early advances towards functional ACC systems to recent CACC approaches, industrial and research agents have employed numerous control techniques to for the gap regulation task. Some of these approaches are listed below:

3.2.1 Control strategies

- Linear Quadratic Regulator (LQR): Using optimal control, LQR-based approaches seek a LQ optimally local controller to act over the states that are fed back. In [Stankovic et al., 2000], an overlapping LQR control framework is proposed for decentralized command of a platoon together with LQ Gaussian observers.

- Fuzzy logic-based: This strategy seeks to imitate how human drivers perform car-following in function of variables of interest, based on the fuzzy logic theory. In [Pérez et al., 2013], a cooperative control solution is proposed on a longitudinal low level structure showing car-following capabilities of fuzzy logic-based control. Fuzzy inference, a rule set for the ego-speed, relative speed and spacing were employed.

- Robust control: Strategies based on robust regulation have been also utilized for car-following control to guarantee not only desired performance for the nominal model, but also the rejection to uncertainties in the model. For instance, in the work of [Ploeg et al., 2014a] feedforward and feedback controllers are designed using $\mathcal{H}_\infty$ optimization strategies. In [Gao et al., 2016], a similar approach is proposed to deal with vehicle dynamics heterogeneity.

- Sliding mode control: It is based on the assumption that the desired equilibrium state where the system should remain, is interpreted as a sliding surface between different structures. The designed controller must ensure the exponential asymptotic convergence to such sliding mode over the surface. For instance, [Lu et al., 2002] proposed a sliding mode approach employable with both ACC and CACC techniques, employing a sliding surface as the equilibrium point where the relative speed and spacing error are zero.

- Model Predictive Control (MPC): This strategy proposes to locally optimize the control input within a finite time horizon, predicting the vehicle states evolution using a model. Global asymptotic stability is ensured in this kind of approach and it results also convenient under constrained performance. The selected cost function strongly defines the behavior of the system, usually for car-following applications it is desired to minimize the spacing and speed error with respect to the preceding vehicle [Stanger and del Re, 2013]. In [Dunbar and Caveney, 2012], a distributed control framework is proposed where each vehicle generates its own set of optimal reference states over a receding horizon and transmits them to its follower through V2V to be further employed.

- Feedforward/feedback with classical control: Constitutes one of the most employed structures. When in ACC mode, it proposes to correct the spacing error with a feedback classical controller that commands directly over the vehicle actuators. If V2V communication links are available, information from forward vehicle(s) is employed to further improve the ego-vehicle response towards disturbance propagations. It constitutes a two degree-of-freedom structure composed by a feedforward and feedback controller, providing flexibility and the capability to fulfill different performance requirements. This strategy has been employed to ensure string stability for ACC [Moon et al., 2008] and CACC-equipped strings [Milanés et al., 2014].

The selection of a control structure not only depends on the desired performance but also on the available communication links between the string vehicles. In function of the communication topology, some control structures are more compatible to manage one or more arriving variables to be employed in the control loop. For this reason, one can find that different network topologies have been employed in the cooperative driving state-of-the-art.

3.2.2 Cooperative driving topologies

The improvement of communication technologies in recent years has encouraged not only information exchange between vehicles, but also the employment of other vehicles' variables inside the ego-control structure showing good results. The solutions based on cooperation augment sensor-based perception, which for automated car-following permits to employ unmeasurable variables in the control loop as reference control variables transmitted through V2V links. It has been widely proven that this enhances reaction capabilities and car-following stability, even for shorter inter-distances. V2V communication links have been employed in the form of different topologies, which are described below:

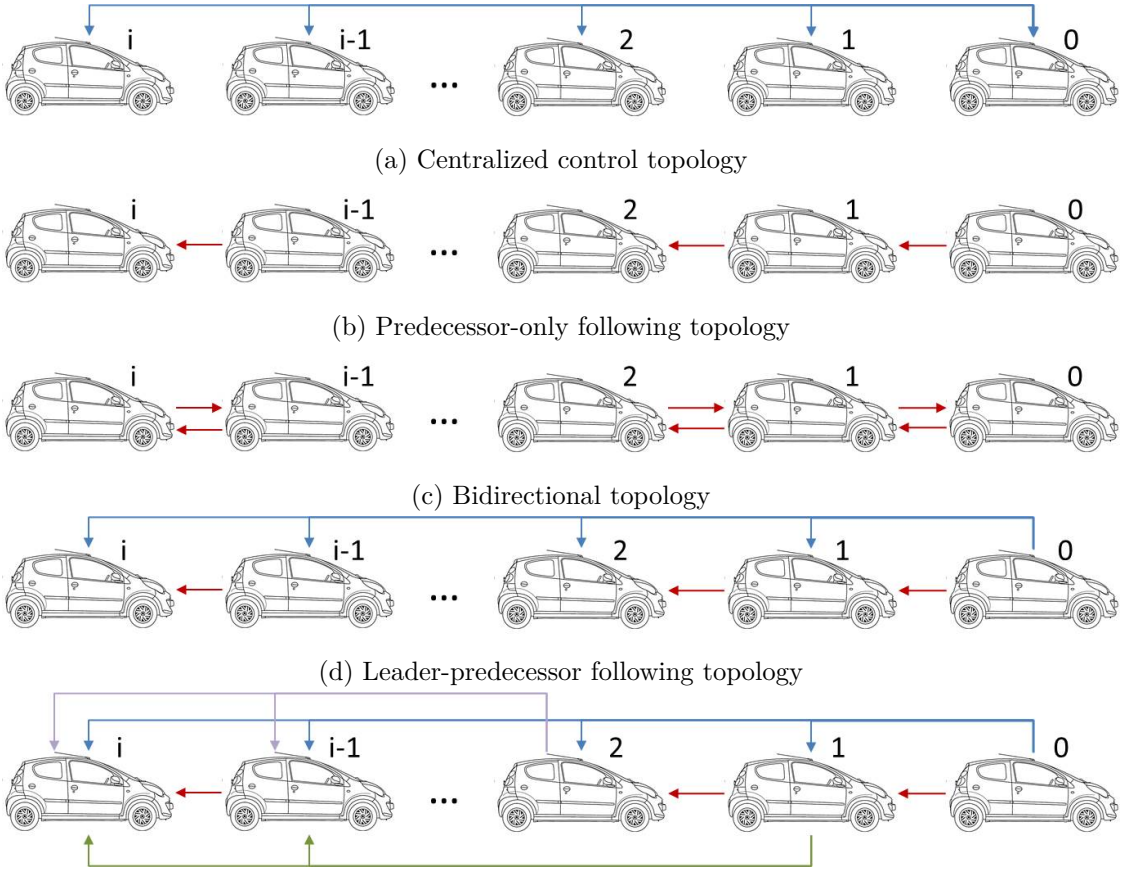

(a) Centralized control topology

(b) Predecessor-only following topology

(c) Bidirectional topology

(d) Leader-predecessor following topology

(e) Multiple predecessor following topology

Figure 3.1: Illustration of cooperative driving topologies in function of the communication links

- Centralized control: This technique consists on having a main and unique control processing unit that commands each of the vehicles low level structures. It takes into consideration all variables of the string members and generates every vehicle reference states in function of the performance expected from the cooperative formation. For instance, in [Stanger and del Re, 2013] an MPC centralized approach is employed to optimize energy consumption for all of platoon members. As expected, this strategy requires a global low latency network to permit the real time data exchange between vehicles and the main controller.

- Predecessor-only following (PF): PF topologies have been extensively employed in the state-

of-the-art since they are the simplest in terms of demanded communication infrastructure. In this case, only information of the immediately preceding vehicle is employed. The required communication structure is an unicast between vehicles of index (i-1)-th and the (i)-th, with data flow in upstream sense. Given that it only considers the next vehicle inside the control loop, the string size can be increased boundlessly and can also be easily merged or split without meaning to a major logistic challenge. The ego-preceding spacing is the most important variable in terms of safety if rear-end collisions are to be avoided, for this reason most of safety-aimed approaches are based on PF topologies. However, the absence of information other than the preceding's, limits ego-vehicle reacting capabilities towards perturbations propagated from the leader in upstream direction.

- Bidirectional following: This technique requires each of the vehicles to have two communication links that support data exchange with the immediately preceding and following vehicles. Some ACC-based approaches employ ranging sensors to measure relative spacing and speed towards the following and preceding vehicle, seeking to improve the string stability considering more vehicles inside the control loop. Another condition that motivates this topology is to have also information flowing in downstream direction to prevent a formation break up–e.g. a vehicle saturates its acceleration and its preceding slows down to remain not far away–. In [Zegers et al., 2016], the benefits of a consensus-based bidirectional CACC are investigated, showing interesting results over homogeneous strings. A drawback of such strategy is that perturbations are not only propagated upstream but also downstream, which makes the string stability analysis complex.

- Leader-predecessor following (LPF): Such topology requires communication links with both the immediately preceding and the first vehicle of the string, with the purpose of employing their information in the control loop. This technique allows each of the vehicles to directly react to leader vehicle states' changes at the moment they are broadcasted, instead of waiting until the perturbation is propagated upstream until the (i-1)-th vehicle. Usually, LPF technologies incorporate a broadcast communication unit in the leader vehicle to a PF infrastructure, so each of the string members can obtain in real time the leader information. For instance, in [Milanés et al., 2014] the position errors with respect to preceding and leader vehicles are fed back and employed by a controller in the deployment of CACC over ACC-equipped vehicles. This approach has been also employed and demonstrated to provide string stability under constant clearance policy with ideal conditions [Seiler et al., 2004].

- Multiple preceding following (MPF): This strategy is the one that demands the most the communication network. It consists on employing several preceding vehicles in the control loop, from the immediately predecessor to the leader vehicle. The idea is to employ weighted information of the forward section of the platoon to achieve an improved performance in case of a braking, merging or splitting. In fact, LPF topology can be interpreted as a special case of MPF where the weight is shared only among leader and predecessor vehicles. It results ideal for cooperative driving where interruptions intra-platoon may occur–e.g. a pedestrian crossing, or accident of one of string members–. This permits the upstream vehicles to react at the interruption moment before perceiving the perturbation over their predecessors. A so-called two-vehicle look-ahead approach is developed in [Ploeg et al., 2014a] and compared with PF strategy, employing information of (i-1)-th and (i-2)-th vehicles, showing good results in terms of string stability. A study on the scalability and stability of platoons is presented in [Zheng et al., 2016] under different MPF approaches. Its capabilities to improve significantly the platoon performance and stability are still in debate.

After reviewing the communication topologies that have been employed in the literature, one can conclude that they all bring benefits but also carry some drawbacks. In this work, the goal is to design a control structure and algorithms, that fulfill the proposed objectives requiring the less complex communication network. This allows to take the most profit of the available information, without requiring a highly demanded V2V infrastructure.

3.3 Proposed control structure

As explained above, a control structure is mandatory for the gap-regulation task. In this work, a hierarchical structure is adopted which consists in a high and low level control layers. The former is in charge of the inter-distance regulation, while the latter receives the generated reference speed and commands the vehicle actuator(s) so the longitudinal speed converges to the reference value. In this work, the following objectives are stated to achieve the desired car-following control performance:

- A defined hierarchy with a clear modularity between high and low level control layers
- Possibility to study the string stability, robustness, as well as disturbances, model uncertainties and noise effect over the overall control performance
- Adaptability to different automated car-following techniques as ACC and CACC with different types of communication topologies
- Online spacing policy adaptation capabilities in function of the operation point or strategy
- Scalability, or possibility to be implemented over any type of vehicle, at any position within the string or platoon

After reviewing the general performance objectives, a structure as the one showed in Fig. 3.2 is proposed for the gap regulation task. One of the fundamental properties of such structure is its adaptability to any spacing policy, given that it permits to directly define the targeted strategy on the outer feedback loop. It takes as an input the measured vehicle state and generates the ideal inter-distance in function of the spacing policy, for further comparison with the measured spacing gap.

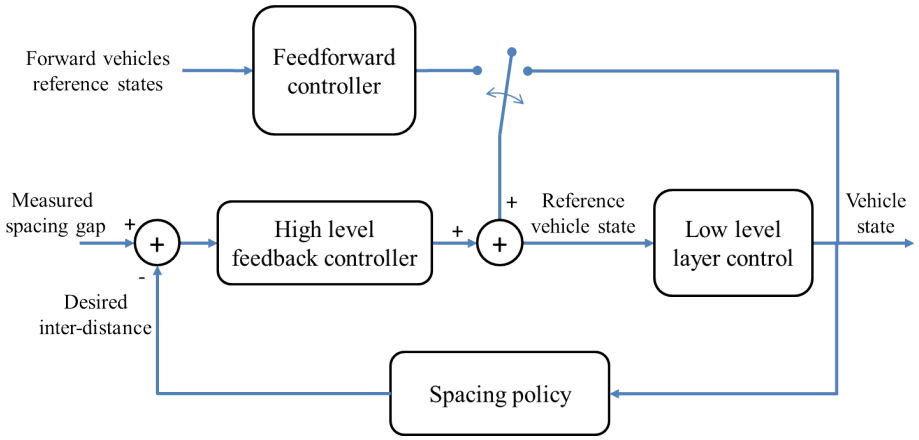

Figure 3.2: Generalized proposed control structure for the gap regulation task

Another advantage of the proposed control structure is its employability on both ACC and CACC strings. For the first, an inner feedback loop is employed which feeds back the vehicle speed, which is added to the high level feedback controller correction. When V2V communication links are available, the inner feedback loop is substituted by the output of a feedforward controller which is in charge of weighing and filtering the received reference speeds of the considered forward vehicles–e.g. preceding, leader, or others. In the case of CACC, the proposed control structure is inspired on the inverse model feedforward strategy.

3.3.1 Inversion-based feedforward control

Feedforward (FF) control follows the idea to have separated controllers for performance enhancement and load disturbance rejection. This strategy provides increased reference tracking capabilities in terms of speed and stability [Devasia, 2000]. It employs a feedforward link to get a faster response towards changes in the input/reference. Instead of using the feedforward link to compensate measured plant perturbations (which is another usage of feedforward approaches), this structure takes the input or reference value and applies the inverse model of the plant. This process consists on injecting the "ideal" input on the controlled plant to reproduce the reference on the output.

In normal conditions, this strategy would require the application of an accurate inverse model approximation of the vehicle dynamics to such reference, in order to feedforward the ideal command. Doing this requires not only invertibility of plant model, but may also lead to non-causal processes, which hinders the employment of such signal. However, when V2V communication links are available, this process is not required since the preceding vehicle sends directly its reference speed at the same moment that it is applied on its low level control layer. This accelerates ego-vehicle reaction capabilities and permits to replicate the preceding vehicle's behavior, according to the spacing policy guidelines. Fig. 3.3 illustrates the main goal of employing inversion-based feedforward control over cooperative automated vehicles.

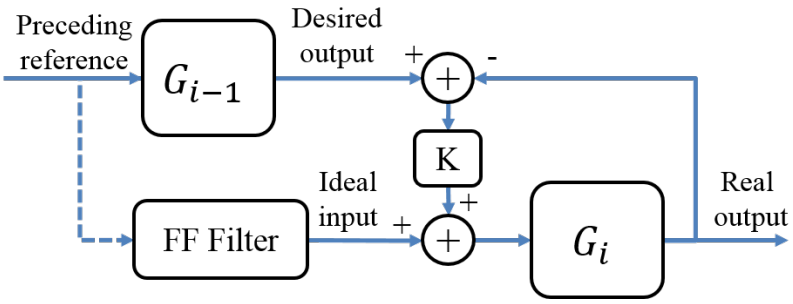

Figure 3.3: Scheme representing proposed inverse feedforward strategy using V2V links (dashed blue line)

One of the fundamental properties that this structure accounts with, is the modularity between each of the blocks. Each of them is independently designed and satisfy different performance objectives, but at the same time their interaction defines the closed loop performance. In the following section, a detailed description is provided of the first structure block to be designed.

3.3.2 Low level control layer

The low level control layer block is in charge of handling the vehicle actuators, with the purpose of tracking the reference vehicle speed. This permits to divide the overall control problem on two: low level reference speed tracking and high level kinematic spacing regulation, permitting to focus on each problem in a modular fashion. The design guidelines for the desired low level control are stated below:

- Predictability of the speed regulation loop performance. This permits to represent the reference speed tracking loop as a simple model with reduced or at least known uncertainties, which is ideal for its posterior implementation in a high level control framework
- Robustness against different road conditions and vehicle operation points. The block must consider that the controlled vehicle's powertrain and actuators account with non-linear behaviors
- Capability to be employed on different types of vehicles, which may have different propulsion and braking systems

Before the design of the low level control layer structure, knowledge of the vehicle dynamics model and its actuation capabilities is required.

3.3.2.1 Vehicle longitudinal model

The present work focuses on the vehicle motion over its longitudinal axis. For this reason, mathematical representations of the states evolution on this axis are analyzed for the design of low and high level control layers. In Fig. 3.4, an illustration of the longitudinal forces that act over the vehicle is presented.

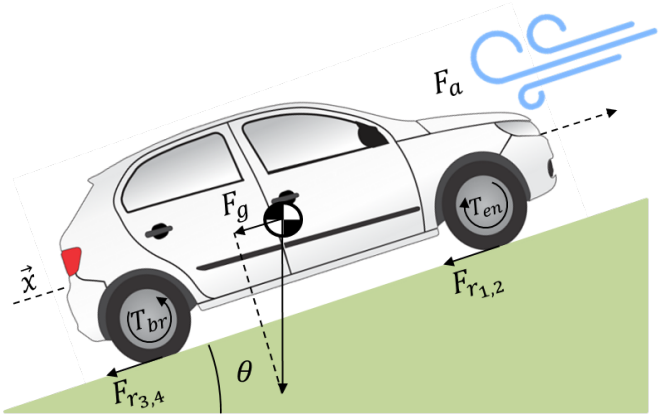

Figure 3.4: Representation of forces that act over the vehicle body on its longitudinal axis

The dynamic forces that act over the vehicle chassis longitudinal axis can be classified as external perturbations or energy losses and forces applied by the vehicle–i.e. due to braking, gear shifting or propulsion. The energy losses that the vehicle encounter when displacing on its longitudinal axis are:

- **Tire rolling resistance**: The tires are the only interaction mean between the vehicle and the road. For this reason, tire-road interaction results fundamental to study the vehicle dynamics. Nevertheless, since tires are not perfectly circular and the tire-road contact surface is not negligible due to the tire rubber deformation, the vehicle suffer from energy losses when displacing. In Eq. 3.1, the mathematical expression of this phenomenon is stated:

$$F_r(\theta, v) = -c_r \cdot M_v \cdot g \cdot cos(\theta) \cdot sign(v);\ c_r > 0 \tag{3.1}$$

  where c_r is the coefficient of rolling friction (CRF), M_v is the vehicle mass (including wheels and rotating parts inertia), g the gravity acceleration, θ the road grade and v the vehicle speed in its longitudinal axis. The CRF is the factor that determines how efficient is the road-tire interaction, which is function of several independent factors: tire properties, road conditions (dry asphalt, rain, ice), vehicle speed, tire temperature and pressure, among others. Generally, this coefficient is left constant and its variations are handled through a robust control layer that can ensure an acceptable performance for the expected values.

- **Aerodynamic friction and drag**: These type of losses are caused by two phenomena related to the air. The first is the viscous friction between the surrounding air and the vehicle surface, acting as a braking entity over the car motion. The second is caused by the drag that appears due to pressure difference between the front and rear part of the vehicle body. Eq. 3.2 describes the mathematical translation of this force:

$$F_a(v) = -0.5 \cdot \rho \cdot A_f \cdot C_d \cdot v^2 \cdot sign(v); \tag{3.2}$$

  where ρ refers to the air density, A_f to the frontal surface of the car body and C_d is the aerodynamic drag coefficient which models how resistant is a body to the fluid displacement around it. To measure this coefficient, wind tunnels tests are required to analyze the vacuum places. Furthermore, aerodynamic drag reduction can be modeled during platooning in function of the inter-vehicular distances and relative yaw angle [Pagliarella, 2009].

- **Gravitational forces**: This force appears at the moment when the vehicle is driving in tilted or non-flat surfaces–i.e. $\theta \neq 0$. Due to the gravitational force induced by the Earth over corps that stands over tilted surfaces, the force can either counteract or assist the vehicle longitudinal motion–i.e. upgrade or downgrade respectively. Eq. 3.3 describe the model of gravitational force over a vehicle of mass M_v:

$$F_g(\theta) = -M_v \cdot g \cdot sin(\theta); \tag{3.3}$$

Concerning the forces applied by the vehicle actuators, one can split them in propulsion and braking forces. The vehicle system that is in charge of delivering torque over the wheels to produce a positive force in the longitudinal axis direction, is named the propulsion system. It covers from the energy storage, engine, transmission and finally the drivetrain [Ioannou and Xu, 1994]. The vehicle energy source defines directly how the propulsion acts over the vehicle chassis. Along the history, most of the vehicles have had internal combustion engines (either with diesel or gasoline), but more recently alternative energy sources as electricity, fuel-cells, hydrogen and hybrid systems have surged as promising solutions for on-board energy storage. In this work, the proposed developments are aimed and implemented on fully electrical vehicles. For the braking forces applied to reduce the vehicle speed, all vehicles account with in-wheel brake system based on a hydraulic pressure

line. When pressing the brake pedal, the system activates each brake to reduce the wheel angular velocity through friction. More details about the operation of a common brake system can be found in [Xu and Ioannou, 1994].

Moving on to the equations that govern vehicle motion, one can start from Newton's second law. It states that the sum of all forces over a single axis is equal to the object mass multiplied by its acceleration. In other words, if vehicle longitudinal dynamics are described assuming no sideslip angles or interaction with lateral dynamics:

$$\begin{aligned} M_v \frac{d^2}{dt^2} x(t) &= \sum_{i=1}^{4} F_i \\ M_v \frac{d^2}{dt^2} x(t) &= \sum_{i=1}^{4} \frac{(t_{th_i} - t_{br_i})}{r_{w_i}} - F_a - F_g - \sum_{i=1}^{4} F_{r_i} \\ M_v \frac{d^2}{dt^2} x(t) &= \sum_{i=1}^{4} \frac{(t_{th_i} - t_{br_i})}{r_{w_i}} - \frac{1}{2}\rho A_f C_d \dot{x}(t)^2 - M_v\, g(sin(\theta) + C_r cos(\theta)) \end{aligned} \tag{3.4}$$

being $x(t)$ the vehicle position over time, r_w the wheel radius and t_{th_i} and t_{br_i} the propulsion and braking torques over each wheel respectively. It is important to state that the rotation inertia of transmission, drivetrain and wheels and can be represented as an added mass in M_v [Guzzella et al., 2007]. The corresponding low level control loop is then in charge of the correct employment and effective synchronization between actuators (t_{th} and t_{br}) to fulfill the aforementioned objectives. The model in Eq. 3.4 is obtained assuming no interaction with the vehicle lateral motion and no sideslip angle.

3.3.2.2 Low level control loop

To develop an appropriate control layer, the actuators operation must be mathematically modeled. Normally, they account with operational limits and temporal lags that define the relation between the commanded signal and the actual torque that is applied over the traction wheels. An accurate model representation in the Laplace frequency domain of throttle and brake actuators is Eq. 3.5.

$$\begin{aligned} \mathcal{L}\{t_{th}(t)\} = T_{th}(s) &= \frac{K_{th}\, e^{-T_{d_t} s}}{\tau_{th} s + 1} \cdot U_{th}(s); = G_{th}(s) \cdot U_{th}(s); \\ \mathcal{L}\{t_{br}(t)\} = T_{br}(s) &= \frac{K_{br}\, e^{-T_{d_b} s}}{s^2 + 2\xi\omega_b s + \omega_b^2} \cdot U_{br}(s) = G_{br}(s) \cdot U_{br}(s); \end{aligned} \tag{3.5}$$

Transport delays T_{d_t} and T_{d_b} appear due to the fact that the low level control layer is a networked embedded system where transmission delays between sensors, processing unit and actuators may appear. The throttle lag τ_{th} represents the stabilization time response of the propulsion actuator, defining the first order behavior. On the other hand, the brake pedal results more complex as it requires an inner brake pedal position control loop, whose closed loop performance is then modeled with a response bandwidth ω_b and damping factor ξ, agreeing with [Milanés et al., 2012]. Signals $U_{th}(s)$ and $U_{br}(s)$ are the throttling and braking commands generated by the automation unit. For sake of simplicity, and to avoid that braking and propulsion actuators are active at the same time, the input signals are unified and considered complementary in a single controller output signal $u(t) = \mathcal{L}^{-1}\{U(s)\}$ defined as follows:

$$u(t) \in \Re : u_{br}^{max} \leq u(t) \leq u_{th}^{max} \tag{3.6}$$

$$\mathcal{L}^{-1}\{U_{th}(s)\} = u_{th}(t) = \begin{cases} u(t);\ \forall\, 0 < u(t) < u_{th}^{max} \\ 0;\ \forall\, u_{br}^{max} < u(t) < 0 \end{cases} \tag{3.7}$$

$$\mathcal{L}^{-1}\{U_{br}(s)\} = u_{br}(t) = \begin{cases} 0;\ \forall\, u_{br}^{min} < u(t) < u_{th}^{max} \\ u(t);\ \forall\, u_{br}^{max} < u(t) < u_{br}^{min} \end{cases} \tag{3.8}$$

where the actuators operational limits u_{br}^{min}, u_{br}^{max} correspond to the minimum and maximum braking, while u_{th}^{max} represents the maximum throttle. Notice that a dead zone is left when $u_{br}^{min} < u(t) < 0$, to avoid not only excessive switching between actuators, but also unnecessary braking given that the vehicle dynamic energy losses produce low decelerations. As one can see, this setting guarantees that only one actuator can be active at most in function of $u(t)$.

The next step on the low level control design is to conceive a controller $C_{ll}(s)$ to fulfill objectives mentioned in the beginning of this section. For its design, robust loop shaping guidelines are applied [Braatz et al., 1996] [Sename et al., 2013], such as high loop gain at low frequencies, stability and good response bandwidth at middle frequencies and noise rejection with low gain at high frequencies. It is important to keep in mind that actuators (brake and throttle) account not only with different dynamics, but also with parameters uncertainties due to their wide operation range, gearbox shifting, efficiency, among other factors. The main purpose is then to remain robust and stable despite such uncertainties, at the same time that the closed loop response for both actuators results consistent both during accelerations and decelerations. This improves the system predictability and guarantees a reliable and consistent low level behavior model, ideal for the high level control layer design. Given that throttle $G_{th}(s)$ and braking $G_{br}(s)$ actuators account with different dynamics, the filters $F_{th}(s)$ and $F_{br}(s)$ are added before the actuators for conditioning purposes. The main objective of this is to guarantee that whichever actuator is used to close the loop, the speed tracking performance and stability result consistent.

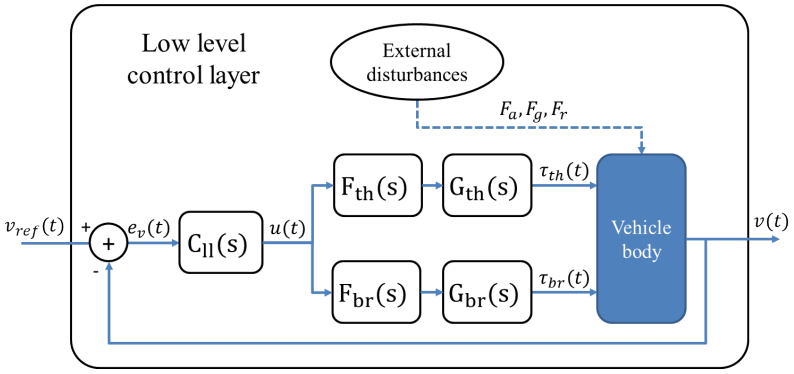

Figure 3.5: Low level speed tracking block description

A more detailed description of conception of the low level control, is provided in chapter 6. Close zoom over the low level control layer is depicted in Fig. 3.5. Finally, the closed loop that governs the given reference speed $v_{ref}(t)$ tracking through the actuators command, is deduced linearizing Eq. 3.4 and considering 3.5:

$$Gp(s) = \frac{V(s)}{V_{ref}(s)} = \frac{K_0 \omega_n^2 e^{-T_d s}}{s^2 + 2\xi\omega_n s + \omega_n^2}; \tag{3.9}$$

where K_0 is the DC gain (which is ideally equal to one), ξ the damping factor, T_d the temporal transport delay and ω_n the system natural frequency. This equation defines the low level control layer behavior, which parameters are of high relevance for the correct design of the remaining blocks of the gap-regulation control structure.

The low level layer design is the first step on the car-following control structure. Regarding the high level layer or gap-regulation loop, its design is carried out in function of the low level layer performance, which evidences the importance of the structure modularity. In fact, an extended version of the control structure in Fig. 3.2 is proposed profiting from such modularity, which accounts with special capabilities for the cooperative driving over urban environments.

3.4 Car-following structure for urban driving

Although platooning systems have been widely explored in recent years with promising developments so far, almost all approaches are designed for highway scenarios. Constant speed changes, interaction with VRU at low speeds or pedestrian protection are still barely explored problems. In fact, almost half of deaths over world's roads are among the most vulnerable users [Chan, 2015]. The addition of communication over transportation systems, has made possible the interaction using V2V, vehicle-to-infrastructure (V2I) and even vehicle-to-pedestrian (V2P) wireless links. This has permitted to increase the cooperation between road users. This is fundamental in the proposed approach to design an automated car-following system with emergency braking and prediction-based pedestrian avoidance [Flores et al., 2018a].

3.4.1 System description

The proposed systems targets the development of a enhanced control algorithm, which is able to handle different situations that may arrive if platooning on urban scenarios. The normal operation of the system requires the platforms to account with on-board ranging sensors (LiDAR) V2V/V2P capabilities and actuators automation. An illustration of the general system outlook is provided in Fig. 3.6. In this section, focus is over the control algorithm that requires an environment detection system and communication layer.

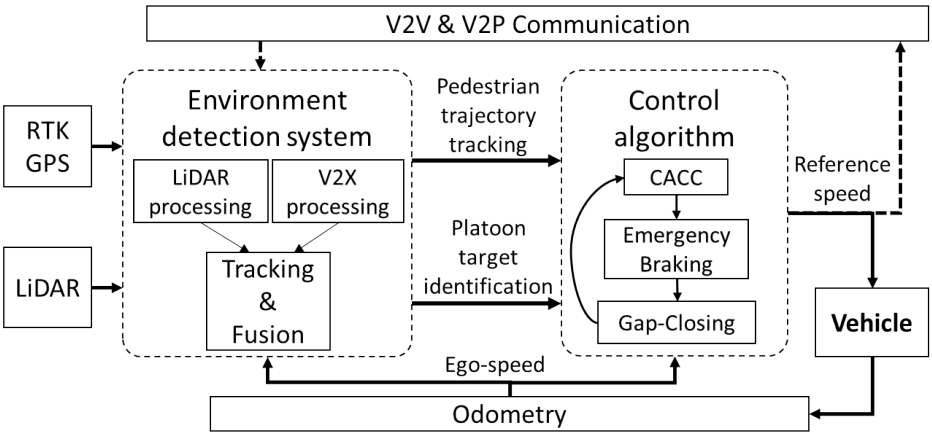

Figure 3.6: Overview of the proposed architecture for urban cooperative driving

The proposed control algorithm focuses on the longitudinal vehicle dynamics, handling emergency braking, platoon splitting/joining and pedestrian interaction. A state machine has been

designed to allow proper integration of the different control strategies (see Fig. 3.7) in the following vehicles–i.e. of index $i \in [2, n]$–. The lateral dynamics can be handled either manually or through a path-following controller [Calzolari et al., n.d.].

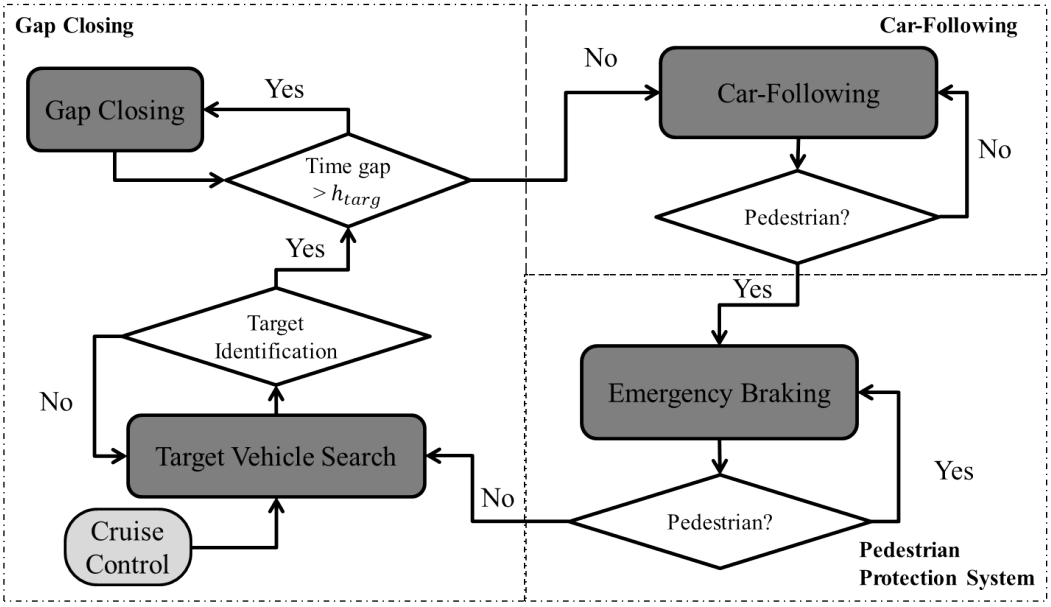

Figure 3.7: State machine of following vehicles with control states and flow diagram

3.4.1.1 Leader speed adaptation

For the string leader vehicle, the low level control layer is implemented to have reference speed tracking capabilities. Over such block, a speed trajectory or profile is generated according to the environment requirements–e.g. traffic lights, crosswalk or else–and tracked through a cruise control system. In the case where a pedestrian is walking around the vehicle string, the fusion system is employed to predict the pedestrian trajectory through LiDAR and a V2P link in case of occlusion, assuming a constant speed model. If leader and pedestrian's trajectories are estimated to intersect at a certain point, the speed profile is interrupted reducing immediately the leader target speed, thus avoiding a possible collision. After the pedestrian has crossed the intersection point and the collision risk is avoided, the speed profile is resumed by the leader vehicle.

3.4.1.2 Car-following control

Three main states are implemented on the follower vehicles: car-following, emergency braking and target vehicle control. The CACC car-following state is the equilibrium state, where the control system should converge to after a possible interruption. It proposes that the gap regulation with respect to its preceding is performed at a target time gap h. For the feedback gap-control, any of the approaches that are described further on Sec. 4.3 can be employed in the proposed structure. The car-following state is set as the initial state of the vehicles string operation. A time gap h is set for the normal car-following driving, whose value is chosen following human factor guidelines that have been provided in [Nowakowski et al., 2010a] for safe and comfortable CACC.

3.4.1.3 Emergency braking

As explained before, platooning over urban scenarios represents a major challenge with respect to highway due to the possible interaction with VRU. In case a pedestrian crosses between the string vehicles, the control algorithm must react safely at any time and break the string formation to avoid a collision. The environment detection system is being surveyed in real-time when vehicles are in car-following state, in case this situation arrives. Furthermore, a very probable scenario is that the pedestrian is detected by the environment detection system only at the moment he/she enters the platoon corridor, which may be caused by possible visual occlusion with another car, tree, corner, etc. For these cases, the control algorithm must interrupt the car-following maneuver and switch to the emergency pedestrian protection system. When a pedestrian is detected by the ego-vehicle to be inside the platooning lane or corridor (polygon area formed between the i-th and $i-1$-th vehicles) the state machine triggers the emergency braking maneuver, whichever the vehicle speed is.

Fig. 3.8 illustrates better this state operation, where two string members are driving at a cruise speed v_0 when a pedestrian enters the platoon corridor. At the detection moment, the ego-vehicle starts the braking maneuver taking into consideration the distance to the pedestrian $d_{detection}$ (or the closest one in case of more than one detection).

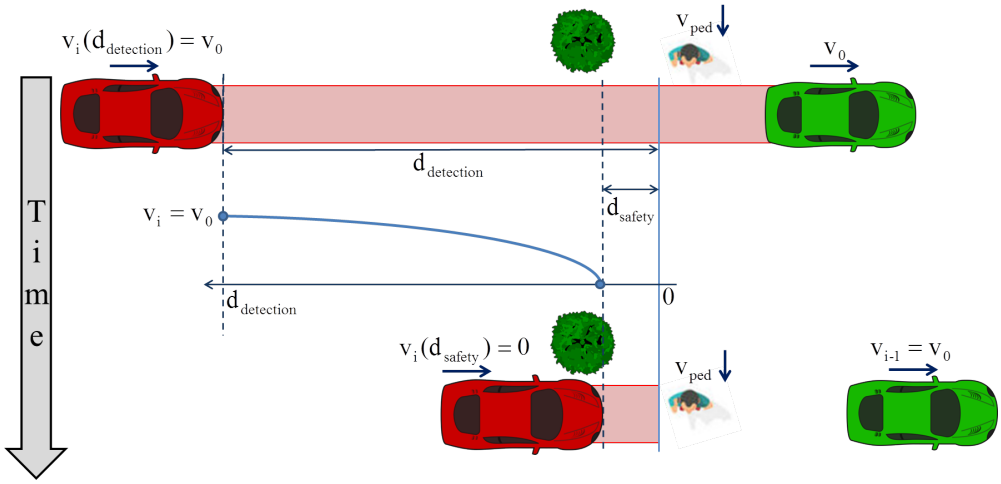

Figure 3.8: Desired behavior in case that a pedestrian crosses the platoon corridor and an emergency braking is required

Right at the crossing moment, the system is initialized by estimating the vehicle deceleration ramp as:

$$a_{ref} = \frac{v_o^2}{2 \cdot (d_{detection} - d_{safety})} < a_{max}; \tag{3.10}$$

where v_0 is the string cruise speed. The term a_{max} stands for the maximum deceleration reachable by the vehicle. With some manipulation, Eq. (3.10) allows to determine also the minimal $d_{detection}$ for a given v_0 for which the emergency braking maneuver is feasible, considering the physical limits of vehicle's braking capabilities. The vehicle should decelerate with the required rate to stop at a safe distance d_{safety} from the pedestrian, avoiding any collision. Taking this estimation as a reference, the target speed is outputted in real time in function of the distance to the pedestrian $d_{2ped}(t)$ received from the environment detection system:

$$v_{targ}(t) = \sqrt{v_0^2 - 2 \cdot a_{ref} \cdot (d_{detection} - d_{safety} - d_{2ped}(t))}; \tag{3.11}$$

To ensure a safe and accurate execution of the stopping maneuver, a speed controller modifies the reference speed sent to the low level control in function of the desired speed in 3.11 and the measured ego-speed. The selected controller is a Proportional-Derivative for its damping properties and stabilizing behavior. The mentioned controller is described by the control law showed in the Eq. 3.12.

$$u(t) = (Kp + Kd \cdot \frac{d}{dt})(v_{targ}(t) - v(t)); \tag{3.12}$$

3.4.1.4 Gap-closing algorithm

Once the pedestrian is no longer inside the platoon corridor, the ego-vehicle can safely rejoin the platoon formation. However, in practice the difference between the reference distance $d_{ref}(t) = hv(t) + d_{std}$ and the relative spacing $d(t)$ measured by the LiDAR may result really large after the stopping maneuver. This would lead to saturation and oscillations in the controller [Bu et al., 2010]. To avoid this scenario, preserve stability and ensure passengers' comfort; a gap closing maneuver is required.

The applied solution to ensure no saturation or oscillation when performing the gap regulation, is that the controller input (spacing error $e_i(t)$) is zero just after finishing emergency braking state. This is attained when the target time gap h and the measured time gap h_{meas} are the same. The latter is calculated as:

$$h_{d,meas}(t) = \frac{x_{i-1}(t) - x_i(t) - d_{std}}{v(t)}; \tag{3.13}$$

When the velocity is low or zero after performing the emergency braking, it could lead to really large $h_{meas}(t)$. To avoid this situation, a maximum allowed time gap h_{max} is set to saturate $h_{meas}(t)$. The gap closing procedure consists on a time gap linear function of the inter-vehicle spacing $d(t)$ and the ego-speed $v(t)$. Then, two steps are followed to close the gap between the preceding and ego-vehicle:

- If the initial inter-vehicle distance $d_{r,start}$ is higher than the term $d_{r,final} = h_{max}v(t)$, a constant and comfortable acceleration a_{gc} is applied until $d_{r,final}$ and the final velocity v_{final} yield a current time gap equal to h_{max} (v_{final} is limited as v_{max}). The term a_{gc} could be chosen depending on driver preferences: $smooth, medium, hard$; the higher a_{gc} is set, the faster h_{max} will be attained.

- Once h_{max} is reached, ACC is executed while reducing the desired time gap h, until it reaches the ACC limit time gap h_{ACC}. Then, the system switches to CACC up to the point where h reaches h_{min}. The time gap decremental ratio depends directly on t_{close}, which is a design parameter that will define the gap closing time between the highest time gap h_{max} and h_{min}. A suitable t_{close} should be chosen considering the trade-off between passengers' comfort and time spent on the transition. The operation is shown in Fig. 3.9.

During the gap closing maneuver, it is important to guarantee that the communication link is correctly resumed at $h_{meas}(t) = h_{ACC}$, where h_{ACC} is set as the minimum time gap where system string stability is ensured using ACC.

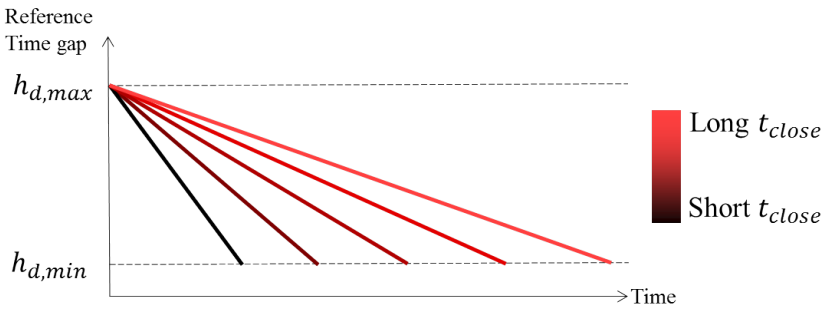

Figure 3.9: Gap closing operation through the time gap adaptation

3.5 Proposed spacing policy

In the structure presented in Fig. 3.2, the spacing policy is defined by the outer feedback loop. This means that the closed loop performance and the system stability are closely related to the choice of this strategy. In the Sec. 2.3.2.1, a state-of-the-art review was provided with the most employed approaches that can be found in the literature. As one can see, all of them bring benefits whereas some drawbacks are also present in every approach. After analyzing most strategies, one can conclude that good results have been demonstrated in function of difference performance criteria and scenarios. Regretfully, almost no approach aims to ensure a framework where string stability and safety are guaranteed over the entire speed range, at the same time that inter-distances are optimized to increase traffic throughput. This encourages the statement of the following design objectives for an enhanced spacing policy:

- Encompass the full speed range, proposing a velocity-dependent spacing strategy that is employable in urban and highway environments
- Reduce/optimize the inter-distances between the vehicles to increase the traffic throughput
- Guarantee safety in case of possible braking of the preceding vehicle, taking into consideration delays and reaction lags
- Ensure the string stability condition over the full speed range, either for ACC or CACC techniques
- Assume that string information is only available from the preceding vehicle (either from on-board sensors or V2V links)

3.5.1 Time gap-based strategy

Previously stated objectives are fulfilled by designing a full-range time gap-based spacing strategy that adapts the inter-vehicle distances in function of the ego-speed. The time gap constitutes the main axis of this strategy because it defines the best how human drivers perform. At the same time, it defines directly not only the traffic throughput–e.g. shorter time gaps increase the road capacity–, but also the string stability.

The proposed car-following spacing policy is divided in urban and highway scenarios–i.e. low and high speeds. In urban driving, CTG is used with a fixed standstill distance is used to gain stop-and-go capabilities, whereas for highway driving the standstill distance is removed relaying

only on constant time gap spacing. Firstly, a CSF is proposed for low speeds, where the time gap is increased as the speed approaches the threshold speed V_{lim}. A smooth transition to high speeds is required, where the CTG strategy is applied seeking a more uniform behavior and the desired car-following stability. The mentioned low speed time gap manipulation also optimizes the spacing, yielding reduced inter-distances for highway driving, at the same time that benefits and performance of CTG are guaranteed. For both cases, the policy design must guarantee that the referenced spacings yield safe car-following without possible rear-end collision in case of preceding vehicle braking.

Focusing on the low speed scenario, the following requirements are stated to obtain the desired behavior: a fixed distance d_{std} at standstill, a smooth and continuous transition to the target time gap h_{targ} at the speed limit V_{lim} between urban and highway scenarios and finally, ensured string stability and safety in the whole speed range. In other words:

$$\begin{aligned} &d_{ref}(0) = d_{std}; \\ &\tfrac{d_{ref}(0)}{dv} = h_{init}; \\ &\tfrac{d_{ref}(V_{lim})}{dv} = h_{targ}; \end{aligned} \tag{3.14}$$

where h_{init} is the time gap held at speed zero, defining the spacing evolution as the speed starts to increase. To satisfy the presented three requirements, a second order polynomial is suggested to describe the function $d_{ref}(v)$ for low speeds. Consequently, a resulting spacing policy of the form:

$$d_{ref}(v) = \begin{cases} \lambda_1 + \lambda_2 v + \lambda_3 v^2;\ 0 \leq v \leq V_{lim} \\ h_{targ} v - c;\ v \geq V_{lim} \end{cases} \tag{3.15}$$

is obtained and can be interpreted as a transition from CSF in low speeds to the CTG policy. The constant c is an offset distance that ensures continuity from low to high speeds, as well as the distance saved with respect to the spacing given by $h_{targ}v$. After some manipulation, the parameters are configured as follows:

$$\begin{aligned} &\lambda_1 = d_{std}; \\ &\lambda_2 = h_{init}; \\ &\lambda_3 = \tfrac{(h_{targ} - h_{init})}{2V_{lim}}; \end{aligned} \tag{3.16}$$

to produce a spacing strategy that satisfies the requirements in Eq. 3.14. After determining the polynomial constants, the selection of the design parameters $(V_{lim}, h_{targ}, h_{init}, d_{std})$ is carried out. Finally, the spacing policy results based on the time gap increase from h_{init} to h_{targ}, which is depicted in Fig. 3.10

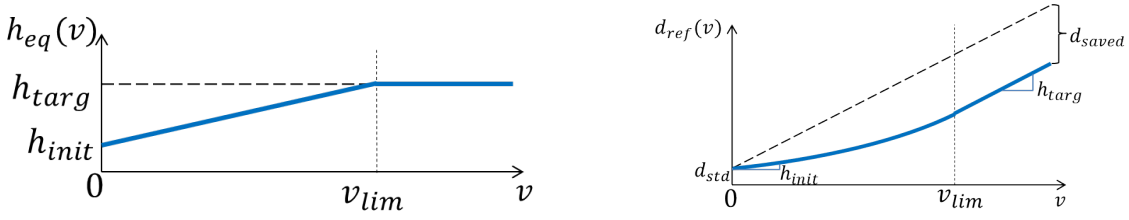

(a) Time gap evolution

(b) Spacing policy in function of the vehicle speed

Figure 3.10: Strategy described through the time gap and spacing evolution

3.5.2 Design parameters choice

As explained before, the proposed strategy is divided in low and high speeds, where V_{lim} sets the limit between both. Consequently, such parameter is selected to be the speed limit in urban areas and set the boundary between both scenarios. Firstly, for ACC it is proposed to set h_{targ} as a time gap chosen by the driver to be maintained in highways (usually between 1 and 1.5 seconds), whereas for CACC a lower time gap is set to increase the traffic throughput and also considering human factors guidelines for CACC driving in highways [Nowakowski et al., 2010b].

Analyzing the low speed scenario (see Eq. 3.15), the CSF policy can be linearized in an equivalent time gap $h_{eq}(v) \in [h_{init}, h_{targ}]$ that increments as the speed increases. In fact, the equivalent time gap results as a smooth function of the ego-speed, given that it corresponds to the derivative of the reference inter-distance with respect to the ego-speed. Then, such value results for the full speed range as:

$$h_{eq}(v) = \begin{cases} h_{init} + \frac{(h_{targ} - h_{init})}{V_{lim}} v;\ 0 \leq v \leq V_{lim} \\ h_{targ};\ v \geq V_{lim} \end{cases} \tag{3.17}$$

Although lower time gaps enhance traffic capacity, they also yield less stable behavior and a more demanding gap-regulation task is then required. Due to this fact, the minimum equivalent time gap (h_{init}) is desired to be the lowest time gap that the employed control structure can afford ensuring string stability. This value is obtained through an iterative process where the time gap is lowered until the infinite norm of the closed loop response–i.e. string stability function $\| \frac{X_i(s)}{X_{i-1}(s)} \|_\infty$–becomes higher than unity.

The parameter r is chosen taking into consideration that the minimum inter-distance for any speed should be safe in case a braking maneuver is performed by the preceding car. The desired inter-distance must be higher than the minimum critical distance $d_{ref,crit}(v)$ required to avoid a possible collision at any speed. The estimation of such distance is done assuming that the vehicles are driving uniformly–i.e. no oscillations or high speed variations–as is the case when performing car-following. In such situation, the available distance $d_{av}(v)$ that the ego-vehicle has to stop is defined by:

$$d_{av}(v) = d_{ref}(v) + \frac{v^2}{2B_{max}}; \tag{3.18}$$

which is composed by the referenced spacing $d_{ref}(v)$ and the distance that covers the preceding vehicle when performing a braking at a deceleration B_{max} starting from speed v. During a preceding vehicle braking situation, the ego-vehicle performs a braking maneuver as the one showed in 3.11.

The total spacing required by the ego-vehicle to fully stop is composed by the addition of three distances D_1, D_2, D_3. These distances are defined as follows:

$$D_1 = \tau v; \tag{3.19}$$

$$D_2 = \frac{B_{max} v}{J_{max}} - \frac{B_{max}^3}{6 J_{max}^2}; \tag{3.20}$$

$$D_3 = \frac{v^2}{2B_{max}} - \frac{B_{max} v}{2J_{max}} + \frac{B_{max}^3}{8 J_{max}^2}; \tag{3.21}$$

where B_{max} and J_{max} are the maximum braking deceleration and jerk respectively. These values are chosen assuming comfortable [ISO, 1997] car-following driving. The distance D_1 results from

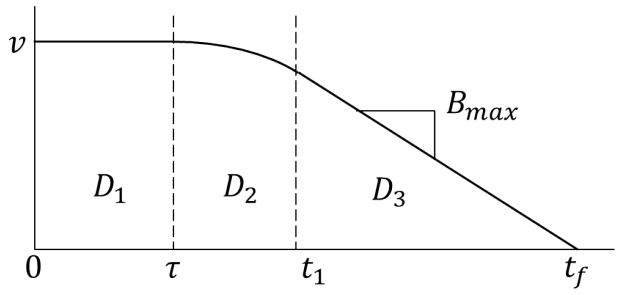

Figure 3.11: Illustration of the distance that covers the ego-vehicle when a stopping maneuver is performed by the preceding one

the time τ that represents actuator response's delay, whereas D_2 results from the traveled distance while reaching maximal deceleration B_{max} with a rate of J_{max}. Finally, D_3 is the covered distance maintaining the mentioned deceleration rate until the car stops. To ensure safety in a possible braking situation, and considering Eq. 3.18 with Eq. 3.19-3.21, the following condition must be fulfilled:

$$d_{ref}(v) \geq d_{ref,crit}(v) = D_1 + D_2 + D_3 - \frac{v^2}{2B_{max}}; \tag{3.22}$$

which constitutes the critical reference inter-distance that can be maintained. For the homogeneous string case it results of the form:

$$d_{ref,crit}(v) = (\tau + \frac{B_{max}}{2J_{max}})v - \frac{B_{max}^3}{24J_{max}^2}; \tag{3.23}$$

and defines the safe region in the spacing vs. speed plane, where the referenced distance has to be maintained above. Transition from low to high speeds is obtained at V_{lim} combining Eq. 3.15 and 3.23. Subsequently, this condition is satisfied when:

$$d_{std} = \frac{V_{lim}(h_{init} - \tau - \frac{B_{max}}{2J_{max}})^2}{2(h_{targ} - h_{init})} - \frac{B_{max}^3}{24J_{max}^2}; \tag{3.24}$$

3.5.3 Strategy evaluation

Once the derivation of the design parameters is explained, an evaluation is provided. Fig. 3.12 shows the comparison between the resulting inter-distance function and other state-of-the-art policies. Black line represents the car-following approach proposed in [Martinez and Canudas-de Wit, 2007]. One can appreciate how its performance in terms of traffic throughput is reduced when speed increases. The red area represents non-safe area where a rear-end collision may occur in case of a preceding vehicle braking scenario, as calculated in Eq. 3.23. Green line depicts the constant time gap strategy. Finally, blue line shows the proposed spacing policy. Comparing the latter with CTG, it can be appreciated that the proposed approach modifies the curve slope in low speeds to optimize the separation between vehicles. This not only improves the traffic capacity if implemented in large scale strings, but also ensures the same desired dynamic response for high speeds.

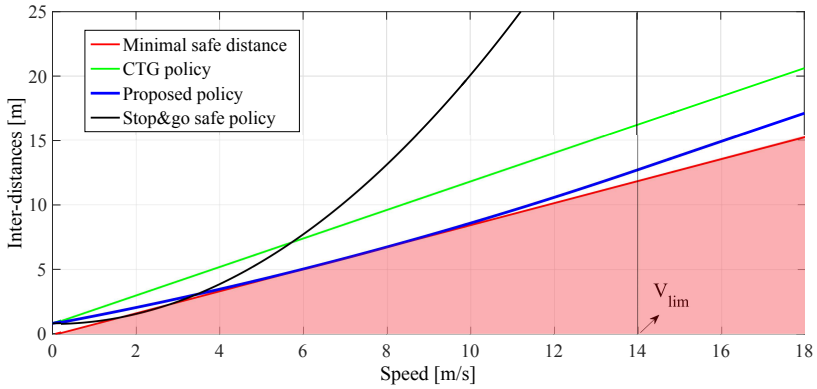

Figure 3.12: Resulting full-range spacing policy (blue line), CTG policy (green line), safe longitudinal distance for ACC and stop&go scenarios (black line) and the minimal spacing to keep (red line)

3.6 Discussion

Along this chapter, the description of the employed control structure for car-following is provided. First, description of the different control strategies and cooperation topologies in the state-of-the-art is provided. From LQR optimal control, MPC, fuzzy logic, sliding mode and classical PD controllers; different techniques have been employed to regulate the spacing gaps on car-following showing good results. Furthermore, different communication topologies have demonstrated to bring benefits at the cost of more complex network architectures. Details have been provided with examples of applications where the mentioned topologies have been successfully applied. Subsequently, the proposed structure has been detailed. Consisting in a cascaded/hierarchical architecture, it is adaptable to ACC and CACC-equipped vehicles. It has been designed focusing on the modularity between the blocks therein.

Given that the focus of this work is over the development of control systems over the longitudinal axis, the model of vehicle's longitudinal dynamics has been described. All the forces that govern the vehicle motion at different speeds and road conditions have been detailed. The vehicle actuators and their control have been also discussed, constituting the low level layer in charge of the reference speed tracking task. This layer is composed by a single feedback controller that generates from the speed error, a control action that is translated either in an acceleration or deceleration is redirected to the required actuator after being filtered. Two major contributions can be distinguished along this chapter.

1. The first major contribution in this chapter is the novel high level global architecture for cooperative driving in urban scenarios. In its equilibrium state, the system performs CACC at the desired time gap until an interruption occurs. Consisting on a state machine algorithm, the architecture manages possible interaction with pedestrians with an emergency braking state, as well as platoon rejoining through a gap closing maneuver based on the time gap manipulation. This developments demonstrates the architecture modularity and the benefits of employing fractional-order calculus for high level control systems design, which will be compared against classical approaches in the chapter 6.

2. The other major contribution of this chapter is the proposal of a full speed range spacing policy, that fulfills different performance criteria and is adaptable for ACC and CACC strings. This

policy ensures string stability at the same time that reduces the vehicle inter-distances for an optimized highway traffic capacity. It is based on a time gap variation from an initial value to a target time gap for highway driving, ensuring that: the time gap is above the minimum time gap that ensures string stability and the desired reference inter-distance is always higher than the minimal required to avoid a rear-end collision. An illustration is provided that shows the benefits with respect to some of the literature spacing policies.

Chapitre 4

Contrôle des convoies homogènes

Below is a French summary of the following chapter "Homogeneous strings control".

Ce chapitre concerne la proposition de différents algorithmes de conception des contrôleurs feedback. Une fois que la politique d'espacement est appliqué pour déterminer l'écart idéal, celui-ci est comparé avec la distance mesurée par rapport au véhicule précédent. L'erreur d'espacement est corrigé par le système de feedback avec l'action de contrôle.

La conception de contrôleurs feedback qui soient capables d'augmenter les avantages du car-following automatisé, notamment la stabilité du convoi, flux de trafique et robustesse; est ciblée. Pour cela, le calcul d'ordre fractionnaire est proposé comme outil de conception. Celui permet d'atteindre des réponses en fréquence dont la forme est plus flexible et précise. Un résumé de l'origine et les techniques de contrôle basés sur cet outil de calcul est fourni, ainsi que les méthodes de'étude de stabilité et mise en œuvre des algorithmes. Trois méthodes de conception sont proposés et expliqués en détail:

1. Un contrôleur Proportionnel Dérivatif d'ordre fractionnaire avec robustesse fractal ou robustesse face aux changements de la gain DC de la plant contrôlé.

2. Un contrôleur Proportionnel Dérivatif d'ordre fractionnaire qui garantisse la stabilité du convoi, tout en réduisant l'écart temporel au minimum possible, sans perdre la stabilité individuelle et en maintenant la même bande passante du système.

3. Un compensateur en avance qui rend une réponse en boucle fermée dans la sensibilité et la stabilité du convoi sont analysées. Spécialement, la sensibilité complémentaire, sensibilité aux perturbations et l'effort du contrôle par rapport à l'entrée du système sont aussi comprises dans la méthode.

Toutes les méthodes sont présentes et expliqués en supposant que les dynamiques des véhicules dans le même convoi sont homogènes.

Chapter 4

Homogeneous Strings Control

Along the previous chapter, different car-following structures were discussed in detail. A modular control scheme has been proposed to get more performing gap-regulation, with the purpose of satisfying more design objectives. The novel full-range spacing policy has been conceived for both ACC and CACC systems, seeking an integral control framework with the ideal separation between vehicles. Although the spacing policy is fundamental for the overall string performance, it is only one of the car-following structure blocks, specifically the outer feedback loop. Once the desired inter-distance is calculated, it has to be compared with the measured spacing to get the position error, which is fed to the feedback controller. Along this chapter, solutions based on feedback control are proposed focusing on gap-regulation under the assumption of identical dynamics among vehicles of the same string (see Fig. 4.1).

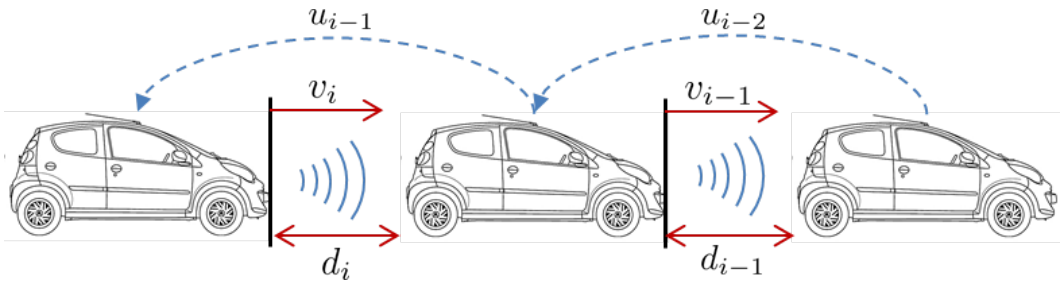

Figure 4.1: Illustration of a homogeneous string of vehicles performing car-following

The design of such controller is fundamental to guarantee not only the string stability but also the robustness against perturbations, disturbances and unmodeled dynamics. In the literature, almost all techniques rely on car-following feedback control. Along this part, the benefits of a novel calculus techniques to design feedback controllers are investigated. The remaining of this chapter is structured as follows: The motivation for employing novel calculus techniques is given in Sec. 4.1. An insight over fractional-order calculus and its applications over several fields including car-following control is described in Sec. 4.2. A list of the different feedback control design algorithms is provided in 4.3, as well as their corresponding motivation and benefits. Explanation of stability validation and discrete implementation of fractional-order solutions are discussed in Sec. 4.2.1.3 and 4.2.1.4 respectively. Finally, a discussion about the conclusions of this chapter is provided in Sec. 4.4.

4.1 Motivation

In this chapter, the proposal of different feedback control algorithms for gap-regulation control is sought that could extend the benefits of car-following systems. Several performance objectives have been sought during the design of these feedback systems. Traffic flow increase with shorter inter-distances, stability and safety are of the main targets of car-following control systems that have been widely scoped in the literature. Nevertheless, strict $\mathcal{L}_\infty$ string stability and robustness are still open challenges that are being studied in the state-of-the-art. To achieve control systems that are able to provide satisfactory solutions to these performance criteria, new techniques as fractional-order calculus could provide significant enhancement.

The major part of nowadays models and systems are based on mathematical representations with integer-order calculus. Regarding control engineering, nearly 95 % of current industrial control systems are PID-based [Åström and Hägglund, 2006], which demonstrates their reliability and proven good performance. However, real systems may not always be representable as an integer-order model, which suggests to remove this restriction and extend to real-order generalizations. This encourages to explore the possible benefits of employing a different calculus tool to represent more accurately a system behavior [Monje et al., 2010]. It has been demonstrated not only that the best fractional-order controller could outperform the best integer-order one for a given plant, but also why it is better to consider non-integer calculus even when high order control works well [Micharet, 2006]. This technique has been chosen as a tool to explore more accurate design algorithms for controllers whose frequency response are required to be more accurately shaped. An introduction of fractional-order calculus theory is provided for a better insight of such technique.

4.2 Fractional-order control

As stated before, integer-order calculus (IOC) has been the most used tool for representing models, systems and controllers in all applied sciences. Nevertheless, a new calculus tool must be considered when it comes to have a more accurate and close-to-reality representation/modeling of real processes, satisfying more strict requirements. In fact, researchers in fields like electrochemistry, biology, viscoelasticity; found that while modeling phenomena behavior through circuits with capacitors, inductors and resistances, the result always remained far from the expected one. Due to this exigency, and considering that not all systems should be generalized to derivatives and integrals of integer order; in the 17th century Leibniz and L'Hôpital raised the question of having a non integer differential order. But it was in the 19th century when eminent scientists like Euler, Laplace, Fourier among others; discussed the possibility of extending the differentiation to a non-integer order.

4.2.1 Fractional-order calculus theory

The first real application of the fractional-order calculus was made by Abel in 1823, when he discovered that the solution for the integral equation for the tautochrone problem could be obtained through an integral of order 1/2. Fractional-order calculus is already a 300 years old mathematics topic. Its rise has permitted to solve numerous scientific issues mostly related to phenomena where memory states are fundamental for describing the system evolution. These advances not only allowed to find solutions that at the moment were far from being understood with integer-order calculus, but also opened different fields of engineering research. In last decades, the growth of fractional calculus has been mainly focused on engineering applications such as transmission

lines modeling, viscoelasticity study, rheology, transport problems, control and systems theory among others. For instance, modeling the voltage-current relation of a semi-infinite lossy RC line, or also the heat diffusion into a semi-infinite solid require the employment of this mathematical tool. For more details in fractional-order calculus advances in physics and engineering, please refer to [Sabatier et al., 2007].

Let introduce the generalized real-order operator ${}_aD_t^\alpha$, which covers differentiation of order $\alpha \in \Re$; as presented in Eq. 4.1

$$ {}_aD_t^\alpha = \begin{cases} \frac{d^\alpha}{dt^\alpha} \rightarrow \alpha > 0 \\ 1 \rightarrow \alpha = 0 \\ \int_a^t (d\tau)^{-\alpha} \rightarrow \alpha < 0 \end{cases} \tag{4.1} $$

where it can be noticed that both derivation and integration process can be modeled using the same operator. At this moment, it is necessary to understand what does real-order differentiation $\frac{d^\alpha}{dt^\alpha}$ mean to remain coherent with integer-order derivation. Some other requirements for the definition of such operator is that it must be linear and the orders must permit addition (semigroup property) [Chen et al., 2009].

One of the most widely known definition for this operator was proposed by Riemann-Liouville [Li et al., 2011], which is presented in Eq. 4.2 for $(n-1 < \alpha < n)$. It can be appreciated that this expression is defined by the convolution operator, which refers to memory phenomena.

$$ {}_aD_t^\alpha = \frac{1}{\Gamma(n-\alpha)} \frac{d^n}{dt^n} \int_a^t \frac{f(\tau)}{(t-\tau)^{\alpha-n+1}} (d\tau), \tag{4.2} $$

In this expression, the term $\Gamma(n)$ corresponds to the Euler's gamma function:

$$ \Gamma(n) = \int_0^\infty t^{n-1} e^{-t} dt; \tag{4.3} $$

Even though this function has been widely accepted, the initial conditions have no simple physical interpretation. For this reason, the mathematician Caputo [Ishteva, 2005] proposed the fractional-order differential operator (see Eq. 4.4), where initial conditions like $y(0) = y_0, \dot{y}(0) = y_1$ can be easily interpreted; and m is the natural number immediately superior to α–i.e. $(m-1 < \alpha < m)$.

$$ {}_aD_t^\alpha = \frac{1}{\Gamma(m-\alpha)} \int_0^t \frac{f^{(m)}(\tau)}{(t-\tau)^{\alpha-m+1}} (d\tau), \tag{4.4} $$

One can observe that in this definition, initial conditions take a more adequate form and the differentiation is carried out inside the integral, avoiding initial conditions conflicts at the lower limit of the integral. Since most of the engineering applications and modeling tools are better described at the frequency domain, an interpretation of the fractional-order differentiation of a function $f(t)$ is provided using Laplace transform in Eq. 4.5.

$$ \mathcal{L}\{{}_aD_t^\alpha f(t)\} = s^\alpha \cdot F(s); \forall\, s > 0,\, \alpha \in \Re \tag{4.5} $$

where $f(t)$ and $F(s)$ stands for the function in its time and frequency domain form respectively, assuming initial conditions as zero. The maturity of fractional-order calculus and its approximations, have made possible their wide employment over different areas. In Fig. 4.2, an illustration of derivation of several orders on a triangular signal with DC level is depicted. The differentiation order is varied from zero to unity, which permits to distinguish the effect of the operator

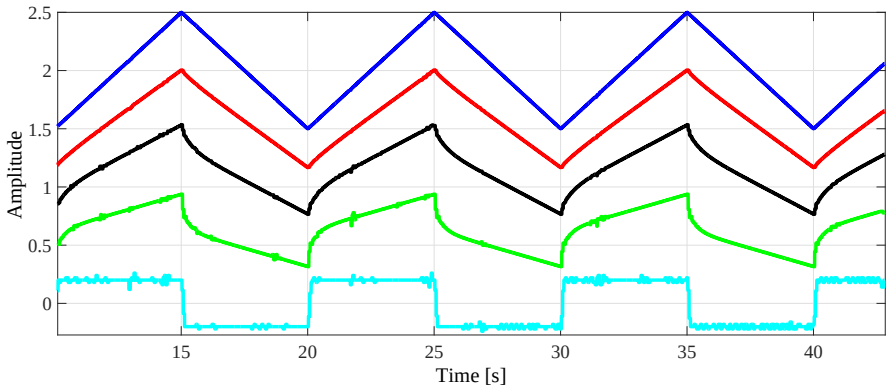

Figure 4.2: Effect of different derivation order α: 0.25 (red), 0.5 (black), 0.75 (green) and 1 (cyan) over a triangular signal (blue line)

as a signal processing tool. This operator presented in Eq. 4.5, has served for numerous signal processing tools and consequently. Hence, it has been extensively employed in the control field in state-of-the-art and industrial approaches with great results [Chen et al., 2009].

4.2.1.1 Fractional-order control techniques

It is important to remind that the main purpose of control systems is to act over a given plant and to make it follow a desired behavior in a feedback structure. Fractional-order control proposes to extend the employment of integrals and derivation to real-order ones, seeking a more appropriate controller form. The growing interest in finding an ideal feedback system robust to infinite plant gain variations has also encouraged the employment of fractional-order calculus. In fact, the fractional-order integrator has been tagged as the reference system for an ideal feedback closed loop response. In other words, the transfer function ω_{gc}/s^{λ}, $0 < \lambda < 2$; (where λ and ω_{gc} are the integration order and gaincross frequency) was denominated by Bode to have the *"ideal cutoff characteristic"* and further named as the *"Bode's ideal loop transfer function"*. This is due to the fact that regardless the plant gain change, the phase margin will remain as $\phi = \pi - \lambda\pi/2$.

Different methods have been proposed in the literature that employ real-order differentiation and integration to attain better results in terms of robustness and control performance.

- **CRONE**: The idea of designing fractional-order systems to control a dynamic plant was introduced by A. Oustaloup [Oustaloup et al., 1993] with the CRONE (in french, *Commande Robuste d'Ordre Non Entier*). For the first generation of the CRONE strategy, its main purpose was to reduce the phase margin variations of the system open loop response, following Bode's ideal loop response.

  On the other hand, the main objective of the second generation of the CRONE approach is to directly cancel the phase variations in the gaincross frequency, by ensuring the so-called *fractal robustness*. To satisfy this requirement, two conditions must be accomplished: a vertical template formed by the open loop Nichols chart, between $-\pi/2$ and $-\pi$ for the nominal parameters of the plant and the sliding of the template when the plant is re-parameterized.

  The frequency template of the transmittance–i.e.-sensitivity function–is given by the function (4.6), where the $arg(\beta(j\omega)) = -\alpha\pi/2$ with $1 < \alpha < 2$, which results in a Nichols chart with a

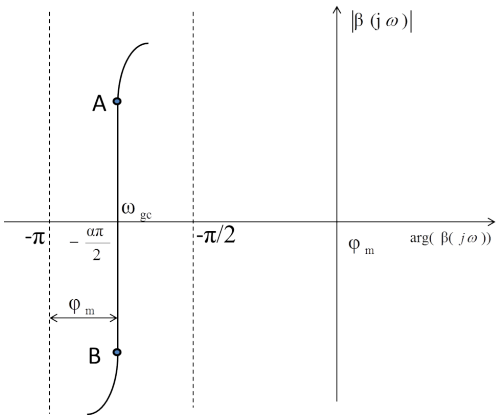

Figure 4.3: Nichols plot from the ideal Bode response β(s)

vertical line that crosses the axis in $-\alpha\pi/2$. This allows the sliding of the system in this straight line when the system parameters vary due to changes in the dynamic behavior, and increases the robustness against plant variations. This fact, explains the main objective of the control design proposed by the CRONE technique, which is to approximate the system open loop response to the frequency template of the transmittance function given by β(s).

$$\beta(s) = \left(\frac{1}{\tau s}\right)^{\alpha} = \left(\frac{\omega_{gc}}{s}\right)^{\alpha} \tag{4.6}$$

Finally, assuming that a negative feedback and cascade control architecture is employed, the transfer function for the controller $C(s)$ is obtained from the expression (4.7), where $G_p(s)$ is the plant that is going to be controlled.

$$C(s) = \frac{\beta(s)}{G_p(s)} \tag{4.7}$$

Numerous applications of this technique has been carried out, such as car suspension control [Oustaloup et al., 1996], hydraulic actuators, among others; bringing great results due to the robustness that this technique provides against model uncertainties or variations.

- **Tilt-Integral-Derivative**:The Tilt-Integral-Derivative Controller [Lurie, 1994] proposes a controller that is a modification of the widely employed classical Proportional Integral Derivative controller. It has the advantages of the PID controller scheme, but the proportional term is substituted by a tilted compensator whose transfer function is $s^{-\frac{1}{n}}$, (where n is a real number usually between 2 and 3) in order to get a response that is reasonably closer to the theoretically optimal Bode response. This compensator is referred as "Tilt", as it provides a tilted feedback gain in function of the frequency, due to the fractional order integrator. This configuration can be easily tuned and allows to maintain the system stable under disturbances, even during parameter variations.

- **PI$^{\lambda}$D$^{\alpha}$**: As it has been demonstrated, PID controllers account with simplicity and provide robustness for the system being controlled. From the Ziegler and Nichols, a wide variety of tuning methods have been proposed to target different objectives. With the introduction of

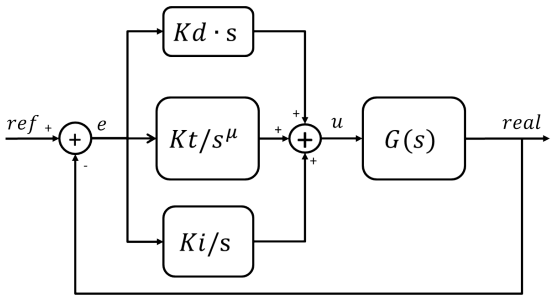

Figure 4.4: Block diagram for TID Control technique

fractional-order calculus and its tools for mathematical developments, great interest was attired to employ this tool on feedback control design. At that moment, I. Podlubny proposed to enhance the classical PID controller, permitting non-integer integral/differential operators. The so-called $PI^{\lambda}D^{\alpha}$ was formally introduced in [Podlubny, 1999]. Initially, the controller was proposed for controlling fractional-order systems, for which a better performance than integer-order control has been demonstrated [Podlubny, 1994]. The controller is of the form:

$$\begin{aligned} u(t) &= K_p e(t) + K_i D_t^{-\lambda} e(t) + K_d D_t^{\alpha} e(t);\ \lambda, \alpha > 0 \\ C(s) &= \frac{U(s)}{E(s)} = K_p + K_i s^{-\lambda} + K_d s^{\alpha}; \end{aligned} \tag{4.8}$$

In Fig. 4.5, illustrations of the difference between classical PID and $PI^{\lambda}D^{\alpha}$ are provided. The plane in Fig. 4.5a depicts the advantage of fractional-order over integer-order controllers in terms of flexibility to graduate the integral/differential action. Classical integer-order controllers can only reach the four red dots, while the gray plane is reachable if real order operators are employed. A Bode plot is presented in Fig. 4.5b comparing the frequency response of PID and $PI^{\lambda}D^{\alpha}$ controllers with $K_p = K_i = K_d = 1$ with and $\lambda = 0.4$ and $\alpha = 0.8$ for the fractional-order PID (FO-PID).

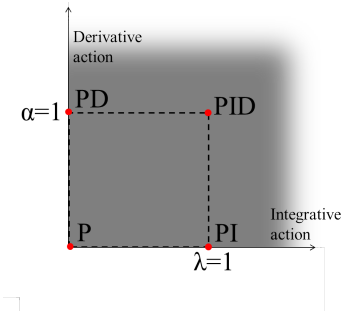

(a) Derivative/integral action plane

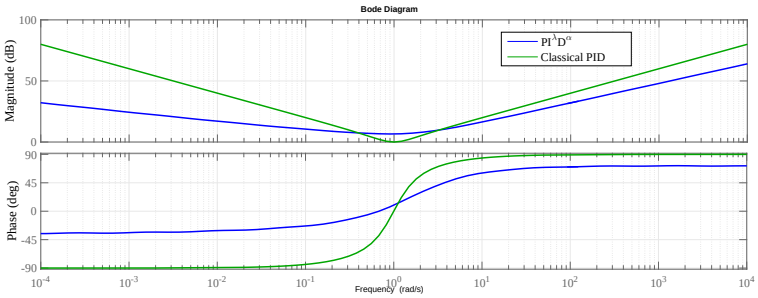

(b) Bode representation of a classical and fractional-order PID

Figure 4.5: Illustration of $PI^{\lambda}D^{\alpha}$ control nature

There is extensive literature on methods for tuning $PI^{\lambda}D^{\alpha}$ controllers for general purposes [Padula and Visioli, 2011], [Monje et al., 2004b]. One can observe that since the FO-PID accounts with two more parameters, a more flexible and moldable frequency response is achieved. The properties of FO-PID are as follows:

1. The phase delays or phase variation rate per decade can be varied in the range $[-\pi/2, \pi/2]$. For the differential operator, it provides a positive phase increment rate of $\frac{\alpha\pi}{4}$ rad/dec; while the integral operator contributes with a negative phase delay rate of $\frac{\lambda\pi}{4}$ rad/dec.
2. Regarding the magnitude increment/decrement that the differential and integral operator introduce, with this generalization the controller is capable to modify the open loop gain among the range $[-20, 20]$ dB/dec.

- **Fractional Lead-Lag Compensator**: The employment of fractional-order calculus over the controller form is not restricted to integral or differential operations. Instead, this technique proposes to extend the classical lead-lag compensation to an non-integer order one [Monje et al., 2004a]. Such compensator is of the form of:

$$C(s) = K_0 \cdot \left(\frac{1 + s/\omega_c}{1 + s/x\omega_c}\right)^{\alpha}; \alpha > 0 \tag{4.9}$$

where K_0 correspond to the compensator DC gain, ω_c is the zero central frequency and α the differentiation order. The parameter x defines whether the pole cuts off before or after the zero, thus defining the compensator nature: if $0 < x < 1$ it results on a lag compensator, while $x > 1$ brings a lead one.

4.2.1.2 Fractional-order control applications

In the literature and also in industrial systems, more and more applications can be found that employ of fractional-order calculus. A comparison of different types of fractional-order control techniques is provided in [Xue and Chen, 2002].

Thanks to advances in this calculus theory with improved methods for its appropriate implementation, great interest has been attired towards exploring its benefits over science and engineering fields. For instance, performing systems for market vehicle suspension have been designed with CRONE-based controllers [Oustaloup et al., 1996]. An entire research area that studies the application of fractional-order control over synchronized fractional and integer-order chaotic systems for several fields, showing promising results [Azar et al., 2017]. One can also find non-linear fractional-order-based control approaches as sliding mode control that have been applied for power electronic Buck converters (chapter 18 on [Monje et al., 2010]). Among others fractional-order control applications, one can find dynamic flexible manipulator control [Feliu and Ramos, 2005], hydraulic canal flux regulation through FO-PI controllers or DC servo-motor control [Luo and Chen, 2009]. Regardless the control technique or the application on which the system is applied, the loop stability must be studied since it is one of the fundamental objectives of feedback control systems.

4.2.1.3 Fractional-order systems stability

In this section, the stability theory of fractional-order systems is presented for further understanding of the control design objectives. First, a representation of a dynamic system is provided through a fractional-order differential equation as:

$$a_n \frac{d^{\alpha_n}}{dt^{\alpha_n}} y(t) + a_{n-1} \frac{d^{\alpha_{n-1}}}{dt^{\alpha_{n-1}}} y(t) + ... + a_0 y(t) = b_n \frac{d^{\beta_n}}{dt^{\beta_n}} u(t) + b_{n-1} \frac{d^{\beta_{n-1}}}{dt^{\beta_{n-1}}} u(t) + ... + b_0 u(t); \tag{4.10}$$

where the constants $a_n, ..., a_0, b_n, ..., b_0; \in \Re$ and the differentiation orders α_n and β_n decrease in magnitude as the index n decreases. In the frequency domain, the system results of the form:

$$G(s) = \frac{Y(s)}{U(s)} = \frac{b_n s^{\beta_n} + b_{n-1} s^{\beta_{n-1}} + ... + b_1 s^{\beta_1} + b_0}{a_n s^{\alpha_n} + a_{n-1} s^{\alpha_{n-1}} + ... + a_1 s^{\alpha_1} + a_0} = \frac{Q(s)}{P(s)} \tag{4.11}$$

If in the previously stated system, all of the derivation orders on the fractional-order polynomials that define $G(s)$ can be represented as integer multiples of a base order α–i.e. $\alpha_n, \beta_n = n\alpha$; $\alpha \in \Re^+$– the system is considered as of *commensurate order* [Chen et al., 2009]. Which means that Eq. 4.11 could be translated to:

$$G(s) = \frac{\sum_{p=0}^{n} b_p \left(s^{\alpha}\right)^p}{\sum_{p=0}^{n} a_p \left(s^{\alpha}\right)^p} \tag{4.12}$$

Furthermore, if the system not only is of commensurate order, but also a parameter q can be found for which $\alpha = 1/q$; $q \in Z^+$, then the system is called to be of *rational-order* [Monje et al., 2010]. A commensurate order system, can also be expressed through a fractional-order LTI state space representation as follows:

$$\begin{aligned} D_t^{\alpha} x(t) &= \mathbf{A}x(t) + \mathbf{B}u(t); \\ y(t) &= \mathbf{C}x(t) + \mathbf{D}u(t); \end{aligned} \tag{4.13}$$

where vectors $(x(t) \in \Re^n)$, $(u(t) \in \Re^r)$ and $(y(t) \in \Re^p)$ are the system states, input and output vectors; whose temporal evolution is defined by the matrices $\mathbf{A} \in \Re^{n \times n}$, $\mathbf{B} \in \Re^{n \times r}$, $\mathbf{C} \in \Re^{n \times p}$ and $\mathbf{D} \in \Re^{p \times r}$. If the variable change $s^{\alpha} = \delta$ is introduced, Eq. 4.13 can be related to the frequency response representation of the system $G(s)$ as:

$$\begin{aligned} G(s^{\alpha}) = G(\delta) = \frac{Y(\delta)}{U(\delta)} &= \mathbf{C}(\delta \mathbf{I} - \mathbf{A})^{-1}\mathbf{B} + \mathbf{D}; \\ G(\delta) &= \frac{\sum_{p=0}^{n} b_p \delta^p}{\sum_{p=0}^{n} a_p \delta^p}; \end{aligned} \tag{4.14}$$

which constitutes the commensurate order representation of the initial fractional-order system. Hence, one can study the stability condition for commensurate order systems through the polynomial charactersitic of the system $G(\delta)$, which is:

$$a_n \delta^n + a_{n-1} \delta^{n-1} + ... + a_1 \delta^1 + a_0 = 0; \tag{4.15}$$

which roots define the overall system stability. For integer-order systems–i.e. $\alpha \in Z^+$, the condition for the system to be stable is that all systems eigenvalues (which correspond to the roots of the characteristic polynomial) or system poles are placed in the left half of the complex plane. The generalization ofsuch definition for fractional-order systems is formally introduced through the Matignon's stability theorem [Matignon, 1998]:

A fractional-order transfer function given by $G(\delta) = P(\delta)/Q(\delta)$ is stable if and only if the following condition is satisfied:

$$|arg(\delta_i)| > \alpha \frac{\pi}{2}; \forall i \in [1, n],\ \delta_i \in \mathcal{C} \,/\, Q(\delta_i) = 0 \tag{4.16}$$

where δ_i is any of the poles of system $G(\delta)$. For $\alpha = 1$, the classical theorem for integer-order systems is met, stating that no pole is in the closed right half of the first Riemann sheet.

Therefore, one can illustrate the unstable and stable region for LTI fractional-order systems as presented in Fig. 4.6b in comparison to integer-order ones Fig. 4.6a.

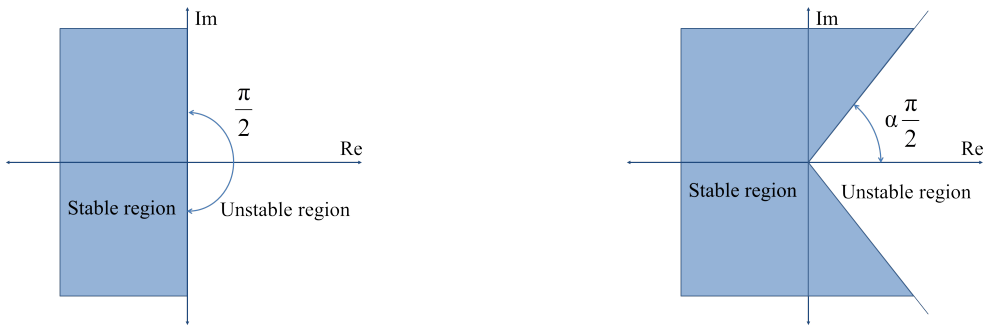

(a) Stability regions for integer-order LTI systems (b) Stability regions for fractional-order LTI sytems

Figure 4.6: Complex plane stability region comparison of integer and fractional order LTI systems

For a more detailed description of the stability theory of fractional-order systems, please refer to [Petráš, 2011], where an extensive explanation of the relation between fractional-order systems poles and Riemann sheets surfaces is provided. At the moment when the controller has been already designed, the next step is to effectively implement its structure over the employed embedded system. Since simulation environments can only resolve integer-order systems and algorithms are executed in the discrete-time domain, a correct translation to continuous and discrete time domain is required.

4.2.1.4 Fractional-order control implementation

FOC theory has seen great advances in recent years, but the practical implementation of FO operators for their employment in real applications has been a major challenge since 1960's. Although fractal circuits have surged as a solution for this, its tuning complexity and difficulty to couple with computer-based control hinder their employment. Ideally, infinite dimensional integer-order systems can perfectly approximate a fractional derivation, but in practice it would require infinite memory. For this reason, the approximations for FO operators are more effectively carried out through a finite dimensional integer-order function. This permits to have the desired performance either for simulations and stability study (continuous-time approximations) or even real implementations (discrete-time approximations), within the desired frequency range.

4.2.1.4.1 Continuous-time approximations Two main strategy types have been employed in the literature for modeling a fractional-order differentiation operator s^α in a continuous time expression. First, the Continuous Fraction Expansion (CFE) and rational approximation methods, used for function evaluations and interpolations respectively. The first method (CFE), which generally overcomes Power Series Expansion (PSE) methods in terms of convergence speed and larger domain, consists on approximating the function $G(s)$ as follows:

$$\hat{G}(s) \simeq a_0(s) + \cfrac{b_1(s)}{a_1(s) + \cfrac{b_2(s)}{a_2(s) + \cfrac{b_3(s)}{a_3(s) + \ldots}}} \tag{4.17}$$

where $a_i(s)$, $b_i(s)$ are rational functions of the Laplace operator s. In [Roy, 1967], a general method for CFE approximation can be found for the operator s^α through rational functions. Carlson's method [Carlson and Halijak, 1964] and Matsuda's method [Khoichi and Hironori, 1993]

are also other approaches based on rational functions, which seek a continuous time integer-order approximation of the fractional-order operator.

Recursive approximations or curve fitting-based methods have also provided good results in the literature. The Oustaloup recursive approximation method [Oustaloup and Coiffet, 1983], the most widely accepted technique for approximating the fractional-order derivation to continuous time integer-order function. The method consists on modeling a function $\hat{G}(s)$ from $G(s)$ in a given frequency range $[\omega_l, \omega_h]$), given as:

$$\begin{gathered} G(s) = s^{\alpha};\ \alpha \in \Re^{+}; \\ G(s) \simeq \hat{G}(s) = K \prod_{k=1}^{N} \frac{s+\omega_k'}{s+\omega_k}; \\ K = \omega_h^{\alpha};\ \omega_k' = \omega_l(\omega_h/\omega_l)^{\frac{2k-1-\alpha}{N}};\ \omega_k = \omega_l(\omega_h/\omega_l)^{\frac{2k-1+\alpha}{N}} \end{gathered} \tag{4.18}$$

where the resulting order of the function $\hat{G}(s)$ is N. This approximation is carried out for $\alpha \in (0, 1]$. For the cases where $\alpha > 1$, the approximation has to be modified as $s^{\alpha} = s^{n}s^{\gamma}$ where n is the integer immediately inferior to α, while γ is its rational part–i.e. $\alpha = n + \gamma$. This method provides a good approximation in the region of interests, as depicted in Fig. 4.7 for different sizes N and orders α.

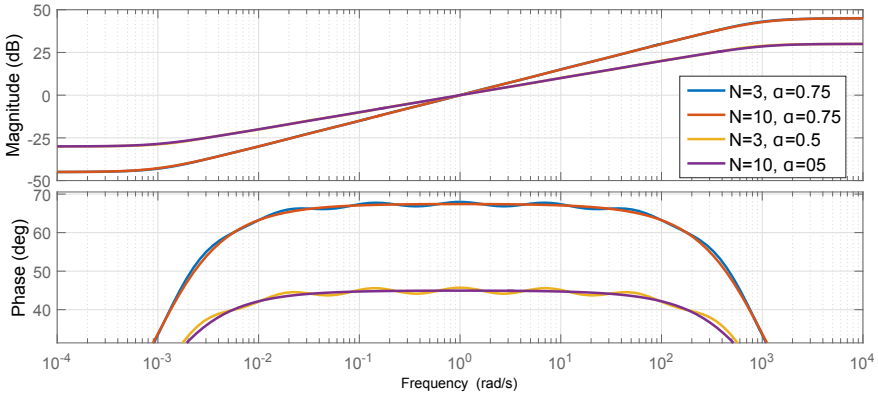

Figure 4.7: Illustration of Oustaloup recursive approximation

An improved version of this method is presented in chapter 12 of [Monje et al., 2010]. The major part of these methods are based on the action of interlacing zeros and poles along the negative real axis to recreate the shape of the fractional-order operator. For this work, Oustaloup method [Oustaloup et al., 2000] is employed for stability study, $\mathcal{H}_{\infty}$ norms' estimations and further frequency domain control analysis.

4.2.1.4.2 Discrete-time approximations For the case of discrete-time model approximations, there are two types of approaches that can be employed, *indirect* and *direct discretization*. In the former, a continuous time function is fitted in the frequency domain using one of the aforementioned methods, for a subsequent discretization of the fitted function. *Direct* methods employ PSE of he Euler operator, CFE of the Tustin operator or even numerical integration based methods.

Different interpretations have been proposed in the literature for translating the Laplace operator s as a function of the discrete-time operator z^{-1} and the sampling period Ts. Some of them are presented below:

$$\begin{aligned} Euler : s &= \frac{1-z^{-1}}{Ts} \\ Tustin : s &= \frac{2}{Ts}\frac{1-z^{-1}}{1+z^{-1}} \\ Simpson : s &= \frac{3}{Ts}\frac{(1-z^{-1})(1+z^{-1})}{1+4z^{-1}+z^{-2}} \\ Al-Alaoui : s &= \frac{8}{7Ts}\frac{1-z^{-1}}{1+z^{-1}/7} \end{aligned} \tag{4.19}$$

For instance, the Euler (backward difference) operator can be used with PSE for continuous to discrete approximation of the operator D^{α} as:

$$D^{\pm\alpha}(z) = \frac{Y(z)}{U(z)} = Ts^{\mp\alpha} PSE\left\{(1-z^{-1})^{\pm\alpha}\right\} \tag{4.20}$$

for which PSE$\{\cdot\}$ denotes the power series expansion, which at the end results in form of polynomials of z^{-1}. Signals $Y(z)$ and $U(z)$ are the $\mathcal{Z}$ transform of output and input time-domain signals $y(t)$ and $u(t)$ respectively. The Tustin (trapezoidal difference) operator can also be employed with this technique. Employing CFE, rational form functions of infinite impulse response-type (IIR) are obtained that, as for continuous time systems, converge faster than PSE in a larger frequency range. In this work, the Tustin operator is employed with CFE using the following expression:

$$D^{\pm\alpha}(z) = \frac{Y(z)}{U(z)} = \left(\frac{2}{Ts}\right)^{\pm\alpha} CFE\left\{\left(\frac{1-z^{-1}}{1+z^{-1}}\right)^{\pm\alpha}\right\} = \left(\frac{2}{Ts}\right)^{\pm\alpha} \frac{P_n(z^{-1})}{Q_n(z^{-1})} \tag{4.21}$$

where $P_n(z^{-1})$ and $Q_n(z^{-1})$ are polynomials of order n=1, 3, 5, 7 or 9. A comparison between discretization methods with different operators is provided in Fig. 4.8, supporting that CFE-Tustin results the most suitable method to discretize the fractional-order derivation operator. In [Vinagre et al., 2003], a more detailed description is provided about the discretization polynomials in function of their order n.

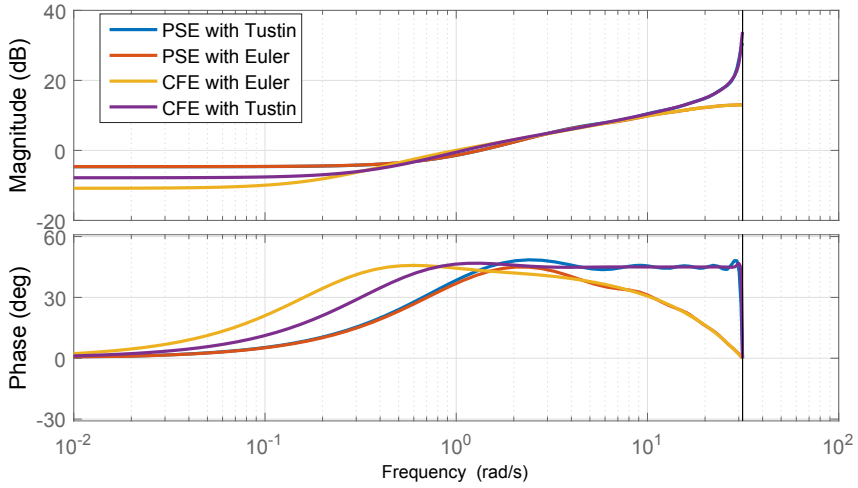

Figure 4.8: Bode plot of different discretization methods for a $s^{0.5}$ with polynomials order of n=9 for a sampling period of Ts=0.1s

4.3 Fractional-order-based car-following control

As stated in Sec. 4.1, the conception of feedback systems is fundamental when designing an automated car-following structure. The gap-regulation controller must be properly set, so the other blocks of the control structure can efficiently be coupled with the feedback controller. The benefits of fractional-order calculus for the design of feedback controllers have been explored in the work of [Hosseinnia et al., 2014], showing good results for ACC between two vehicles. This further encouraged to employ fractional-order controllers together with new and more exigent design methods and target control objectives.

Along this thesis, different controllers have been developed following several performance criteria and control applications. In the subsequent sections, the design methods are detailed.

4.3.1 String stability with reduced time gap

This first approach seeks to optimize the traffic capacity through lower time gaps, at the same time that strict $\mathcal{L}_\infty$-strict string stability is ensured with internal stability and constrained loop bandwidth [Flores and Milanés, 2018]. The design algorithm is applied over the structures depicted in Fig. 4.9:

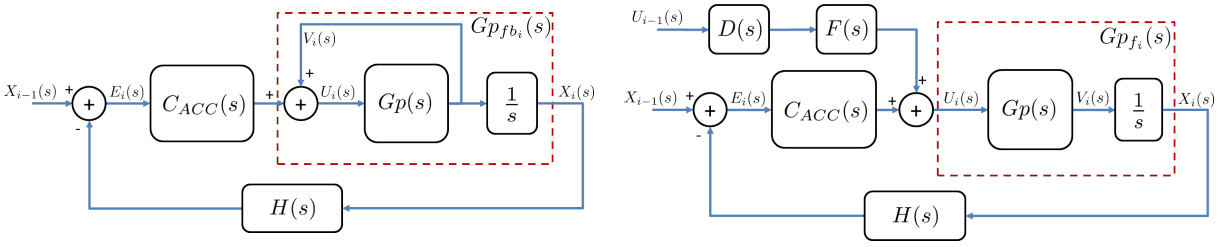

(a) ACC closed loop system

(b) CACC structure closed loop system

Figure 4.9: Control structures for ACC and CACC techniques

The blocks $D(s) = e^{-\theta s}$ and $H(s) = h \cdot s + 1$ represent the communication temporal delay and constant time gap spacing policy. For ACC car-following $Gp_{fb_i}(s)$ is considered as the controlled plant (red dashed square on Fig. 4.9a), while $Gp_{f_i}(s)$ is taken into account for the CACC design (red dashed square on Fig. 4.9a).

4.3.1.1 Control objectives

The considered controller for the application of the design algorithm is the so-called fractional-order proportional-derivative (FOPD) controller. Its form is described as follows:

$$C(j\omega) = K_p \left(1 + j\frac{\omega^\alpha}{\omega_c}\right); \forall \omega > 0 \tag{4.22}$$

The FOPD controller design procedure is aimed not only to ensure the loop stability for the gap-regulation task with a desired system bandwidth and phase margin, but also to increase the string stability when applied on a homogeneous string of vehicles. To achieve so, the procedure demands to obtain the optimal configuration of the controller gain Kp, central frequency ω_c and the differentiation order α to fulfill the three requirements: maintain the vehicle response bandwidth when closing the loop, a desired phase margin and guarantee the string stability for the lowest time gap possible.

4.3.1.2 Methodology

The estimation of the system bandwidth and phase margin when applying the CTG policy is studied over the loop expression $L_{ACC}(s) = Gp_{fb}(s)C(s)H(s)$. Its gaincross frequency ω_{gc} should be similar to the vehicle's one (it is proposed $\omega_{gc} = \omega_n \pm 0.1\,rad/sec$), lower values of ω_{gc} limit the system reaction speed and higher values may lead to actuator saturation and non-linearities consequently. A phase margin of $\phi = (60 \pm 1)^\circ$ is targeted so the system is robust and stable, but not overdamped so it loses output-to-reference convergence speed. For ACC, the string stability requirement is analyzed over the closed loop response of the structure in Fig. 4.9a, which results as:

$$||\Gamma_{ACC}(s)||_\infty = \left|\left|\frac{X_i(s)}{X_{i-1}(s)}\right|\right|_\infty = \left|\left|\frac{C(s)Gp_{fb}(s)}{1 + C(s)Gp_{fb}(s)H(s)}\right|\right|_\infty \leq 1;\ i \geq 2 \tag{4.23}$$

For CACC, where communication links are available, the string stability is studied over the closed loop response of structure in Fig. 4.9b, given by:

$$||\Gamma_{CACC}(s)||_\infty = \left|\left|\frac{X_i(s)}{X_{i-1}(s)}\right|\right|_\infty = \left|\left|\frac{D(s)F(s) + C(s)Gp_f(s)}{1 + C(s)Gp_f(s)H(s)}\right|\right|_\infty \leq 1;\ i \geq 2 \tag{4.24}$$

To retrieve the controller parameters, an optimization algorithm is executed for different values of h using the Matlab command $fsolve$, which allows to solve multi-objective non-linear optimization problem. The function to minimize results from the design requirements and interpreted as follows:

$$F(h) = w_1 \cdot |\omega_{gc} - \hat{\omega}_{gc}| + w_2 \cdot |\phi - \hat{\phi}| + w_3 \cdot (||\Gamma(s)||_\infty - 1.00); \tag{4.25}$$

where $F(h)$ is the weighted function to be minimized for a given time gap h, $\hat{\omega}_{gc}$ the desired loop bandwidth, $\hat{\phi}$ the desired phase margin and $\Gamma(s)$ is the closed loop response of the system–i.e. $\Gamma_{ACC}(s)$ for ACC and $\Gamma_{CACC}(s)$ for CACC–. The general guideline to set the weights w_1, w_2 and w_3 is to define a considerably higher cost to the string stability condition, given that it is strictly required that $||\Gamma(s)||_2 \leq 1$.

The algorithm is executed lowering the time gap until a Pareto-front is reached and one or more design requirements are no longer fulfilled due to the more demanding performance necessary to hold shorter time gaps. If a lower time gap is desired with string stable performance, one of the other design requirements must be relaxed.

4.3.2 Robustness against plant gain variations

The control approach is focused on designing feedback control to be employed over automated cooperative car-following systems [Flores et al., 2016]. Among the entire speed range, the low level control block in Eq. 3.9, might slightly change its behavior due to gear shift or limited dynamic response. This changes are reflected on the plant DC gain K_0, which can either increase or decrease with respect to the considered nominal value. This development is mainly focused for CACC applications, where the DC gain has higher impact on the loop response. For ACC systems, the inner feedback loop in Fig. 3.2 provides the necessary robustness towards these uncertainties.

4.3.2.1 Control objectives

This algorithm focuses on designing a high level control layer that ensures that the desired loop stability is maintained, even if small changes in the plant gain are faced due to modeling uncertainties. It considers the low level control layer as the plant upon which the control signal is applied. The development is carried out in the framework of structure in Fig. 3.2. Generally, PD controllers are employed in car-following applications, which have demonstrated stabilizing properties with fast responses. The proposed controller is a FOPD with a cutoff filter, profiting from its damping capabilities and flexibility to define not only the central frequency location, but also the contribution in phase and magnitude due to its non-integer differential order. The proposed controller form is as follows:

$$C(s) = \frac{K_p + K_d \cdot s^{\alpha}}{1 + h \cdot s};\ K_p, K_d, \alpha, h > 0 \tag{4.26}$$

If the Euler identity is employed over this expression, the fractional-order controller can be rewritten as:

$$C(j\omega) = \left[Kp + Kd\left(\omega^{\alpha} cos\left(\frac{\alpha\pi}{2}\right) + j\omega^{\alpha} sin\left(\frac{\alpha\pi}{2}\right)\right)\right] \cdot (1 + jh\omega)^{-1} \tag{4.27}$$

where K_p, K_d, α, and h are the proportional gain, derivative gain, differentiation order and time gap respectively. Since the feedback loop response $L(j\omega) = Gp_f(j\omega)C(j\omega)H(j\omega)$ defines the control stability, it is considered following the structure in Fig. 3.2. The study is done at the gaincross frequency ω_{gc} since it defines the phase margin and the loop bandwidth. The plant $Gp_f(j\omega)$ takes the form of Eq. 4.28:

$$Gp_f(s) = Gp(s)/s = \frac{K_0\omega_n^2}{s(s^2 + 2\xi\omega_n s + \omega_n^2)}; \tag{4.28}$$

Since the controller accounts with three parameters for tuning, three control specifications are set as follows:

1. Guarantee a desired phase margin for system stability, $\phi_m \approx \frac{\pi}{4}$ rad:

$$arg(L(j\omega_{gc})) = -\pi + \phi_m \tag{4.29}$$

2. Make the loop response within the vehicle low level bandwidth to avoid actuator saturation. In other words, open loop gaincross frequency $\omega_{gc} \approx \omega_n$:

$$|L(j\omega_{gc})|_{dB} = 0 \tag{4.30}$$

3. Ensure fractal response with flat phase on gaincross frequency, or robustness to plant gain variations:

$$\left(\frac{d(arg(L(j\omega))}{d\omega}\right)_{\omega=\omega_{gc}} = 0 \tag{4.31}$$

4.3.2.2 Methodology

The first two design specifications are set to guarantee the controller bandwidth and the phase margin. The third design specification, which aims on having a flat phase around the gaincross frequency, guarantees the good performance to a certain type of unmodeled dynamics–i.e. model

gain changes will not reduce the phase margin–. For the first step in the controller design, the plant gain and phase can be described as presented in Eq. 4.32 and 4.33 respectively.

$$|Gp_f(j\omega)| = \frac{\omega_n^2}{\omega\sqrt{\omega_n^4 + 4\xi\omega_n^2 - 2\xi\omega_n^2\omega^2 + \omega^4}} \tag{4.32}$$

$$arg(Gp_f(j\omega)) = -\frac{\pi}{2} - tan^{-1}\left(\frac{2\xi\omega}{\omega_n^2 - \omega^2}\right); \tag{4.33}$$

It is important to highlight that the employed controller in Eq. 4.26 employs the inverse of spacing policy $H(j\omega)$ to cancel the effect of the outer feedback loop. This is done to produce a loop stability that is independent from the reference time gap. In the same line, the gain and phase of the controller with the spacing policy are determined through the Eq. 4.34 and 4.35.

$$|C(j\omega)H(j\omega)| = \sqrt{K_p^2 + 2K_pK_dcos\left(\frac{\alpha\pi}{2}\right) + K_d^2\omega^{2\alpha}} \tag{4.34}$$

$$arg(C(j\omega)H(\omega)) = tan^{-1}\left(\frac{K_d\omega^\alpha sin(\frac{\alpha\pi}{2})}{K_p + K_d\omega^\alpha cos(\frac{\alpha\pi}{2})}\right) \tag{4.35}$$

Eq. 4.34 and 4.32 are put into Eq. 4.30; to derive the expression that ensures the loop gaincross frequency condition.

$$\frac{\omega_n^4 \cdot K_p^2 + 2K_pK_dcos\left(\frac{\alpha\pi}{2}\right) + K_d^2\omega_{gc}^{2\alpha}}{\omega^2\omega_n^4 + 4\xi\omega_n^2 - 2\xi\omega_n^2\omega_{gc}^2 + \omega_{gc}^4} = 1 \tag{4.36}$$

To study the loop stability condition, the Eq. 4.33 and 4.35 are used with Eq. 4.29 to ensure the phase margin.

$$-\frac{\pi}{2} - tan^{-1}\left(\frac{2\xi\omega_{gc}}{\omega_n^2 - \omega_{gc}^2}\right) + tan^{-1}\left(\frac{K_d\omega_{gc}^\alpha sin(\frac{\alpha\pi}{2})}{K_p + K_d\omega_{gc}^\alpha cos(\frac{\alpha\pi}{2})}\right) = \phi_m; \tag{4.37}$$

Finally, the third condition for the design algorithm corresponds to the flat phase around the gaincross frequency. It regards the differentiation of Eq. 4.37 over the frequency axis:

$$\frac{K_pK_d\alpha sin(\frac{\alpha\pi}{2})\omega_{gc}^{\alpha-1}}{K_p^2 + 2K_pK_dcos(\frac{\alpha\pi}{2})\omega_{gc}^\alpha + K_d^2\omega_{gc}^{2\alpha}} = \frac{2\omega_{gc}(\omega_n^4 - 2\omega_n^2\omega_{gc}^2 + \omega_{gc}^4)}{(\omega_n^4 - 2\omega_n^2\omega_{gc}^2 + \omega_{gc}^4 + 4\xi^2\omega_n^2)cos\left(\phi_m - \frac{\pi}{2} + \tan^{-1}\left(\frac{2\xi\omega_n}{\omega_n^2 - \omega_{gc}^2}\right)\right)}; \tag{4.38}$$

Given the procedure described previously, one obtains a non-linear equation system composed by Eq. 4.36-4.38. To retrieve the controller values, an optimization algorithm is used–e.g. *fsolve* from MATLAB optimization toolbox, with the *lsqnonlin* method–. Given that the problem is interpreted as a non-convex optimization algorithm, where one can find local or sub-optimal solutions, several seeds are tested until a solution is found that satisfies the aforementioned specifications.

4.3.3 Loop shaped fractional-order compensator

The main purpose of this control design algorithm is to shape the loop response $L(s)$ to fulfil different closed loop performance criteria over the CACC structure in Fig. 4.9b. For control applications, the ideal loop shape that is desired is as shown in Fig. 4.10a. The Nyquist principle is taken into consideration for the analysis of system sensitivity, to meet robustness and stability

requirements. It studies the proximity of closed loop transfer function denominator (see Eq. 4.24) to zero. In other words, corresponds to the distance between the loop $L(j\omega)$ and the critical point $(-1, j0)$ in the complex plane, as depicted in Fig. 4.10b. The general enhancement with respect to previous points is that the present approach seeks not only to satisfy three robust performance criteria, but also the controller transfer function along the entire frequency axis is analyzed. For this task, template functions are used to shape the loop and consequently the controller form with respect to the proposed objectives.

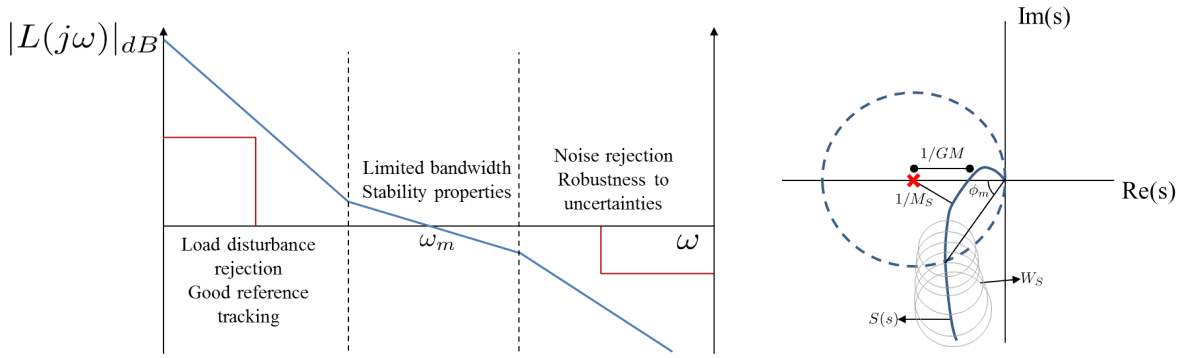

(a) Ideal loop $L(j\omega)$ magnitude shape

(b) Nyquist plot of the loop sensitivity $S(j\omega)$

Figure 4.10: Loop shaping principles with robustness study over the system sensitivity

4.3.3.1 Control objectives

The performance objectives can be described as follows:

- Strict $\mathcal{L}_\infty$ string stability and high frequency noise rejection. The string stability condition requires that for the entire frequency range, preceding vehicle oscillations are attenuated upstream in form of a filter $H(s)^{-1}$ in the ideal case, described by the time gap. Such expression can also be understood in the framework of this work, as the complementary sensitivity or string stability function $\Gamma_i(j\omega) = T_i(j\omega) = \frac{X_i(j\omega)}{X_{i-1}(j\omega)}$. Hence, to meet the requirements in [Ploeg et al., 2014b], template function is defined as:

$$W_T(j\omega) = 1; \forall\omega > 0 \tag{4.39}$$

  Generally, for control systems the complementary sensitivity is a first order low pass filter, but since strict $\mathcal{L}_\infty$ string stability is required for the closed loop response, the limit is set as one for the entire frequency range. Similar approach has been proposed in [Ploeg et al., 2014a].

- Disturbance rejection within the system loop bandwidth. The possible modeling errors may cause that the overall behavior is harmed, for this reason, the control loop must reject the possible uncertainties over the ego-vehicle low level control layer or feedforward term. It is important to highlight that the robustness to disturbances is dependant on Bode's Sensitivity Integral principle. It states that the frequencies for which $|S(j\omega)| < 1$ are balanced over those where the $|S(j\omega)| > 1$. The system sensitivity in this case is considered as $S_i(j\omega) = \frac{E_i(j\omega)}{X_{i-1}(j\omega)}$. The suggested sensitivity template function considers this is in the form of:

$$W_S(j\omega)^{-1} = \frac{j\omega}{\omega_S + j\omega/M_S}; \forall\omega > 0 \tag{4.40}$$

where the bandwidth or frequency region for which disturbance rejection is desired is given by $\omega_S \approx \omega_n$. M_S refers to the maximum magnitude value permitted for the sensitivity.

- Reduced control effort and saturation avoidance. High frequency noise may induce that the actuators are overemployed in the reference tracking process. The control effort behavior is studied through the term $C_i(j\omega)S_i(j\omega) = \frac{U_i(j\omega)}{X_{i-1}(j\omega)}$. Its ideal behavior is thus shaped using the template function:

$$W_U(j\omega)^{-1} = \frac{\omega_u}{j\omega + \omega_u/M_u} \forall\omega > 0 \tag{4.41}$$

where ω_u is the spacing error roll off frequency. The peak magnitude M_U defines the maximum allowed control effort change with respect to a given reference change, which is desired to be at low frequencies. The magnitude and bandwidth limitation of this transfer function ensures that the vehicle low level actuators $Gp_i(s)$ are not demanded over their operational limits.

4.3.3.2 Methodology

A different type of controller is considered for this design method, to meet the loop shaping requirements. Since car-following feedback controllers should be lead-based to provide stability, a lead compensator is suggested. Furthermore, fractional-order calculus is applied to derive a fractional lead compensator. The controller transfer function is as follows:

$$C(j\omega) = Kp\left(\frac{1 + j\frac{\omega^\alpha}{\omega_c}}{1 + j\frac{\omega^\delta}{\omega_p}}\right); Kp > 0; \omega_p > \omega_c > 0; \delta > \alpha > 0 \tag{4.42}$$

The parameters are determined by translating the control objectives into a minimization problem. It consists on using the template functions with the loop transfer functions to get the optimal parameters configuration of the controller in Eq. 4.42. Let consider $\mathcal{S}$ the set of compensator parameters that exist in the space $\Re^+$–i.e. $\mathcal{S} = \langle Kp, \omega_c, \omega_p, \alpha, \delta\rangle$–. The optimization algorithm is based on minimizing the following cost function:

$$F(\mathcal{S}) = \cdot\|W_T T(j\omega)\|_\infty + \cdot\|W_S S(j\omega)\|_\infty + \cdot\|W_U C(j\omega)S(j\omega)\|_\infty; \tag{4.43}$$

The function $F(\mathcal{S})$ is evaluated through a non-convex optimization process, over different seeds of Θ and surveying their convergence. This procedure allows to avoid getting stocked on not local minima that provide non-satisfying solutions in terms of the design criteria. Hence, the desired solution is formally expressed as:

$$\hat{\mathcal{S}} = \arg\min_{\mathcal{S}}(F(\mathcal{S})); \tag{4.44}$$

where the resulting parameters configuration $\hat{\mathcal{S}}$ is employed to define $C(j\omega)$. It is important to highlight that since the controller design is closed-loop-based, the definition of $S(j\omega)$ and $T(j\omega)$ requires to set car-following operational values. These are the desired time gap h to define $H(s)$ and the maximum communication delay $\theta = \theta_{max}$ that the V2V network could present. This

assumption is taken to ensure a control design that is robust to communication losses. For values different than θ_{max}, the overall closed loop performance improves as θ decreases.

All of the aforementioned algorithms are proposed for designing a gap-regulation system that commands a low level control layer in function of different expected behaviors. Each of them target different performance objectives related to reference tracking capabilities, robustness to disturbances or stability, at the same time that actuators limited bandwidth and operational limits are considered. The developed controllers are conceived for ACC and CACC techniques, employed over the structure presented in Fig. 3.2.

In the same framework, the proposed high level feedback controllers can be employed with a variable time gap spacing policy as the one presented in chapter 3, or within a more complex framework as the one presented for urban cooperative car-following in Sec. 3.4. The modularity of the proposed control structure in Fig. 3.2 permits that any of the selected control systems developed along this chapter can be employed therein, in function of the desired performance objectives.

4.4 Discussion

This chapter has been oriented to the design and implementation of feedback control systems for gap regulation of homogeneous ACC and CACC strings. The conception of more performing controllers with an accurate frequency response, motivated to explore the benefits of extending from integer to real-order controllers for the gap regulation task. An extensive review is provided about the fractional-calculus theory, its origins and some scientific areas where it has been applied. Control techniques as CRONE, TID Control, $PI^{\lambda}D^{\alpha}$ and fractional lead-lag compensation; have been proposed and applied to real solutions, demonstrating the usefulness of non-integer order systems. To study fractional-order linear systems stability, two main methods have been depicted: study the commensurate order system poles placement and approximate the fractional-order differentiation operator to an integer order polynomial using CFE or Oustaloup approximations. An overview of the discrete-time approximation methods for implementing fractional-order derivation on real embedded controllers is provided, concluding that CFE based on Tustin operator transformation performs sufficiently good for this work.

It has been widely demonstrated in the literature that for car-following gap regulation, lead-based controllers perform the best. For this reason, one of the major contributions of this work is focused on the proposal of three novel methods for designing feedback fractional-order lead control systems. The first one proposes a method to design ACC and CACC FOPD controllers based on a Pareto front-seeking algorithm that minimizes the time gap, while keeping string stable behavior and loop stability and bandwidth. The second algorithm seeks the design of a FOPD that permits a flat phase in the surroundings of the gaincross frequency, guaranteeing robustness to loop gain changes and the desired phase margin. The last proposed method consists on shaping the loop magnitude through a fractional-order lead compensator based on the desired loop sensitivity, string stability and control effort function. Template functions are employed to define the required objectives, which are further used in the $\mathcal{H}_{\infty}$-norm optimization of the loop shaping functions.

The main contribution presented in this chapter has been the proposal of design algorithms for different feedback control systems, focusing on important performance objectives that extend the car-following control capabilities. Special focus has been put on the string stability performance, due to its great importance defining traffic behavior, capacity and safety. For this task, the employment of fractional-order calculus has been encouraged due to its proven potential to attain more flexible and accurate frequency responses. To guarantee the correct implementation of the

designed control systems, two conditions are required: 1) knowledge of the vehicle longitudinal behavior and its uncertainties, 2) validate that the CFE expansion of the fractional-order operator successfully represents the desired operator theoretical frequency response.

Chapitre 5

Contrôle des convoies hétérogènes

Below is a French summary of the following chapter "Heterogeneous strings control".

Dans le chapitre précédent, la conception des systèmes de régulation de l'espacement est examinée pour le cas où les véhicules du convoi sont des dynamiques identiques. Par contre, lors que les véhicules présentent différents réponses au même stimulus, cet assomption n'est plus valable. Pour étendre l'utilisation des techniques de car-following automatisé et connecté, il faut permettre la formation des séries des véhicules avec dynamiques hétérogènes. Ce chapitre traite le problème de la commande des convois hétérogènes à travers l'emploi des systèmes de contrôle en feedforward. D'abord, l'état-de-l'art du contrôle des convois hétérogènes est résumé, ainsi que les problèmes qui restent à résoudre et qui sont ciblés lors de ce travaux de thèse. La stratégie proposée demande une modélisation en temps réel des dynamiques du véhicule précédant, permettant l'adaptation de la structure en fonction de cela et la garantie de la performance désirée malgré la différence des véhicules.

Un filtre des particules est proposé pour la modélisation 'online', dont sa sortie est utilisé pour adapter le filtre feedforward. Deux topologies sont analysées: 1) celle où chaque véhicule est connecté qu'avec son véhicule précédent, 2) celle où tous les véhicules se communiquent avec le premier véhicule du convoi (leader) et son immédiatement précédant. Ce dernier approche a pour but d'éviter la sur-amplification de la consigne venant du véhicule précédant, ce qui pourrait emmener à saturer les actionneurs du véhicule. La forme des filtres feedforward est présentée pour les deux topologies, ainsi que l'algorithme pour concevoir ses paramètres. Finalement, une discussion sur les développements de ce chapitre est fournie, avec les conclusions dérivés.

Chapter 5

Heterogeneous Strings Control

In the previous chapter, focus was put on developing feedback control algorithms following different performance objectives in function of the desired string behavior. So far, the strongest assumption that has been done is that all vehicles that belong to the string account with the same dynamics, and hence same feedback controller, FF filter and spacing policy. Most of developments over automated car-following take this assumption as well, stating that the preceding vehicle's low level control layer performs similarly enough so it can be assumed equal as the ego–i.e. $Gp_{i-1}(s) = Gp_i(s)$. This assumption simplifies significantly both the string control development and stability study, specially for predecessor-only following (PF) topologies. For this strategy, the performance would result similar and replicated for every vehicle index $i \in [2, n]$ being 1 the index of leader and n the size of the string formation. It would require that all vehicles' actuator lags and delays should be identical, hindering for instance a possible cooperation between heavy duty trucks and conventional passenger cars. As a consequence of this assumption, most of car-following systems are restricted only for strings or platoons where all vehicles have very similar dynamics.

Relaxing this assumption permits to contemplate different type of vehicles on the same formation (see Fig. 5.1). This is fundamental to further expand the impact of automated car-following applications, knowing that in reality vehicles account with non-identical dynamics. The possibility of vehicles of different types to cooperate as a platoon, would significantly increase the number of strings that could be formed both on highways and urban scenarios. For this reason, the case where $Gp_{i-1}(s) \neq Gp_i(s)$; $\forall\, i \in [2, n]$ is not only of great interest in most recent works of cooperative automated driving, but also the main focus of this chapter.

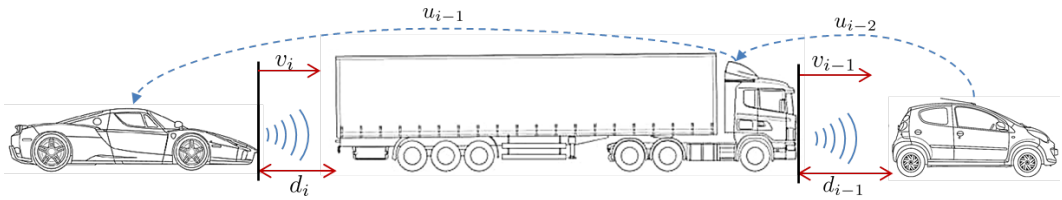

Figure 5.1: Illustration of a heterogeneous string of vehicles performing car-following under a PF topology

The rest of this chapter is structured as follows. First, the motivation of focusing on mixed strings is described in Sec. 5.1. A literature review of heterogeneous strings control strategies is provided in Sec. 5.2. In Sec. 5.3, a novel approach is proposed to profit from the FF link to enhance the car-following overall performance, aiming to mitigate the disturbances introduced by the difference in adjacent vehicle dynamics. For a first approach, only information from the

predecessor vehicle (PF topology) is considered to seek a solution that permits boundless platoon size. Subsequently, a novel leader-predecessor-following (LPF) algorithm is proposed in Sec. 5.4 to investigate the possible benefits of its employment in the control structure. Conclusions of the proposed approaches are discussed in Sec. 5.5

5.1 Motivation

There are two main differences between the control of homogeneous and heterogeneous strings over CACC. 1) The assumption of identical plant response is no longer valid, for which the coupling between vehicles become more complex. 2) Disturbances propagation in upstream direction are closely dependent on each of the string elements dynamics and their relation, evolving differently than for identical vehicles. For instance, in [Sheikholeslam and Desoer, 1992b] it has been demonstrated through time domain simulations that spacing errors are not propagated uniformly in a string of non-identical vehicles. In reality, not only the vehicle actuators' lags and possible delays are relevant to design the control system, but also to be aware of possible actuator saturation and difference in the braking capabilities.

When performing CACC over consecutive vehicles that are different, the reference speed that is sent through the V2V link is not tracked symmetrically by both vehicles. Hence, even if no communication delays are present, the same reference speed would produce different follower vehicles' speeds $v_{i-1}(t)$ and $v_i(t)$, in contrast with the homogeneous case where both speeds will evolve symmetrically. Since the inverse model FF approach is possible with the employment of V2V links, the performance results highly dependent on the precision over the vehicle model. So far, the assumption of all vehicles with the same dynamics has made possible to use a simple first order filter as the FF transfer function. For heterogeneous cases, more complex real-time processing is required over the information that arrives through the FF link to ensure the desired car-following performance. In recent years, this issue has been gaining more interest and solutions have been proposed in the literature to mitigate the effects of non-identical dynamics. A state-of-the-art review is provided of current developments on heterogeneous strings control.

5.2 State-of-the-art of heterogeneous strings control

Research on car-following of non-identical vehicles is a relatively recent topic, since most of prior efforts were put on homogeneous formations. Among the first attempts for having non-identical vehicles in the same string, one can find that in projects Energy ITS [Tsugawa, 2013] and SARTRE [Chan et al., 2012] platooning application systems have been demonstrated over mixed traffic. Nevertheless, most of performed tests were over focused on validating the platooning logistics and communication protocols, without determining the control capabilities and limits of the operational system on the different vehicles. On the more recent projects GCDC 1 [Ploeg et al., 2012] and 2 [Ploeg et al., 2018], CACC over passenger vehicles and trucks was demonstrated showing promising results and the feasibility of CACC over mixed strings with different technologies.

Although these advances have encouraged to put more efforts on developing CACC for mixed formations, the exploration of solutions that ensure individual and string stability for any configuration were still a remaining issue. Bounded string stability of spacing errors was studied in [Shaw and Hedrick, 2007b], [Shaw and Hedrick, 2007a] through the usage of a LPF topology for a constant spacing strategy. Regretfully, only time-domain simulations are presented and strict $\mathcal{L}_\infty$ string stability is not demonstrated as well as robustness to possible communication delays. Another LPF strategy is proposed in [Rödönyi, 2015], where also robust string stability is studied

for different string configurations, yet effects of communication temporal delays are not considered. A direct model predictive control is developed in [Zheng et al., 2017] and tested in simulation over vehicles with slightly different parameters and small speed changes. Good results were shown for constant spacing under PF, LPF, two-PF and two-predecessor-leader-following, although model uncertainties are not considered in the receding horizon strategy as well as communication losses. In [di Bernardo et al., 2015], a consensus control-based approach is implemented in simulation showing asymptotic stability. An adaptive switched control approach is investigated in [Harfouch et al., 2017] and validated through numerical tests with communication losses, but string stability is not guaranteed during the switching transitions. Heterogeneity in the sense of communication connectivity is analyzed in [Zhang and Orosz, 2016], showing robustness to network failures while only weak string stability is ensured and safety is also compromised. A sliding mode control is proposed in [Guo et al., 2016] with a leader following constant spacing strategy, where global stability is demonstrated but string stability and robustness to initial conditions remain unsolved.

Robust control approaches are proposed in [Gao et al., 2015], [Gao et al., 2016] that employ $\mathcal{H}_\infty$ notions to design a CTG-aimed platoon control that deals with heterogeneity as model uncertainties. The main issue comes when the difference between adjacent vehicles' models is high enough to exceed the robustness bounds. For this reason, FF strategies have been investigated in several works for their benefits and implementation simplicity. For instance, [Wang and Nijmeijer, 2015a] proposed for the first time to implement a FF filter that depends on both the preceding and ego vehicle model. Similar approach is presented in [Al-Jhayyish and Schmidt, 2018], where three different types of FF strategies are implemented to evaluate the potential benefits over strings of non-identical vehicles. In both works the contribution is demonstrated for control systems of heterogeneous strings, providing a string stability region where communication delays and time gap conditions are stated.

5.2.1 Proposed design considerations

Even though these approaches have provided different good results with both benefits and drawbacks, they encourage to pursue a solution to improve the impact of heterogeneous cooperative strings. Some work objectives can be stated in function of the aforementioned work contributions, setting the guidelines followed during the development of this section work:

- Strict $\mathcal{L}_\infty$ string stability must be ensured regardless the dynamics of the preceding and ego vehicles. This condition should be maintained for all possible combinations of fast, medium and slow vehicles (being the reaction speed proportional to the vehicle low level bandwidth ω_n).
- Safety towards rear-end collision in case of leader vehicle speed change must be guaranteed. This requirement must not lead to large inter-distances so benefits of traffic capacity increase are harmed.
- The proposed solution should not only be robust to communication temporal delays but should also require simple communication network topology–e.g. PF or LPF–.
- Yield the desired string performance in terms of states propagations. Since the CTG is adopted for this work, the behavior of the ego-vehicle should be a filtered version (with $1/H(s)$) of the preceding vehicle states

Given that the chosen spacing policy defines not only the geometry of the string, but also the stability of the car-following control system, the choice of desired time gap is fundamental for the

string performance. Besides, shortening the time gap between vehicles increases traffic throughput and fuel saving capabilities, but could also lead to string unstable behavior and unsafe operation. The latter is of highest importance, given that in case of a braking stop of the preceding vehicle, the ego-vehicle must be able to brake with no rear-end collision. The main condition stated for the design of the spacing strategy is that all vehicles should keep inter-distances in the full speed range that are collision free. To assess a time gap value that is safe for all vehicles to track, the braking scenario is recalled.

For this case, since the string is composed by non-identical vehicles, the maximal decelerations that each of them can reach may not be the same. A consequence of this is that the required braking distance will not only depend on the reaction time but also on the ego and preceding vehicles deceleration capacities–i.e. $B_{max_i} \neq B_{max_{i-1}}$. An illustration of this condition is presented in Fig. 5.2a and 5.2b, where braking scenarios are illustrated for vehicles with different braking capabilities.

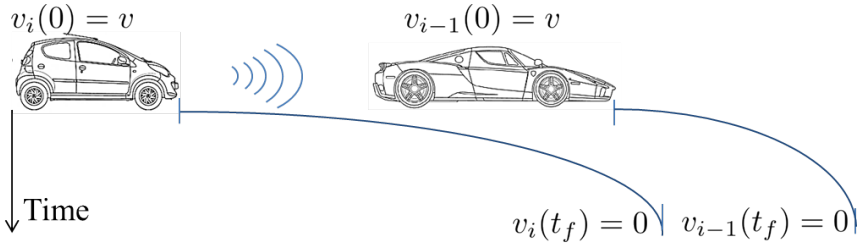

(a) Ego vehicle has less braking capacity than the preceding one

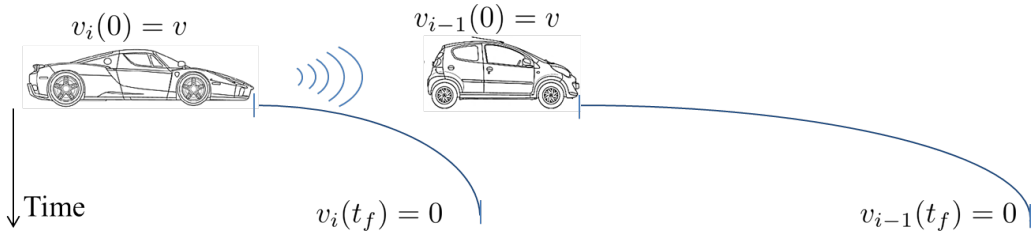

(b) Ego vehicle has more braking capacity than the preceding one

Figure 5.2: Non-identical ego and preceding vehicles' trajectory evolution over time during a braking scenario

One can observe that when the ego vehicle accounts with higher deceleration capabilities (Fig. 5.2a), the final inter-distance at the stopping point results higher than in the less favorable case (Fig. 5.2b). This phenomenon can be mathematically modeled by extending Eq. 3.22, assuming different braking capabilities to derive the safe inter-distance area in the ego-speed vs. spacing gap plane:

$$d_{ref}(v) \geq \tau_i v + \frac{B_{max_i} v}{J_{max_i}} - \frac{B_{max_i}^3}{6J_{max_i}^2} + \frac{v^2}{2B_{max_i}} - \frac{B_{max_{i-1}} v}{2J_{max_{i-1}}} + \frac{B_{max_{i-1}}^3}{8J_{max_{i-1}}^2} - \frac{v^2}{2B_{max_{i-1}}}; \tag{5.1}$$

where it is visible that the terms quadratically dependent on the speed, are no longer canceled due to $B_{max_i} \neq B_{max_{i-1}}$ and $J_{max_i} \neq J_{max_{i-1}}$. Hence, the minimum braking distance to ensure no collision is illustrated for three cases in Fig. 5.3. For an ego vehicle that can reach lower deceleration rates (orange line), a spacing gap that increases quadratically is required as the speed is higher. On the other hand, if the preceding vehicle has less braking capacities (yellow line),

the spacing gap decreases quadratically from the initial value. The general guideline to chose the desired time gap (which is the inter-distance vs. speed curve slope) is to yield a spacing gap that satisfies Eq. 5.1 in the speed range of interest. This is done considering the worst ego-preceding vehicle combination in the string, to ensure that no collision may occur in a possible braking situation.

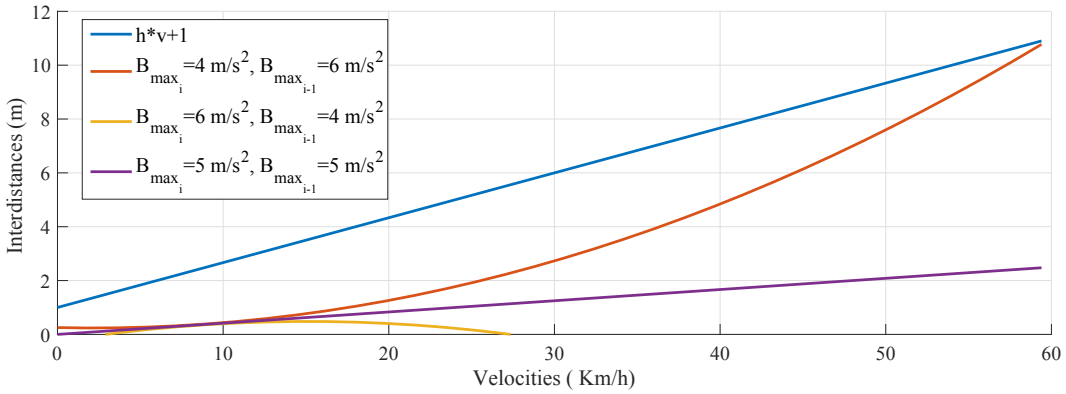

Figure 5.3: Illustration of three possible braking scenarios, varying ego and preceding braking capabilities (orange, purple and yellow lines). Resulting safe CTG spacing policy (blue line)

If the vehicles in the string only account with on-board sensors (ACC-equipped), the closed loop behavior depends on the ego-vehicle dynamics, selected spacing policy and feedback controller. The car-following performance is determined only by the feedback loop capability to track the preceding position evolution $X_{i-1}(s)$. On the other hand if V2V links are available, performance is significantly enhanced permitting more stable and reduced inter-distances, due to the received reference speed in feedforward. However, this requires an appropriate feedforward link configuration due to the dependence on the ego-preceding dynamics relation, otherwise the obtained behavior results degraded.

Considering the time gap selection and following the aforementioned design objectives, two main strategies are proposed focusing on feedforward CACC-based solutions for the control of heterogeneous strings. The first seeks a solution to be implemented over vehicle strings where V2V links are available only from each vehicle to its immediately follower (predecessor-following topology). The second approach relaxes this assumption and permits the addition of broadcast wireless links from the leader vehicle to all the vehicles in the string (leader-predecessor-following topology).

5.3 CACC under predecessor-following topology

As mentioned in Sec. 3.2.2, PF topologies have been the most widely employed cooperative driving strategy for its simplicity and implementation benefits. It proposes that each vehicle of index i-th accounts with information coming only from the $i-1$-th one, both from on-board sensors and V2V communications. For this reason, the string size can easily be extended boundlessly without leading to a major logistical problem. Another advantage of this approach is that if all vehicles account with DSRC (which is the most common technology for vehicular V2V links), the wireless transmission range is not a constraint to increase the string size boundlessly.

For the case where no communication links are available over a heterogeneous string, the individual and string stability depends only on the ego-vehicle reference speed tracking model,

high level controller and the desired spacing policy. Whichever the car-following dynamics of the preceding vehicles are, the stability of the ego-vehicle is not affected (assuming no actuator saturation and driving within vehicle operational limits). In the case of CACC and platooning, several solutions based on PF have been proposed using FF strategies showing promising results. Regretfully, none handles the case where the preceding vehicle dynamics are unknown due to initialization or possible cut-in/cut-out.

In this section, an online-adapted control structure is proposed that employs an identification algorithm in real time over the preceding vehicle dynamics [Flores et al., 2018b]. This is carried out to adapt the FF filter in function of the identified parameters, enhancing the closed loop performance of the ego-vehicle when using CACC. CTG spacing policy is proposed together with a feedback controller that ensures loop stability and robustness to possible modeling uncertainties or disturbances. The FF filter is adapted with the purpose of mitigating the effects of having different vehicle low level control capabilities–i.e. $Gp_{i-1}(s) \neq Gp_i(s)$–, thus approximating the FF filter to the ideal inverse model expression.

5.3.1 System description

The proposed solution is aimed for CACC techniques for strings where different vehicles are interconnected on string. The PF topology-based controller structure is presented in Fig. 5.4, where the dashed lines are the wireless V2V communication links.

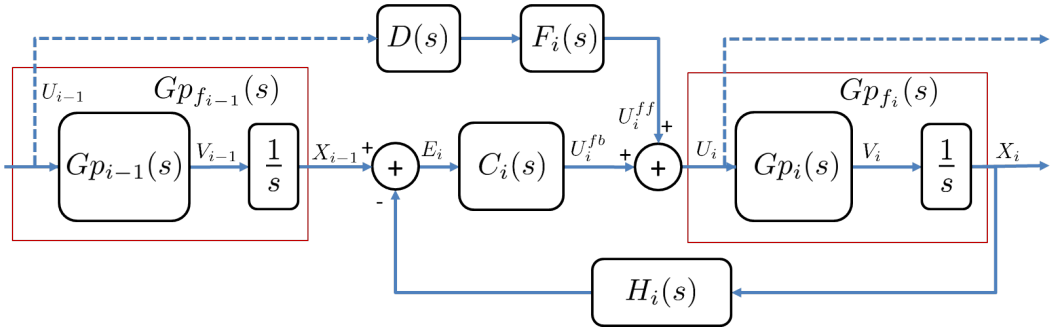

Figure 5.4: Control structure illustration for CACC applications

One can observe that the main differences with the structure previously presented in Fig. 4.9b are related to the distinction between $Gp_i(s)$ and $Gp_{i-1}(s)$. This is intended to clarify that string vehicles' dynamics are no longer approximated similar, which also forces to add the index notation to the FF filter, controller and spacing policy. The block $D(s)$ represents the V2V network delay in the preceding vehicle's reference speed. It is modeled on the frequency domain as $D(s) = e^{-\theta s}$, where θ is the time delay in seconds. The model $Gp_{f_i}(s)$ represents the relation between the vehicle position given a control input or reference speed–i.e. $\frac{X_i(s)}{U_i(s)}$. For this CACC application, it is equivalent to add a pole in the origin to the low level control layer model $Gp_i(s)$.

Given that the string stability is of the main performance targets of the current work, its evolution is studied in the proposed control structure. In the literature, prior approaches have considered different variables for the study of this condition. Nevertheless, control inputs and spacing errors evolve differently in strings of vehicles with non-identical dynamics, controllers and spacing policies. For this reason, in the GCDC mixed CACC demonstrations the vehicles' longitudinal accelerations was adopted as the string stability criteria [Wang and Nijmeijer, 2015a]–i.e. $\left\| \frac{A_i(s)}{A_{i-1}(s)} \right\|_\infty$. The strict $\mathcal{L}_2$ string stability is analyzed through the closed loop response of the

structure in Fig. 5.4, resulting as:

$$\Gamma_i(s) = \frac{A_i(s)}{A_{i-1}(s)} = \frac{sV_i(s)}{sV_{i-1}(s)} = \frac{s^2X_i(s)}{s^2X_{i-1}(s)} = \frac{D(s)F_i(s)P_i(s) + Gp_{f_i}(s)C_i(s)}{1 + Gp_{f_i}(s)C_i(s)H_i(s)};\ i > 2 \tag{5.2}$$

where the term $P_i(s)$ represents the relation between the ego and preceding vehicle models, $\frac{Gp_i(s)}{Gp_{i-1}(s)}$. The $\mathcal{H}_\infty$-norm of the expression above is evaluated according to the definition of strict $\mathcal{L}_2$ string stability. When the vehicles can be assumed to have similar dynamics, the term $P_i(s)$ results as one, thus obtaining the expression in Eq. 4.24. The fact that term $P_i(s)$ is no longer negligible introduces disturbances in the system closed loop performance with respect to the homogeneous case.

5.3.1.1 Inverse model-based FF strategy

To solve this issue, it is proposed to manipulate the FF filter to mitigate the effect of the different dynamics, at the same time that the closed loop performance and sensitivity is enhanced. An inverse model FF approach is proposed, which has demonstrated to provide faster system response, improve disturbance rejection and increase significantly the reference tracking performance, as explained in Sec. 3.3. The error evolution of simple FB $E_{fb}(s)$ and inverse model-based FF/FB $E_{ff}(s)$ conventional structures are as follows:

$$\begin{aligned} E_{fb}(s) &= \frac{1}{1 + G(s)C(s)}U(s); \\ E_{ff}(s) &= \frac{1 - G(s)\tilde{G}^{-1}(s)}{1 + G(s)C(s)}U(s); \end{aligned} \tag{5.3}$$

where $U(s)$ is the closed loop reference input, $C(s)$ the feedback controller and $G(s)$ the model whose inversion is employed in the FF link approximated as $\tilde{G}(s)$. Notice that if $\tilde{G}(s) = G(s)$, perfect tracking of any reference is achieved with error sensitivity equal to zero for the FF/FB technique. It is important to consider that the model $\tilde{G}(s)$ must satisfy the conditions for being inverted with traditional methods, which are: being minimum-phase system with no zeros/poles in the origin.

In practice, it is difficult to determine exactly the inverse model and attain a perfect model inversion with ideal reference tracking. However, a sufficient condition to demonstrate that the proposed strategy with the feedforward/feedback (FF/FB) structure increases the system performance over FB-only despite the model uncertainty, is to study the worst-case tracking error with and without the FF strategy [Devasia, 2002], [Faanes and Skogestad, 2003]. Given that tracking error $E(s)$ is in function of the loop sensitivity and the reference input, dependence on the latter can be removed by normalizing the tracking error by the 2-norm of the input. The worst case error $\hat{E}(s)$ of both structures is then determined as follows:

$$\begin{aligned} \hat{E}_{(fb)}(s) &= \left\| \frac{1}{(1 + G(s)C(s))} \right\|_\infty; \\ \hat{E}_{(ff)}(s) &= \left\| \frac{\Delta(s)}{(1 + G(s)C(s))\tilde{G}(s)} \right\|_\infty; \end{aligned} \tag{5.4}$$

where the uncertainty over the inverted model is defined as $\Delta(s) = \tilde{G}(s) - G(s)$. Notice that $\|\hat{E}_{ff}(s)\|_\infty \leq \|\hat{E}_{fb}(s)\|_\infty$, if the following condition is fulfilled:

$$|\Delta(s)| \leq \left|\tilde{G}(s)\right|; \tag{5.5}$$

demonstrating that the FF/FB is capable of improving the reference tracking performance and stability, if such condition is satisfied. For the case of the structure presented in Fig. 5.4, the guidelines proposed in [Naus et al., 2010] for the design of FF filter under CTG spacing policies are extended for the heterogeneous case using a FF filter $F_i(s) = (\tilde{P}_i(s)H_i(s))^{-1}$. The term $\tilde{P}_i(s)$ refers to the relation between $\tilde{Gp}_{i-1}(s)$ and $\tilde{Gp}_i(s)$. The ego-vehicle real reference speed tracking control $Gp_i(s)$ is approximated by the model $\tilde{Gp}_i(s)$. Notice that $F_i(s)$ is employable to filter the preceding vehicle's reference speed, given that $P_i(s)$ fulfills the invertibility condition. The term $H_i(s)$ is employed in the filter to guarantee string stability for every time gap $h > 0$, in case the FF link presents no communication delays [Naus et al., 2010]. This also limits the FF filter action bandwidth to the interest frequency region. Since modeling uncertainties are greater for higher frequencies, the addition of $H_i(s)$ increases the robustness towards these uncertainties. With some modifications, the condition in Eq. 5.5 can be translated for the case of structure Fig. 5.4 to:

$$\left|\tilde{P}_i(j\omega) - P_i(j\omega)\right| = |\Delta_i(s)| \leq |\tilde{P}_i(j\omega)|; \tag{5.6}$$

To satisfy this condition, the objective is to reduce as much as possible the model uncertainty $|\Delta_{P_i}(j\omega)| = |\tilde{P}_i(j\omega) - P_i(j\omega)|$ in the interest frequency region–i.e. the closed loop bandwidth $\omega \in (0, 1/h]$–to yield the best reference tracking as possible, being h the employed time gap. In practice, the ego-vehicle behavior is known a priori when designing the control loop, which means that for the estimation of $\tilde{P}_i(s)$, $\tilde{Gp}_i(s)$ should describe accurately $Gp_i(s)$. On the other hand, the preceding vehicle model is unknown a priori, due to possible cut-in/cut-out where the string order changes. The key element of this approach is then to approximate $\tilde{Gp}_{i-1}(s) \rightarrow Gp_{i-1}(s)$, so the condition in Eq. 5.6 is fulfilled. An identification algorithm is proposed for this task, with the purpose of estimating the dynamics of $Gp_{i-1}(s)$ and obtain an approximation of $P_i(s)$.

5.3.2 Proposed algorithm

In the literature there exists several parameter identification methods such as linear regression, least square-based strategies, gradient descent, particle swarm optimization or particle filtering. Given that the state measurements might be corrupted with observation noise and the optimization must be robust to non-convexity, particle filtering or Sequential-Monte-Carlo (SMC) based on least square error results ideal for the modeling of $\tilde{Gp}_{i-1}(s)$. This algorithm has been proven to perform well when applied on non-linear distributed problems, while its stochastic nature permits to avoid local minima within determined state space boundaries.

5.3.2.1 Particle filtering

In this section, basics of particle filtering are provided for a better understanding on the algorithm principles. The particle filters have been conceived as a powerful tool to solve state space models and non-linear systems problems. With the introduction of the bootstrap filter [Gordon et al., 1993] or Sampling Importance Resampling (SIR) filter, it has been applied over Bayesian filtering problems showing good results. Based on Monte Carlo methods, it proposes to approximate numerically the probability density function (PDF) of the process current state, given the current observation. Consider the stochastic system:

$$\begin{aligned} x_k &= f_k(x_{k-1}) + v_{k-1}; \\ y_k &= h_k(x_k) + v_k; \end{aligned} \tag{5.7}$$

where $f_k(\cdot), h_k(\cdot)$ are the discrete non-linear functions of state dynamics and measurements respectively, at the time frame k. The system and observation errors $v_k, n(k)$ are independent identically distributed functions. Given a set of observations $y_{0:k} = y_0...y_k$ and states $x_{0:k} = x_0...y_x$, the algorithm objective is to compute sequentially each time frame the posterior PDF of the system states–i.e. $p(x_k|y_k)$. For its prediction, the recursive Bayesian filter is employed of the form:

$$p(x_k|y_{0:k}) = \frac{p(y_k|x_n)p(x_k|y_{0:k})}{p(y_k|y_{0:n-1})} \tag{5.8}$$

which is also called as the update step in Bayesian inference. However, analytical computation of the PDF is not feasible due to the lack of an exact model error and/or non-linearities. For this reason, particle filters-based methods approximate the distributions using samples or particles defined as $x_k^j \sim p(x_k|y_{0:k})$; $j \in [1, N]$ where j is the particle index and N is the number of particles, usually large for better convergence to the PDF. The algorithm key is the choice of the prior density $p(x_k|x_{k-1}^j)$, which defines the particles' evolution and further weighting. The PDF is proposed to be estimated as:

$$p(x_k|y_{0:k}) \simeq \sum_{j=1}^{N} \hat{\omega}_k^j \delta(x_k - x_k^j); \tag{5.9}$$

having $\delta(\cdot)$ as the Dirac delta function and $\hat{\omega}_k^j$ the normalized weight assigned to the particle of index j in the frame k. As one can see, if $N \leftarrow \infty$, the estimated PDF converges to $p(x_k|y_k)$. For importance sampling-based algorithms as the SIR, the particles are weighted as:

$$\begin{aligned} \omega_k^j &= \frac{p(y_{0:k}|x_k^j)p(x_k^j)}{p(x_k^j|y_{0:k})} \\ \hat{\omega}_k^j &= \frac{\omega_k^j}{\sum_{m=1}^{N} \omega_k^m} \end{aligned} \tag{5.10}$$

The remaining steps are related to the output expectation and the resampling process. The former considers the particles estimation and their normalized weight to generate the states expectation as follows:

$$\hat{x}_k = \sum_{i=1}^{N} \hat{\omega}_k^j \cdot x_k^j; \tag{5.11}$$

Subsequently, the resampling process is carried out to generate a new equally weighted $(1/N)$ particles set for the next time frame $k+1$. This improves the approximation of the PDF, discarding stochastically the particles which weight is lower and avoiding their degeneracy over the iterations. The resampling is based on the assumption that the probability of a particle to be repeated is proportional to its weight–i.e. $p(x_{k+1}^j = x_k^j) = \hat{\omega}_k^j$. The process is repeated sequentially for each time frame with the novel observation. An applied version of this algorithm is proposed in this work, with the purpose of identifying the parameters of the preceding vehicle low level control layer.

5.3.2.2 Online preceding vehicle identification

The implementation of a particle filtering method over the preceding vehicle low level behavior $Gp_{i-1}(s)$, is proposed. For this application, the process parameters are estimated, instead of the states evolution as described in the previous section. A linear state space representation of the system described in Eq. 5.7 is used, that considers model input and parameters:

$$\begin{aligned} \dot{x}(t) &= A(\Theta) \cdot x(t) + B(\Theta) \cdot u(t); \\ y(t) &= C(\Theta) \cdot x(t); \end{aligned} \tag{5.12}$$

where Θ holds for the set of model parameters intended to be identified. Model in Eq. 3.9 is considered for the identification algorithm, since it represents accurately the bandwidth and damping properties of the vehicle low level control dynamics. Considering then Eq. 3.9 and 5.12.

$$\begin{aligned} \begin{bmatrix} \dot{x}(t) \\ \ddot{x}(t) \end{bmatrix} &= \begin{bmatrix} 0 & 1 \\ -\omega_n^2 & -2\xi\omega_n \end{bmatrix} \cdot \begin{bmatrix} x(t) \\ \dot{x}(t) \end{bmatrix} + \begin{bmatrix} 0 \\ \omega_n^2 \end{bmatrix} \cdot u(t); \\ y(t) &= \begin{bmatrix} 0 & 1 \end{bmatrix} \cdot \begin{bmatrix} x(t) \\ \dot{x}(t) \end{bmatrix}; \end{aligned} \tag{5.13}$$

To identify the model parameters $\Theta = \langle \omega_n, \xi \rangle$, observation over the model output $y(t)$ and input $u(t)$ are required. For the case of the preceding vehicle system, the input and output correspond to the reference $u_{i-1}(t)$ and measured speed $v_{i-1}(t)$ respectively. These variables are obtained in real time through the V2V communication link. Given that the entire CACC algorithm is executed in a computer (discrete time), a discrete version of the model in Eq. 5.13 is employed. For this task, the Tustin discretization method is applied, whose formula is shown in Eq. 4.19. Through this transformation, the system results in a discrete transfer function as follows:

$$\frac{v_{i-1}[k]}{u_{i-1}[k]} = \frac{y[k]}{u[k]} = \frac{\omega_n^2 Ts^2(1 + z^{-1} + z^{-2})}{4 + \omega_n^2 Ts^2 + 4\xi\omega_n Ts + (2\omega_n^2 Ts^2 - 8)z^{-1} + (4 - 4\xi\omega_n Ts + \omega_n^2 Ts^2)z^{-2}}; \tag{5.14}$$

having Ts as the sampling period and z^{-1} as the discrete time operator. Any possible low level control response model can be described from the set Θ. Since the particle filters require a bounded parameters space, the model parameters are bounded as $\xi \in [\xi_{min}, \xi_{max}]$ and $\omega_n \in [\omega_{n_{min}}, \omega_{n_{max}}]$. The parameter bounds are set in function of the expected dynamics of the string vehicles (experimental values are provided in chapter 6). On the algorithm implementation, the j-th particle represents a candidate model, defined as the vector $\theta^j = \langle log(\omega_n^j), \xi^j \rangle$; $j \in [1, N]$. Notice that the model bandwidth logarithm is considered instead of the ω_n for two reasons: first, to avoid irregular initial random distribution of the particles in the model bandwidth axis (since frequencies evolve with a logarithmic behavior), and lastly, to guarantee an effective appliance of the artificial Gaussian noise in the resampling stage over the distribution of ω_n^j. The online identification algorithm is detailed in Algo. 1.

Initially, a set of particles S_0 is generated with a random distribution over the 2D bounded parameter space. The particle filter is executed and updated at a sample period of Ts recommended to be less than π/ω_{max} to agree with the Nyquist principle, but also high enough to fulfill real-time constraints. With respect to the process input/observation pairs $\langle u_k, y_k \rangle$ (reference and measured vehicle longitudinal speed respectively), they are received through V2V at each time frame k. As they are received, they are also queued on a vector $\bar{Z}_{k_0:k}$, which contains all input/output pairs from time frame k_0 to the current k. Given that embedded systems are memory limited and due to

Algorithm 1 SIR-based particle filter algorithm for parameters identification

$\tilde{\theta}_0 = \theta_{ego}$ ▷ Assume homogeneous case at beginning
1. Initial sampling at $k = 0$
$\theta_1^j \sim p(\theta_1^j);\ j \in [1, N_p]$ ▷ Generate uniform distribution
for $\theta_k^j in\ \Theta_k$ **do** ▷ Iterate over the particles
    2. Compute particle estimation
    $\tilde{y}_{k_0:k}^j = ComputeEstimations(u_{k_0:k}^j, \theta_k^j)$
    3. Particle score calculation
    $w_k^j = 1/\sum_{n=k_0}^{k}(\tilde{y}_n^j - y_n)^2$ ▷ Estimate score with RMSE
end for
4. Normalize weights and output estimation
$w_k^j = w_k^j / \sum_{m=1}^{N_p} w_k^m$
$E(\theta_k) = argmax_{\theta_k^j}(w_k^j)$ ▷ Estimation with highest score
if $\sigma_{\tilde{\theta}_k} \geq \sigma_{max}$ **then** ▷ Supervise estimation convergence
    $\tilde{\theta}_k = \theta_{ego}$ ▷ Unstable solution, set homogeneous case
else
    $\tilde{\theta}_k = E(\theta_k)$ ▷ Stable PF output, preceding model is updated with parameters estimation
end if
5. Particles resampling ▷ Generate new set Θ_{k+1}
$p(\theta_{k+1}^j = \theta_k^j) = w_k^j$
$\theta_{k+1}^j = \theta_{k+1}^j + \nu_k^j;\ \nu_k^j \sim \mathcal{N}(0, dev^{\tilde{\theta}})$

processing time constraints, $\bar{Z}_{k_0:k}$ cannot grow boundlessly. For this reason, a sliding time window is adopted where N_s is the maximal amount of input/output pairs that are considered for the weighting. In other words, the vector size increases as values arrive until the condition $k - k_0 = N_s$ is reached. Then, most recent values are stored while the oldest ones are being removed.

At each sample time k, the algorithm computes every particle $\theta^j;\ j \in [1, Np]$ estimation within the time window between k_0 to k as $\tilde{y}_{k_0:k}^j$, employing the discrete-time state space model in Eq. 5.14. In case the preceding vehicle presents time varying parameters or non-consistent behavior, a forgetting factor can be introduced in Eq. 5.15 to give priority to the most recent input/output pairs during the particles' weights assignment process. Each particle weight is assigned using the Root Mean Square Error (RMSE) between each particle's estimations $\tilde{y}_{k_0:k}^j$ and the observations $y_{k_0:k}$ along the time window, given the inputs $u_{k0:k}$:

$$\begin{aligned} \omega_k^j &= \frac{1}{\sum_{m=k_0}^{k}(\tilde{y}_m^j - y_m)^2}; \\ \hat{\omega}_k^j &= \frac{\omega_k^j}{\sum_{j=0}^{Np} w_k^j}; \end{aligned} \tag{5.15}$$

The normalized weight $\hat{\omega}_k$ is obtained for all particles in S_k for the subsequent resampling process [Carvalho et al., 2010], to discard low-scored estimations and increase the particles' density over the bounded parameter space areas where high fitting has been obtained. The resampling generates a new set of particles S_{k+1} for the next frame, where the scoring weight defines the probability of a particle to be resampled. Afterwards, each resampled particle is corrupted with normally distributed noise $\nu \sim \mathcal{N}(0, \sigma_\theta)$ to avoid particles degeneracy and continue exploring the bounded parameter space. The noise σ_θ is determined as the standard deviation of the observation error due to the encoders measurement error.

For the first executions of the algorithm, the vector $\bar{Z}_{k_0:k}$ does not account with sufficient

sampled information to provide a good estimation of the model parameters. During this initialization period, the preceding vehicle's model is assumed to be similar than the ego-vehicle one–i.e. $P_i(s) = 1$. As the size of $\bar{Z}_{k_0:k}$ increases, the particles converge to a stable solution which variance is less than a maximal tolerated value ($\sigma < \sigma_{max}$). At each time frame, the estimated model parameters are outputted following $E(\theta_k) = \arg\max_{\theta_k^j} \hat{\omega}_k^j$. Such values $\tilde{\theta}_k = \langle log(\tilde{\omega}_n), \tilde{\xi} \rangle$ are employed to adapt $\tilde{Gp}_{i-1}(s)$ in the FF filter $F_i(s)$.

Even though the particle filter algorithm provides a good estimation of $\tilde{Gp}_{i-1}(s)$, measurement noise and uncertainties produce a variance over the algorithm output with respect to the real model $Gp_{i-1}(s)$. As explained in Sec. 5.3.1.1, the FF/FB structure demands a low magnitude of the uncertainty $|\Delta_{Gp_{i-1}}(s)|$ to guarantee an enhanced reference tracking performance. In other words, as the magnitude of $|\Delta_{Gp_{i-1}}(s)|$ results higher, the inverse model strategy loses its benefits–i.e. $P_i(s)\tilde{P}_i^{-1}(s) \neq 1$. To mitigate the effect of modeling uncertainties on the FF filter, the cutoff filter $1/H(s)$ results ideal since it limits the response bandwidth of the FF filter and attenuates possible disturbances. The final form of $F_i(s)$ is defined as:

$$F_i(s) = \frac{\tilde{Gp}_{i-1}(s)}{H(s)Gp_i(s)} \tag{5.16}$$

An illustration of the FF filter $F_i(s)$ is provided in Fig. 5.5 for several preceding vehicles with 10 different dynamics of $\omega_{n_{i-1}}$ from 0.45 rad/s to 1.8 rad/s (black to light gray plot), while ego-vehicle's bandwidth is fixed at $\omega_{n_i} = 1\,rad/s$. The CACC structure is set for a time gap of $h = 0.4s$.

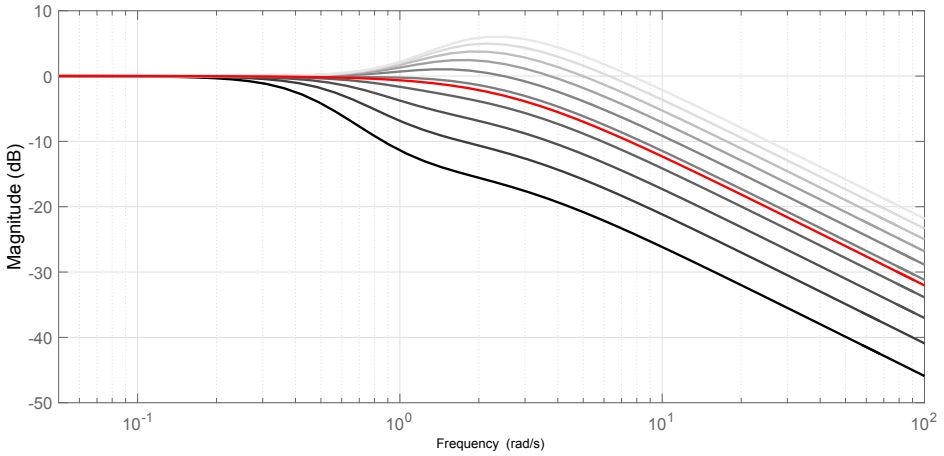

Figure 5.5: Different resulting feedforward filter $F_i(s)$ (black to light gray lines) and $H(s)^{-1}$ (red line)

One can observe that the filter adopts its frequency response in function of the dynamics relation $P_i(s)$ and the spacing policy. From the scenarios where the ego-vehicle has faster dynamics (black and dark gray) to the cases where its dynamics are slower (lighter gray), the filter magnitude response changes from attenuating to amplifying the received V2V signal respectively at middle frequencies. The term $H(s)^{-1}$ (red line) is also depicted, showing the cutting frequency that not only describes the ideal closed loop response of vehicles on CTG policy, but also limits the frequency region of $F_i(s)$.

Analyzing the two border cases, it is possible to understand the physical purpose of the response of $F_i(s)$. When having ($\omega_{n_i} > \omega_{n_{i-1}}$), the ego-vehicle real speed converges faster than the preceding

vehicle for the same reference speed change. If the FF filter is not adapted, excessive control effort is put on the ego-vehicle actuators, at the same time that preceding vehicle's behavior is amplified. When the proposed FF filter is introduced, a low pass response on $U_{i-1}(s)$ is produced with a cutoff on $\omega_{n_{i-1}}$, thus attenuating speed changes for higher frequencies and avoiding overreaction to preceding vehicle speed changes.

On the other hand, if $(\omega_{n_i} < \omega_{n_{i-1}})$ a slight amplification of $U_{i-1}(s)$ is yielded within the region $\omega \in [\omega_{n_i}, \omega_{n_{i-1}}]$ to compensate the convergence speed difference between both vehicles' low level control layers. This means that to yield the ideal behavior–i.e. $V_i(s) = V_{i-1}(s)H(s)^{-1}$–the lack of convergence speed in $V_i(s)$ due to the limited low level response bandwidth must be compensated by amplifying the reference speed sent through the V2V link.

Although the adopted $F_i(s)$ provides the necessary conditions for an ideal reference speed tracking, when $\omega \in [\omega_{n_i}, \omega_{n_{i-1}}]$ longitudinal actuators' saturation may occur if the filtered signal $(F_i(s)U_{i-1}(s))$ cannot be tracked by the ego-low level control layer. Two solutions can be proposed to solve this problem. The first one consists on relaxing the spacing policy by targeting a higher time gap, reducing the required closed loop response bandwidth and permitting the ego-vehicle to track the reference speed without actuators saturation. The second solution is adopted if the targeted spacing policy is not modified. It consists on employing leader vehicle information from a V2V link, in addition to the preceding vehicle's. This permits less reactive vehicles to take advantage of the leader speed changes to anticipate preceding vehicle behavior change, without requiring to overreact to predecessor's reference speed in the FF filter.

5.4 CACC under leader-predecessor-following topology

In the literature, LF and LPF strategies have been employed for car-following techniques demonstrating their benefits in terms of string performance. An illustration of a LPF topology is provided in Fig. 5.6:

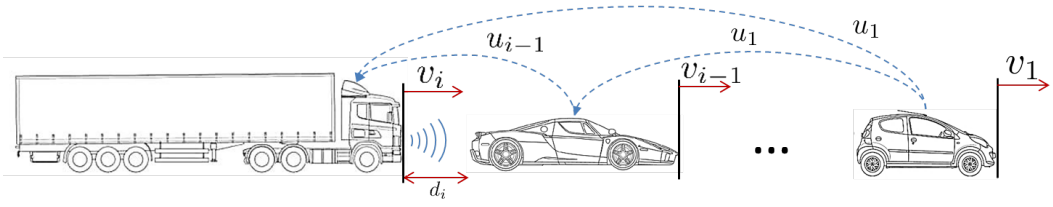

Figure 5.6: Illustration of the proposed LPF strategy

For instance, it has been proved that stability is ensured for constant spacing strings with ideal communications, if the leader is tracked by every vehicle in the string [Seiler et al., 2004]. Nevertheless, considering that practical platooning and CACC employ V2V links with delays and periodic signal sampling, string stability of vehicle position, speed or acceleration can only be achieved in the weak sense with constant spacing [Swaroop and Hedrick, 1999] [Shladover, 1991]. An extensive list of literature approaches on LPF is provided in [Li et al., 2017a]. Among the most relevant ones, one can find [Swaroop and Hedrick, 1999] where a mini-platoon strategy is adopted splitting the formation in several groups seeking to attenuate spacing errors. In [Milanés et al., 2014], two independent PD controllers for regulation of ego-predecessor and ego-leader spacing gaps have been designed, demonstrating the benefits of LPF topologies on CACC strings. In [Xiao et al., 2009], conditions on the scalability of LPF platoons are deduced for both constant spacing and CTG policies, targeting weak string stable closed loop performance with a fixed controller for

spacing errors with respect to preceding and leader vehicles. An adaptive control is proposed to prove Lyapunov-Krasovskii asymptotic stability under a delayed dynamical network in [Petrillo et al., 2018], while in [Rödönyi, 2015] a robust control strategy is demonstrated to provide good performance but assuming no parasitic and network delays. In conclusion, although LPF strategies require a more complex communication network, they have demonstrated to ensure weak string stability even under delayed V2V networks. In [Peters et al., 2014], communication delay problem is considered by regulating the spacing error of with respect to the preceding vehicle and tracking the leader speed.

Specifically for heterogeneous vehicles, a handful of works have been done to explore the benefits of this topology for non-identical strings [Rödönyi, 2015]. In the work of [Peters et al., 2016] a controller is developed to regulate weighted position errors with respect to preceding and leader vehicles under a constant spacing policy, regretfully string stability is not assessed. In [Shaw and Hedrick, 2007b] and [Shaw and Hedrick, 2007a], bounded string stability of the spacing error is demonstrated for constant spacing using the leader and preceding vehicles' relative position in feedback. Sensitivity to parameter disturbances is also studied in such work, as well as simulations over a platoon of three types of vehicles demonstrating spacing error boundedness. Some guidelines for the design of feedback controllers to process leader and predecessor spacing errors are provided in [Shaw and Hedrick, 2007a], which are adopted in this work. A modified LPF structure is proposed in [Ali et al., 2014] employing a flatbed tow truck model with a modified time gap policy.

5.4.1 Motivation

However the aforementioned strategies have achieved promising results, only bounded and weak string stability have been guaranteed by employing LPF strategies. Strict $\mathcal{L}_2$ string stability of vehicles position, speed or acceleration is still an open challenge for V2V networks with transmission delays. In addition, most of approaches consider in the feedback loop the position errors with respect to both the preceding and leader vehicles, which may result non ideal since the addition of a supplementary controller for the leader-ego inter-distance modifies the loop response stability. An extra spacing policy with respect to the leader would also be required, considering that it depends on the string size and vehicles' length and positions. For this reason, the following design objectives are aimed in the proposed LPF framework:

- Reduce the demand on vehicle actuators due to a possible fast-slow preceding-ego vehicle combination, by employing leader vehicle information to anticipate perturbations coming from downstream
- Develop a CTG-based string strategy, considering only the ego and preceding vehicles' positions
- Search a solution for CACC under degraded communication networks with considerable transmission delays
- Study the strict $\mathcal{L}_2$ string stability conditions of a LPF topology of heterogeneous CACC strings
- Ensure the fulfillment of strict $\mathcal{L}_2$ string stability conditions without modifying the individual stability

To approach these objectives, a novel LPF strategy based on FF is proposed with a feedback control loop to reject disturbances and modeling errors. A time gap spacing policy is employed to remain robust to communication delays and limit the closed loop response to a feasible frequency region.

5.4.2 Proposed system

The leader and preceding vehicle's reference speed ($u_1(t)$ and $u_{i-1}(t)$) are received through V2V wireless links and further weighted to be employed in the FF structure. This permits to have an additional degree of freedom on the control structure, specifically on the FF link. The management of such link is carried out in function of the relation between preceding and ego vehicle low level responses $P_i^{i-1}(s)$. The signals received through V2V are employed in FF after being processed by the filters $F_{i,i-1}(s)$ and $F_{i,1}(s)$, for the preceding and leader vehicles' reference speeds respectively. Given that the platoon or string can be understood as a whole interconnected system whose unique exogenous input is $u_1(t)$ (the other $u_i(t)$; $i > 2$ are inner propagations of such exogenous input), this value can be employed by less reactive vehicles to anticipate the oscillations propagated from downstream, instead of waiting for the preceding vehicle to adapt its control input due to the propagated perturbation. In Fig. 5.7, the proposed LPF control structure is depicted.

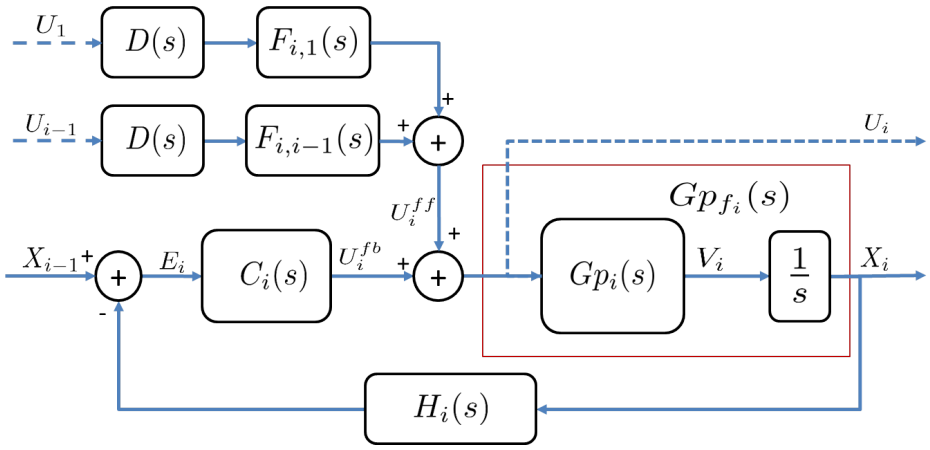

Figure 5.7: Proposed control structure based on a LPF topology

One can observe that the difference with respect to the structure in Fig. 5.4 is the addition of the FF link that processes leader vehicle reference speed and its FF filter $F_{i,1}(s)$. To derive sufficient conditions for the structure blocks design, one has to study first the closed loop form of the structure. The ego-vehicle position results as follows:

$$X_i(s) = \frac{Gp_{f_i}(s)[C_i(s)X_{i-1}(s) + D(s)[F_{i,i-1}(s)U_{i-1}(s) + F_{i,1}(s)U_1(s)]]}{1 + Gp_{f_i}(s)C_i(s)H(s)}; \; i \geq 3 \tag{5.17}$$

Since the closed loop is studied with respect to the vehicle positions, the identity $X_i(s) = Gp_{f_i}(s)U_i(s)$ is employed to get:

$$X_i(s) = \frac{D(s)F_{i,i-1}(s)\frac{Gp_i(s)}{Gp_{i-1}(s)} + Gp_{f_i}(s)C_i(s)}{1 + Gp_{f_i}(s)C_i(s)H(s)}X_{i-1}(s) + \frac{D(s)F_{i,1}(s)\frac{Gp_i(s)}{Gp_1(s)}}{1 + Gp_{f_i}(s)C_i(s)H(s)}X_1(s); \; i \geq 3 \tag{5.18}$$

It is worth to highlight that these developments are valid for all string vehicles of index $i \geq 3$. The leader vehicle performs cruise speed control and in the case of the second vehicle, the leader is also its preceding one, thus its closed loop response results as in Eq. 5.2. For the rest of string vehicles, the closed loop response results of two parts, one that depends on the leader position and

the other on the preceding vehicle's one. The obtained closed loop form results of the same than in Eq. 5.2, except for the addition of the term influenced by the leader vehicle motion.

At this point, the response can be studied as a MISO system to evaluate the loop stability, but the adopted definition of strict $\mathcal{L}_2$ string stability requires to study the $\mathcal{H}_\infty$-norm of the closed loop response $\Gamma_i(s) = \frac{X_i(s)}{X_{i-1}(s)}$. A relation between the leader and preceding vehicles' positions is required to derive the expected closed loop form. Considering the vehicles string property of being an interconnected system, it can be stated that:

$$\begin{aligned} \frac{X_{i-1}(s)}{X_1(s)} &= \frac{X_{i-1}(s)}{X_{i-2}(s)}\frac{X_{i-2}(s)}{X_{i-3}(s)}\cdots\frac{X_2(s)}{X_1(s)}; \\ \frac{X_{i-1}(s)}{X_1(s)} &= \Gamma_{i-1}(s)\Gamma_{i-2}(s)\cdots\Gamma_2(s); \end{aligned} \tag{5.19}$$

An assumption is taken to approximate the form of $\Gamma(s)$, so it can be employed in the closed loop form in Eq. 5.18. A first order response of the form $H^{-1}(s)$ can accurately approximate the states propagation within the string, given that vehicles' car-following system are designed to be strictly string stable. In fact, as the communication delay converges to zero $\theta \to 0$, the closed loop form converges to the ideal string stable response $\Gamma(s) \to H^{-1}(s)$ [Naus et al., 2009]. Nevertheless, communication delay are considered in this case and the ego-vehicle cannot react in a shorter time than such temporal delay to a change in the preceding behavior. The following approximation is proposed to derive the string stability closed form:

$$\Gamma_i(s) \approx \frac{D(s)}{H(s)};\ \forall i \geq 2 \tag{5.20}$$

The closed loop in function of all preceding vehicles result then as:

$$\begin{aligned} \frac{X_2(s)}{X_1(s)} &= \frac{D(s)F_{2,1}(s)\frac{Gp_2(s)}{Gp_1(s)} + Gp_{f_2}(s)C_2(s)}{1 + Gp_{f_2}(s)C_2(s)H(s)}; \\ \frac{X_i(s)}{X_{i-1}(s)} &= \frac{Gp_{f_i}(s)C_i(s) + D(s)[F_{i,i-1}(s)\frac{Gp_i(s)}{Gp_{i-1}(s)} + F_{i,1}(s)\frac{Gp_i(s)}{Gp_1(s)}\left(\frac{H(s)}{D(s)}\right)^{i-2}]}{1 + Gp_{f_i}(s)C_i(s)H(s)};\ \forall i \geq 3 \end{aligned} \tag{5.21}$$

which ∞-norm must be maintained equal or less than one to guarantee strict $\mathcal{L}_\infty$ string stability. The block $C_i(s)$ is a fractional-order feedback compensator designed following the guidelines presented in Sec. 4.3.3, with the addition of the inverted spacing policy to make the closed loop poles independent from the adopted policy:

$$C_i(s) = \frac{Kp}{H(s)}\frac{\left(1 + \frac{s^\alpha}{\omega_c}\right)}{\left(1 + \frac{s^\alpha}{x\omega_c}\right)};\ Kp, \omega_c, \alpha > 0,\ x > 1 \tag{5.22}$$

where one can observe that the resulting loop stability is in function of the controller and the ego-vehicle low level behavior, regardless the adopted spacing policy.

5.4.3 LPF feedforward structure design

With respect to the FF filters design, the guidelines provided in [Ploeg et al., 2014a] for two-predecessor following structures are adopted for the FF structure DC gain. The following condition is required:

$$|F_{i,i-1}(s) + F_{i,1}(s)| \rightarrow 1;\ s \rightarrow 0; \tag{5.23}$$

which means that the DC gain of the two FF links should be complementary. This is intuitive given that at equilibrium, all string vehicles' reference speeds should converge to the same value–i.e. $U_{i-1}(0) = U_1(0) = U_i(0)$–once the spacing errors are zero. The middle and high frequency regions of $F_{i,i-1}(s)$ and $F_{i,1}(s)$ are designed following the same inverse model-based FF strategy that has been proposed on the Sec. 5.3.1.1, aiming to get the ideal reference tracking given the FF inputs (in this case, $u_1(t)$ and $u_{i-1}(t)$). Approximations of $P_{i,i-1}(s) = \frac{Gp_i(s)}{Gp_{i-1}(s)}$ and $P_{i,1}(s) = \frac{Gp_i(s)}{Gp_1(s)}$ are used in the inverse model strategy as explained before. The low level control models of preceding and leader vehicles can be obtained employing the identification method in Sec. 5.3.2.2. The FF filter $F_{i,i-1}(s)$ that process preceding vehicle's reference speed is set as:

$$F_{i,i-1}(s) = \beta_i \frac{\tilde{Gp}_{i-1}(s)}{Gp_i(s)H(s)} = \frac{\beta}{\tilde{P}_{i,i-1}(s)H(s)};\ i \geq 3 \tag{5.24}$$

where $\beta \in \Re : 0 < \beta < 1$. For the leader reference speed FF filter $F_{i,1}(s)$, a similar form is adopted based on an estimation of leader vehicle speed, but using the cutoff filter $H(s)^{i-1}$ of an order that increases as the vehicle index is higher [Ploeg et al., 2014a]. The proposed form is adopted due to the approximation in Eq. 5.20, which introduces $i-2$ zeros with frequency in $1/h$ in the closed loop form numerator. By adopting a filter as:

$$F_{i,1}(s) = (1-\beta_i) \frac{\tilde{Gp}_1(s)}{Gp_i(s)H(s)^{i-1}} = \frac{(1-\beta_i)}{\tilde{P}_{i,1}(s)H(s)^{i-1}};\ i \geq 3 \tag{5.25}$$

not only the aforementioned zeros are canceled, but also the desired string behavior with constant time gap geometry is ensured. In other words, since the string exogenous input $u_1(t)$ is propagated downstream being filtered with $H(s)^{-1}$ as the vehicle index increases, the control input for the i-th vehicle that would produce the ideal behavior is $U_i(s) = U_1(s)H(s)^{-i+1};\ i \geq 2$. Notice that by employing β in $F_{i,i-1}(s)$ and $(1-\beta)$ in $F_{i,1}(s)$ the condition in Eq. 5.23 is fulfilled. Finally, by adopting the proposed feedforward LPF strategy, the strict $\mathcal{L}_\infty$ string stability results as:

$$\Gamma_i(s) = \frac{X_i(s)}{X_{i-1}(s)} = \frac{D(s)\Delta P_{i,i-1}(s) + D(s)^{-i+1}\Delta P_{i,1}(s) + Gp_{f_i}(s)C_i(s)H(s)}{H(s)(1 + Gp_{f_i}(s)C_i(s)H(s))} \tag{5.26}$$

where $\Delta P_{i,i-1}(s)$ denotes the product $P_i(s)\tilde{P}_i(s)^{-1}$ which should be equal to one to get the ideal performance. The main advantage of this approach is visible in the fact that there exists a temporal advance $D(s)^{-i+1} = e^{(i-1)\theta s}$ over the preceding vehicle (see numerator in Eq. 5.26). Even if normally this is not feasible due to non-causalities, for the frequency domain representation, the term appears as a consequence of the time lead with respect to the preceding vehicle's behavior by taking the also leader reference speed in FF.

5.4.3.1 Management of FF filters

As explained before, the structure in Fig. 5.7 employs the combination of leader and preceding vehicles' reference speeds. The filters $F_{i,i-1}(s)$ and $F_{i,1}(s)$ are designed following the aforementioned guidelines for inverse model-based FF, aiming the ideal string performance given the signals $u_1(t)$ and $u_{i-1}(t)$. A weight assigning policy over each FF link is required for the filters. If $\beta_i = 1$ the PF topology is yielded, while if $\beta_i = 0$, the ego vehicle employs only the leader vehicle's reference speed

as feedforward. Such strategy is not ideal given that it would prompt a reaction too advanced in time, thus leading to undesired spacing error. For this reason, a trade-off between both scenarios is sought to remain slightly advanced with respect to preceding vehicle, while avoiding spacing errors due to overreacting behavior.

As stated in previous section, the main motivation of employing the leader vehicle on the control loop is to permit less reactive vehicles to anticipate the perturbations propagated downstream, before a more reactive preceding vehicle reacts in consequence. It is intuitive to set as design policy that the relation between ego-preceding vehicles' low level responses is evaluated to set the parameter β. Similar strategies has been applied in the state-of-the-art for weighted LPF constant spacing topologies but only at feedback level, instead of feedforward. For instance, in [Peters et al., 2014] and [Peters et al., 2016], complementary weights are assigned to the spacing errors with respect to the preceding and leader vehicles, but with in the form of more complex dynamic filters. In [Shaw and Hedrick, 2007a], guidelines specifically for heterogeneous strings are provided for the design of linear combinations of feedback controllers to regulate spacing error with respect to leader and predecessor vehicles. As a conclusion of such work, it is stated that the general strategy is to keep faster vehicles more coupled to their preceding, while slower vehicles should be more coupled to the leader vehicle. Simulations and frequency response studies therein demonstrate the benefits in terms of overall bounded string stability and robustness to disturbances.

The same principle is adopted in this work to design the parameter β. For this, not only the vehicle index in the string is considered, but also the ego-preceding dynamics relation. Analyzing the Fig. 5.5, it is visible that the cases where the preceding vehicle accounts with faster dynamics, the term $(\tilde{P}_i(s)H(s))^{-1}$ induces an amplification of the signal $u_{i-1}(t)$, which is non desired due to possible actuator saturation. In addition, the higher the terms $(\omega_{n_{i-1}}/\omega_{n_i})$ and (ω_{n_i}/h); the higher will be the peak magnitude or $\mathcal{H}_\infty$-norm of the non-weighted FF filter $(\tilde{P}_i(s)H(s))^{-1}$. On the other hand, if ω_{n_i} is not lower than $\omega_{n_{i-1}}$ or $1/h$; the ∞-norm results equal to one, given that the DC gain will result equal to one regardless the models parameters and adopted time gap. Finally, it is proposed to design β_i following the policy:

$$\beta_i = \begin{cases} \beta_{max}; \left\|(\tilde{P}_i(s)H(s))^{-1}\right\|_\infty^{-1} \geq \beta_{max} \\ \left\|(\tilde{P}_i(s)H(s))^{-1}\right\|_\infty^{-1}; \left\|(\tilde{P}_i(s)H(s))^{-1}\right\|_\infty^{-1} < \beta_{max} \end{cases} \tag{5.27}$$

obtaining a framework to assign mathematically the weight β_i in function of the spacing policy and ego-preceding dynamics relation. The parameter β_{max} bounds the possible weight assigned to all followers, which agrees with the results obtained in [Shaw and Hedrick, 2007a]. By adopting this strategy, the maximum peak gain of FF filter $F_{i,i-1}(s)$ is normalized to one, reducing the chance of actuator saturation due to a more aggressive control action from the preceding vehicle.

5.5 Discussion

The consideration of vehicles with different dynamics, controllers and braking capabilities in the same string significantly increases the complexity of the car-following task. When the string is composed by similar vehicles, the architecture design can be replicated for all vehicles. But when this assumption is no longer valid, the control structure design requires to consider not only each vehicle characteristics, but also the preceding ones for CACC control. In case of heterogeneous strings, it has been showed that the safe region for the reference inter-distance in function of the speed, is determined by the ego and preceding braking capabilities. The choice of a time gap that

respects this safe region is not only fundamental in terms of safety, but also will determine the way states are propagated upstream and its stability.

Two CACC approaches were proposed, seeking a solution for heterogeneous strings with ensured string stability for a desired time gap. The first approach is based on predecessor-only following topology. It has been proposed to adapt in real time the FF filter, to mitigate the disturbances introduced when the low level control layers of consecutive vehicles are different. Based on an inverse-model FF strategy, the preceding vehicle model is identified online employing a variation of sequential Monte Carlo or particle filtering, thus learning in real time the model parameters (damping factor and frequency bandwidth). A description of the novel identification algorithm has been provided. Conditions for the correct implementation of the proposed approach have been given in function of the modeling uncertainties. The FF filter have been proposed to depend on the relation between ego and preceding low level control models, as well as their spacing policy. The spacing policy term has been added not only to limit the FF action to the desired closed-loop bandwidth, but also to ensure the ideal string behavior for CTG-based car-following. Nevertheless, in case the ego-vehicle response bandwidth is shorter than both the preceding's and the required closed loop bandwidth, it has been demonstrated that the FF filter would produce an amplification over the received reference speed, causing non-desired actuator saturation.

To mitigate this problem, the addition of leader vehicle information has been investigated. A novel FF-based LPF structure has been proposed that employ dynamic filters over the leader and preceding vehicles' reference speeds. A linear combination of both is employed in FF, with the purpose of permitting less reactive vehicles to anticipate speed changes of its preceding vehicle, by employing the leader vehicle's information. The design of the FF filters has been introduced, as well as the conditions for strict $\mathcal{L}_\infty$ string stability under the LPF structure. Finally, the management of the reference speeds through the parameter β_i has been detailed, resulting in function of the relation between ego and preceding low level models.

Chapitre 6

Résultats de validation

Below is a French summary of the following chapter "Validation results".

Différents algorithmes de contrôle ont été présentés et décrits dans les chapitres précédents. Lors de ce chapitre, ces méthodes seront validés en considérant les plateformes de l'équipe RITS et ses dynamiques. D'abord, la conception de la couche de contrôle bas niveau est décrite, responsable du suivi de la vitesse de référence. Le bon fonctionnement de l'architecture de car-following capable de gérer l'interaction avec piétons est démontré à l'aide des expérimentation où tous les étapes de la machine d'état sont illustrées et expliquées. Puis, le développement de la politique d'espacement est validé pour des applications ACC et CACC, avec des simulations et expérimentations réelles. Les méthodes de conception des contrôleurs feedback basées sur le calcul d'ordre fractionnaire sont utilisées et validées aussi en démontrant l'accomplissement des objectifs de conception et leur avantages sur des autres solutions de l'état-de-l'art.

Ensuite, l'assomption d'homogénéité n'est plus considéré pour valider les méthodes proposés dans le chapitre 5. La méthode proposée pour modéliser les dynamiques des véhicules en temps réel est illustré pour différents types de réponses, cela permet de déterminer la convergence de l'algorithme ainsi que l'incertitude finale sur les paramètres du modèle. Pour la suite, les deux approches feedforward (topologie PF et LPF) pour CACC sont évalués sur des convois avec véhicules des différents dynamiques. Finalement, des conclusions et une discussion sont présentés par rapport aux résultats obtenues et les considérations les plus importantes lors de la conception des systèmes de contrôle car-following.

Chapter 6

Validation results

Different approaches have been proposed along this thesis work targeting both homogeneous and heterogeneous strings of ACC and CACC-equipped vehicles. To validate the developments, design examples and experimental results are provided in this chapter. These are carried out considering the INRIA RITS team platforms and their dynamics.

First, the design algorithm of the low level control layer is depicted for the experimental platforms, as well as its validation for further employment in the car-following control framework. Subsequently, a design procedure of the novel full range spacing policy introduced in chapter 3 is provided, taking into consideration the parameters of the experimental platforms. The algorithm is validated for ACC and CACC strategies for further testing over the experimental platforms. The car-following architecture for CACC in urban environments is depicted in Sec. 6.3.2. All of the states composing the proposed state machine are demonstrated through the real experimentations scenarios with pedestrian interaction. Subsequently, the feedback control design algorithms proposed in chapter 4 are employed for the conception of controllers for the team platforms, demonstrating their benefits and design objectives fulfilment. Comparison with other state-of-the-art approaches is also provided.

The heterogeneous string control methods developed in chapter 5 are validated. First, the identification algorithm is tested to examine its convergence and efficiency to retrieve the dynamics model parameters. Subsequently, the predecessor-only strategy is evaluated considering CACC strings with vehicles whose low level control layers are different, requiring the adaptation of the FF filter in real time. Finally, the motivation for a leader-predecessor structure is supported through extensive analytical results. Concluding remarks and discussion about the obtained results are provided in Sec. 6.5, as well as some insights of most important considerations when designing car-following systems for experimental platforms.

6.1 Validation platforms

Validation process is divided in two stages: 1) a simulation study using INRIA vehicles' models is carried out; and 2) the algorithm is implemented over the experimental platforms for real testing. In this section, the simulation tools are described as well as the vehicles over which the car-following algorithms are tested.

6.1.1 Simulation tools

Two software for the implementations of the developed algorithms are employed. MATLAB[1] is used to study the frequency response and stability analysis of the different developed systems. The optimization toolbox is also employed to solve the non-convex optimization problems to find the control parameters during the design phase. Simulink modeling tool is employed to simulate the system data flow, which permits to evaluate and compare the different designed controllers over driving scenarios.

The control algorithms are coded and tested on the developing tool RTMaps 4[2]. It consists in a multi-thread tool that executes and manages the data flow between processes, permitting parallel executions and the communication with different sensors and actuators. Since it is based on modular development, it results ideal to implement different processing blocks as the high and low level control layers. The algorithms are coded in C++, which are compiled and further employed in the execution diagram in the form of input-process-output packages.

6.1.2 Real vehicles

To implement the developed control algorithms over the vehicle platforms, RTMaps is also employed. Since this tool permits connection with on-board sensors and embedded processing units through CAN, Ethernet, serial ports; it results ideal for the validation of automation algorithms over real vehicles. The INRIA RITS team, where this work has been carried out, accounts with two types of vehicles, the Cycabs and the Citröen C1.

6.1.2.1 Cycabs

The RITS team accounts with three cycabs, which are low speed electrical vehicle prototypes that are equipped with drive-by-wire capabilities and four in-wheel motors for propulsion. These are vehicles conceived for last mile on-demand transportation, mainly for urban environments with full automation [Parent and de La Fortelle, 2005]. They are equipped with on-board sensors as LiDAR, cameras, wheels encoders, GPS-RTK, inertial unit; that permit the environment perception and vehicle positioning. A picture of the Cycab platforms is provided in Fig. 6.1.

Figure 6.1: Illustration of the cycab platform during the experiments

Concerning the car-following applications, the Cycabs measure the inter-vehicular distances with four-layer Ibeo Lux LiDARs with 110° of field view, while the V2V communications links are established using IEEE 802.11g standard. The vehicle accounts also with an embedded processing unit dedicated to the low level control layer, which receives the steering wheel and the four wheels'

[1]https://mathworks.com/
[2]https://intempora.com/

encoders signals to determine the steering angle and vehicle longitudinal speed. It is also in charge of applying the reference speed tracking low level control law, with the purpose of driving the input to the motors in form of a Pulse Width Modulation (PWM) signal.

6.1.2.2 Citröen C1 Ev'ie

The Citröen C1 Ev'ie, is an electrical conversion of the classical Citröen C1. It is equipped with a 30 Kw fully electrical engine with transmission towards the front wheels, as well as a battery bank of 96 V. As on-board sensors, the C1 accounts with GPS-RTK, two Ibeo Lux LiDAR in front for obstacles detection, wheels encoders, inertial unit, brake pedal and steering wheel position encoders. A computer with RTMaps is in charge of the automation layer and communication with the different sensors and actuators.

For the longitudinal automation, the vehicle has been modified to be commanded through drive-by-wire. A 8-bit signal between 0-255 is directly sent to the vehicle propulsion system for acceleration. For the braking, a servomotor is placed beside the brake pedal, permitting to push and release the pedal by applying a desired torque. Pictures of the described vehicle and its modified braking system are provided in Fig. 6.2a and 6.2b.

(a) Picture of the C1 platform

(b) Picture of the modified braking system

Figure 6.2: Illustration of the experimental platform and its embedded braking system

6.2 Low level control layer

Along this section, a detailed description of the implemented low level control layers on the Cycabs and C1 is provided. From the actuators testing and modeling to the design of the control law over the vehicles' industrial PCs, the full implementation of the reference speed tracking block is presented. All mathematical models that are obtained to represent the low level control layer are based on offline identification of its experimental performance.

6.2.1 Cycabs

For the case of the Cycabs platforms, the embedded processing unit is programmed with the automation law for the speed tracking, sensors lecture and actuators command. The vehicle accounts with DC motors over each wheel axis. Each of them has a wheel encoder that measures the angular speed. Following the vehicle Ackermann geometry and its dimensions, the longitudinal speed is determined. The motors are commanded with PWM signals outputted by the processing

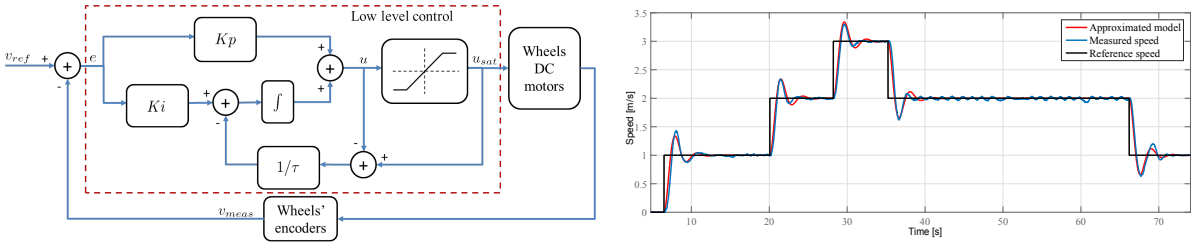

(a) Cycabs low level control architecture for reference speed tracking

(b) Approximated model, reference and measured speed for several speed change steps

Figure 6.3: Vehicle propulsion modeling

unit to a motor driver, which increases the signals power for their further delivery to the DC motors.

For the reference speed tracking task, a PI-based control strategy is employed, to ensure a fast rising time and no stationary state error. The controller tuning is done based on the vehicle open loop behavior. Different PWM values are generated and the speed evolution is observed respectively. Once the plant is approximated through a mathematical expression, the PI controller is tuned to place the closed loop poles in the desired complex plane region.

After some tests, it has been noticed that for considerable accelerations/decelerations the vehicle power-train was not able to track efficiently fast speed changes due to lack of power. For this reason, a wind-up phenomenon was appreciated. An anti-wind-up loop was introduced to mitigate the effect of saturation over the controller integrator. Finally, the control loop for the Cycab low level control layer has been implemented as in Fig. 6.3a, where v_{ref}, v_{meas}, u and u_{sat} are the reference speed, measured speed, generated control input and saturated control input. Experimental tests are depicted in Fig. 6.3b to validate the correct reference speed tracking behavior of the designed low level control. One can observe that the vehicle is able to track efficiently the speed changes with no stationary state error. The speed tracking behavior can be modeled as described in chapter 3, with a second order response:

$$Gp(s) = \frac{V_{meas}(s)}{V_{ref}(s)} = \frac{5.55}{s^2 + 8.547s + 5.55}; \tag{6.1}$$

A small overshoot is appreciated, though it does not lead to a degraded performance since for the low level control scheme it is desired to have faster rising time than less overshoot. Transport delay T_d is observed to be negligible. The further implementation of a high level gap regulation control provides the required stability that enhances the system damping.

6.2.2 Citröen C1 Ev'ie

The conception of the C1 low level control layer is more complex than the one for the Cycabs. Given that the vehicle has braking and throttling systems as conventional cars, the design must be carried out differently. The development is done in a two step process: first the action over the vehicle speed for different operation points is modeled, after the control layer is designed considering the actuators behavior and the guidelines provided in chapter 3.

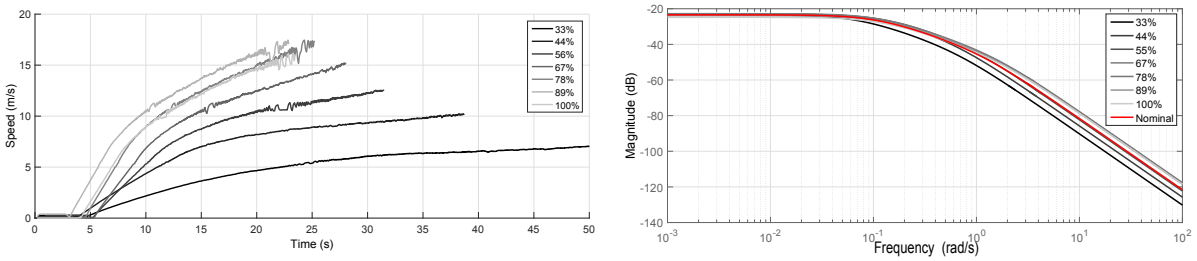

(a) Speed trajectories for different throttle level steps

(b) Approximated models and nominal model of throttle response over different operation points

Figure 6.4: Vehicle propulsion modeling

6.2.2.1 Actuators modeling

Open loop modeling is performed to determine the actuators dynamics and their effect over the vehicle longitudinal speed. First, different input levels are set to the throttle actuator and with the brake pedal.

6.2.2.1.1 Throttle Different PWM levels are introduced to the vehicle propulsion in open loop, to study the longitudinal speed evolution. Values under 30% does not yield enough propulsion torque to overcome the vehicle inertia, for which only values over 33% are presented in Fig. 6.4a. Tests with higher accelerations were not continued due to the limited length of the testing track. One can see that the vehicle speed takes form of a damped second order response. This is due to the fact that the higher the velocity, the less acceleration the vehicle is able to provide due to the fixed delivered power and increasing force losses (see chapter 3).

The throttling steps are modeled as overdamped second order transfer functions depicted in Fig. 6.4b. From all the transfer functions described by the different step responses, a nominal model is derived that approximates the best the throttle performance. The throttle nominal response results as:

$$G_{th}(s) = \frac{V_{meas}(s)}{U_{th,pwm}(s)} = \frac{2.8621}{s^2 + 1.3392s + 0.1302}; \tag{6.2}$$

where $U_{th,pwm}(s)$ is the signal driven to the vehicle propulsion which $\mathcal{L}^{-1}\{U_{th,pwm}(s)\} = u_{th,pwm}(t) \in [0, 100]$. This model is further employed in the control layer design to provide the desired closed loop performance and stability.

6.2.2.1.2 Braking system For the vehicle braking, a cascade control approach is proposed. First a nested control loop is designed to regulate the brake pedal position, by commanding through a PWM signal the servomotor that governs the brake pedal position. Subsequently, the vehicle speed evolution is modeled in function of different brake positions. This model is employed for the design of the reference speed tracking control during decelerations.

In Fig. 6.5a, the position evolution in time is studied for different PWM levels applied on the brake pedal servomotor. The brake pedal position is limited as $u_{br,pos}(t) \in [0, 5000]$, where only positions as $u_{br,pos} > 1200$ apply effectively a decelerating force on the vehicle chassis. In addition, control signal values below 30%, does not provide enough power for the motor to push the brake pedal beyond the minimal value. For this reason, 30% of PWM is assumed as the minimal control input value that is applied in case that braking is required.

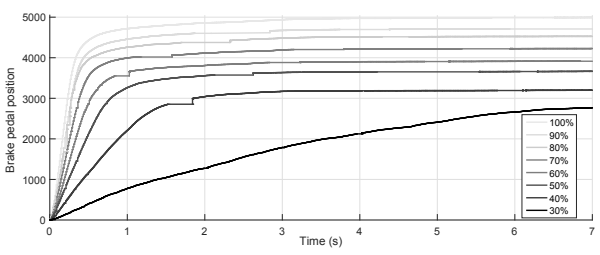

(a) Brake pedal position responses towards torque steps

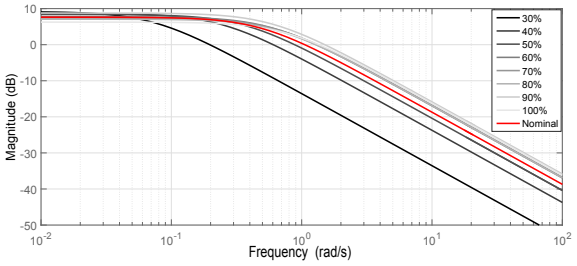

(b) Brake pedal motor models (black to light gray lines) and resulting nominal model (red line)

Figure 6.5: Brake pedal actuator modeling

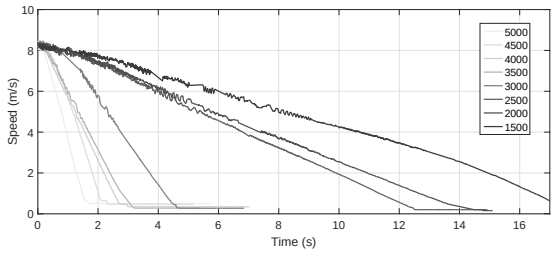

(a) Vehicle speed evolution for different brake pedal positions

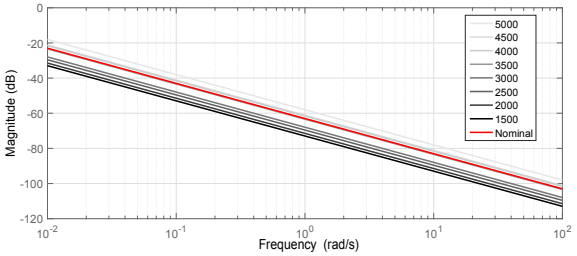

(b) Models for different braking positions (black to light gray lines) and nominal model (red line)

Figure 6.6: Modeling of the braking position action over the vehicle speed

The brake pedal position response to different motor torque steps (Fig. 6.5a) result as first order responses. These are approximated in the Bode plot in Fig. 6.5b and their nominal model in red line, whose mathematical form is as follows:

$$G_{br,pwm}(s) = \frac{U_{br,pos}(s)}{U_{br,pwm}(s)} = \frac{1.1606}{s + 0.4826}; \tag{6.3}$$

A classical PI controller is proposed for the brake pedal position control, aiming a fast response and no stationary state error over the nominal model in Eq. 6.3. Using K_p=0.0404 and K_i=0.0516, different brake pedal positions are set to study the brake system action over the vehicle speed. The closed loop responses are depicted in Fig. 6.6a and the obtained models are illustrated in Fig. 6.6b. Finally, the braking system nominal model in red line, can be mathematically expressed as:

$$G_{br,pos}(s) = \frac{V_{meas}(s)}{U_{br,pos}(s)} = -0.0007079/s \tag{6.4}$$

6.2.2.2 Control design

The nominal models of the vehicle actuators on Fig. 6.2 and 6.4, are considered for the design of the feedback speed regulation control. As can be appreciated, the actuators' models $G_{br,pos}(s)$ and $G_{th}(s)$ result of different frequency response. For each of them, conditioning filters are implemented that process the controller output $u(t)$ and delivers it into the actuators as their input signals (positive values of $u(t)$ are for throttling, while negative values for braking) agreeing with the guidelines in Sec. 3.3.2.2. PWM value $u_{th}(t)$ for the throttle and reference brake pedal position

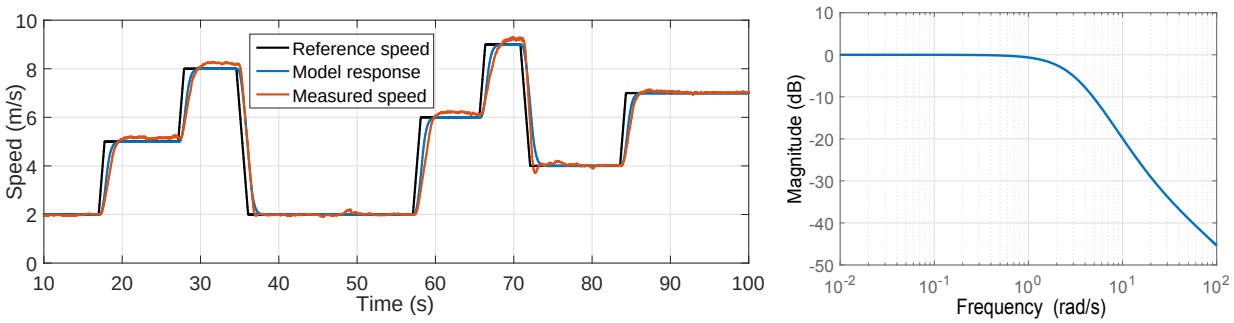

(a) Reference (black line) and measured speed (red line) compared to the model response (blue line)

(b) Approximated model (see Eq. 6.5) frequency response

Figure 6.7: Validation of the longitudinal low level control layer through reference speed steps

$u_{br,pos}(t)$ for the braking system loop respectively. These filters are designed with the purpose to obtain speed tracking responses as consistent as possible regardless if its acceleration or braking. They also permit to low-pass the signals and reduce the risk of actuator saturation. With respect to the design of the feedback controller, loop shaping guidelines in [Zhou and Doyle, 1998] are followed seeking robustness and output tracking performance. Robustness is fundamental in this case given that although the identified actuator models approximate correctly their frequency behavior, the different operation points introduce uncertainties that modify the actuators' responses.

The low level system design is validated and modeled through the application of different reference speed steps with $\pm 4 \mathrm{m/s}^2$ rates, for which the longitudinal speed evolution is studied and modeled. Fig. 6.7a depicts the results, where it is visible that the speed tracking performance is satisfactory. For both accelerations and decelerations, the vehicle speed is adjusted with almost no overshoot and with an acceptable stabilizing time, being aware of the actuators operational limits. It is important to highlight that despite the difference between actuators frequency behavior, the speed tracking performances results very similar during both throttling and braking. This property improves the validity of an unified response model that describes the speed tracking closed loop system, which is modeled with the expression in Eq. 6.5.

$$Gp(s) = \frac{V_{meas}(s)}{V_{ref}(s)} = \frac{9.454}{s^2 + 5.689s + 9.462}; \tag{6.5}$$

6.3 Homogeneous strings control

This section presents the application of the algorithms proposed in chapters 3 and 4, under the assumption of homogeneity between vehicles dynamics in the same string. Firstly, the fulfillment of the proposed full range spacing policy objectives is demonstrated. Simulations and real experiments are described on ACC and CACC-equipped vehicles. A full demonstration of the enhanced CACC algorithm for urban environments is provided, where interaction with pedestrians is included to validate the proposed state machine solution. Finally, the motivation for employing fractional-order calculus on the design of feedback gap-regulation controllers is justified with stability studies and experimental validations.

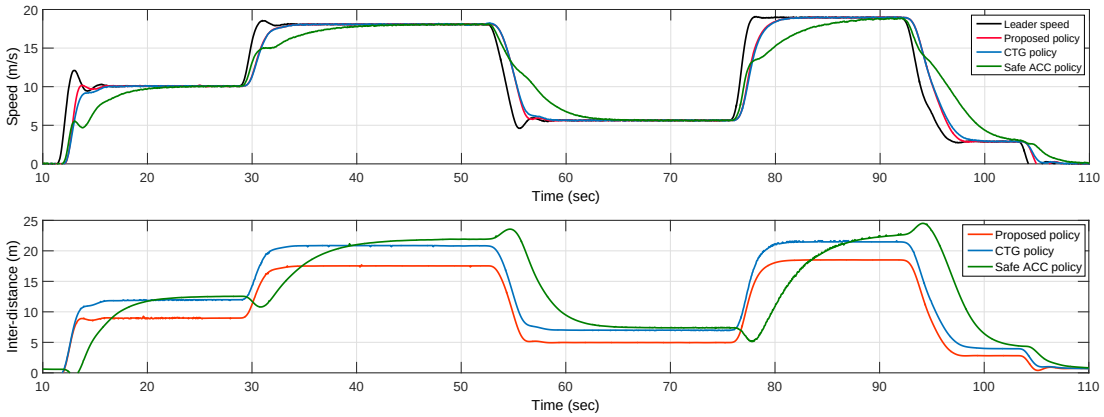

Figure 6.8: Speed comparison between vehicles employing the three different policies

6.3.1 Full-range spacing policy

To demonstrate the correct performance and the benefits of the proposed spacing policy, simulations and a comparison with other spacing policies employed in the literature are provided. A two-vehicle string is used to evaluate the performance in simulation, considering the Cycabs longitudinal model. Three car-following policies are compared employing the ACC technique: the proposed full-range spacing policy [Flores et al., 2017], CTG and the safety distance policy [Ioannou and Chien, 1993]. The vehicles' speeds and spacings are evaluated in the Fig. 6.8 in the upper and lower plot respectively. The employed standstill distance is set to 0.35 meters and the target time gap is 1.1 seconds.

It can be appreciated that in terms of speed the proposed approach and the CTG policies are similar, which is due to the fact that both strategies employ a time gap-based control loop. On the other hand, the safe ACC policy tracks the preceding vehicle in a more conservative manner. This can be noticed in the inter-distances plot, which shows that this technique produces higher spacings with slower speed transitions. In the same plot, the proposed full-range and the CTG policies perform similarly in low speeds in terms of spacing, but as the speed increases one can distinguish that the former strategy suggests to maintain lower inter-distances than the CTG. Regarding the string stability, it is clear that the car-following maneuver is executed in a stable way, given that the leader vehicle oscillations are attenuated as they are propagated to the ego-vehicle. This permits that the amount of vehicles that composes the string could be increased without leading to a possible rear-end collision. The proposed algorithm was also tested on the experimental platform at INRIA test tracks and compared against the CTG policy, considering the parameters expressed in Tab. 6.1.

Table 6.1: Spacing policies validation parameters

Strategy	V_{lim}	h_{targ}	h_{init}	std	B_{max}	J_{max}	τ
CTG-based ACC	4 m/s	1.1 s	-	0.38 m	1.5 m/s^2	1.5 m/s^3	0.4 s
Proposed ACC	4 m/s	1.1 s	0.65 s	0.38 m	1.5 m/s^2	1.5 m/s^3	0.4 s
CTG-based CACC	4 m/s	0.6 s	-	0.38 m	1.5 m/s^2	1.5 m/s^3	0.09 s
Proposed CACC	4 m/s	0.6 s	0.38 s	0.38 m	1.5 m/s^2	1.5 m/s^3	0.09 s

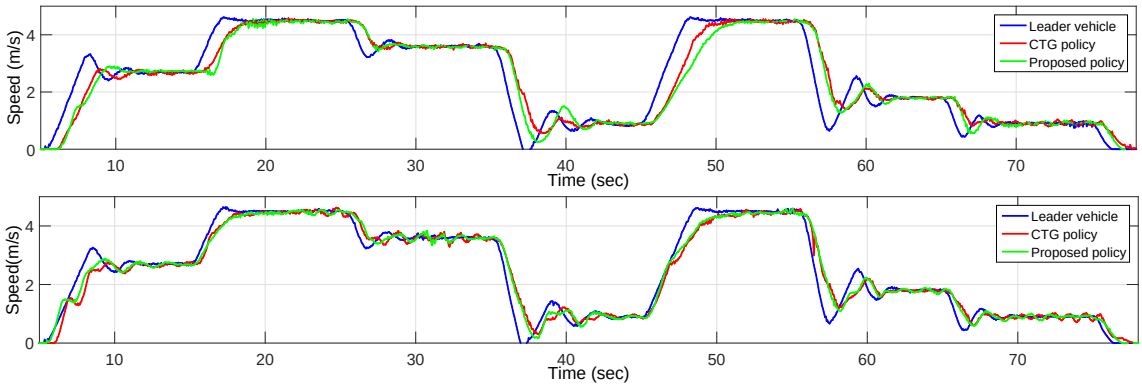

Figure 6.9: Speed evolution comparison employing the CTG strategy and the proposed spacing policy, for ACC (top figure) and CACC (bottom figure)

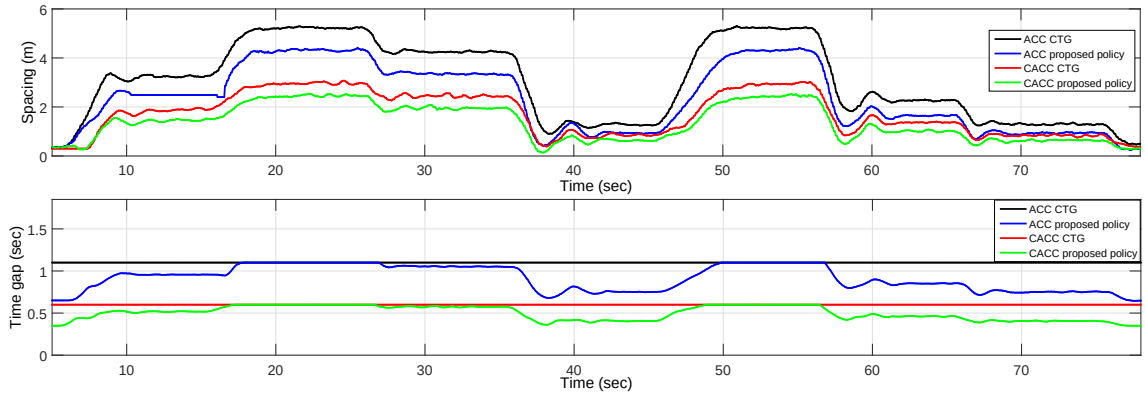

Figure 6.10: Inter-distances (top figure) and time gaps (bottom figure) evolution comparison employing the CTG strategy and the proposed spacing policy, for ACC and CACC

The first vehicle follows a speed profile with several speed changes to see the inter-distance evolution of the follower vehicle, as well as the tracked time gap that outputs the algorithm for both cases. Due to the fact that the Cycabs are not able to drive at speeds higher than 5 m/s, the tests are scaled to the speed range of such platform. The speed boundary V_{lim} between low and high speeds is configured as 4 m/s. The tests are carried out using firstly ACC and afterwards the same speed profile is performed using CACC. Notice that the maximum jerk and deceleration values are chosen to remain in the comfort limits of driving, following the guidelines in [Karjanto and Yusof, 2015].

Fig. 6.9 depicts two experimental use cases, one with the CTG policy and another with the proposed full range spacing policy. A speed profile is set for the leader vehicle and the following cars are tracking it both for ACC and CACC (see top and bottom graphs respectively). As expected, the CACC followers react in a faster way towards leader speed changes than the ACC-equipped vehicles, which is produced by the lower time gaps that are targeted and the communication links.

In the upper plot of Fig. 6.10, a comparison between the spacing evolution when employing CTG and the proposed strategy is depicted, applying ACC and CACC strategies. At low speeds the behavior results similar in terms of spacing, but as the speed increases to $V_{lim} = 4$ m/s

the inter-distance reduction yielded by the proposed approach becomes more and more visible in comparison to the CTG strategy. This is due to the adaptation of the equivalent time gap from the initial value (0.65 s for ACC and 0.35 s for CACC) to the target time gap (1.1 sec for ACC and 0.6 sec for CACC) as the speed increments (see lower plot of Fig. 6.10). It is also possible to distinguish the transition moment between low speeds zone and high speeds, since the time gap stays at the targeted value and the inter-distance difference between CTG and the full-range policy remains fixed. It is also visible that the oscillations of the leader vehicle are not amplified by its follower (string stable), which is one of the main motivations for the spacing policy design.

6.3.2 Enhanced Car-Following Structure

This section presents the integration of the CACC structure in a more complex framework, leading to a full longitudinal control system that takes into account not only car-following capabilities, but also interaction with other road agents as pedestrians. Three *Cycabs* and three pedestrians, including one equipped with V2P communication, are used for an experimental validation of the proposed system. A speed profile emulating an urban driving scenario with several speed transitions is set for the platoon leader, while the other two *Cycabs* are performing car-following. The experiment is composed by several scenarios for the test and validation of the leader speed reduction, car-following, emergency braking and gap closing systems. Finally, a complete demonstration of all systems showing the integration and transitions is provided.

6.3.2.1 Leader speed reduction

Fig. 6.11 displays the distance to the pedestrian tracked by V2P (blue line) and LiDAR (red line) in the upper plot. It is shown that the V2P communication system can serve as a predictive tool since the distance to pedestrian is available even when he/she is not visible for the LiDAR. Fusion between these two sources is then useful in urban environments where occlusion degrades the performance of LiDAR-based protection systems.

Besides, as the first vehicle follows its reference speed profile, a speed reduction is performed by the platoon leader after detecting a possible collision (time t=29s in Fig. 6.11). Once the risk of collision with the pedestrian is avoided (at time t=32s), the desired speed profile is resumed. This deceleration is performed in function of the vehicle and pedestrian motion (speeds and positions) as they approach the intersection point. This is done in a way that the motion prediction yields no collision at the crossing point. At this moment, the speed profile is resumed permitting the pedestrian to cross the intersection point first.

6.3.2.2 CACC Car-following

Each follower vehicle implements the FF/FB CACC car-following structure described in chapter 3. A time gap of $h_{min} = 0.7s$ is applied so that string stability is ensured using a CACC car-following technique. A controller robust to plant gain variations is proposed to be implemented over each of the follower vehicles as presented in Sec. 4.3.2.

Fig. 6.12 shows the time response of the leader vehicle to the reference speed given by the speed profile and the rest of the string members regulating the inter-vehicle distances. The plot shows that the behavior results string stable, since during leader speed transitions the rest of the vehicles track their precedings' speeds attenuating the oscillations. Such behavior would permit to extend the string size ensuring safety and comfort. This response is more visible when the leader reference

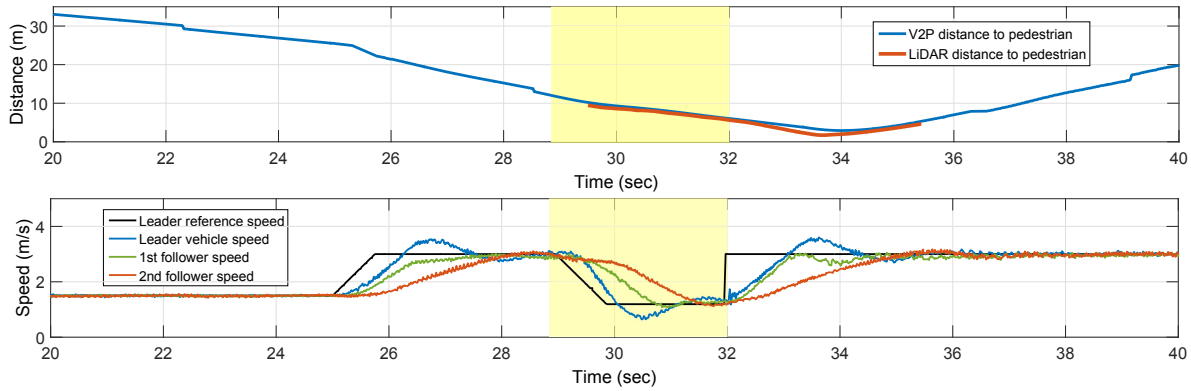

Figure 6.11: Platoon performance when the leader vehicle detects a crossing pedestrian with the V2P system and the LiDAR, as well as the speed reduction zone (light yellow background)

speed changes and the rest of the string members must adjust their speed smoothly (time=80, 100, 120 sec).

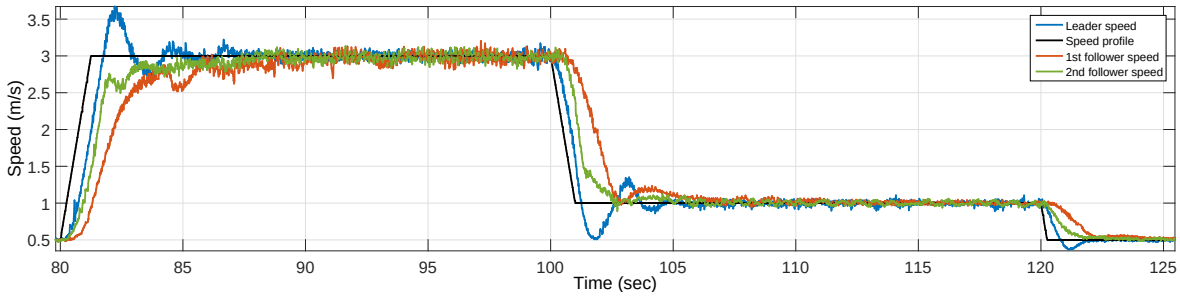

Figure 6.12: Leader and followers performing car-following maneuvers in stop&go scenarios

6.3.2.3 Emergency braking

Whenever a pedestrian crosses the platoon between the string members, the emergency braking state is triggered. In this situation, the relative distance to the obstacle is output by the environment detection system and a stopping maneuver is started. Here, the distance to pedestrian, reference and real speeds of the different vehicles are examined in Fig. 6.13 for a desired stopping distance $d_{safety} = 1.5\,m$.

The controller outputs the target speed (black line) to perform the maneuver, while the leader and first follower (blue and green lines) continue in car-following state. The brown line shows how the ego-vehicle is quickly approaching the pedestrian, but the displacement rate decreases during the braking until it stops at d_{safety} from the obstacle. Finally, the vehicle stands still waiting for the pedestrian to leave of the platoon corridor and switch to the gap closing state. It is observed that the control loop performs correctly, since the vehicle stops at the desired safety distance in spite of the actuator lag between reference and measured speeds.

6.3.2.4 Gap-closing

After the pedestrian is out of the platoon corridor, the ego-vehicle has to close the gap with respect to the preceding car through the time gap manipulation. In Fig. 6.14 two plots are presented, the

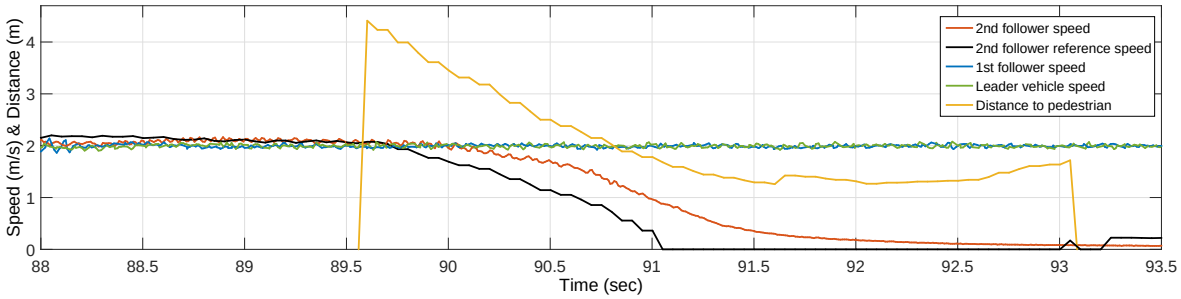

Figure 6.13: Demonstration of the emergency braking maneuver with the control variables

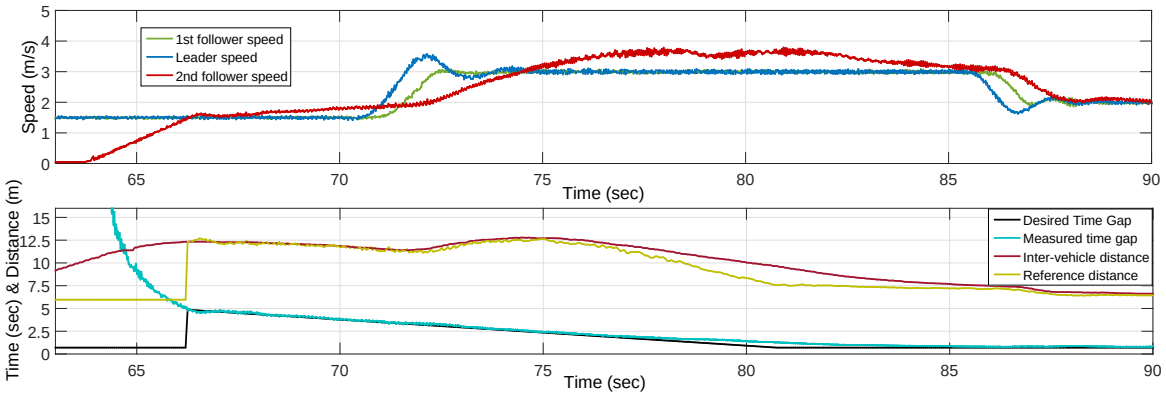

Figure 6.14: a) Upper plot shows the performance of the three string members by showing each vehicles' speed. b) Lower plot depicts the control variables of the ego-vehicle

upper one shows the general platoon overview with the string members' speeds. The lower plot details control variables such reference and current spacing, and desired and measured time gap.

Firstly, the vehicle starts the platoon rejoining maneuver by accelerating at $a_{gc} = 1.5m/s^2$ (time t=62s to t=67s), until the gap-closing time gap range (between h_{max} and h_{min}) is reached. Then, the time gap (blue line) decreases as the speed is incremented, completing the target identification process. The reference time gap reduction starts from h_{max} to h_{min} with a t_{close} = 15s. This process is depicted by the reference time gap h (black line) and the real time gap h_{meas}. In the upper plot, one can highlight how the gap closing maneuver requires the vehicle to speed up at the beginning to rejoin the string and reduce the inter-distance, even if the leader vehicle also accelerates (time t=72s). The platoon coupling is carried out in a stable and smooth way as can be noticed from time t=80s to t=90s, when finally the ego-vehicle is again at the car-following state with the desired time gap h_{min}.

6.3.2.5 State machine demonstration

A complete scenario has been set to validate the transitions between the three states that composes the architecture. Fig. 6.15 shows the three vehicles string performing a CACC car-following with a time gap of $h_{min} = 0.7sec$. Suddenly the last follower vehicle performs an emergency stopping due to a pedestrian that crossed in front (time t=100s), and the speed decreases. Time gap with respect to the preceding vehicle is reduced when performing the gap-closing state (time t=103s to t=121s). During this period, another pedestrian crosses but this time in front of the leader vehicle, requiring the pedestrian detection system to stop following the speed profile and reduce the platoon speed

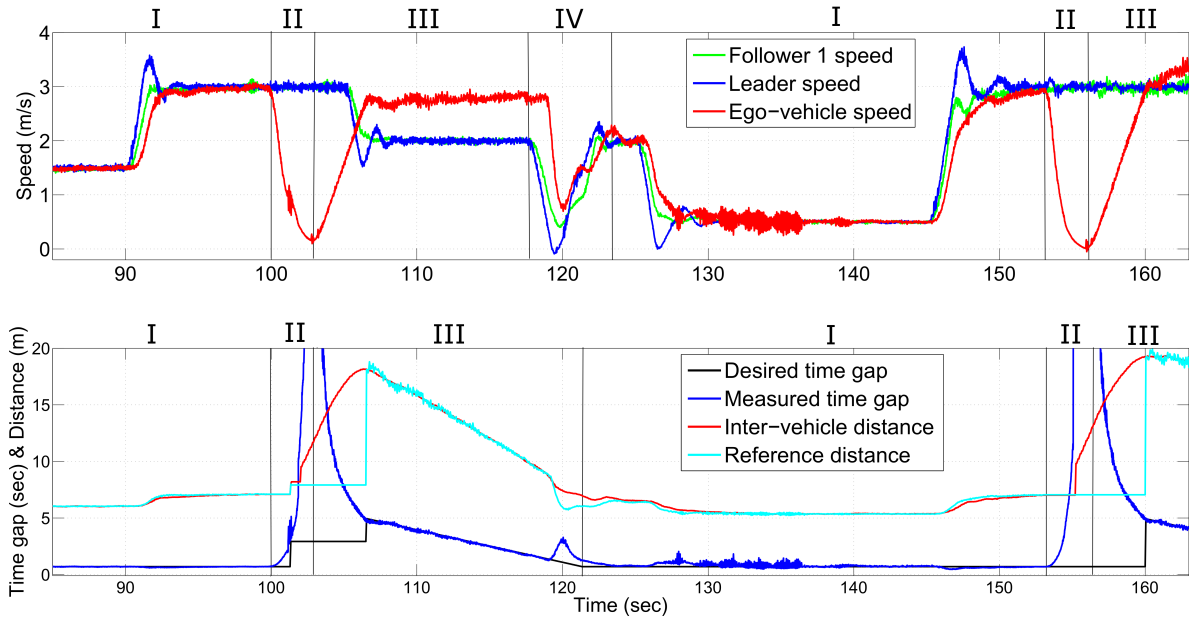

Figure 6.15: State machine integration: V2P protection maneuver (IV), car-following (I), emergency braking (II) and gap-closing (III). Their transitions are shown through a speed plot (upper plot) and the control variables of the ego-vehicle (lower plot).

to avoid further collision with it. From time t=121s to t=154s, the car-following state is correctly resumed by following the speed profile in a string stable way. Afterwards, another pedestrian goes through the platoon corridor (time 154-157s) which activates the emergency braking system followed by the gap-closing when the pedestrian exits the ego-corridor.

6.3.3 Feedback controllers design validation

The control algorithms for the design of feedback controllers are demonstrated in this section, employing the vehicles' models. Experimentations are provided to validate the performance and prove the motivation for employing the designed control strategies. First, the algorithm for improving string stability with optimized time gap is executed over a real vehicle dynamics model, which is after applied on the Cycabs. The fractional-order controller for optimized robustness towards plant gain changes is also presented with simulation results. Finally, the loop-shaped fractional-order lead compensator is tested over the vehicle C1 to observe its performance and robustness benefits.

6.3.3.1 String stability with reduced time gap

To validate the proposed method, a comparison with state-of-the-art feedback control approach is proposed for ACC and CACC. Literature review shows several implementations using IOPD-based feedforward controllers for ACC/CACC systems [Shaw and Hedrick, 2007b], [Milanés and Shladover, 2014], [Naus et al., 2010], exhibiting good performance. A comparison with the FOPD controller proposed is carried out in this section. Since IOPD controllers have two parameters, only two design requirements can be fulfilled. For this reason, two IOPD controllers are designed to do a proper comparison. The first controller is aimed to guarantee the loop bandwidth and its phase margin (referred as $IOPD^{PM}$), while the other should ensure loop bandwidth and maximize

the string stability (referred as $IOPD^{SS}$). For both IOPD controllers, the solutions are sought for the lowest time gap possible that allows string stability.

In Tab. 6.2, the designed FOPD and IOPD controllers are presented for ACC and CACC control structures, as well as the obtained system loop bandwidth, phase margin and minimum time gap for string stability. The controllers are designed for the Cycabs dynamics model.

Table 6.2: Controller parameters, minimum time gap allowed and stability metrics

$Controller$	Kp	ω_c	α	$h[s]$	$\phi[^\circ]$	$\omega_{gc}[rad/s]$	$\|\|\Gamma(s)\|\|_\infty$
$FOPD_{ACC}$	2.079	2.640	1.075	0.536	59.148	3.556	1.000
$IOPD^{PM}_{ACC}$	1.613	2.015	1.000	0.572	60.078	3.505	1.000
$IOPD^{SS}_{ACC}$	1.919	2.399	1.000	0.538	54.153	3.504	1.000
$FOPD_{CACC}$	2.483	3.625	1.188	0.254	60.031	3.556	1.000
$IOPD^{PM}_{CACC}$	1.613	2.395	1.000	0.308	60.103	3.507	1.000
$IOPD^{SS}_{CACC}$	2.367	3.734	1.000	0.260	42.851	3.501	1.000

All controllers produce the desired loop bandwidth, but it is observed that when designing an IOPD for the phase margin requirement, the time gap cannot be lowered as much as if the design requirement was maximizing string stability. On the other hand, the $FOPD_{ACC}$ controller is capable not only to ensure the string stability for the same time gap than $IOPD^{SS}_{ACC}$ does, but also to provide the desired phase margin. This demonstrates the compromise that exists when enhancing both the system performance and loop stability, which can be improved with the more flexible structure of the fractional-order controller.

This is depicted as well in Fig. 6.16. In the left figure, the frequency response of $L_{ACC}(s)$ is presented when using the three controllers for their resulting minimum time gaps. The magnitude of their closed loop responses is illustrated in the right figure setting a $h = 0.536$ sec. A clear difference is observed in the performance provided by the $IOPD^{PM}_{ACC}$ which results string unstable as the time gap set is lower than its limit. For the other controllers, the results showed in the table are also visible in Fig. 6.16b since their closed loop performance results equal (a $||\Gamma(s)||_\infty$=1) for the same time gap, but the phase margin is reduced in the case of the $IOPD^{SS}_{ACC}$ (see Fig. 6.16a) with respect to what the $FOPD_{ACC}$ controller yields.

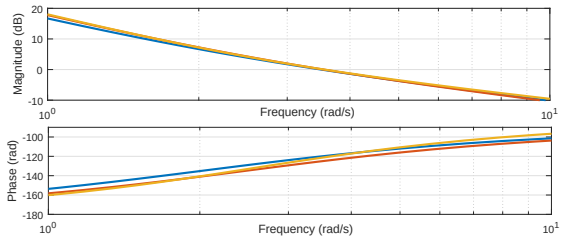

(a) Magnitude and phase of the loop response $L_{ACC}(s)$

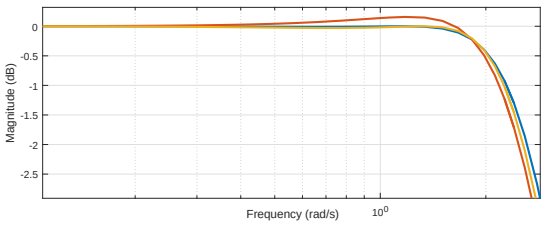

(b) Magnitude of the closed loop response if a time gap of $h = 0.536$ sec is set

Figure 6.16: Frequency analysis of the control structure having as feedback controller: $FOPD_{ACC}$ (yellow line), $IOPD^{SS}_{ACC}$ (blue line) and $IOPD^{PM}_{ACC}$ (red line)

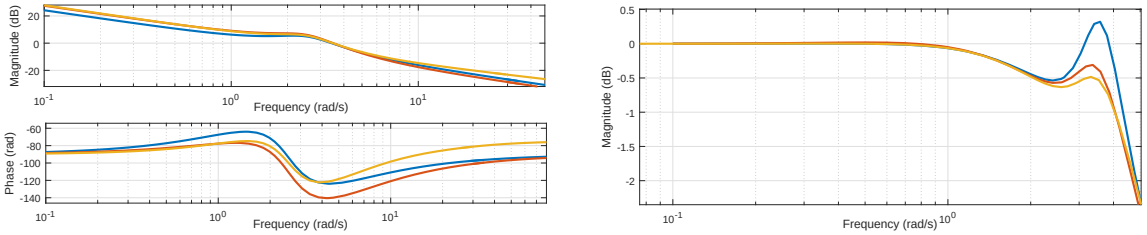

(a) Magnitude and phase of the loop response $L_{CACC}(s)$

(b) Magnitude of the closed loop response if a time gap of $h = 0.254$ sec is set

Figure 6.17: Frequency analysis of the control structure having as feedback controller: $FOPD_{CACC}$ (yellow line), $IOPD^{SS}_{CACC}$ (blue line) and $IOPD^{PM}_{CACC}$ (red line)

It can be observed that the $FOPD_{CACC}$ attains the three objectives for a minimum time gap of $h = 0.254$ sec. On the other hand, when employing an IOPD controller for the same time gap, one must decide between either improving the system stability or increasing the closed loop performance with string stable behavior at a lower time gap. This is noticed in the properties of $IOPD^{SS}_{CACC}$ controller, where even if it ensures string stability for almost the same time gap than the $FOPD_{CACC}$, the resulting phase margin is compromised. If the desired phase margin must be guaranteed with an IOPD controller, the time gap exigence must be relaxed to provide a string stable behavior. This is illustrated in Fig. 6.17, where the left figure depicts the bode response of $L_{CACC}(s)$ for the three mentioned controllers. In the right plot, the closed loop magnitude response is studied using each of the three controllers with a time gap of $h = 0.254$ sec. In such figure, the $IOPD^{PM}_{CACC}$ controller presents string unstable behavior, amplifying leader's oscillations. For the other two controllers the performances result almost similar. However, a difference is observed around $\omega = 0.5$ rad/sec where the closed loop magnitude yielded by the $IOPD^{SS}_{CACC}$ results slightly higher than unity.

Since the V2V temporal delay affects directly the string stability, the minimum time gap that can be set is modified. Having the three CACC controllers presented in Tab. 6.2, the communication delay in $D(s)$ is varied as $\theta \in (0, 0.3)s$ to study the minimum time gap for which string stability is guaranteed. Fig. 6.18 shows the study, where it is observed that lower time gaps require low latency communications as would be expected. This evidences the relevance of the FF term in this type of control structures, where ideal communications provide string stability

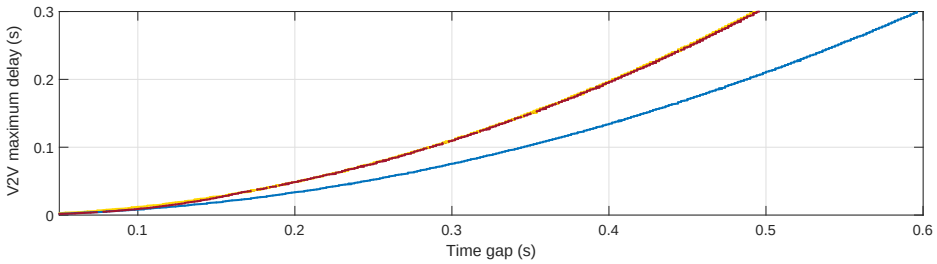

Figure 6.18: Maximum tolerable communication delay time for each time gap ensuring string stability for CACC strings for the $FOPD_{CACC}$ (yellow line), $IOPD^{SS}_{CACC}$ (red line) and $IOPD^{PM}_{CACC}$ controllers

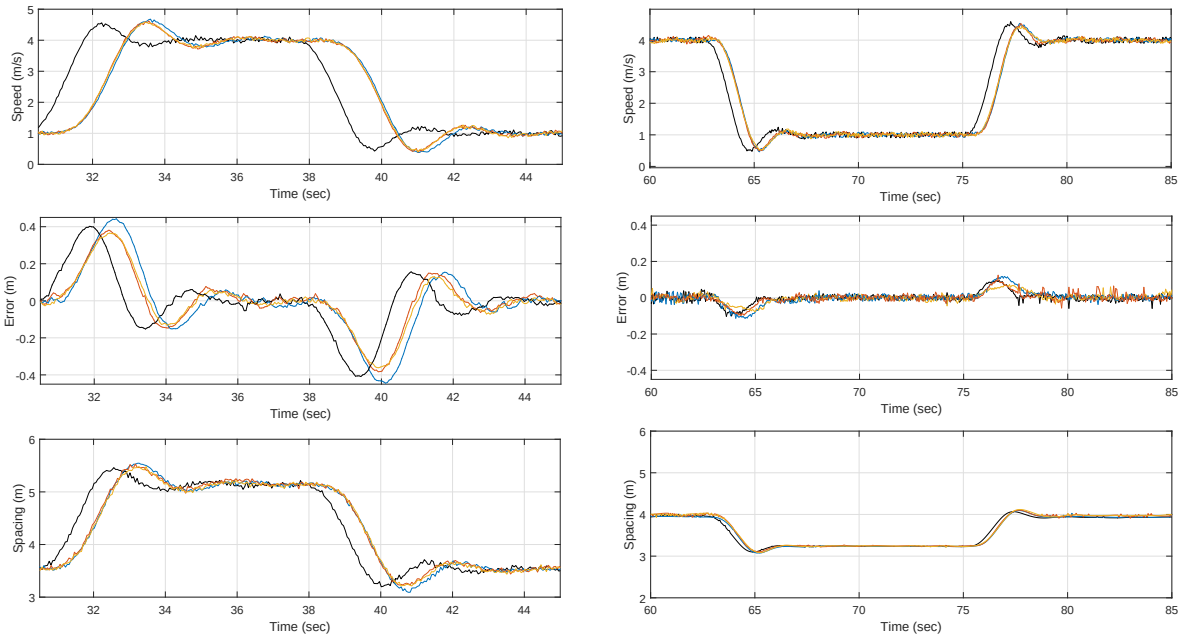

(a) ACC-equipped vehicles string evaluation (b) CACC-equipped vehicles string evaluation

Figure 6.19: State variables evolution applying $IOPD^{SS}$ (red line), $IOPD^{PM}$ (blue line) and $FOPD$ (yellow line) controllers; over ACC and CACC-equipped vehicles

for all time gaps higher than zero [Naus et al., 2010]. It is also worthy to mention that feedback loop robustness plays a key role for assuring string stability, overall when V2V temporal delays increase.

For the real tests (see Fig. 6.19), a 3-vehicle string is used. ACC and CACC scenarios are tested to compare the performances of the three controllers previously designed. For the sake of clarity, the graphics will show the leader speed (black line) and the speed of the third vehicle in the platoon for the three experiments. With respect to spacing errors and inter-distances, second and third vehicles' variables are depicted. For the ACC technique, a distance corresponding to a time gap of $h = 0.55$ sec is added to a standstill distance of three meters. The behavior observed in the simulations is also repeated in the real experiments.

The speed evolution results very similar for the three scenarios, except the $IOPD^{PM}_{ACC}$ controller which oscillations result slightly higher with respect to the others. Such behavior is more visible from the second to the third vehicle, where the spacing error is amplified rather than attenuated, as a consequence of the weaker string stability limit that this controller yields. A smaller difference in the stabilization period is observed between the $IOPD^{SS}_{ACC}$ and $FOPD_{ACC}$ controllers performance due to the phase margin difference. The string stability results similar between both controllers since their limits are equal according to the theoretical analysis.

The available communication links are now employed to perform the CACC tests. The three CACC controllers in Tab. 6.2 are implemented following the proposed control structure CACC. As it was previously stated, measured communication delay is 0.08 sec. A time gap of 0.26s is set for all vehicles in the string with a standstill distance of three meters.

Comparing to the ACC scenario, it is clear that shorter distances and faster gap-regulation maneuvers are achieved, which also leads to smaller peak errors. Even though the results are

observed similar in terms of speed evolution, the spacing errors of the $FOPD_{CACC}$ controller shows an enhanced stability with more attenuation upstream, while the $IOPD^{SS}_{CACC}$ is at the stability limit and $IOPD^{PM}_{CACC}$ shows an amplification of the spacing error.

6.3.3.2 Robustness against plant gain variations

Over this section, results are provided using the feedback control design method for robustness against plant gain variations. The algorithm is applied considering the Cycabs model as in the previous section, in a CACC control structure. As loop design objectives, a phase margin around 90° is sought with a gaincross frequency of 1 rad/s. The fractional-order controller parameters are obtained solving the non-convex optimization algorithm. The parameters are: K_p=0.77, K_d=0.495 and α=1.025. Loop response is presented in Fig. 6.20a, fulfilling the phase margin and loop bandwidth requirements.

The loop response $L_{CACC}(s)$ attains the flat phase condition around the gaincross frequency ω_{gc}. In other words, the phase derivative results zero ensuring that if the plant DC gain is slightly perturbed, the phase margin remains of the same value. To demonstrate the effectiveness of the obtained controller, a string of CACC vehicles is tested following a CTG policy with a 0.6s time gap. Fig. 6.20b presents the vehicles' speeds for different Cycab models which DC gains are modified randomly with a 10% of their nominal value. One can appreciate that despite the variations in the plants' gain, the algorithm is able to provide the car-following stability. The condition of string stability is also ensured, which is visible in the vehicles speed evolution. The oscillations over the speeds are attenuated as they are propagated in upstream direction.

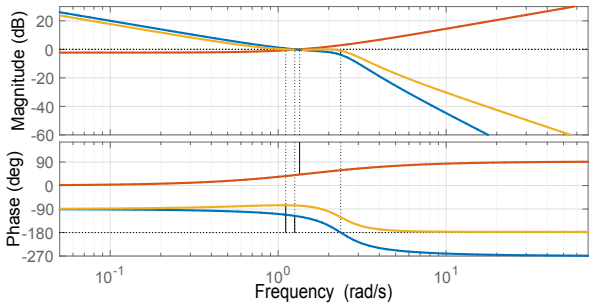

(a) Bode plot of the plant $Gp_f(s)$ (blue line), controller $C(s)$ and the loop response $L_{CACC}(s)$ (yellow line)

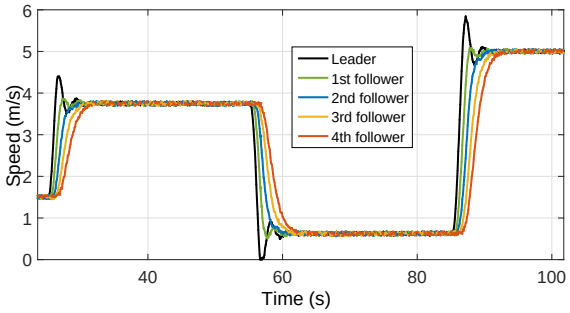

(b) Simulation of a CACC string of vehicles with perturbed DC gains

Figure 6.20: Stability study and simulation of vehicles' speeds evolution with the proposed control approach

6.3.3.3 Loop shaped fractional-order compensator

The algorithm for the design of a fractional-order compensator is evaluated considering the dynamics of the Citröen C1 in Eq. 6.5. As described in the Sec. 4.3.3, template functions are used to shape the loop response. They define the desired performance, robustness and control effort that the closed loop system should have. The template functions are:

$$\begin{aligned} W_T(s) &= 1; \\ W_S(s)^{-1} &= \frac{s}{\omega_S + s/M_S}; \\ W_U(s)^{-1} &= \frac{\omega_u}{s + \omega_u/M_u}; \end{aligned} \tag{6.6}$$

where ω_S is set equal as the plant bandwidth, $M_S = 2$ ensuring at least $\pi/3$ of phase margin [Zhou and Doyle, 1998], and finally $M_U = 2$ with a $\omega_u = 1/h$. The CACC control structure is employed, which means that the closed loop response depends as well on the feedforward link and the communication delay. A time gap of h=0.6s is set following human factor guidelines [Nowakowski et al., 2010a], while a communication lag of θ=0.08s is set given the maximum observed value during experimental tests. The optimization algorithm is applied to retrieve the controller parameters, minimizing the cost function that penalizes non ideal closed loop results. The fractional-order feedback compensator for the model in Eq. 6.5 results as follows:

$$C(s) = \frac{0.788}{(1 + 0.6s)} \frac{(1 + \frac{s^{0.3}}{4.386})}{\left(1 + \frac{s^{0.3}}{17.53}\right)} \tag{6.7}$$

In Fig. 6.21, the resulting closed loop functions are studied using the obtained controller, to verify the fulfillment of the control design objectives. The template functions are depicted for the three specifications (red lines), while the resulting complementary sensitivity, disturbance sensitivity and control effort functions are depicted (blue lines).

In the left figure, it can be seen that the string stability condition is satisfied given that the ∞-norm of the complementary sensitivity results equal to one. The system sensitivity is presented in the middle figure, where the desired shape is achieved with a peak sensitivity of 2dB, at the desired frequency ω_S. This guarantees that the loop is stable and robust to possible load disturbances. The right figure describes the resulting control effort response to changes in the reference input. It is visible that the function bandwidth condition is satisfied, meaning that input noise is not amplified. Nevertheless, at low frequencies the function presents low gain given that the compensator DC gain does not tends to infinite as $\omega \to 0$. This is due to the fact that for CACC systems, the reference input tracking task is performed mainly by the feedforward system, while the feedback controller provides robustness and loop stability at middle frequencies.

In Fig. 6.22, experimental results are presented when applying the designed compensator in Eq. 6.7. The experiment is performed using three C1 vehicles, performing CACC at a time

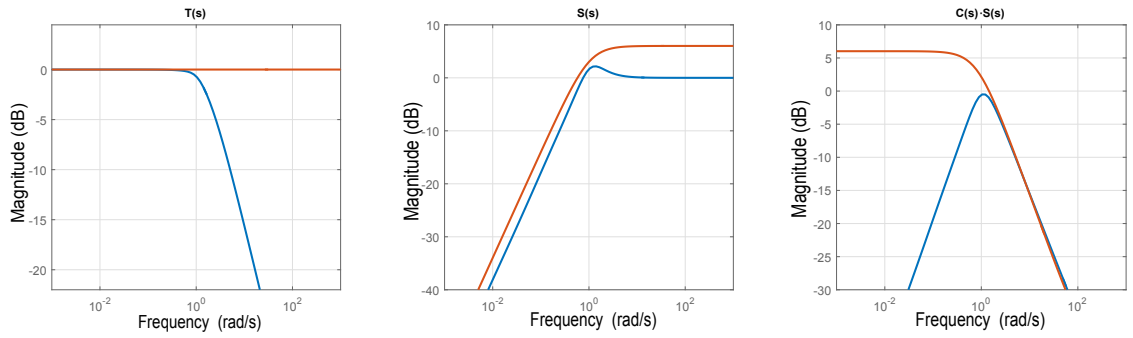

Figure 6.21: Template (red lines) and resulting closed loop functions (blue lines), applying the designed controller

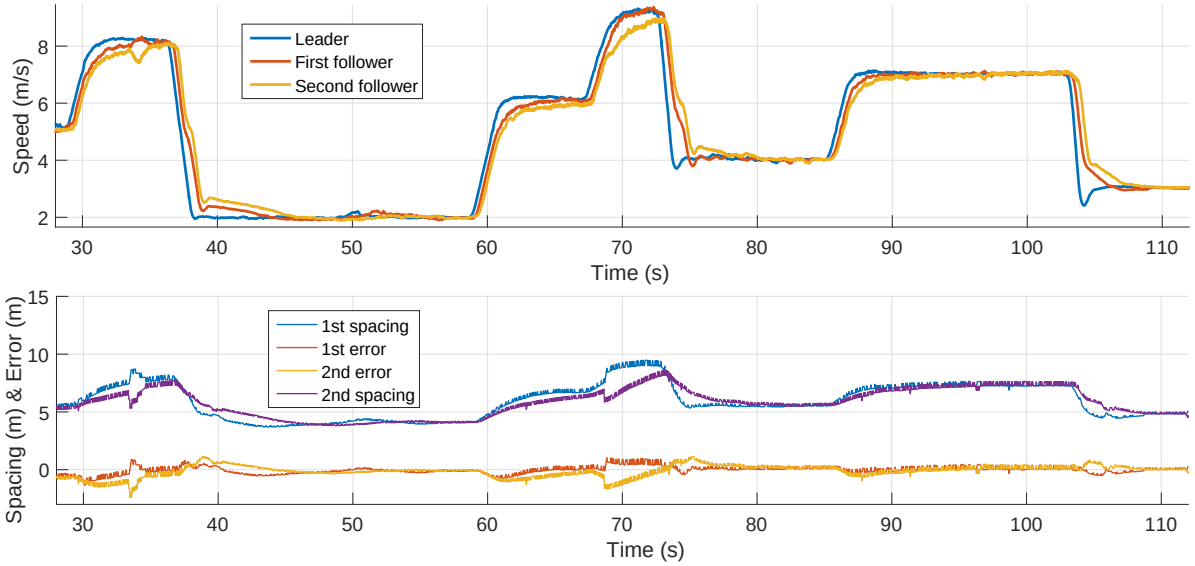

Figure 6.22: CACC validation experiment employing the loop shaped fractional-order compensator

gap of 0.6s with V2V communication links of θ=0.08s of delay. A standstill distance of three meters is adopted. As one can appreciate in the plot, the follower vehicles track correctly the leader vehicle speed changes. This is carried out in a damped way with no overshoots during the speed propagation in upstream direction, demonstrating the fulfillment of the string stability requirement. It is important to highlight that despite some failures in the inter-distance perception system (t=34s and t=67s), the control algorithm is able to stabilize the car-following behavior and maintain the spacing error below 2 meters.

6.4 Heterogeneous strings control

The remaining of this chapter concerns the validation and results related to the control of heterogeneous strings. This section is divided in two parts: first, the strategies where information only from the preceding vehicle is available (PF topologies) and second, the approach where the leader vehicle is also considered in the control structure (LPF topology). The vehicle dynamics in the same string are non-identical, which increases the complexity of the control design and the stability study. For this reason, several vehicle types are considered with different damping properties and response bandwidths.

6.4.1 CACC under predecessor-only topologies

As detailed in the Sec. 5.3, PF topologies are the most employed strategies for CACC car-following, requiring the less complex communication network. An inverse model-based FF approach has been proposed that employs an identification algorithm to obtain the preceding vehicle longitudinal model. It is employed to adapt in real-time the FF filter, improving significantly the reference tracking performance and the string stability. First, the particle filter algorithm is evaluated with different data to observe its convergence properties and the resulting preceding vehicle modeling uncertainty. A stability study is provided when using the adapted FF filter for the worst case modeling uncertainty, as well as experimental results when using the online adapted FF structure

with the particle filter.

6.4.1.1 Identification algorithm

The preceding vehicle longitudinal model is obtained using the particle filter. This section evaluates its performance to determine the algorithm convergence properties and output uncertainties. The lower the magnitude of such modeling disturbances, the better the FF filter performs attaining a good model inversion. For the convergence validation, the algorithm is applied over nine different vehicles' responses to a reference speed profile. Vehicles' parameters are selected as $\omega_n \in [0.95, 5]$ and $\xi \in [0.2, 1]$. In Fig. 6.23, the experimental convergence test is depicted. Each individual experiment consists on modeling the vehicle response with 200 particles over 10 resampling iterations, given the speed observations corrupted by noise $\mathcal{N}(0, 0.15)$ and sampled at 0.1s of sampling period.

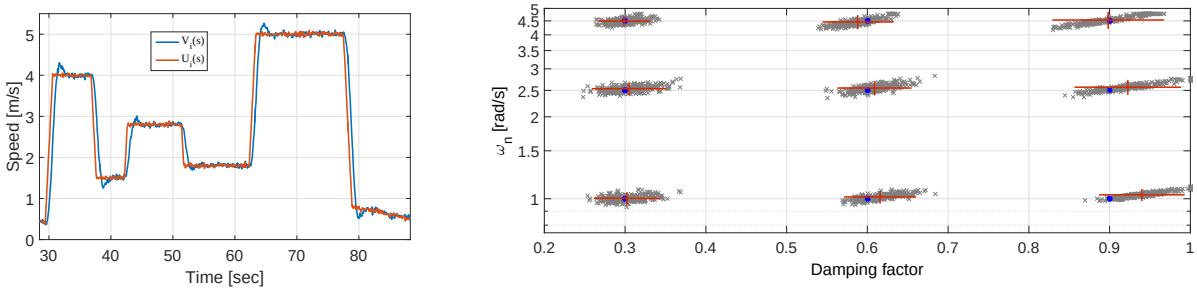

(a) Speed profile with speed observations for a vehicle longitudinal model

(b) Particle filter tests outputs (gray dots), with ground truth (blude dots) and output variance (red lines)

Figure 6.23: Stability study and simulation of vehicles' speeds evolution with the proposed control approach

As one can see, since the reference and measured speeds are corrupted by noise, the algorithm output may differ from the ground truth. Nevertheless, this study permits to analyze the algorithm convergence and the magnitude of modeling uncertainties. From the results depicted in Fig. 6.23b, the uncertainties over the preceding vehicle model parameters result as follows:

$$\begin{aligned} \xi &= \tilde{\xi} + \Delta_\xi;\ |\Delta_\xi| < 0.11; \\ \omega_n &= \tilde{\omega}_n \cdot (1 + \Delta_{\omega_n});\ |\Delta_{\omega_n}| < 0.12; \end{aligned} \tag{6.8}$$

which can be translated as a unstructured multiplicative uncertainty $\Delta_{Gp_{i-1}}$ from $\tilde{Gp}_{i-1}(s)$ over the model $Gp_{i-1}(s)$. It is known that FF-only control does not provide satisfactory results, given that perfect model inversion is never attained due to the uncertainty $\Delta_{Gp_{i-1}}$. For this reason, feedback control is designed to ensure not only the desired closed loop performance but also the required robustness to modeling uncertainties. It is proposed to employ the fractional-order feedback loop-shaped compensator developed in Sec. 6.3.3.3 to provide the required load disturbance rejection towards these modeling uncertainties, as well as reduced control effort.

6.4.1.2 Sensitivity and string stability study

Three vehicle dynamics were identified to evaluate the system sensitivity and string stability. These are: fast/underdamped (type 1), medium/damped (type 2) and slow/overdamped (type 3). To demonstrate the benefits of the proposed method, a comparison with state-of-the-art

solutions is provided. The methods that are evaluated are: FB-only car-following, FF/FB car-following with a conventional FF filter $F_i(s) = 1/H(s)$ and the proposed adapted FF system with $F_i(s) = (H(s)\tilde{P}_i(s))^{-1}$. The proposed vehicle plants and respective designed compensators are depicted in Tab. 6.3.

Table 6.3: Controller parameters considering three different type of dynamics

Vehicle	ω_n	ξ	Kp	α	ω_c	ω_p
Type 1	3.22	0.33	1.24	0.97	8.64	15.70
Type 2	1.85	0.40	0.95	1.06	2.40	5.17
Type 3	1.12	0.67	0.98	1.32	0.29	3.89

As performance metrics for the method comparison, the ∞-norm of the sensitivity–i.e.$S_i(s) = E_i(s)/X_{i-1}(s)$–and string stability functions are determined. All combinations of type 1,2 and 3 vehicles are analyzed to survey all methods' performance for all possible ego-preceding configurations. The sensitivities for FB-only ($\|S_i^{fb}\|_\infty$), conventional FF/FB ($\|S_i^{ff,conv}\|_\infty$) and proposed FF/FB approach ($\|S_i^{ff,adap}\|_\infty$) are compared in Tab. 6.4. The analysis is done considering the worst uncertainty over the preceding vehicle model in Eq. 6.8 . A time gap of 0.6s is used.

Table 6.4: Controller parameters for three different type of vehicles

Ego	Prec.	$\|S_i^{fb}\|_\infty$	$\|S_i^{ff,conv}\|_\infty$	$\|S_i^{ff,adap}\|_\infty$
1	1	3.85	0.60	0.60
-	2	3.85	1.20	0.39
-	3	3.85	1.50	0.34
2	1	4.08	4.44	0.60
-	2	4.08	0.49	0.49
-	3	4.08	1.05	0.32
3	1	1.77	21.89	0.72
-	2	1.77	4.76	0.44
-	3	1.77	0.44	0.36

For the FB-only approach, one can see that the system stability is independent from the preceding vehicle dynamics as the ACC closed loop response is independent from the preceding vehicle. In the case where $F_i(s) = 1/H(s)$, it is clear that when $P_i(s) \approx 1$ the performance improves. This is due to the fact that the conventional approach assumes both vehicles models to be the same. But when the vehicle dynamics differ, the system stability decreases as the magnitude of $P_i(s)$ becomes higher, introducing undesired behavior on the closed loop. When the ego-model has faster dynamics the performance results better, while the worst behavior is obtained when its dynamics are slower than the preceding ones. For the proposed structure, the system robustness/stability is improved for all possible scenarios (see Fig. 6.24). The enhancement with respect to the other solutions becomes more noticeable as the magnitude of $P_i(s)$ is higher. Generally, better results are obtained with the proposed solution if the ego-vehicle presents a faster model than the preceding one.

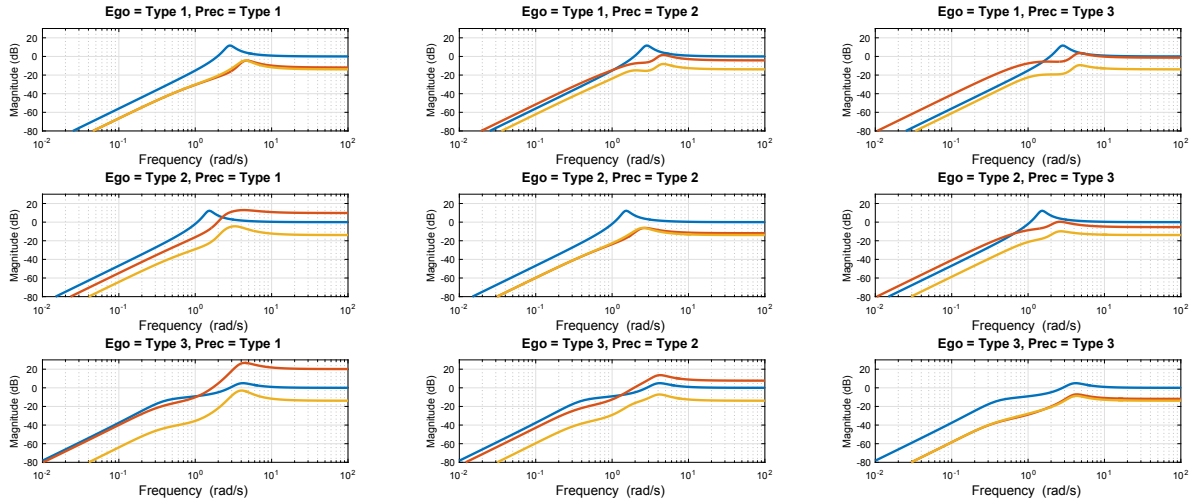

Figure 6.24: Sensitivity comparison between S_i^{fb} (blue line), $S_i^{ff,conv}$ (red line) and $S_i^{ff,adap}$ (yellow line) for all vehicle type combinations

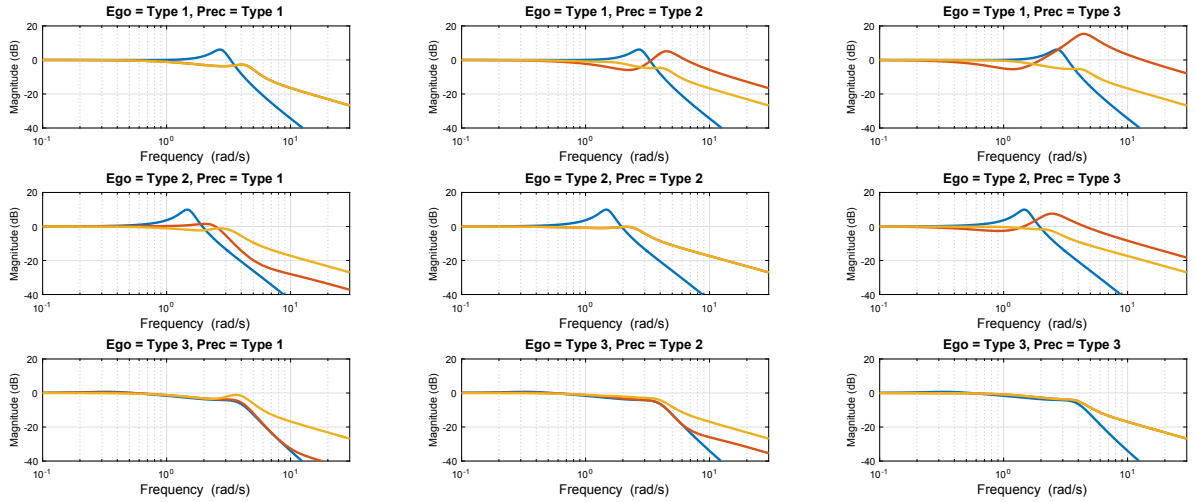

Figure 6.25: String stability function comparison between T_i^{fb} (blue line), $T_i^{ff,conv}$ (red line) and $T_i^{ff,adap}$ (yellow line) for all vehicle type combinations

Finally, the string stability condition is analyzed in Fig. 6.25. As in the previous study, the performances of FB-only, FF/FB with the conventional FF filter and the proposed approach are compared for all possible ego-preceding combinations in Tab. 6.3. As the communication delay directly affects the system string stability, a $\theta = 0.1$s is set.

For the FB-only and the FF/FB structures with conventional FF filter, the string stability presents an overshoot over unity at higher frequencies if the ego-model has a low ω_n. This is due to the bandwidth limitation of slower vehicles, that hinders the correct tracking of high frequency speed changes. If the ego-model accounts with a bigger ω_n, an overshoot is observed at lower frequencies given that faster vehicles overreact to the preceding speed changes. It is also appreciated that for some cases the FF filter with conventional form performs worst than the FB solution, specially when the ego-vehicle is faster than the preceding. As the magnitude distance between the FF filter and the ideal inverse model form $(H(s)P_i(s))^{-1}$ increases, the closed loop response

becomes worst, agreeing with the conclusions in [Devasia, 2002]. When the proposed adapted-FF filter is employed, although in some frequency regions the magnitude of $|T_i(s)|$ may be higher than for the other static structures, its peak value is maintained below unity in all frequencies for all the possible scenarios, satisfying the string stability condition.

6.4.1.3 Experimental validation

A four vehicle scenario is disposed considering the vehicle types on Tab. 6.3 and their controllers. A CACC string is set with a time gap of 0.6s, employing a network with θ=0.1s. For this case, only the conventional FF/FB and the proposed adapted FF/FB structure are analyzed. The string configuration in terms of vehicle dynamics is as follows, from leader to last: type 2, type 1, type 3 and type 2.

Fig. 6.26 shows the vehicles' speed evolution. When the conventional FF filter is applied, the vehicles' speeds do not evolve uniformly as desired. It can be appreciated that slower vehicles present a higher speed overshoot than the faster ones, which introduces considerable spacing errors (see Fig. 6.27) that can reach up to 1.6 meters in the case of the third vehicle. When the proposed adapted FF filter is applied, in the first speed step the vehicles' speeds do not evolve uniformly as in the conventional scenario due to the lack of knowledge of their preceding vehicle model. For the following speed changes, one can observe in Fig. 6.28 that the modeling parameters converge to their solutions as more V2V data is received to be modeled. This permits a more stable speed evolution as each vehicle is able to adapt its FF filter with the identified preceding vehicle parameters, compensating the dynamics difference. The spacing error peak value is reduced from 1.8 up to 0.4 meters.

In CACC homogeneous strings, when the leader accelerates or decelerates, the rest of the string members should face a positive or negative spacing error respectively due to the temporal delay in the V2V link. Instead, when the CACC string is heterogeneous, faster vehicles overreact to the speed change with respect to their slower preceding vehicle, which produces a negative distance error (see 2nd and 4th vehicle in upper plot of Fig. 6.27). If the ego-vehicle accounts with slower dynamics, the spacing error becomes positive as would be expected given an increment in the

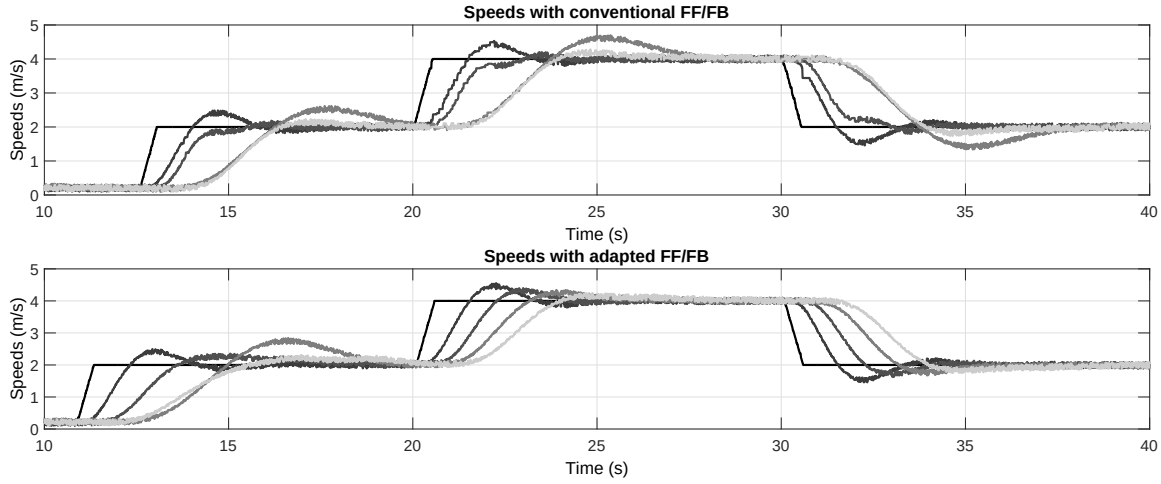

Figure 6.26: Speed evolution of the CACC string from leader (black line) to the last vehicle (light gray) applying the conventional and the proposed FF/FB approaches (top and bottom figure respectively)

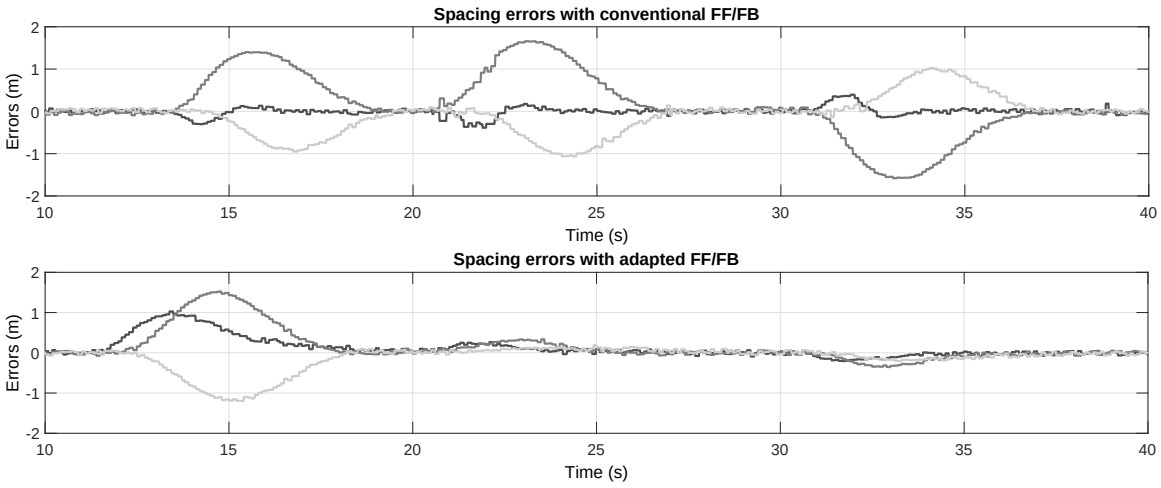

Figure 6.27: Spacing errors evolution of the CACC string from the first follower (dark gray) to the last vehicle (light gray) applying the conventional and the proposed FF/FB approaches (top and bottom figure respectively)

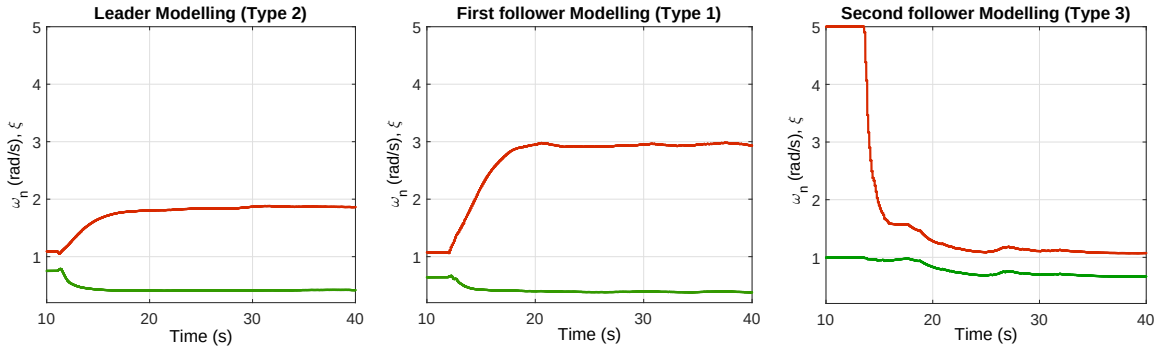

Figure 6.28: Identified response bandwidth (red line) and damping factor (green line) during the experimental validation by the second, third and fourth vehicles, on their precedings

leader speed. Nevertheless, its magnitude is higher than desired due to the ego-vehicle limitation to track efficiently its faster preceding vehicle speed changes. This also agrees with the results obtained in Sec. 6.4.1.2.

To deal with this problem, the adapted FF filter is configured to process the preceding vehicle's reference considering both vehicles' models. This can be appreciated on the lower plot of Fig. 6.27, where for the first speed change in time t=10s the spacing errors evolve differently. Instead, as each vehicle adapts its structure, not only the errors' peak values are reduced but also their evolution results more likely as an homogeneous string scenario (positive or negative speed changes produce spacing errors of equal sign).

6.4.2 CACC under leader-predecessor topologies

The proposed particle filter-based method has exhibited promising performance when used on a PF topology. Next step is to compare different topologies, specially against the LPF structure explained in Sec. 5.4. The benefits of adding the leader reference speed on feedforward are

explored in this section with extensive simulations of CACC-controlled strings under PF and LPF topologies. The remaining of this section is organized as follows: experimental setup is detailed with the considered experiment parameters and a result analysis section to compare both strategies and revise the proposed approach benefits.

6.4.2.1 Experimental setup

For each of the scenarios, CACC strings of N_s vehicles are considered that follow CTG spacing policy. Each of the vehicles has different dynamics from slower to faster. The main purpose of the experiment is to investigate existing performance differences between PF and LPF CACC structures. For each time gap-delay combination, a series of N_e experiments is performed where the platoon order is varied and evaluated on each iteration applying both topologies. This is done to average the results of several different vehicle dynamics configurations on the string, avoiding to benefit one strategy over the other, while seeking the regular performance tendency regardless the platoon order. For the sake of simplicity, the following vehicles dynamics are set to be described as first order models with an actuator lag time of $\tau \in \{0.1, 0.2, 0.4, 0.9\}$. Concerning the leader vehicle, an actuator lag value of $\tau = 0.3$ is set, constituting a middle frequency response with respect to the follower vehicles. Each of the vehicles adapt its feedforward structure in function of its own dynamics and those of the preceding (for PF topologies) and leader vehicles (for LPF topologies). The models' parameters are set to be known with a modeling uncertainty of Δ_τ. The feedback control is designed in function of the ego-model, following the design guidelines in Sec. 4.3.3. In Tab. 6.5, the experiment setup parameters are presented.

Table 6.5: Experimental setup parameters

h_{min}	h_{max}	θ_{min}	θ_{max}	N_e	Δ_τ	β_{max}	N_s
0.2	0.6	0.02	0.2	100	0.12	0.9	6

The comparison between both strategies consists on evaluating performance metrics as: theoretical string stability, measured string stability, peak spacing error, integrated absolute spacing error, peak acceleration and integrated absolute control effort. Since the first follower is limited to employ the PF control strategy for every case, only the variables from the second follower (or third vehicle), to the last follower are evaluated. To permit a more accurate string stability study and excite the required spectral regions, an acceleration profile is built based on a random phase multisine signal [Pintelon and Schoukens, 2012]. Different weights are assigned to the sines in function of their frequencies and with respect to the interest regions where the model magnitude peaks of string stability are expected to occur. In Fig. 6.29 the sines weights $W(\omega)$ are depicted in function of their frequencies $\omega \in \Omega$, as well as the resulting time domain signal built from the random phase combination of the sines. The time signal is finally set with the total time length T_{end} and sampling time Ts following the formula:

$$\dot{u}_1(t) = \sum_{i=0}^{\Omega} W_i \, cos(\omega_i t + \phi_i);\; t = \{0, Ts, ..., T_{end}\} \tag{6.9}$$

6.4.2.2 Results analysis

For a fair comparison between both methods, variables of vehicles whose index higher than 2 are averaged for both strategies, since the second vehicle performs the same for both topologies.

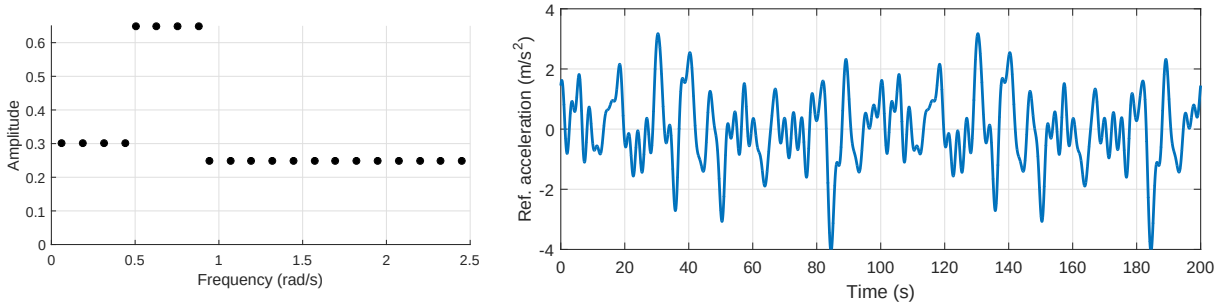

(a) Sine weights

(b) Time domain signal

Figure 6.29: Assigned weights for the multisine random phase signal and resulting time domain reference acceleration profile

Subsequently, for each experiment the mean performance on the PF topology string is divided by the LPF-based one–e.g. PF would outperform LPF if the performance ratio is higher than one. The resulting ratios for all the N_e are finally averaged, providing a general tendency representation that is robust to the vehicles order for all considered time gap-communication delay combinations. In other words, the resulting values $\Omega(h,\theta)$ represented on Fig. 6.30 can be interpreted as:

$$\Omega(h,\theta) = \frac{1}{N_e} \cdot \sum_{k=1}^{N_e} \frac{1}{N_s} \cdot \sum_{i=3}^{N_s} \left| \frac{Z_{i,LPF}(h,\theta)}{Z_{i,PF}(h,\theta)} \right| \tag{6.10}$$

The terms corresponding to LPF ($Z_{i,LPF}(h,\theta)$) and PF topologies ($Z_{i,PF}(h,\theta)$) represent: $\mathcal{H}_\infty$-norm of the transfer function $\Gamma_i(s)$ given in Eq. 5.26, ∞-norm of the approximated response model $\frac{X_i(s)}{X_{i-1}(s)}$, peak acceleration $\|a_i(t)\|_\infty$, integrated absolute control effort or action $\int |\dot{u}_i(t)|dt$, peak spacing errors $\|e_i(t)\|_\infty$ and integrated absolute spacing error $\int |e_i(t)|dt$. All the results concerning the aforementioned performance metrics are depicted in Fig. 6.30, where it is possible to see the regions in the time gap/communication delay plane where LPF-based control performs better (green), equal (black) or worse (red) than the PF approach.

One of the fundamental points to evaluate, is the validation of the strict $\mathcal{L}_2$ string stability study method for strings controlled under LPF topologies, proposed in 5.4.3. It is compared against the measured string stability, which is approximated modeling the ego-vehicle response towards changes in its preceding–i.e. $\frac{X_i(s)}{X_{i-1}(s)}$. The results concerning the $\mathcal{H}_\infty$-norms of both the theoretical and measured string stability functions are presented in Fig. 6.30a and 6.30b. For the theoretical string stability, no cases are observed where the PF strategy outperforms the LPF one. They result almost similar for very short communication delays and high time gaps, but as the delay increases and the time gap is reduced, the difference between both techniques becomes more significant in favor of LPF-based control. The same tendency is observed as well when comparing the modeled string stability results, validating the employment of the proposed string stability study method for LPF-based CACC strings. The main difference between both plots is observed in some red regions. This is due to the fact that string stability is measured with the ∞-norm of the modeled closed loop response, which for some scenarios where a low β is employed (ego-vehicle dynamics are slower than precedings'), behavior does not result causal due to the time advance that provides the employment of leader reference speed instead of preceding vehicle's.

With respect to the vehicles peak accelerations (see Fig. 6.30c), it can be observed that for all communication delays and time gaps, the LPF strategy provides a gap regulation control

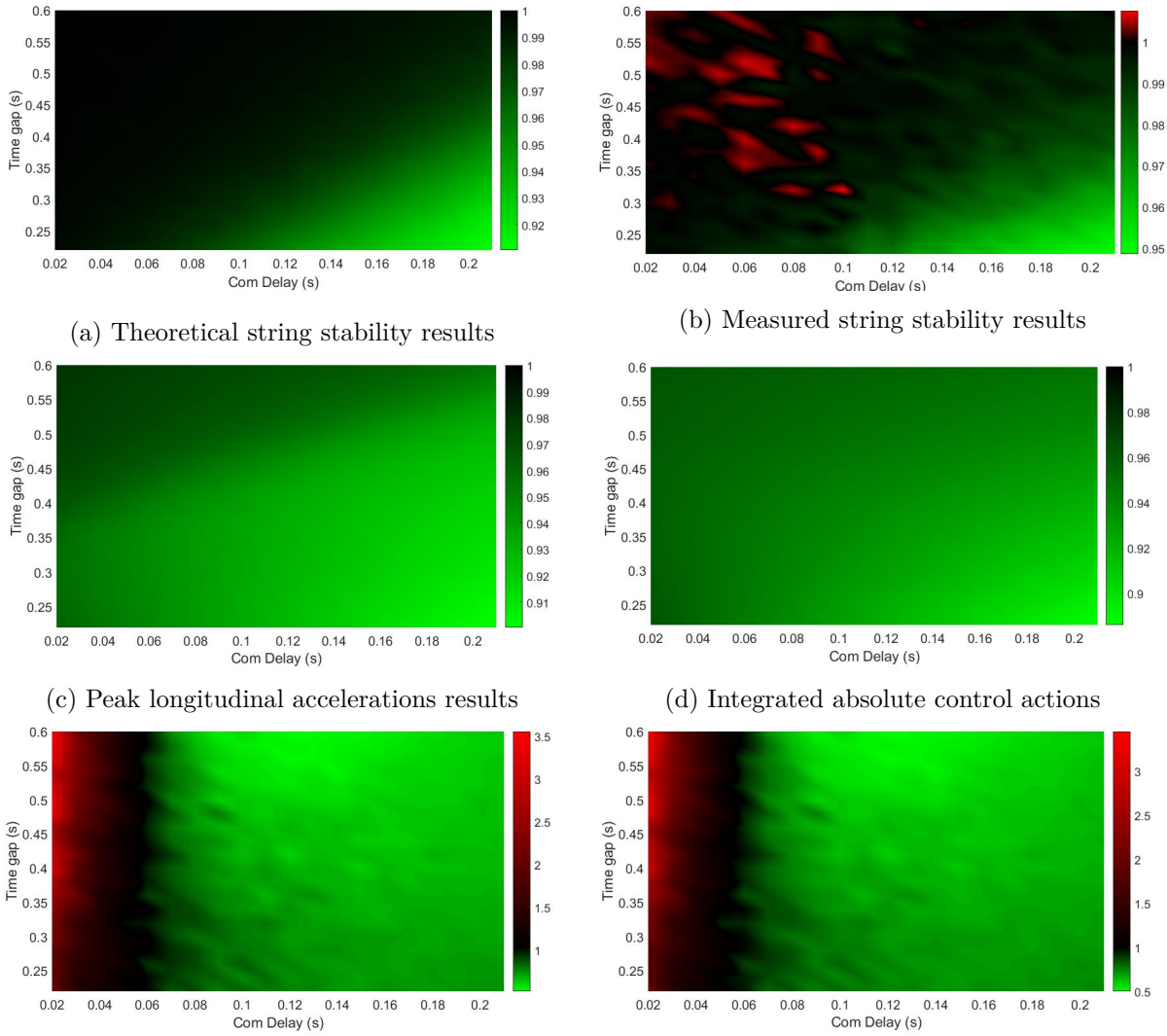

(a) Theoretical string stability results

(b) Measured string stability results

(c) Peak longitudinal accelerations results

(d) Integrated absolute control actions

(e) Peak spacing errors results

(f) Integrated absolute spacing errors results

Figure 6.30: Performance results ratio between PF and LPF topologies on CACC strings under CTG spacing policy and communication delays

that demands lower peak accelerations. As for the string stability, this tendency becomes more important as the communication delay increases and the time gap is reduced. These results are consistent with the motivation for the proposed LPF strategy, since it permits to reduce the required acceleration magnitude and the control effort (as appreciated in Fig. 6.30d) up to an 11% without losing string stability. Specially for vehicles with slower dynamics, this results convenient since their capacity to track faster vehicles speed changes are limited with respect to those of faster dynamics.

Additional conclusions can be derived from the peak spacing errors (Fig. 6.30e) and integrated absolute errors (Fig. 6.30f) results. The time gap value is observed to have very small influence in the performance ratio between PF and LPF strategies. On the other hand, the communication delay results of great importance concerning the spacing error behavior. For θ lower than 0.05s, using PF structures yields significantly better performance than including the leader vehicle in

this case. As the communication delay is increased, the performance ratio tendency changes at $\theta > 0.06$ in favor of the LPF approach, getting fixed in an average of 0.7 for short time gaps and 0.5 for higher time gaps. This agrees with the expected behavior when of introducing the leader vehicle on the FF structure, given that the benefits of LPF over PF are more significant as the communication delay is higher. Such condition is not only visible through the stabilizing properties given by the time advance in the closed loop form Eq. 5.26, but also intuitive because slower vehicles are able to anticipate further in advance preceding vehicles' state changes before they are either detected or received through V2V links.

6.5 Discussion

Stability studies, simulations and real platforms experiments have been provided to validate the algorithms proposed in this thesis work. The design process of low level control systems has been detailed, considering the RITS team platforms, which dynamics and actuators models have been employed for further validation. The correct design of such low level block is fundamental to ensure the desired modularity and high level time gap-based structure behavior. The latter has been scoped firstly through the validation of the full range spacing policy approach, for which simulations and low speed real platforms experiments have been provided. By comparing this strategy with state-of-the-art spacing policies and CTG overall, the approach benefits over traffic capacity increase, string stability and safety have been demonstrated over the whole defined speed range; both for ACC and CACC techniques.

One of the fundamental contributions of this thesis has been validated in real scenarios, which is the CACC algorithm for platooning over urban environments. It permits to operate CACC-equipped strings in scenarios where interaction with VRU may occur, for which emergency braking and gap closing capabilities are implemented under a state machine framework. Results show the benefits and stability of the proposed approach, providing safe operation for both vehicle drivers and VRU. The proposed algorithms for the design of high level feedback control systems have been demonstrated and tested on simulations. Firstly, the design procedure for fractional-order PD controllers has been proved to outperform a classical PD controller both in ACC and CACC structures, in terms of permitting shorter time gaps without losing string and individual stability. In second place, the fractional-order controller designed to be robust to plant gain variations has been also validated through frequency response studies and tested over simulations. Finally, the benefits of using the loop-shaped fractional-order compensator algorithm are demonstrated through the study of sensitivity, closed loop and input-to-control action responses, as well as in real platform experiments. In summary, the introduction of fractional-order calculus has been proved to bring several benefits and permit more flexible frequency responses, thus more exigent control design criteria can be fulfilled.

The benefits of the two proposed approaches for heterogeneous strings control have been demonstrated. Firstly, the case where communication is available only with the predecessor vehicle is considered, for which the performance of the dynamics identification algorithm has been tested. The solution convergence for the proposed particle filtering approach has been extensively tested for different dynamics, providing an approximation of the modeling uncertainty. String stability and sensitivity evaluations are carried out, confirming that adaptation of the feedforward structure in function of the ego-preceding dynamics relation significantly improves the car-following performance. It has been demonstrated that this approach allows to ensure robustness and strict $\mathcal{L}_2$ string stability for all slow, medium and fast dynamics ego-preceding combination. Experimental tests have been carried out showing that not only string stability is ensured in contrast with

conventional approaches, but also the spacing errors are significantly reduced as every vehicle's feedforward system is adapted. Finally, the inclusion of the leader vehicle reference speed in the feedforward structure is verified with extensive simulations. The proposed LPF approach is evaluated against the PF validated previously, with the purpose of determining under which conditions it results more convenient to employ LPF topologies over PF-only. Results show a general tendency that indicates performance enhancement as the time gap gets shorter and the communication delay higher. In other words, employing the leader information is encouraged mainly for more exigent scenarios where low time gaps are targeted and the V2V network may present considerable lags.

Chapter 7

Conclusions

This chapter encloses this thesis report with the concluding remarks of the presented state-of-the-art review, proposed methods and validation results. Subsequently, the research lines that are encouraged to pursue are described, as well as future work that can be derived from the accomplished goals along this thesis.

7.1 Concluding remarks

The recent growing interest on solutions based on vehicle automation has not only busted the employment of on-board cutting-edge technologies, but also the research and development of strategies that extend their benefits. The state-of-the-art review presented the evolution from cruise control systems to CACC or platooning evidences the impact that these techniques achieve over road mobility. The guarantee of safety, increment of traffic capacity, reduction of CO_2 emissions and shockwaves mitigation; are some of the automated car-following advantages that have been demonstrated in research projects around the world. Furthermore, the increasing interest on standardizing the V2V communications and vehicular connectivity have further encouraged the investment on cooperative solutions. Nevertheless, some challenges remain. This thesis provides a solution to some of these challenges through the following contributions: 1) the proposal of a modular architecture for automated (and cooperative) car-following focused on time gap-based spacing policies; 2) the exploration of novel calculus tools and control design methods to further improve individual and string stability with robustness; and 3) functional control systems to ensure the string performance despite the heterogeneity between vehicles.

The analysis of different car-following control architectures has been conducted, which motivated the employment of feedforward/feedback structures due to their effectiveness for embedded processing and proven good performance. The proposed strategy has been based on a modular hierarchical approach, that separates the spacing gap-regulation task (high level layer) from the longitudinal speed control (low level layer). The consistency and awareness between the two layers design has been found to be a fundamental property to achieve the desired performance, for which the design of the low level control layer should be the first step for the automated car-following system. It has been also concluded that the choice of a spacing policy or reference car-following model, not only defines the string geometry but also how demanded the system is. For this reason, the correct time gap selection is of utmost importance to guarantee robust string stability, based on the actuator lags and V2V communication delay values. To maximize the benefits of cooperative automated car-following while ensuring safety and string stability, two complementary research lines have been conducted in parallel: the full range spacing policy shaping and the proposal of

different feedback controller design methods. The former fulfills the need to have an operational spacing strategy over the entire speed range in ACC and CACC modes optimizing inter-distances, while the latter focuses on employing fractional-order calculus to achieve more flexible frequency responses, optimizing string stability, robustness and load sensitivity.

With the purpose of encouraging the widespread employment of cooperative automated car-following solutions, a novel architecture has been proposed for CACC over urban environments where interaction with VRU may occur. A state machine that switches from cooperative car-following mode to emergency braking when a possible front-end collision is detected, and then to a gap-closing platoon rejoining maneuver when the collision danger disappears. This strategy, together with the full speed range spacing policy introduces CACC and platooning to urban environments, which is one of the targeted challenges on the state-of-the-art.

The study of feedforward-based strategies for strings of non-identical vehicles is another major contribution that has been made in this thesis work. The adaptation of the control structure on PF topologies in function of the ego and preceding vehicles has been demonstrated to outperform existing solutions, specially in terms of string stability an load sensitivity for all fast-medium-slow dynamics ego-preceding configurations. Simulation results validate the stability studies and demonstrate the strategy potential to not only guarantee string stability, but also reduce considerably the spacing errors magnitude, despite the string heterogeneity. Actuators' saturation and communication delays effects have been also tackled with respect to the string performance. This is done employing a LPF approach with a novel weighting strategy between leader and preceding vehicles reference speed. Extensive experimental simulations were conducted to compare PF and LPF performances, concluding that in more demanding scenarios (short time gap and relatively high V2V delay), employing the leader information results of great advantage to maintain the desired string stability and performance.

7.2 Research perspective and future work

In the upcoming years, an imminent increase of vehicle automation capabilities is expected over most of commercial cars. At the same time, the introduction of V2V communication links over commercial vehicles encourages to develop enhanced car-following solutions based on cooperation. As a research perspective, more efforts should be put to investigate additional applications and benefits that could be derived from cooperation, which would directly stimulate their widespread incorporation over vehicles.

Another fundamental aspect that must be taken into account in future research works is the awareness of the relevance of the time gap choice. As the time gap tends to zero–i.e. constant clearance–, a higher closed loop bandwidth response is demanded, which is not always feasible. Although several approaches have proposed to employ constant clearance, the guarantee of strict $\mathcal{L}_\infty$ string stability under such spacing policy would require to have almost zero V2V transmission delays, as well as no sensing and actuation lags; which in reality is not feasible. Besides, time gap policy is a powerful solution designed to relax the car-following demanded performance, gaining robustness towards system delays. For this reason, the trade-off between in one hand car-following performance, traffic capacity increase and fuel consumption reduction; and in the other hand safety, robustness and comfort, is fundamental for the choice of the time gap set.

Forthcoming research should not only be focused on extending CACC control capabilities, but also measuring the impact that these techniques have over drivers–i.e. human factors. For instance, extensive studies were done in [Nowakowski et al., 2010a] to determine drivers' time gap choice over CACC-equipped vehicles, showing acceptance for CACC and preferences for the smallest time

gap system setting values (0.6s in this case). In [Yang et al., 2018] similar study has been carried out testing truck drivers gap preferences, showing that time gaps less than 0.9s were too close and higher than 1.8s were too far. Future field studies should investigate the minimum accepted time gap for which the drivers feel comfortable, without losing the system benefits and positive impact over traffic, safety and even fuel consumption reduction.

In reality ideal homogeneity between string vehicles is very improbable, for which the algorithms proposed along this thesis constitute a promising solution. Nevertheless, if the high heterogeneity– i.e. high magnitude distance between vehicle responses' models–is filtered at the platoon formation moment, the risk of actuators saturation, complexity and undesired performance is considerably reduced. For this reason, another research perspective that could be derived from this work is the study of formal requirements and strategies for clustering of platoons according to each vehicle performance.

One of the most important properties of the proposed string control framework is its modularity, which permits its employment over future developments in the same field. As a continuation of the developed work, several future works are encouraged to be pursued:

- Include inter-lanes vehicle interaction, with merging and splitting capabilities. Given that cut-in maneuvers are of the main causes of traffic shockwaves, extending control capabilities to handle not only one, but also multiple vehicles cutting in the controlled string. Solving this issue with cooperative strategies has been recently gaining attention. As a matter of fact, it has been approached by several research institutions in the second edition of GCDC [Ploeg et al., 2018]. Including vehicles heterogeneity and strict $\mathcal{L}_\infty$ string stability should be included in future interaction handling policies.

- Perform an exhaustive validation study of the macroscopic impact of the proposed algorithms in terms of traffic capacity and shockwave mitigation, accounting with real communication and traffic simulators. This should include the presence of human-driven vehicles represented by some of the models described in chapter 2, which may interact with the controlled vehicles as mentioned previously.

- Permit different time gaps within the cooperative string. It results intuitive that in considerably heterogeneous strings, vehicles with faster dynamics are able to hold shorter time gaps than slower ones. The consequences of having different spacing policies in the same formation to maximize traffic throughput is a subject to be investigated, under the string stability constraint. This consideration would also affect the vehicles' states propagation, since each vehicle would perform car-following differently in function of its response capabilities.

- Investigate more accurate discrete-time approximations for the fractional-order systems representation. Fractional-order controllers have been proven to provide a more flexible frequency response design framework. Nevertheless, since fractional-order systems ideally require infinite memory to be correctly represented, the accuracy of the finite order discrete approximation methods are of utmost importance to guarantee the control design effectiveness. An evaluation of different methods could be considered in function of the controller type and required bandwidth validity.

- Focus on extending the low level control capabilities to adapt its behavior in function of external disturbances. Study as well different reference speed tracking strategies to ensure a constant closed loop response model behavior. This would guarantee that the desired high level performs as expected at the design stage. In the same line, strategies as anti windup or

optimization-based techniques could be explored to manage the actuators to avoid saturation, as well as the non-linearities that these may introduce.

- Research different control algorithms that would reduce significantly the energy consumption. The design of control systems that take into account not only the aerodynamic drafting capabilities of short-separation platooning, but also the regenerative braking capacities of electrical vehicles. Although shorter separations ensure less energy consumption, more aggressive actuator responses are demanded and consequently more energy is consumed. This trade-off should be the focus of future research for extending fuel economy capabilities of platooning techniques.

Bibliography

[Al-Jhayyish and Schmidt, 2018] Al-Jhayyish, A. M. and Schmidt, K. W., 2018. Feedforward strategies for cooperative adaptive cruise control in heterogeneous vehicle strings. IEEE Transactions on Intelligent Transportation Systems 19(1), pp. 113–122.

[Ali et al., 2014] Ali, A., Garcia, G. and Martinet, P., 2014. Safe platooning in the event of communication loss using the flatbed tow truck model. In: Control Automation Robotics & Vision (ICARCV), 2014 13th International Conference on, IEEE, pp. 1644–1649.

[Ali et al., 2015] Ali, A., Garcia, G. and Martinet, P., 2015. Urban platooning using a flatbed tow truck model. In: Intelligent Vehicles Symposium (IV), 2015 IEEE, IEEE, pp. 374–379.

[Åström and Hägglund, 2006] Åström, K. J. and Hägglund, T., 2006. Advanced pid control. In: The Instrumentation, Systems, and Automation Society, Citeseer.

[Azar et al., 2017] Azar, A. T., Vaidyanathan, S. and Ouannas, A., 2017. Fractional order control and synchronization of chaotic systems. Vol. 688, Springer.

[Bishop, 2005] Bishop, R., 2005. Intelligent vehicle technology and trends.

[Bose and Ioannou, 2003] Bose, A. and Ioannou, P. A., 2003. Analysis of traffic flow with mixed manual and semiautomated vehicles. IEEE Transactions on Intelligent Transportation Systems 4(4), pp. 173–188.

[Braatz et al., 1996] Braatz, R. D., Morari, M. and Skogestad, S., 1996. Loopshaping for robust performance. International Journal of Robust and Nonlinear Control 6(8), pp. 805–823.

[Brackstone and McDonald, 1999] Brackstone, M. and McDonald, M., 1999. Car-following: a historical review. Transportation Research Part F: Traffic Psychology and Behaviour 2(4), pp. 181–196.

[Brackstone and McDonald, 2000] Brackstone, M. and McDonald, M., 2000. A comparison of eu and us progress in the development of longitudinal advanced vehicle control and safety systems (avcss). Transport Reviews 20(2), pp. 173–190.

[Browand et al., 2004] Browand, F., McArthur, J. and Radovich, C., 2004. Fuel saving achieved in the field test of two tandem trucks. California Partners for Advanced Transit and Highways (PATH).

[Bu et al., 2010] Bu, F., Tan, H.-S. and Huang, J., 2010. Design and field testing of a cooperative adaptive cruise control system. In: IEEE American Control Conference (ACC), IEEE, pp. 4616–4621.

[Burger et al., 2017] Burger, C., Orzechowski, P. F., Taş, Ö. Ş. and Stiller, C., 2017. Rating cooperative driving: A scheme for behavior assessment. In: Intelligent Transportation Systems (ITSC), 2017 IEEE 20th International Conference on, IEEE, pp. 1–6.

[Calzolari et al., n.d.] Calzolari, D., Schürmann, B. and Althoff, M., n.d. Comparison of trajectory tracking controllers for autonomous vehicles.

[Carlson and Halijak, 1964] Carlson, G. and Halijak, C., 1964. Approximation of fractional capacitors (1/s)ˆ(1/n) by a regular newton process. IEEE Transactions on Circuit Theory 11(2), pp. 210–213.

[Carvalho et al., 2010] Carvalho, C. M., Johannes, M. S., Lopes, H. F., Polson, N. G. et al., 2010. Particle learning and smoothing. Statistical Science 25(1), pp. 88–106.

[Chan et al., 2012] Chan, E., Gilhead, P., Jelinek, P., Krejci, P. and Robinson, T., 2012. Cooperative control of sartre automated platoon vehicles. In: 19th ITS World CongressERTICO-ITS EuropeEuropean CommissionITS AmericaITS Asia-Pacific.

[Chan, 2015] Chan, M., 2015. Global status report on road safety. Technical report, World Health Organization.

[Chandler et al., 1958] Chandler, R. E., Herman, R. and Montroll, E. W., 1958. Traffic dynamics: studies in car following. Operations research 6(2), pp. 165–184.

[Chen et al., 2009] Chen, Y., Petras, I. and Xue, D., 2009. Fractional order control-a tutorial. In: American Control Conference, 2009. ACC'09., IEEE, pp. 1397–1411.

[Chu, 1974] Chu, K.-C., 1974. Optimal dencentralized regulation for a string of coupled systems. IEEE Transactions on Automatic Control 19(3), pp. 243–246.

[Curtain et al., 2009] Curtain, R., Iftime, O. V. and Zwart, H., 2009. System theoretic properties of a class of spatially invariant systems. Automatica 45(7), pp. 1619–1627.

[D. and R., 1999] D., S. and R., R., 1999. Intelligent cruise control systems and traffic flow stability. Transportation Research Part C: Emerging Technologies 7(6), pp. 329–352.

[De Winter et al., 2017] De Winter, J., Gorter, C., Schakel, W. and van Arem, B., 2017. Pleasure in using adaptive cruise control: A questionnaire study in the netherlands. Traffic injury prevention 18(2), pp. 216–224.

[Delis et al., 2016] Delis, A. I., Nikolos, I. K. and Papageorgiou, M., 2016. Simulation of the penetration rate effects of acc and cacc on macroscopic traffic dynamics. In: Intelligent Transportation Systems (ITSC), 2016 IEEE 19th International Conference on, IEEE, pp. 336–341.

[Devasia, 2000] Devasia, S., 2000. Robust inversion-based feedforward controllers for output tracking under plant uncertainty. In: American Control Conference, 2000. Proceedings of the 2000, Vol. 1number 6, IEEE, pp. 497–502.

[Devasia, 2002] Devasia, S., 2002. Should model-based inverse inputs be used as feedforward under plant uncertainty? IEEE Transactions on Automatic Control 47(11), pp. 1865–1871.

[di Bernardo et al., 2015] di Bernardo, M., Salvi, A. and Santini, S., 2015. Distributed consensus strategy for platooning of vehicles in the presence of time-varying heterogeneous communication delays. IEEE Transactions on Intelligent Transportation Systems 16(1), pp. 102–112.

[Diamond and Lawrence, 1966] Diamond, H. and Lawrence, W., 1966. The development of an automatically controlled highway system. university of michigan. Transportation Research Institutes's Report UMR1266.

[Dunbar and Caveney, 2012] Dunbar, W. B. and Caveney, D. S., 2012. Distributed receding horizon control of vehicle platoons: Stability and string stability. IEEE Transactions on Automatic Control 57(3), pp. 620–633.

[Eckhardt et al., 2015] Eckhardt, J., Aarts, L., van Vliet, A. and Alkim, T., 2015. European truck platooning challenge 2016. The Hague, Delta3.

[Eilers et al., 2015] Eilers, S., Mårtensson, J., Pettersson, H., Pillado, M., Gallegos, D., Tobar, M., Johansson, K. H., Ma, X., Friedrichs, T., Borojeni, S. S. et al., 2015. Companion–towards cooperative platoon management of heavy-duty vehicles. In: Intelligent Transportation Systems (ITSC), 2015 IEEE 18th International Conference on, IEEE, pp. 1267–1273.

[El Ghouti et al., 2009] El Ghouti, N., Serrarens, A., Van Sambeek, D. and Ploeg, J., 2009. " connect & drive"-c-acc for reducing congestion dynamics.

[Eyre et al., 1998] Eyre, J., Yanakiev, D. and Kanellakopoulos, I., 1998. A simplified framework for string stability analysis of automated vehicles. Vehicle System Dynamics 30(5), pp. 375–405.

[Faanes and Skogestad, 2003] Faanes, A. and Skogestad, S., 2003. Feedforward control under the presence of uncertainty. In: European Control Conference (ECC), 2003, IEEE, pp. 1387–1392.

[Feliu and Ramos, 2005] Feliu, V. and Ramos, F., 2005. Strain gauge based control of single-link flexible very lightweight robots robust to payload changes. Mechatronics 15(5), pp. 547–571.

[Fenton and Mayhan, 1991] Fenton, R. E. and Mayhan, R. J., 1991. Automated highway studies at the ohio state university-an overview. IEEE transactions on Vehicular Technology 40(1), pp. 100–113.

[Flores and Milanés, 2018] Flores, C. and Milanés, V., 2018. Fractional-order-based acc/cacc algorithm for improving string stability. Transportation Research Part C: Emerging Technologies 95, pp. 381–393.

[Flores et al., 2018a] Flores, C., Merdrignac, P., de Charette, R., Navas, F., Milanés, V. and Nashashibi, F., 2018a. A cooperative car-following/emergency braking system with prediction-based pedestrian avoidance capabilities. IEEE Transactions on Intelligent Transportation Systems (99), pp. 1–10.

[Flores et al., 2016] Flores, C., Milanés, V. and Nashashibi, F., 2016. Using fractional calculus for cooperative car-following control. In: Intelligent Transportation Systems (ITSC), 2016 IEEE 19th International Conference on, IEEE, pp. 907–912.

[Flores et al., 2017] Flores, C., Milanés, V. and Nashashibi, F., 2017. A time gap-based spacing policy for full-range car-following. In: Intelligent Transportation Systems (ITSC), 2017 IEEE 20th International Conference on, IEEE, pp. 1–6.

[Flores et al., 2018b] Flores, C., Milanés, V. and Nashashibi, F., 2018b. Online feedforward/feedback structure adaptation for heterogeneous cacc strings. In: 2018 Annual American Control Conference (ACC), IEEE, pp. 49–55.

[Fritz et al., 2004] Fritz, H., Gern, A., Schiemenz, H. and Bonnet, C., 2004. Chauffeur assistant: a driver assistance system for commercial vehicles based on fusion of advanced acc and lane keeping. In: Intelligent Vehicles Symposium, 2004 IEEE, IEEE, pp. 495–500.

[Gao et al., 2015] Gao, F., Dang, D. and Li, S. E., 2015. Control of a heterogeneous vehicular platoon with uniform communication delay. In: Information and Automation, 2015 IEEE International Conference on, IEEE, pp. 2419–2424.

[Gao et al., 2016] Gao, F., Li, S. E., Zheng, Y. and Kum, D., 2016. Robust control of heterogeneous vehicular platoon with uncertain dynamics and communication delay. IET Intelligent Transport Systems 10(7), pp. 503–513.

[Gipps, 1981] Gipps, P. G., 1981. A behavioural car-following model for computer simulation. Transportation Research Part B: Methodological 15(2), pp. 105–111.

[González-Villaseñor et al., 2007] González-Villaseñor, A., Renfrew, A. C. and Brunn, P. J., 2007. A controller design methodology for close headway spacing strategies for automated vehicles. International Journal of Control 80(2), pp. 179–189.

[Gordon et al., 1993] Gordon, N. J., Salmond, D. J. and Smith, A. F., 1993. Novel approach to nonlinear/non-gaussian bayesian state estimation. In: IEE Proceedings F (Radar and Signal Processing), Vol. 140number 2, IET, pp. 107–113.

[Guo et al., 2016] Guo, X.-G., Wang, J.-L., Liao, F. and Teo, R. S. H., 2016. String stability of heterogeneous leader-following vehicle platoons based on constant spacing policy. In: Intelligent Vehicles Symposium (IV), 2016 IEEE, IEEE, pp. 761–766.

[Guzzella et al., 2007] Guzzella, L., Sciarretta, A. et al., 2007. Vehicle propulsion systems. Vol. 1, Springer.

[Harfouch et al., 2017] Harfouch, Y. A., Yuan, S. and Baldi, S., 2017. An adaptive switched control approach to heterogeneous platooning with inter-vehicle communication losses. IEEE Transactions on Control of Network Systems.

[Helly, 1959] Helly, W., 1959. Simulation of bottlenecks in single-lane traffic flow.

[Hosseinnia et al., 2014] Hosseinnia, S. H., Tejado, I., Milanés, V., Villagrá, J. and Vinagre, B. M., 2014. Experimental application of hybrid fractional-order adaptive cruise control at low speed. IEEE transactions on control systems technology 22(6), pp. 2329–2336.

[Ioannou and Chien, 1993] Ioannou, P. A. and Chien, C.-C., 1993. Autonomous intelligent cruise control. IEEE Transactions on Vehicular technology 42(4), pp. 657–672.

[Ioannou and Xu, 1994] Ioannou, P. and Xu, Z., 1994. Throttle and brake control systems for automatic vehicle following. IVHS Journal 1(4), pp. 345–377.

[Ishteva, 2005] Ishteva, M., 2005. Properties and applications of the Caputo fractional operator. PhD thesis, Msc. Thesis, Dept. of Math., Universität Karlsruhe (TH), Sofia, Bulgaria.

[ISO, 1997] ISO, 1997. Mechanical Vibration and Shock: Evaluation of Human Exposure to Whole-body Vibration. Part 1, General Requirements: International Standard ISO 2631-1: 1997 (E). ISO.

[Karjanto and Yusof, 2015] Karjanto, J. and Yusof, N., 2015. Comfort determination in autonomous driving style. Proceedings of the AutoUI, Nottingham, UK pp. 1–3.

[Khoichi and Hironori, 1993] Khoichi, M. and Hironori, F., 1993. Hinf optimized waveabsorbing control: Analytical and experimental result. Journal of Guidance, Control, and Dynamics 16(6), pp. 1146–1153.

[Kikuchi and Chakroborty, 1992] Kikuchi, S. and Chakroborty, P., 1992. Car-following model based on fuzzy inference system. Transportation Research Record pp. 82–82.

[Kometani, 1959] Kometani, E., 1959. Dynamic behavior of traffic with a nonlinear spacing-speed relationship. Theory of Traffic Flow (Proc. of Sym. on TTF (GM)) pp. 105–119.

[Kunze et al., 2010] Kunze, R., Ramakers, R., Henning, K. and Jeschke, S., 2010. Efficient organization of truck platoons by means of data mining-application of the data mining technique for the planning and organization of electronically coupled trucks. In: ICINCO (1), pp. 104–113.

[Künzli et al., 2000] Künzli, N., Kaiser, R., Medina, S., Studnicka, M., Chanel, O., Filliger, P., Herry, M., Horak Jr, F., Puybonnieux-Texier, V., Quénel, P. et al., 2000. Public-health impact of outdoor and traffic-related air pollution: a european assessment. The Lancet 356(9232), pp. 795–801.

[Li et al., 2011] Li, C., Qian, D. and Chen, Y., 2011. On riemann-liouville and caputo derivatives. Discrete Dynamics in Nature and Society.

[Li et al., 2017a] Li, S. E., Zheng, Y., Li, K., Wang, L.-Y. and Zhang, H., 2017a. Platoon control of connected vehicles from a networked control perspective: Literature review, component modeling, and controller synthesis. IEEE Transactions on Vehicular Technology.

[Li et al., 2017b] Li, Y., Li, Z., Wang, H., Wang, W. and Xing, L., 2017b. Evaluating the safety impact of adaptive cruise control in traffic oscillations on freeways. Accident Analysis & Prevention 104, pp. 137–145.

[Li et al., 2017c] Li, Y., Wang, H., Wang, W., Xing, L., Liu, S. and Wei, X., 2017c. Evaluation of the impacts of cooperative adaptive cruise control on reducing rear-end collision risks on freeways. Accident Analysis & Prevention 98, pp. 87–95.

[Liang and Peng, 2000] Liang, C.-Y. and Peng, H., 2000. String stability analysis of adaptive cruise controlled vehicles. JSME International Journal Series C Mechanical Systems, Machine Elements and Manufacturing 43(3), pp. 671–677.

[Lu et al., 2002] Lu, X.-Y., Hedrick, J. K. and Drew, M., 2002. Acc/cacc-control design, stability and robust performance. In: American Control Conference, 2002. Proceedings of the 2002, Vol. 6, IEEE, pp. 4327–4332.

[Luo and Chen, 2009] Luo, Y. and Chen, Y., 2009. Fractional-order [proportional derivative] controller for robust motion control: Tuning procedure and validation. In: American Control Conference, 2009. ACC'09., IEEE, pp. 1412–1417.

[Lurie, 1994] Lurie, B. J., 1994. Three-parameter tunable tilt-integral-derivative (tid) controller.

[Mammar et al., 2012] Mammar, S., Oufroukh, N. A., Yacine, Z., Ichalal, D. and Nouveliere, L., 2012. Invariant set based variable headway time vehicle longitudinal control assistance. In: American Control Conference (ACC), 2012, IEEE, pp. 2922–2927.

[Marsden et al., 2001] Marsden, G., McDonald, M. and Brackstone, M., 2001. Towards an understanding of adaptive cruise control. Transportation Research Part C: Emerging Technologies 9(1), pp. 33–51.

[Martinez and Canudas-de Wit, 2007] Martinez, J.-J. and Canudas-de Wit, C., 2007. A safe longitudinal control for adaptive cruise control and stop-and-go scenarios. IEEE Transactions on control systems technology 15(2), pp. 246–258.

[Matignon, 1998] Matignon, D., 1998. Generalized fractional differential and difference equations: stability properties and modelling issues. In: Mathematical Theory of Networks and Systems symposium, pp. 503–506.

[Mazzola and Schaaf, 2014] Mazzola, M. and Schaaf, G., 2014. Modeling and control design of a centralized adaptive cruise control system. International Journal of Computer, Electrical, Automation, Control and Information Engineering 8(7), pp. 1142–1146.

[McAuliffe et al., 2018] McAuliffe, B., Lammert, M., Lu, X., Shladover, S., Surcel, M. and Kailas, A., 2018. Influences on energy savings of heavy trucks using cooperative adaptive cruise control. SAE Technical Paper pp. 01–1181.

[Melson et al., 2018] Melson, C. L., Levin, M. W., Hammit, B. E. and Boyles, S. D., 2018. Dynamic traffic assignment of cooperative adaptive cruise control. Transportation Research Part C: Emerging Technologies 90, pp. 114–133.

[Michael et al., 1998] Michael, J. B., Godbole, D. N., Lygeros, J. and Sengupta, R., 1998. Capacity analysis of traffic flow over a single-lane automated highway system. Journal of Intelligent Transportation System 4(1-2), pp. 49–80.

[Michaels, 1963] Michaels, R., 1963. Perceptual factors in car-following. Proc. of 2nd ISTTF (London) pp. 44–59.

[Micharet, 2006] Micharet, C. A. M., 2006. Design methods of fractional order controllers for industrial applications.

[Middleton and Braslavsky, 2010] Middleton, R. H. and Braslavsky, J. H., 2010. String instability in classes of linear time invariant formation control with limited communication range. IEEE Transactions on Automatic Control 55(7), pp. 1519–1530.

[Milanés and Shladover, 2014] Milanés, V. and Shladover, S. E., 2014. Modeling cooperative and autonomous adaptive cruise control dynamic responses using experimental data. Transportation Research Part C: Emerging Technologies 48, pp. 285–300.

[Milanés and Shladover, 2016] Milanés, V. and Shladover, S. E., 2016. Handling cut-in vehicles in strings of cooperative adaptive cruise control vehicles. Journal of Intelligent Transportation Systems 20(2), pp. 178–191.

[Milanés et al., 2014] Milanés, V., Shladover, S. E., Spring, J., Nowakowski, C., Kawazoe, H. and Nakamura, M., 2014. Cooperative adaptive cruise control in real traffic situations. IEEE Transactions on Intelligent Transportation Systems 15(1), pp. 296–305.

[Milanés et al., 2012] Milanés, V., Villagrá, J., Pérez, J. and González, C., 2012. Low-speed longitudinal controllers for mass-produced cars: A comparative study. IEEE Transactions on Industrial Electronics 59(1), pp. 620–628.

[Monje et al., 2004a] Monje, C. A., Calderon, A. J., Vinagre, B. M. and Feliu, V., 2004a. The fractional order lead compensator. In: Computational Cybernetics, 2004. ICCC 2004. Second IEEE International Conference on, IEEE, pp. 347–352.

[Monje et al., 2010] Monje, C. A., Chen, Y., Vinagre, B. M., Xue, D. and Feliu-Batlle, V., 2010. Fractional-order systems and controls: fundamentals and applications. Springer Science & Business Media.

[Monje et al., 2004b] Monje, C., Vinagre, B., Chen, Y., Feliu, V., Lanusse, P. and Sabatier, J., 2004b. Proposals for fractional piλdμ tuning. In: Proceedings of The First IFAC Symposium on Fractional Differentiation and its Applications (FDA04).

[Moon et al., 2008] Moon, S., Yi, K. and Moon, I., 2008. Design, tuning and evaluation of integrated acc/ca systems. IFAC Proceedings Volumes 41(2), pp. 8546–8551.

[Naus et al., 2009] Naus, G., Vugts, R., Ploeg, J., Van de Molengraft, M. and Steinbuch, M., 2009. Towards on-the-road implementation of cooperative adaptive cruise control. Proc. 16th World Congr. Exhib. Intell. Transp. Syst. Serv.

[Naus et al., 2010] Naus, G., Vugts, R., Ploeg, J., van de Molengraft, R. and Steinbuch, M., 2010. Cooperative adaptive cruise control, design and experiments. In: American Control Conference (ACC), 2010, IEEE, pp. 6145–6150.

[Nowakowski et al., 2010a] Nowakowski, C., O'Connell, J., Shladover, S. E. and Cody, D., 2010a. Cooperative adaptive cruise control: Driver acceptance of following gap settings less than one second. In: Proceedings of the Human Factors and Ergonomics Society Annual Meeting, Vol. 54number 24, SAGE Publications Sage CA: Los Angeles, CA, pp. 2033–2037.

[Nowakowski et al., 2010b] Nowakowski, C., Shladover, S. E., Cody, D., Bu, F., O'Connell, J., Spring, J., Dickey, S. and Nelson, D., 2010b. Cooperative adaptive cruise control: Testing drivers' choices of following distances. California PATH Program, Institute of Transportation Studies, University of California at Berkeley.

[Oustaloup and Coiffet, 1983] Oustaloup, A. and Coiffet, P., 1983. Systèmes asservis linéaires d'ordre fractionnaire: théorie et pratique: par Alain Oustaloup. Masson.

[Oustaloup et al., 2000] Oustaloup, A., Levron, F., Mathieu, B. and Nanot, F. M., 2000. Frequency-band complex noninteger differentiator: characterization and synthesis. IEEE Transactions on Circuits and Systems I: Fundamental Theory and Applications 47(1), pp. 25–39.

[Oustaloup et al., 1993] Oustaloup, A., Moreau, X. and Nouillant, M., 1993. From the second generation crone control to the crone suspension. In: Systems, Man and Cybernetics, 1993.'Systems Engineering in the Service of Humans', Conference Proceedings., International Conference on, IEEE, pp. 143–148.

[Oustaloup et al., 1996] Oustaloup, A., Moreau, X. and Nouillant, M., 1996. The crone suspension. Control Engineering Practice 4(8), pp. 1101–1108.

[Padula and Visioli, 2011] Padula, F. and Visioli, A., 2011. Tuning rules for optimal pid and fractional-order pid controllers. Journal of process control 21(1), pp. 69–81.

[Pagliarella, 2009] Pagliarella, R., 2009. On the aerodynamic performance of automotive vehicle platoons featuring pre and post-critical leading forms.

[Parent and de La Fortelle, 2005] Parent, M. and de La Fortelle, A., 2005. Cybercars : Past, present and future of the technology. CoRR.

[Peppard, 1974] Peppard, L., 1974. String stability of relative-motion pid vehicle control systems. IEEE Transactions on Automatic Control 19(5), pp. 579–581.

[Pérez et al., 2013] Pérez, J., Milanés, V., Godoy, J., Villagra, J. and Onieva, E., 2013. Cooperative controllers for highways based on human experience. Expert Systems with Applications 40(4), pp. 1024–1033.

[Peters et al., 2016] Peters, A. A., Mason, O. and Middleton, R. H., 2016. Leader following with non-homogeneous weights for control of vehicle formations.

[Peters et al., 2014] Peters, A. A., Middleton, R. H. and Mason, O., 2014. Leader tracking in homogeneous vehicle platoons with broadcast delays. Automatica 50(1), pp. 64–74.

[Petráš, 2011] Petráš, I., 2011. Fractional-order nonlinear systems: modeling, analysis and simulation. Springer Science & Business Media.

[Petrillo et al., 2018] Petrillo, A., Salvi, A., Santini, S. and Valente, A. S., 2018. Adaptive multi-agents synchronization for collaborative driving of autonomous vehicles with multiple communication delays. Transportation research part C: emerging technologies 86, pp. 372–392.

[Piccinini et al., 2014] Piccinini, G. F. B., Rodrigues, C. M., Leitão, M. and Simões, A., 2014. Driver's behavioral adaptation to adaptive cruise control (acc): The case of speed and time headway. Journal of safety research 49, pp. 77–e1.

[Pintelon and Schoukens, 2012] Pintelon, R. and Schoukens, J., 2012. System identification: a frequency domain approach. John Wiley & Sons.

[Pipes, 1953] Pipes, L. A., 1953. An operational analysis of traffic dynamics. Journal of applied physics 24(3), pp. 274–281.

[Ploeg et al., 2018] Ploeg, J., Englund, C., Nijmeijer, H., Semsar-Kazerooni, E., Shladover, S. E., Voronov, A. and Van de Wouw, N., 2018. Guest editorial introduction to the special issue on the 2016 grand cooperative driving challenge. IEEE Transactions on Intelligent Transportation Systems 19(4), pp. 1208–1212.

[Ploeg et al., 2012] Ploeg, J., Shladover, S., Nijmeijer, H. and van de Wouw, N., 2012. Introduction to the special issue on the 2011 grand cooperative driving challenge. IEEE Transactions on Intelligent Transportation Systems 13(3), pp. 989–993.

[Ploeg et al., 2014a] Ploeg, J., Shukla, D. P., van de Wouw, N. and Nijmeijer, H., 2014a. Controller synthesis for string stability of vehicle platoons. IEEE Transactions on Intelligent Transportation Systems 15(2), pp. 854–865.

[Ploeg et al., 2014b] Ploeg, J., Van De Wouw, N. and Nijmeijer, H., 2014b. Lp string stability of cascaded systems: Application to vehicle platooning. IEEE Transactions on Control Systems Technology 22(2), pp. 786–793.

[Podlubny, 1994] Podlubny, I., 1994. Fractional-order systems and fractional-order controllers. Institute of Experimental Physics, Slovak Academy of Sciences, Kosice 12(3), pp. 1–18.

[Podlubny, 1999] Podlubny, I., 1999. Fractional-order systems and pi/sup/spl lambda//d/sup/spl mu//-controllers. IEEE Transactions on automatic control 44(1), pp. 208–214.

[Rajamani, 2011] Rajamani, R., 2011. Vehicle dynamics and control. Springer Science & Business Media.

[Rajamani and Shladover, 2001] Rajamani, R. and Shladover, S. E., 2001. An experimental comparative study of autonomous and co-operative vehicle-follower control systems. Transportation Research Part C: Emerging Technologies 9(1), pp. 15–31.

[Rios-Torres and Malikopoulos, 2017] Rios-Torres, J. and Malikopoulos, A. A., 2017. A survey on the coordination of connected and automated vehicles at intersections and merging at highway on-ramps. IEEE Transactions on Intelligent Transportation Systems 18(5), pp. 1066–1077.

[Rödönyi, 2015] Rödönyi, G., 2015. Leader and predecessor following robust controller synthesis for string stable heterogeneous vehicle platoons. IFAC-PapersOnLine 48(14), pp. 155–160.

[Roy, 1967] Roy, S., 1967. On the realization of a constant-argument immittance or fractional operator. IEEE Transactions on Circuit Theory 14(3), pp. 264–274.

[Ryus et al., 2011] Ryus, P., Vandehey, M., Elefteriadou, L., Dowling, R. G. and Ostrom, B. K., 2011. New trb publication: Highway capacity manual 2010. Tr News.

[Sabatier et al., 2007] Sabatier, J., Agrawal, O. P. and Machado, J. T., 2007. Advances in fractional calculus. Vol. 4Number 9, Springer.

[SAE, 2016] SAE, 2016. Taxonomy and definitions for terms related to driving automation systems for on-road motor vehicles.

[Santhanakrishnan and Rajamani, 2003] Santhanakrishnan, K. and Rajamani, R., 2003. On spacing policies for highway vehicle automation. IEEE Transactions on Intelligent Transportation Systems 4(4), pp. 198–204.

[Schakel et al., 2010] Schakel, W. J., Van Arem, B. and Netten, B. D., 2010. Effects of cooperative adaptive cruise control on traffic flow stability. In: Intelligent Transportation Systems (ITSC), 2010 13th International IEEE Conference on, IEEE, pp. 759–764.

[Seiler et al., 2004] Seiler, P., Pant, A. and Hedrick, K., 2004. Disturbance propagation in vehicle strings. IEEE Transactions on automatic control 49(10), pp. 1835–1842.

[Sename et al., 2013] Sename, O., Gaspar, P. and Bokor, J., 2013. Robust control and linear parameter varying approaches: application to vehicle dynamics. Vol. 437, Springer.

[Shaout and Jarrah, 1997] Shaout, A. and Jarrah, M., 1997. Cruise control technology review. Computers & electrical engineering 23(4), pp. 259–271.

[Shaw and Hedrick, 2007a] Shaw, E. and Hedrick, J. K., 2007a. Controller design for string stable heterogeneous vehicle strings. In: Decision and Control, 2007 46th IEEE Conference on, IEEE, pp. 2868–2875.

[Shaw and Hedrick, 2007b] Shaw, E. and Hedrick, J. K., 2007b. String stability analysis for heterogeneous vehicle strings. In: American Control Conference, 2007. ACC'07, IEEE, pp. 3118–3125.

[Sheikholeslam and Desoer, 1992a] Sheikholeslam, S. and Desoer, C. A., 1992a. Control of interconnected nonlinear dynamical systems: The platoon problem. IEEE Transactions on Automatic Control 37(6), pp. 806–810.

[Sheikholeslam and Desoer, 1992b] Sheikholeslam, S. and Desoer, C. A., 1992b. A system level study of the longitudinal control of a platoon of vehicles. Journal of dynamic systems, measurement, and control 114(2), pp. 286–292.

[Shladover, 2009] Shladover, S., 2009. Ahs demo'97 "complete success.". Available at:)(Accessed August 3, 2009) http://www. path. berkeley. edu/PATH/Intellimotion/intel63. pdf View in Article.

[Shladover, 1991] Shladover, S. E., 1991. Longitudinal control of automotive vehicles in close-formation platoons. Journal of dynamic systems, measurement, and control 113(2), pp. 231–241.

[Shladover, 1995] Shladover, S. E., 1995. Review of the state of development of advanced vehicle control systems (avcs). Vehicle System Dynamics 24(6-7), pp. 551–595.

[Shladover, 2017] Shladover, S. E., 2017. Connected and automated vehicle systems: Introduction and overview. Journal of Intelligent Transportation Systems pp. 1–11.

[Shladover et al., 2015] Shladover, S. E., Nowakowski, C., Lu, X.-Y. and Ferlis, R., 2015. Cooperative adaptive cruise control: Definitions and operating concepts. Transportation Research Record: Journal of the Transportation Research Board (2489), pp. 145–152.

[Shladover et al., 2014] Shladover, S. E., Nowakowski, C., Lu, X.-Y. and Hoogendoorn, R., 2014. Using cooperative adaptive cruise control (cacc) to form high-performance vehicle streams.

[Shladover et al., 2012] Shladover, S., Su, D. and Lu, X.-Y., 2012. Impacts of cooperative adaptive cruise control on freeway traffic flow. Transportation Research Record: Journal of the Transportation Research Board (2324), pp. 63–70.

[Stanger and del Re, 2013] Stanger, T. and del Re, L., 2013. A model predictive cooperative adaptive cruise control approach. In: American Control Conference (ACC), 2013, IEEE, pp. 1374–1379.

[Stankovic et al., 2000] Stankovic, S. S., Stanojevic, M. J. and Siljak, D. D., 2000. Decentralized overlapping control of a platoon of vehicles. IEEE Transactions on Control Systems Technology 8(5), pp. 816–832.

[Swaroop and Hedrick, 1999] Swaroop, D. and Hedrick, J., 1999. Constant spacing strategies for platooning in automated highway systems. Journal of dynamic systems, measurement, and control 121(3), pp. 462–470.

[Swaroop and Hedrick, 1996] Swaroop, D. and Hedrick, J. K., 1996. String stability of interconnected systems. IEEE transactions on automatic control 41(3), pp. 349–357.

[Swaroop and Yoon, 1999] Swaroop, D. and Yoon, S. M., 1999. Integrated lateral and longitudinal vehicle control for an emergency lane change manoeuvre design. International journal of vehicle design 21(2-3), pp. 161–174.

[Swaroop et al., 1994] Swaroop, D., Hedrick, J., Chien, C. and Ioannou, P., 1994. A comparision of spacing and headway control laws for automatically controlled vehicles1. Vehicle System Dynamics 23(1), pp. 597–625.

[Toledo, 2007] Toledo, T., 2007. Driving behaviour: models and challenges. Transport Reviews 27(1), pp. 65–84.

[Treiber and Helbing, 2003] Treiber, M. and Helbing, D., 2003. Memory effects in microscopic traffic models and wide scattering in flow-density data. Physical Review E 68(4), pp. 046119.

[Treiber et al., 2000] Treiber, M., Hennecke, A. and Helbing, D., 2000. Congested traffic states in empirical observations and microscopic simulations. Physical review E 62(2), pp. 1805.

[Tsugawa, 2013] Tsugawa, S., 2013. An overview on an automated truck platoon within the energy its project. IFAC Proceedings Volumes 46(21), pp. 41–46.

[Van Arem et al., 2006] Van Arem, B., Van Driel, C. J. and Visser, R., 2006. The impact of cooperative adaptive cruise control on traffic-flow characteristics. IEEE Transactions on Intelligent Transportation Systems 7(4), pp. 429–436.

[Vinagre et al., 2003] Vinagre, B. M., Chen, Y. Q. and Petráš, I., 2003. Two direct tustin discretization methods for fractional-order differentiator/integrator. Journal of the franklin institute 340(5), pp. 349–362.

[Wang and Nijmeijer, 2015a] Wang, C. and Nijmeijer, H., 2015a. String stable heterogeneous vehicle platoon using cooperative adaptive cruise control. In: Intelligent Transportation Systems (ITSC), 2015 IEEE 18th International Conference on, IEEE, pp. 1977–1982.

[Wang and Nijmeijer, 2015b] Wang, C. and Nijmeijer, H., 2015b. String stable heterogeneous vehicle platoon using cooperative adaptive cruise control. In: Intelligent Transportation Systems (ITSC), 2015 IEEE 18th International Conference on, IEEE, pp. 1977–1982.

[Winkelman and Liubakka, 1993] Winkelman, J. R. and Liubakka, M. K., 1993. Self-tuning speed control for a vehicle. US Patent 5,235,512.

[Xiao and Gao, 2010] Xiao, L. and Gao, F., 2010. A comprehensive review of the development of adaptive cruise control systems. Vehicle System Dynamics 48(10), pp. 1167–1192.

[Xiao et al., 2009] Xiao, L., Gao, F. and Wang, J., 2009. On scalability of platoon of automated vehicles for leader-predecessor information framework. In: Intelligent Vehicles Symposium, 2009 IEEE, IEEE, pp. 1103–1108.

[Xu and Ioannou, 1994] Xu, Z. and Ioannou, P. A., 1994. Modeling of the Brake Line Pressure to Tire Brake Force Subsystem. California PATH Program, Institute of Transportation Studies, University of California, Berkeley.

[Xue and Chen, 2002] Xue, D. and Chen, Y., 2002. A comparative introduction of four fractional order controllers. In: Intelligent Control and Automation, 2002. Proceedings of the 4th World Congress on, Vol. 4, IEEE, pp. 3228–3235.

[Yanakiev and Kanellakopoulos, 1995] Yanakiev, D. and Kanellakopoulos, I., 1995. Variable time headway for string stability of automated heavy-duty vehicles. In: Decision and Control, 1995., Proceedings of the 34th IEEE Conference on, Vol. 4, IEEE, pp. 4077–4081.

[Yang et al., 2018] Yang, S., Shladover, S. E., Lu, X.-Y., Spring, J., Nelson, D. and Ramezani, H., 2018. A first investigation of truck drivers' on-the-road experience using cooperative adaptive cruise control.

[Zegers et al., 2016] Zegers, J. C., Semsar-Kazerooni, E., Ploeg, J., van de Wouw, N. and Nijmeijer, H., 2016. Consensus-based bi-directional cacc for vehicular platooning. In: American Control Conference (ACC), 2016, IEEE, pp. 2578–2584.

[Zhang and Orosz, 2016] Zhang, L. and Orosz, G., 2016. Motif-based design for connected vehicle systems in presence of heterogeneous connectivity structures and time delays. IEEE Transactions on Intelligent Transportation Systems 17(6), pp. 1638–1651.

[Zhao et al., 2009] Zhao, J., Oya, M. and El Kamel, A., 2009. A safety spacing policy and its impact on highway traffic flow. In: Intelligent Vehicles Symposium, 2009 IEEE, IEEE, pp. 960–965.

[Zheng et al., 2017] Zheng, Y., Li, S. E., Li, K., Borrelli, F. and Hedrick, J. K., 2017. Distributed model predictive control for heterogeneous vehicle platoons under unidirectional topologies. IEEE Transactions on Control Systems Technology 25(3), pp. 899–910.

[Zheng et al., 2016] Zheng, Y., Li, S. E., Wang, J., Cao, D. and Li, K., 2016. Stability and scalability of homogeneous vehicular platoon: Study on the influence of information flow topologies. IEEE Transactions on Intelligent Transportation Systems 17(1), pp. 14–26.

[Zhou and Peng, 2005] Zhou, J. and Peng, H., 2005. Range policy of adaptive cruise control vehicles for improved flow stability and string stability. IEEE Transactions on intelligent transportation systems 6(2), pp. 229–237.

[Zhou and Doyle, 1998] Zhou, K. and Doyle, J. C., 1998. Essentials of robust control. Vol. 104, Prentice hall Upper Saddle River, NJ.

[Zwaneveld and Van Arem, 1997] Zwaneveld, P. J. and Van Arem, B., 1997. Traffic effects of automated vehicle guidance systems: a literature survey.

Résumé

L'adoption récente et généralisé des systèmes d'automatisation des véhicules, avec l'incorporation de la connectivité entre voitures, a encouragé l'utilisation des techniques comme le Contrôle Croisière Adaptatif Coopératif (CACC) et la conduite en convoi. Ces techniques ont prouvé l'amélioration du flux de trafic et la sécurité de la conduite, tout en réduisant la consommation d'énergie et les émissions CO_2. Néanmoins, la robustesse et la stabilité $\mathcal{L}_\infty$ stricte du convoi, malgré les délais de communication et l'hétérogénéité des convois, restent des sujets de recherche en cours. Cette thèse a pour sujet la conception, l'analyse et validation de systèmes de contrôle pour le car-following automatisé et coopératif, en ciblant l'augmentation de ses avantages et son usage, en se concentrant sur la robustesse et la stabilité du convoi même sur des séries de véhicules hétérogènes avec des retards de communication. Une structure feedforward/feedback est développée, dont sa modularité est fondamentale pour la mise au point des approches avec des objectifs différents mais complémentaires. L'architecture permet non seulement l'adoption d'une stratégie d'espacement pour la range entière de vitesse, mais elle peut aussi être employée dans le cadre d'un CACC basé sur une machine d'état pour la conduite en convoi sur des environnements urbains avec des capacités de freinage d'urgence et de rejoint du convoi. Des différents algorithmes pour la conception de systèmes de contrôle feedback pour la régulation des distances sont présentés, pour quoi le calcul d'ordre fractionnaire démontre fournir des réponses fréquentielles de boucle fermé plus précises et satisfaire des besoins plus exigeantes. La performance est assurée malgré l'hétérogénéité avec la proposition de deux approches feedforward différents. Le premier est basé sur une topologie en considérant que le véhicule précédente dans la boucle, tandis que le deuxième inclue le véhicule leader pour améliorer la performance de suivi. Les algorithmes propos és sont validés avec des études de stabilité dans le domaine du temps et fréquence, ainsi que simulations et expérimentations réelles.

Mots Clés

Car-following automatisé, Contrôle coopératif, Stabilité du convoi, Convois hétérogènes, Contrôle d'ordre fractionnaire

Abstract

Recent widespread adoption of vehicle automation and introduction of vehicle-to-vehicle connectivity has opened the doors for techniques as Cooperative Adaptive Cruise Control (CACC) and platooning, showing promising results in terms of traffic capacity and safety improvement, while reducing fuel consumption and CO_2 emissions. However, robustness and strict $\mathcal{L}_\infty$ string stability, despite communication delays and string heterogeneity is still an on-going research field. This thesis deals with the design, study and validation of control systems for cooperative automated car-following, with the purpose of extending their benefits and encourage their employment, focusing on robustness and string stability, despite possible V2V communication delays and string heterogeneity. A feedforward/feedback hierarchical control structure is developed, which modularity is fundamental for the proposal of approaches that target different but complementary performance objectives. The architecture not only permits the adoption of a full speed range spacing policy that target multiple criteria, but can also be employed in a state machine-based CACC framework for urban environments with emergency braking and platoon re-joining capabilities in case of pedestrian interaction. Different feedback control design algorithms are presented for the gap-regulation, for which the fractional-order calculus is demonstrated to provide more accurate closed loop frequency responses and satisfy more demanding requirements. Desired performance is ensured in spite of string heterogeneity through the proposal of two feedforward methods: one based on predecessor-only topology, while the second includes the leader vehicle information on feedforward to gain tracking capabilities. Proposed control algorithms are validated through time and frequency-domain stability studies, simulation and real platforms experiments.

Keywords

Automated car-following, cooperative control, string stability, heterogeneous strings, fractional-order control